

博士論文

S1c22a4 欠損による
pentylenetetrazole
誘発けいれん抑制と untargeted
metabolomics による
メカニズム解析

金沢大学大学院医薬保健学総合研究科創薬科学専攻
分子薬物治療学研究室

学籍番号	1629012014
学生氏名	西山 美沙
主任指導教員	加藤 将夫 教授
論文提出	令和2年7月

目次

緒言	-1-
方法	-4-
結果	-16-
考察	-23-
引用文献	-31-
図表	-43-
謝辞	-58-

緒言

てんかんは世界で 5 億人が罹患していると推測される最も一般的な脳神経疾患のひとつである(Beghi et al., 2019)。てんかんは海馬や大脳皮質を含む大脳の神経細胞の過剰な興奮によって引き起こされ、繰り返しのけいれん発作や意識消失を特徴とする(Bozzi et al., 2018)。正常な脳では神経細胞の興奮/抑制のバランスが興奮性のグルタミン酸や抑制性の GABA によって制御されている。遺伝学的研究により様々な遺伝子がてんかん関連遺伝子として同定された(Thomas and Berkovic, 2014; Magalhães et al., 2019)。グルタミン酸トランスポーター 1 やグルコーストランスポーター 1 (GLUT1) はてんかん原因遺伝子として知られており、変異による機能低下により脳の過剰な興奮を引き起こす(Mattison et al., 2018; Koch and Weber, 2019)。しかしながらてんかんが起こるメカニズムは完全には解明されていない。てんかん患者の 20%は抗てんかん薬により発作をコントロールできない治療抵抗性である(Picot et al., 2008)。てんかんのコントロール不良は日常生活の制限や寿命の短縮などを起こすことから(Tian et al., 2018)、さらなるメカニズムの解明が望まれている。

Organic cation/carnitine transporter OCTN1(SLC22A4)は脳、腎、小腸など多様な臓器に発現し(Tamai et al., 1997, 2000)、種々の有機カチオンや両性化合物を輸送する。

OCTN1 は薬に加えて、food-derived compound である ergothioneine (ERGO) や stachydrine, endogenous 化合物である acetylcholine、spermine、carnitine を輸送する(Pelteková et al., 2004; Gründemann et al., 2005; Grigat et al., 2007; Urban et al.,

2008; Kato et al., 2010; Pochini et al., 2012a, 2012b; Drenberg et al., 2017; Masuo et al., 2018)。その中で ERGO は、野生型マウス(wild-type)の血液や臓器中で μM から sub mM のレベルで存在する一方、*octn1* 遺伝子欠損マウス(*Octn1*^{-/-})では脳を含むほとんどの組織中で検出限界以下となることから、in vivo で OCTN1 の基質として輸送されることが示唆されている(Kato et al., 2010)。脳において OCTN1 は神経幹細胞や神経細胞、ミクログリアに発現し、神経分化や神経成熟、ミクログリアの活性化抑制に関与していることが示唆されている(Nakamichi et al., 2012; Ishimoto et al., 2014, 2018)。一方で基質となる ERGO は、抗うつ薬様作用、睡眠異常の改善、社交性の改善や、正常マウスとアルツハイマー病モデルマウスでの認知機能向上に働く(Yang et al., 2012; Song et al., 2014; Nakamichi et al., 2016, 2020; Matsuda et al., 2020)。OCTN1 と同じ SLC22A ファミリーに属する OCT 2 や OCT3 の機能異常は不安行動や強迫性障害などの精神神経疾患に関与することが報告されている(Wultsch et al., 2009; Nina et al., 2011)。しかしながら OCTN1 が脳でのどのような病態生理学的意義をもつのかは未解明である。

酸化ストレスはてんかんの発症や増悪に関与することが知られており(Pearson-smith and Patel, 2017)、抗酸化物質である α トコフェノールやメラトニンは抗けいれん作用を示す(Freitas, 2010; Banach et al., 2011)。OCTN1 の in vivo 基質 である ERGO は抗酸化物質である。また OCTN1 の基質となるスペルミンやカルニチンには抗けいれん

作用があり (Kumar and Kumar, 2017; Hussein et al., 2018)、同じく基質となるアセチルコリンの受容体の異常は常染色体優性夜間前頭葉てんかんを起こす (Becchetti et al., 2015)。したがって OCTN1 は、これらの基質の脳内濃度の制御を介して、てんかんの発症や増悪に関与する可能性があると考えた。しかしながら OCTN1 とてんかんの関与は明らかになっていない。

そこで本研究は、OCTN1 がてんかん発作にどのような影響を及ぼすのかを解明することを目指し、てんかんモデルマウスにおける OCTN1 の役割解明を目的とした。まず、wild-type と *Octn1*^{-/-} で GABA 受容体アンタゴニストである pentylenetetrazole (PTZ) 投与によりてんかんモデルを作製し、けいれんを評価したところ、*Octn1*^{-/-} マウスではけいれんが抑制された。そこでそのメカニズムを解明するため untargeted metabolomics の手法を用いて OCTN1 基質の探索を行った。その結果、食物に含まれる化合物である homostachydrine が新規 OCTN1 基質として同定されたため、homostachydrine が PTZ 誘発性けいれんに与える影響を調べた。最後に OCTN1 の基質かつ阻害剤である ERGO の投与が長期 PTZ 投与によるけいれんに影響を与えるか評価した。

方法

Materials

PTZ は Sigma–Aldrich Inc. (St. Louis, MO) から購入した。ERGO と d9-ERGO はそれぞれ雪国まいたけ (南魚沼、日本) の田中昭弘博士と TETRAHEDRON (Paris, France) の Dr. Jean-Claude Yadan から提供された。他のすべての試薬は市販特級試薬を用いた。

動物

Octn1^{-/-} マウスは、C57BL/6J wild-type マウスとのバッククロスを 6 回以上行ったマウスを実験に用いた (Ishimoto et al., 2018)。WT マウスは三協ラボから購入もしくは金沢大学学際科学実験センター実験動物研究施設で繁殖、飼育されたものを用いた。

Octn1^{-/-} マウスは、金沢大学学際科学実験センター実験動物研究施設で繁殖、飼育されたものを用いた。特に記載がない場合、8 から 9 週齢のマウスを実験に用いた。生後 3-4 週目に離乳し、離乳後のマウスはすべて標準食で飼育され、水及び食餌は自由に与えられた。動物実験は金沢大学動物実験指針に従って実施した。

PTZ 急性けいれんモデルの作製

Wild-type と *Octn1*^{-/-} に 35、40、50 mg/kg の PTZ を腹腔内投与した。PTZ は投与直

前に生理食塩水に溶解して用いた。投与後、マウスは個別にプラスチックケージにいれ、20分間けいれん行動を観察した。けいれんのレベルは Mizoguchi らの論文(Mizoguchi et al., 2011)を modify して作製したクライテリアに従いスコア化し、20分間で見られた 1 番高いスコアを記録した。ここで、Stage0: No behavioral change、Stage1: Hypoactivity and immobility、Stage2: Two or more isolated, myoclonic jerks、Stage3: Generalized clonic convulsions with preservation of righting reflex、Stage4: Generalized or tonic-clonic seizure with loss of righting reflex、Stage5: Death と定義した。2回の投与後、PCR 測定用サンプルに 2 時間後、ELISA 測定用サンプルに 4 時間後に海馬を回収し、測定に使用するまで-80℃で保管した。Homostachydrine の PTZ 急性けいれんに与える影響を調べる実験では、PTZ 投与の 4 時間前に麻酔下で静脈内から homostachydrine を投与した。20 分の観察後、血漿と海馬、大脳皮質前部を回収し、PCR と homostachydrine 濃度測定に用いた。

Real-time PCR

回収された海馬もしくは大脳皮質前部から total RNA を抽出した。視床下部より前の大脳皮質を大脳皮質前部とした。Total RNA は標準的な ISOGEN(NIPPON GENE, Tokyo, Japan)もしくは RNAiso-plus(TAKARA BIO, Shiga, Japan)のプロトコルにしたがい抽出した。cDNA は RiverTra Ace qPCR RT master mix with gDNA remover

(TOYOBO, Osaka, Japan) により作製し、cDNA テンプレートと各プライマー、THUNDERBIRD SYBR qPCR Mix (TOYOBO, Osaka, Japan)を加えて Mx3005P (Agilent Technologies, Santa Clara, CA)で増幅させた。プライマー配列は以下の通り

(c-fos forward, GGGACAGCCTTTCCTACTACC and reverse, TTGGCACTAGAGACGGACAG; Arc forward, GAGTTCTTAGCCTGTTCGGA and reverse, GCTCGGCACTTACCAATCT; Egr1 forward, AGCCTTCGCTCACTCCACTATCC and reverse, GCGGCTGGGTTTGATGAGTTGG; Bdnf forward, GCGGCAGATAAAAAGACTGC and reverse, TCAGTTGGCCTTTGGATAACC; Ngf forward, TCTATACTGGCCGCAGTGAG and reverse, GGACATTGCTATCTGTGTACGG; Nt-3 forward, GGAGGAAACGCTATGCAGAA and reverse, GTCACCCACAGGCTCTCACT; 36B4 forward, ACTGGTCTAGGACCCGAGAAG and reverse, TCCCACCTTGTCTCCAGTCT)。

PCR の反応条件は以下の通り (95 ° C、15 分 → (95 ° C、10 秒 → 60 ° C、30 秒) x 40 サイクル)。mRNA 発現量は、相対定量の $\Delta\Delta Ct$ 法を用いて定量した。相対定量では、ハウスキーピング遺伝子である acidic ribosomal phosphoprotein P0 (36B4)によって補正を行った。

ELISA による BDNF タンパク質濃度の測定

PTZ を 2 回目に投与 4 時間後に wild-type と *Octn1*^{-/-} の海馬を摘出し、測定まで-80°C で保管した。10 mg の海馬に対して 100 μ L の extraction buffer (50 mmol/L 酢酸アンモニウム、1 mol/L NaCl、0.1 % Triton X-100 を酢酸で pH 4.0 に調整) を加え、懸濁液を氷上でソニケーション (Handy Sonic UR20-P、TOMMY SEIKO、Japan) を組織破片が目で確認できなくなるまで行った後、21,500 g で 30 分間、遠心した。上清を Mature BDNF Rapid ELISA Kit (Biosensis, Thebarton, South Australia, Australia) を用いてキットプロトコルに基づいて BDNF 濃度を定量した。

LC-QTOFMS による untargeted metabolomics

7 週齢の Wild-type と *Octn1*^{-/-} を 1 週間同一ケージで飼育した後、血漿を回収し、海馬と大脳皮質前部を摘出し-80°C で保管した。大脳皮質の視床下部より前の部分を大脳皮質前部とした。組織を秤量し海馬 10 mg あたり 60 μ L、大脳皮質前部 10 mg あたり 50 μ L の IS を溶かしたメタノールを加えた後、ジルコニアシリカビーズ 1.2 mm (Biomedical Science, Tokyo, Japan) を入れ、ビーズ式 homogenizer (Precellys 24 homogenizer, Bertin Technologies, Montigny-le-Bretonneux, France) を用い、6,500 rpm で 90 秒 (30 秒×3 回、インターバル 30 秒) かけて homogenize した。血漿は 100 μ L に対して 500 μ L の IS を溶かしたメタノールを加えて vortex した。これらを 21,500 g で 10 分間遠心した上清 30 μ L に 120 μ L のアセトニトリルを加えた。21,500

g で 10 分間遠心した上清を LC-QTOFMS の測定に用いた。候補化合物の検出には、Waters ACQUITY Arc-System と Xevo G2 TOF (Waters, Milford, MA) を接続した装置を使った。移動相は(A) 0.1% formic acid, 10 mM CH₃COONH₄ in 80% H₂O/20% AcCN (B) 0.1% formic acid, 10 mM CH₃COONH₄ in 5% H₂O/95% AcCN を使用した。流速は 0.4 μL/min で行なった。グラジエントは以下の通り (0-0.5min, 1% A/99% B; 0.5-6.5min, 1% A/99% B to 50% A/50% B; 6.5-7.5 min, 50% A/50% B to 70% A/30% B; 7.5-8.5 min, 70% A/30% B; 8.5-9.0 min, 70% A/30% B to 1% A/99% B; 9.0-13.5 min, 1% A/99% B)。カラムは ACQUITY UPLC® BEH Amide (1.7 μm particle size, 2.1 mm I.D.×100 mm; Waters, Milford, MA)、カラム温度は 50°C、ポジティブモードで測定を行った。スキャンレンジは *m/z* 50~600 とした。

Untargeted metabolomics データからのピークピッキングと候補化合物の絞り込み

測定データからの自動ピーク検出は、MS システムの制御ソフトである MassLynx(Waters, Milford, MA)を用いて行った。MassLynx のメタボロミクス用オプションアプリケーションマネージャである MarkerLynx で解析を行った。解析時のピーク強度の閾値は以下の様に設定した (海馬:2,000、大脳皮質前部 : 1,700、血漿 : 400)。シグナル強度が 1 未満、それぞれのグループで 4/6 未満のサンプルにしか検出されないピークはノイズとして除いた。ピーク高さを内部標準物質 (gabapentin) で補

正した。Wild-type と *Octn1*^{-/-} でピーク高さの平均値を算出し、*Octn1*^{-/-} のピーク高さの平均値が wild-type に対して 1/2 倍以下か 2 倍以上に変動したピークを選び、その中から有意な差が見られたもののみを選んだ。最後にピーク形状を目視で確認し、形状が悪いものは除いた。LC-QTOFMS 測定で得られた parent ion の精密質量を用いて、データベース METLIN (<https://metlin.scripps.edu>)と HMDB(<http://www.hmdb.ca>)を検索することにより、候補化合物の同定を試みた。

Homostachydrine の合成

Homostachydrine と d-homostachydrine は過去の報告に従い(Servillo et al., 2012)、ピペコリン酸からヨードメタンもしくは重水素ヨードメタンと KHCO_3 で処理することにより合成した。合成された homostachydrine は $^1\text{H-NMR}$ と electrospray ionization mass spectrometry ($m/z = 157$)により確認した。合成された d-homostachydrine は $^1\text{H-NMR}$ により確認した。

Product ion scan

Wild-type 血漿サンプルと合成した homostachydrine 標品について、Nexera X2 LC system を接続した LCMS-8040(Shimadzu, Kyoto, Japan)を用いて product ion scan を行った。カラムは ACQUITY UPLC® BEH Amide (1.7 μm particle size, 2.1 mm

I.D.×100 mm; Waters, Milford, MA)、移動相は(A) 0.1% formic acid, 10 mM CH₃COONH₄ in 80% H₂O, 20% AcCN、(B) 0.1% formic acid, 10 mM CH₃COONH₄ in 5% H₂O, 95% AcCN を 0.4 μL/min で流した。グラジエントは以下の通り (0 to 0.5min, 1% A/99% B; 0.5 to 3.5min, 1% A/99% B to 15% A/85% B; 3.5 to 4.5 min, 15% A/85% B to 35% A/65% B; 4.5 to 4.8min, 35% A/65% B to 60% A/40% B; 4.8 to 5.8min, 60% A/40% B; 5.8 to 6.0min, 60% A/40% B to 1% A/99% B; 6.0 to 8.0min, 1% A/99% B)。カラム温度は 50 °C、モードは positive、parent ion は m/z 158.00、collision energy は-10, -20, -40 V、product ion scan レンジは m/z 50-200 で行なった。

MRM 測定

Homostachydrine、homostachydrine-d の測定は Exera X2 LC system を接続した LCMS-8040(Shimadzu, Kyoto, Japan)を用いて行った。カラムは ACQUITY UPLC® BEH Amide (1.7 μm particle size, 2.1 mm I.D.×100 mm; Waters, Milford, MA)。移動相は(A) 0.1% formic acid, 10 mM CH₃COONH₄ in 80% H₂O, 20% AcCN、(B) 0.1% formic acid, 10 mM CH₃COONH₄ in 5% H₂O, 95% AcCN を 0.4 μL/min で流した。グラジエントは以下の通り (0 to 0.5min, 1% A/99% B; 0.5 to 3.5min, 1% A/99% B to 15% A/85% B; 3.5 to 4.5min, 15% A/85% B to 35% A/65% B; 4.5 to 4.8min, 35% A/65% B to 60% A/40% B; 4.8 to 5.8min, 60% A/40% B; 5.8 to 6.0min, 60% / 40% B to 1%

A/99% B, 6.0 to 8.0min, 1% A/99% B)。ERGO-d 測定のグラジエントは以下の通り (0 to 0.5min, 1% A/99% B, 0.5 to 1.5min, 1% A/99% B to 25% A/85% B; 1.5 to 6.3 min, 25% A/85% B; 6.3 to 7.0 min, 25% A/85% B to 60% A/40% B; 7.0 to 8.0 min, 60% A/40% B; 8.0 to 8.2 min, 60% A/40% B to 1% A/99% B; 8.2 min to 11.5 min, 1% A/99% B)。Cephalexin の測定は Exera X2 LC system を接続した LCMS-8040 を用いて行った。カラムは a Cosmosil C18-MS-II packed column (3 mm particle size, 2.0 mm I.D.×50 mm; Nacalai Tesque, Kyoto, Japan)。移動相は(A) 0.1% formic acid, H₂O、(B) 0.1% formic acid,100% AcCN を 0.4 μL/min で流した。測定のグラジエントは以下の通り (0 to 0.3 min, 99% A/1% B; 0.3 to 2.8 min, 99% A/1% B to 5% A/95% B; 2.8 to 3.4 min, 5% A/95% B; 3.4 to 4.5 min, 5% A/95% B to 99% A/1% B)。Homostachydrine の precursor ion は m/z 158.00、product ion は m/z 58.00。Homostachydrine-d の precursor は m/z 164.00、product ion は m/z 64.15。ERGO-d の precursor は m/z 239.15、product ion は m/z 127.00。Cephalexin の precursor ion は m/z 348.00、product ion は m/z 157.90。homostachydrine、homostachydrine-d、ERGO-d に対する内部標準 gabapentin の precursor ion は m/z 172.05, product ion は 154.15。Cephalexin に対する内部標準の verapamil の precursor ion は m/z 455.20、product ion は 165.05 に設定した。

臓器中 homostachydrine 測定

Wild-type と *Octn1*^{-/-} は一晩絶食し、血漿と各臓器を回収した。血漿、臓器サンプルに内標の gabapentin 入りメタノールを加え、それぞれボルテックスもしくはビーズ式 homogenizer を用いて 90 秒 homogenize した。21,500 g、4 °C で 10 分間遠心し、上清を回収後、もう一度遠心し、上清を測定に用いた。

Homostachydrine の取り込み実験

HEK293 細胞にヒト OCTN1 遺伝子(*hOCTN1*)もしくはベクター(pcDNA3)のみを安定発現させた HEK293/hOCTN1 と HEK293/mock 細胞を poly-l-lysine コートした 4 ウェルディッシュに 3.8×10^4 cells/cm² で播種した。培地は Dulbecco's modified Eagle's medium に 10% FBS と抗生物質 (ペニシリン K、ストレプトマイシン) を加えたものを用いた。播種から 48 時間後に培地を新しいものに交換した。播種から 72 時間後、培地を除き、トランスポートバッファー(123 mM NaCl, 4.8 mM KCl, 5.6 mM glucose, 1.2 mM CaCl₂, 1.2 mM KH₂PO₄, 1.2 mM MgSO₄, 20 mM HEPES, 4.2 mM NaHCO₃/NaOH, pH 7.4)で wash したのち 10 分間プレインキュベーションした。時間依存性取り込み試験では 10 μM の homostachydrine-d を含んだトランスポートバッファーを加えて反応を開始し、所定の時間に ice-cold バッファーで 3 回 wash した。濃度依存性試験では以下の様に homostachydrine-d と homostachydrine を含んだトラン

スポーツバッファーを添加し、15秒後に ice-cold buffer を約7倍容積加えることにより反応をストップさせたのち、速やかに細胞を ice-cold バッファーで3回 wash した。薬液の組成は以下の通り (Homostachydrine-d 5 μ M, homostachydrine-d 5 μ M + homostachydrine 20 μ M, homostachydrine-d 5 μ M + homostachydrine 100 μ M, homostachydrine-d 6 μ M + homostachydrine 300 μ M, homostachydrine-d 12 μ M + homostachydrine 600 μ M, homostachydrine-d 20 μ M + homostachydrine 1mM)。細胞を乾かした後、300 μ Lの水とともに細胞をセルスクレーパーで回収し、ソニケーションで細胞を破壊した。サンプルは内標 (gabapentin) を含んだアセトニトリルを加えて 21,500 g、4 $^{\circ}$ Cで10分間遠心し、上清をもう一度遠心して上清を測定に用いた。LSMS-8040(Shimadzu, Kyoto, Japan)を用いて homostachydrine-d を測定した。ERGO 阻害試験では1 μ Mの ERGO-d と様々な濃度の homostachydrine を含んだトランスポートバッファーで5分インキュベートした。LSMS-8040で ERGO-d の細胞内濃度を測定した。タンパク濃度はブラッドフォード法で測定した。

Homostachydrine の血漿中濃度推移

Wild-type と *Octn1*^{-/-} は一晩絶食し、homostachydrine-d を静脈内、もしくは経口投与した。一定時間後に静脈から血液を回収し、血漿を回収後、測定まで-80 $^{\circ}$ Cで保存した。血漿に内標を含んだメタノールを加えて 21,500g、4 $^{\circ}$ Cで10分間遠心し、上清を

回収後、もう一度遠心し、上清を測定に用いた。投与後 1、5、10 分のサンプルはあらかじめ水で 10 倍に希釈してから用いた。LSMS-8040 を用いて homostachydrine-d を測定した。血漿中濃度プロファイルから moment 解析を用いて動態パラメーターを算出した。モーメント解析のプログラムは <https://www.pharm.kyoto-u.ac.jp/byoyaku/Kinetics/download.html#chuui> から入手した。

Homostachydrine の尿中排泄

Wild-type と *Octn1*^{-/-} を代謝ケージに入れて慣らし飼育した。24 時間後、生理食塩水に溶解した homostachydrine-d を 1 mg/kg 静脈内投与、もしくは 3 mg/kg 経口投与し、ただちに代謝ケージで尿の回収を始めた。実験のコントロールとして、セファレキシン 50 μmol/kg を homostachydrine-d と同じ薬液に溶解し投与した。尿の回収開始後 24 時間で尿の回収チューブを交換し、さらに 24 時間後にもう一度尿を回収することで、48 時間までの尿を回収した。尿中の homostachydrine-d と cephalexin の濃度を、LSMS-8040 を用いて測定し、回収した尿量と投与量から尿への排泄率を算出した。

PTZ-induced kindling

Wild-type と *Octn1*^{-/-} に 1 日おきに 35 mg/kg の PTZ を腹腔内投与し、けいれんを観

察した。スコアは PTZ 急性けいれんと同様とした。マウスが途中でけいれんにより死亡した場合はそれ以降を Stage5 として扱った。ERGO が PTZ-induced kindling に与える影響を調べるために 7 週齢の wild-type に 50 mg/kg の ERGO を毎日投与した。ERGO 投与開始から 1 週間後に PTZ の投与を開始した。PTZ の投与中も ERGO の投与は継続したが、ERGO 投与時のイソフルラン麻酔の影響を避けるため、PTZ 投与と ERGO 投与が重なる日は PTZ 投与のあとに ERGO を投与した。11 回目の PTZ の投与後、海馬と大脳皮質前部を回収した。海馬、大脳皮質前部サンプルに内標の gabapentin 入りメタノールを加え、ビーズ式 homogenizer を用いて 30 秒 homogenize した。21,500 g、4°C で 10 分間遠心し、上清を回収後、もう一度遠心し、上清を測定に用いた。LSMS-8040 を用いて ERGO と homostachydrine 濃度を測定した。

統計

データは平均値±標準偏差で表記した。Microsoft Excel 2010 で Student の t 検定を適用し、統計学的に解析した。一元配置分散分析を用いてデータを分析し有意な差が得られたときは、Dunnett's multiple comparison test を適用し、統計学的に解析した。生存率の有意差検定はケプランマイヤー法を適用した。p 値が 0.05 未満を統計学的に有意差ありとした。

結果

Octn1^{-/-}ではPTZ急性けいれんが抑制された

OCTN1がPTZの急性けいれんに与える影響を調べるために、PTZを投与後のけいれんをWild-typeとOctn1^{-/-}で比較した。Wild-typeではけいれんスコアはPTZ投与量依存的に上昇が見られた (Fig. 1A)。一方、Octn1^{-/-}ではPTZ 40mg/kg投与群でwild-typeに比べて有意に低いスコアを示した (Fig.1A)。50 mg/kgではOctn1^{-/-}でもけいれんが確認された (Fig.1A)。45 mg/kgのPTZを2回投与したところ、同様にwild-typeに比べてOctn1^{-/-}ではスコアが低かった (Fig. 1B)。PCRとELISAのためにPTZを2回目の投与 (48時間後) のさらにそれぞれ2時間後、4時間後に海馬を回収した。

Octn1^{-/-}ではPTZ投与によるc-fos、Arc、BDNFの発現上昇が抑制された

PTZによる神経細胞の興奮を評価するため神経興奮関連遺伝子の発現をPCRで調べた。Wild-typeではPTZ投与群で神経興奮マーカーのc-fosと細胞への刺激に応じて発現が上昇する最初期遺伝子のひとつであるArcが有意に上昇した (Fig. 2A-B)。一方、Octn1^{-/-}ではPTZによるc-fos, Arcの顕著な発現上昇は見られなかった (Fig. 2A-B)。また、てんかんの発症、進行に関与すると言われていたBDNFの発現をPCR (Fig. 2D) とELISA (Fig. 2F) で測定した。Wild-typeではPTZ投与によりmRNA, タンパク質両

方で BDNF 発現量が上昇したが、*Octn1*^{-/-} では顕著な上昇が見られなかった(Fig. 2D, F)。なお、PTZ 1 回投与 2 時間後の *c-fos*、*Arc*、*Egr1*、*Bdnf* の mRNA 発現も測定したが、*wild-type* のばらつきが大きかったため、明確な違いは検出できなかった。

Untargeted metabolomics による OCTN1 基質の探索

OCTN1 は、基質の細胞内への取り込みに働く膜輸送体である。そこで、*Octn1*^{-/-} だけいれんが抑制された理由として、OCTN1 が輸送し、PTZ 誘発性けいれんに関係する何らかの生体内基質が輸送できなかったことに起因すると考え、*wild-type* の海馬に存在し、*Octn1*^{-/-} では低下する OCTN1 の *in vivo* 基質を探索するため untargeted metabolomics 解析を行った。*Wild-type* と *Octn1*^{-/-} を同一ケージで 1 週間飼育後、海馬、大脳皮質前部、血漿を採取し前処理後、LC-TOF/MS を用い untargeted metabolomics を行った。ピークピッキングの結果、それぞれ、2,599、2,676、1,697 個のイオンが検出された。ここからノイズを除去し、*wild-type* と *Octn1*^{-/-} マウス間に有意差があり、ピーク高さが 2 倍以上もしくは 2 分の 1 以下のものを拾ったところ、5、3、3 個のピークにまで絞り込まれ、さらに chromatogram でピーク形状を確認したところ十分なシグナル強度を有するピークをそれぞれ 4、2、2 個を選別できた。このうち *m/z* 158 は、海馬、大脳皮質前部、血漿で共通して両マウス間に差のあるピークであったため、以降の解析対象とした(Fig. 3A-C)。LC-QTOFMS 測定で得られた parent ion、product ion

から m/z 158 は homostachydrine であると推定された。そこで、有機合成した homostachydrine 標品と血漿を用いた product ion scan を行なったところ、少なくとも m/z 56, 58, 70, 84 が共通 product ion として検出された (Fig. 3D,E) ことから、 m/z 158 は homostachydrine であると同定された。Wild-type と *Octn1*^{-/-} の血漿と各臓器中の homostachydrine 濃度を測定したところ、小腸中部以外の部位で homostachydrine 濃度が *Octn1*^{-/-} で有意に低かった (Fig. 3F,G)。

hOCTN1 を介した Homostachydrine の取り込み

Homostachydrine が OCTN1 によって輸送されるかを確認するため、HEK293/hOCTN1 細胞と HEK293/mock 細胞を用いて取り込み実験を行った。hOCTN1 による時間依存的な homostachydrine-d の取り込みが見られた (Fig. 4A)。500 μ M ERGO の添加で homostachydrine の取り込みが阻害された (Fig. 4A)。また 15 秒まで取り込みの直線性が確認されたことから (data not shown)、取り込み時間を 15 秒として濃度依存性を検討した。Homostachydrine は濃度依存的だが飽和性のある取り込みを示した (Fig. 4B)。Eadie-Hofstee プロットにより homostachydrine 取り込みの K_m , V_{max} を算出したところ、それぞれ 236 μ M, 102 nmol/mg protein/min となった。Homostachydrine による OCTN1 輸送の阻害効果を評価するために、ERGO-d に様々な濃度の homostachydrine を添加して取り込み試験を行った。Homostachydrine は

ERGO-d に対して弱い阻害を示した(Fig. 4C)。

Homostachydrine の体内動態に及ぼす OCTN1 の影響

OCTN1 の homostachydrine 体内動態における役割を調べるため、wild-type と *Octn1*^{-/-} に homostachydrine-d を静脈内または経口投与し、血漿中濃度推移を比較した。静脈内投与では投与後 1 分、5 分、10 分では *Octn1*^{-/-} の方が wild-type に比べて高い血中濃度を示したが、*Octn1*^{-/-} では投与後 4 時間以降は速やかな消失が見られた(Fig. 5A)。経口投与では投与後 6 時間以降 *Octn1*^{-/-} では wild-type に比べて homostachydrine-d は速やかに消失した(Fig. 5B)。投与後 24 時間では homostachydrine-d は定量限界以下であった。Moment 解析により動態パラメーターを算出した (Table 1)。静脈内投与の半減期は wild-type と *Octn1*^{-/-} で有意差はなかったものの、*Octn1*^{-/-} の方が短い傾向だった一方、経口投与後の半減期は wild-type に比べ *Octn1*^{-/-} で有意に短縮された (Table 1)。定常状態分布容積 (Vdss) は wild-type に対して *Octn1*^{-/-} で有意な低下が見られた (Table 1)。全身クリアランスは wild-type と *Octn1*^{-/-} で差はみられなかった。興味深いことに bioavailability は wild-type と *Octn1*^{-/-} で同等であった。したがって、homostachydrine が *Octn1*^{-/-} で低かった原因は、吸収よりも消失過程に起因すると考えられた。

Homostachydrine の尿中排泄に及ぼす OCTN1 の影響

Homostachydrine の消失経路と、homostachydrine の尿中排泄に対する OCTN1 の影響を調べるため、homostachydrine-d を静脈内投与または経口投与してのち、48 時間尿を回収した (Table 2)。静脈内投与後の homostachydrine-d の尿中排泄率は wild-type と Octn1^{-/-}の両方で 70%程度となり、差はみられなかった (Table 2)。経口投与後の homostachydrine-d の排泄率もほぼ同様であった (Table 2) Octn1^{-/-} でやや低い傾向にあった。同時に測定したセファレキシンの尿中排泄率は両系統において静脈内投与、経口投与後 50%程度であった (Table 2)。

Homostachydrine は PTZ 誘発急性けいれんを悪化させる

Homostachydrine の PTZ 誘発けいれんへの影響を調べるため、wild-type に homostachydrine を静脈内投与してけいれんを評価した。PTZ 40 mg/kg 投与時、homostachydrine 投与群では、対照 (生食投与) 群に比べて、けいれんスコアが有意に上昇した (Fig. 6A)。20 分間のけいれん観察終了後血漿と脳を回収し、homostachydrine 濃度を測定した。血漿中 homostachydrine 濃度は対照群に比べて顕著に高かった (Fig. 6B)。海馬、大脳皮質前部での濃度は homostachydrine 投与群で対照群に比べ 8 倍程度となり、海馬と大脳皮質前部で濃度差はなかった (Fig. 6C)。海馬、大脳皮質前部の神経興奮関連遺伝子の発現を PCR にて確認したところ、海馬では Arc

の発現が homostachydrine 投与群で有意に上昇していた(Fig. 6D)。大脳皮質前部では Arc と Egr1、Bdnf の発現が有意に増加していた(Fig. 6E)。

***Octn1*^{-/-} では PTZ による Kindling の形成が抑制される**

PTZ の単回投与モデルはけいれんを評価するものであるのに対し、低投与量の PTZ を連続投与する PTZ-induced kindling モデルはてんかんの発症や進行を評価するモデルである。後者のモデルでは、PTZ 開始時はけいれんがほとんど見られないが、徐々に同じ刺激に対してけいれんを起こすようになり、けいれんを起こしやすい脳の構造を獲得する。PTZ-induced kindling model では神経脱落や苔状繊維の異常発芽などてんかん患者と同様の脳の変化が見られるため、より臨床に近いてんかんモデルであると考えられている(Morimoto et al., 2004; Becker, 2018)。OCTN1 の PTZ による kindling の形成に与える影響を調べるため、wild-type と *Octn1*^{-/-} に 35 mg/kg の PTZ を 48 時間隔で 11 回連続投与した。Wild-type ではけいれんスコアは徐々に上昇が見られたが、*Octn1*^{-/-} では PTZ 投与期間にほとんどけいれんが見られず、けいれんスコアは wild-type に比べ有意に低く(Fig. 7A)、高い生存率を示した (Fig. 7B)。次に OCTN1 の阻害剤が PTZ による kindling の形成を抑制できるかを検討した。OCTN1 には特異的な阻害剤が見つかっていないため、in vivo で投与のできる ERGO を阻害剤として用いた。ERGO の長期投与によりけいれんのスコアは有意に抑制され (Fig. 7C)、ERGO

投与群は高い生存率を示した(Fig. 7D)。最終 PTZ 投与後生存していたマウスの海馬と
大脳皮質前部の ERGO と homostachydrine 濃度を測定した。ERGO 濃度は対照（水
投与）群に比べて ERGO 投与群で上昇が確認された(Fig. 7E)。Homostachydrine 濃度
は ERGO 投与群で対照群に比べて約 1/2 に低下した(Fig. 7F)。

考察

本研究の結果は *octn1* 遺伝子の欠損がマウスで PTZ によるけいれんと神経興奮の抑制に働くことを示す (Figs. 1, 2)。OCTN1 は、食物由来抗酸化物質 ERGO に加えて、アセチルコリン、カルニチン、スペルミンなどの抗けいれん作用のある化合物を輸送する (Kato et al., 2010; Pochini et al., 2012a; Masuo et al., 2018)。したがって、本研究開始当初は *Octn1*^{-/-} では、けいれんが悪化すると予測していた。しかしながら、結果は正反対になった。OCTN1 は両性アミノ酸である ERGO を輸送すること、in vitro で OCTN1 によるアセチルコリン輸送を GABA が阻害することから (Pochini et al., 2012b)、OCTN1 が Glu や GABA を輸送する可能性も考えられる。しかしながら、saline もしくは PTZ 投与後の wild-type と *Octn1*^{-/-} で脳の海馬と大脳皮質前部中の Glu、GABA 濃度を測定したところ、両系統の間に明確な差はなかった (data not shown)。また、PTZ (50 mg/kg) を腹腔内投与 30 分後の脳中 PTZ 濃度や、PTZ (35 mg/kg) を腹腔内投与後に microdialysis 法を用いて測定した脳細胞外液中濃度にも差はなく、また、hOCTN1 発現細胞を用いた実験でも PTZ の OCTN1 を介した取り込みは見られなかった (data not shown)。したがって、両系統間のけいれんの違いは、Glu や GABA、PTZ の動態の違いによるものではないと考えられた。

OCTN1 と同じ SLC22 ファミリーの OCT2 は神経毒であるサルソリノールを細胞内へ取り込むことで OCT2 発現細胞選択的に毒性を示す (Taubert et al., 2007)。そこで

OCTN1 が未知のけいれん誘発物質を細胞内へ輸送しているという仮説を立て、untargeted metabolomics を行ったところ、OCTN1 の新規基質として homostachydrine が同定された (Figs. 3,4)。Homostachydrine は欠損マウスで臓器中濃度が変化するという意味で、ERGO、spermine に続く 3 つ目の in vivo 基質である。Homostachydrine は柑橘類やアルファルファ、ライ麦等に含まれるアルカロイドである (Wiehler and Marion, 1958; Servillo et al., 2012, 2018)。Homostachydrine は植物ではピペコリン酸から合成されると推測されているが (Servillo et al., 2012)、哺乳類では生合成は報告されておらず、食餌から摂取されると考えられている。その点においては、同じく哺乳類で生合成されず、もっぱら食餌から摂取される ERGO と同様である。*Octn1*^{-/-} では homostachydrine-d は wild-type に比べて速やかな消失が見られた (Fig. 5)。一方、bioavailability は wild-type と *Octn1*^{-/-} で差が見られなかった (Table 1)。したがって、homostachydrine の消化管吸収において OCTN1 の寄与は少ないことが示唆された。OCTN1 は腎臓の lumen 側に発現しており、ERGO は腎臓で OCTN1 によって再吸収を受ける (Kato et al., 2010)。Homostachydrine も ERGO と同様に腎から再吸収され、*Octn1*^{-/-} では再吸収が行われないうことにより速やかな homostachydrine の消失につながっている可能性がある。実際、腎臓中の homostachydrine 濃度は、wild-type に比べて *Octn1*^{-/-} で顕著に低く (Fig. 3G)、この仮説を支持している。Homostachydrine-d の尿中排泄率が静脈内投与後約 70% であっ

たことから (Table 2)、homostachydrine の主要な消失経路は腎であると考えられる。一方で、今回の尿中排泄の検討では、wild-type と *Octn1*^{-/-}での違いは見られなかった (Table 2)。48 時間という長時間のサンプリングであったため、より短い時間での検討によって尿中排泄速度を比較する必要がある。。

Homostachydrine の静脈内投与 は PTZ によるけいれんを悪化させた (Fig. 6)。血漿中 homostachydrine 濃度は、統合失調症、注意欠陥・多動性障害 (ADHD) との相関が報告されている (Yang et al., 2020)。また多発性硬化症研究に用いられる実験的自己免疫性脳脊髄炎 (experimental autoimmune encephalitis: EAE) モデルマウスでは homostachydrine の血漿中濃度が上昇する (Mangalam et al., 2013)。しかしながら homostachydrine の生理的機能を直接示したのは本研究が初めてである。植物における homostachydrine の前駆体であり構造が類似しているピペコリン酸は、いくつかのてんかんと関係を示す報告がある。ピリドキシン依存性てんかん患者の血漿と脳脊髄液中では、ピペコリン酸濃度の上昇が見られる (Plecko et al., 2000, 2005)。また、ピペコリン酸を高濃度で脳室内に直接投与すると重篤なけいれんを起こす (Takahama et al., 1982; Plecko et al., 2005)。一方で、ピペコリン酸の腹腔内投与と低濃度 i.c.v.投与では、PTZ によるけいれんに対してむしろ抗けいれん効果を示す (Yung-Feng Chang et al., 1988)。これらの報告はピペコリン酸が低濃度と高濃度の脳への暴露で、けいれんに対して異なる振る舞いをする可能性を示す。Homostachydrine が、このように相反

する活性を示すかどうかについては、今回の検討からは示されておらず、今後のさらなる検討が必要である。*Octn1* のピペコリン酸は GABA 受容体に結合し、GABA の再取り込みを抑制し、GABA の放出を促進することから (Feigenbaum and Chang, 1986; Gutierrez and Delgado-coello, 1989; Takagi et al., 2003)、GABA 神経伝達系のモジュレーターであると考えられている。Homostachydrine が GABA 神経伝達に影響を与えるか否かは報告がないが、GABA 受容体に何らかの作用をすることで PTZ 誘発性けいれんに影響を与えたと考えれば今回の結果は説明できるかもしれない。今後 homostachydrine と GABA 神経伝達系の関係についてさらなる検討が必要である。

本研究の結果を考えると、homostachydrine を含む柑橘類やライ麦などの食品を多く摂取することでけいれんが悪化するかどうかを臨床において解明することは重要であるかもしれない。本研究でけいれんの増悪が見られた 50 mg/kg homostachydrine 静脈内投与群では、血漿中 homostachydrine 濃度はコントロールに比べて約 7 倍であった (Fig. 6B)。ヒトにおける homostachydrine の血漿中濃度は 7.0 ng/mL ほどであり (Tuomainen et al., 2019)、今回の結果では、マウス血漿中濃度は、絶食下で 0.35 µg/mL 程度であったため (Fig. 3F)、マウスと比べてヒトは 50 分の 1 程度である。一方で、ヒトの血漿中 homostachydrine 濃度は食事の影響を受けることが分かっており (Guertin et al., 2014; Kärkkäinen et al., 2018)、高度な塩分制限や healthy Nordic diet によりそれぞれ 1.47 倍、1.41 倍になることが報告されている (Derkach et al., 2017;

Tuomainen et al., 2019)。Homostachydrine は herbal medicine として使われる *Medicago sativa* (alfalfa) や *Achillea millefolium* に多く含まれるため(Wood et al., 1991; Tunón et al., 1994)、食事だけでなくこれらの服用により血中濃度が高くなる可能性もある。Homostachydrine がヒトでけいれんを悪化させるかを結論付けるには食事やハーブによる homostachydrine の体内濃度の変化についても合わせて研究することが必要である。

ERGO は食事由来の抗酸化物質であり、きのこや腸内細菌によって合成される (Genghof and Damme, 1964; Genghof, 1970; Cheah and Halliwell, 2012)。ERGO は抗酸化作用を介してシスプラチンや β アミロイドによる細胞障害に対して保護作用を示すと考えられている (Song et al., 2010; Yang et al., 2012)。本研究で用いた ERGO の投与量はこれらの論文より高いことから、本研究で確認された長期 PTZ 投与における ERGO のけいれん抑制作用 (Fig.7) は、同様に抗酸化作用を介している可能性がある。一方で ERGO の投与により脳中 homostachydrine 濃度は低下しているため (Fig. 7F)、homostachydrine の低下がけいれんの抑制につながった可能性も考えられる。すなわち、ERGO は抗酸化作用だけでなく、homostachydrine 濃度を低下させるという二つのメカニズムでてんかんを抑制できる可能性がある。同じ抗酸化物質であるメラトニンは、非臨床、臨床で抗けいれん効果があることが示されている (Banach et al., 2011)(Goldberg-Stern et al., 2012)。メラトニンは比較的副作用が少ないものの、睡眠

に関する研究で頭痛や眠気の報告が確認されている(Boeve et al., 2003)。一方、ヒトにおける ERGO の投与においては今のところ副作用は報告されていない(Cheah et al., 2017)。動態の面ではメラトニンの半減期 30 分から 2 時間程度であるが(Harpsøe et al., 2015)、ERGO はマウスとヒトで極めて長時間血中に滞留することから、一度の服用で長い効果が期待できるかもしれない(Kato et al., 2010; Cheah et al., 2017)。

PTZ-induced kindling はてんかんの発症や進行過程である epileptogenesis を評価できるモデルであり、てんかん患者で見られる神経細胞の脱落や苔状繊維の異常発芽などが見られるため、ヒトのてんかんにより近いモデルと考えられている(Morimoto et al., 2004)(Becker, 2018)。Kindling では低投与量の PTZ 投与を繰り返すことで、けいれんを起こしやすい脳の構造を獲得する。本研究において、*Octn1*^{-/-} では単回投与と kindling の両方で、wild-type に比べけいれんの抑制が見られた(Figs. 1, 7)ため、OCTN1 はけいれんだけでなく epileptogenesis に関与する可能性がある。

ヒト *OCTN1* 遺伝子の SNPs として Caucasians に多く見られる L503F(allele frequency: 0.458)や Caucasians と日本人に多い I306T が知られている(Urban et al., 2007; Toh et al., 2013)。OCTN1 の SNPs では輸送活性が低下するものと上昇するものがあり、さらに SNPs によっては基質により輸送が変動する。たとえば L503F では ERGO や tetraethylammonium の取り込みに関する intrinsic clearance(V_{max}/K_m)は野生型 OCTN1 に比べて高くなる一方で、carnitine や gabapentin の取り込みの

intrinsic clearance は野生型に比べて小さくなる(Peltekova et al., 2004)。一方、I306T の ERGO 取り込みに関する intrinsic clearance は野生型と同程度だが gabapentin の取り込みの intrinsic clearance は野生型に比べ低下する(Futatsugi et al., 2016)。Homostachydrine の取り込み活性がこれらの多型によってどのような影響を受けるかについては未解明であるが、homostachydrine がけいれんを悪化させること(Fig. 6)や、ERGO が kindling を改善すること(Fig. 7)を考慮すれば、OCTN1 の SNPs がてんかんの症状にも影響を及ぼすかもしれない。

本研究において、*Octn1*^{-/-} ではけいれんや kindling が顕著に低い(Figs. 1, 7)ことから、OCTN1 の機能的な障害がこれらの症状を抑制できる可能性が示された。*Octn1*^{-/-} は通常の飼育環境下では明確なフェノタイプを示さないことから、OCTN1 の機能的な障害が劇的な副作用を引き起こす可能性は少ないと予想されるため、OCTN1 障害剤は抗てんかん薬として期待できる。一方で注意点として、OCTN1 の SNPs はクローン病との関係が示されていること(Peltekova et al., 2004)、*Octn1*^{-/-} では炎症性腸疾患モデルの症状を悪化させること(Shimizu et al., 2015)から、炎症性腸疾患を持つ患者に対しては避けた方がよいかもしれない。

結論として、OCTN1 の遺伝子欠損が PTZ によるけいれんを抑制することを示した。またそのメカニズムとして新規 OCTN1 基質 homostachydrine がけいれん増悪物質として働く可能性を示した。OCTN1 の基質かつ障害剤である ERGO が homostachydrine

濃度を低下させ、けいれんを抑制することを示した。今後 homostachydrine が PTZ によるけいれんを悪化させる詳細なメカニズムの解明と他のてんかんモデルを用いた解析を行うことによって、OCTN1 が治療標的となりうるかについて検討する必要がある。

引用文献

Banach M, Gurdziel E, Jédrych M, Borowicz KK (2011) Melatonin in experimental seizures and epilepsy.

Becchetti A, Aracri P, Meneghini S, Brusco S, Amadeo A (2015) The role of nicotinic acetylcholine receptors in autosomal dominant nocturnal frontal lobe epilepsy. *Front Physiol* 6:22.

Becker AJ (2018) Review: Animal models of acquired epilepsy: insights into mechanisms of human epileptogenesis. *Neuropathol Appl Neurobiol* 44:112–129.

Beghi E et al. (2019) Global, regional, and national burden of epilepsy, 1990–2016: a systematic analysis for the Global Burden of Disease Study 2016. *Lancet Neurol* 18:357–375.

Boeve BF, Silber MH, Ferman TJ (2003) Melatonin for treatment of REM sleep behavior disorder in neurologic disorders: Results in 14 patients. *Sleep Med* 4:281–284.

Bozzi Y, Provenzano G, Casarosa S (2018) Neurobiological bases of autism-epilepsy comorbidity: a focus on excitation/inhibition imbalance. *Eur J Neurosci* 47:534–548.

Cheah IK, Halliwell B (2012) Ergothioneine; antioxidant potential, physiological function and role in disease. *Biochim Biophys Acta - Mol Basis Dis* 1822:784–793.

Cheah IK, Tang RMY, Yew TSZ, Lim KHC, Halliwell B (2017) Administration of Pure

- Ergothioneine to Healthy Human Subjects: Uptake, Metabolism, and Effects on Biomarkers of Oxidative Damage and Inflammation. *Antioxid Redox Signal* 26:193–206.
- Derkach A, Sampson J, Joseph J, Playdon MC, Stolzenberg-Solomon RZ (2017) Effects of dietary sodium on metabolites: The Dietary Approaches to Stop Hypertension (DASH)–Sodium Feeding Study. *Am J Clin Nutr* 106:1131–1141.
- Drenberg CD, Gibson AA, Pounds SB, Shi L, Rhinehart DP, Li L, Hu S, Du G, Nies AT, Schwab M, Pabla N, Blum W, Gruber TA, Baker SD, Sparreboom A (2017) OCTN1 Is a High-Affinity Carrier of Nucleoside Analogues. *Cancer Res* 77:2102–2111.
- Feigenbaum P, Chang Y (1986) Pipecolic acid antagonizes barbiturate-enhanced GABA binding to bovine brain membranes. *J Neurochem* 46:176–179.
- Freitas DFRM (2010) The Effects of Alpha-Tocopherol on Hippocampal Oxidative Stress Prior to in Pilocarpine-Induced Seizures. *Neurosci Lett* 478:580–587.
- Futatsugi A, Masuo Y, Kawabata S, Nakamichi N, Kato Y (2016) L503F variant of carnitine/organic cation transporter 1 efficiently transports metformin and other biguanides. *J Pharm Pharmacol* 68:1160–1169.
- Genghof DS (1970) Biosynthesis of Ergothioneine and Hercynine by Fungi and Actinomycetales.

- Genghof DS, Damme O Van (1964) BIOSYNTHESIS OF ERGOTHIONEINE AND HERCYNINE BY MYCOBACTERIA. Available at: <http://jb.asm.org/> [Accessed June 30, 2020].
- Goldberg-Stern H, Oren H, Peled N, Garty B-Z (2012) Effect of melatonin on seizure frequency in intractable epilepsy: a pilot study. *J Child Neurol* 27:1524–1528.
- Grigat S, Harlfinger S, Pal S, Striebinger R, Golz S, Geerts A, Lazar A, Schömig E, Gründemann D (2007) Probing the substrate specificity of the ergothioneine transporter with methimazole, hercynine, and organic cations. *Biochem Pharmacol* 74:309–316.
- Gründemann D, Harlfinger S, Golz S, Geerts A, Lazar A, Berkels R, Jung N, Rubbert A, Schömig E (2005) Discovery of the ergothioneine transporter. *Proc Natl Acad Sci U S A* 102:5256–5261.
- Guertin KA, Moore SC, Sampson JN, Huang W-Y, Xiao Q, Stolzenberg-Solomon RZ, Sinha R, Cross AJ (2014) Metabolomics in nutritional epidemiology: identifying metabolites associated with diet and quantifying their potential to uncover diet-disease relations in populations. *Am J Clin Nutr* 100:208–217.
- Gutierrez CM, Delgado-coello BA (1989) Influence of Pipecolic Acid on the Release and Uptake of [3H] GABA from Brain Slices of Mouse Cerebral Cortex. 14:405–408.

- Harpsøe NG, Andersen LPH, Gögenur I, Rosenberg J (2015) Clinical pharmacokinetics of melatonin: A systematic review. *Eur J Clin Pharmacol* 71:901–909.
- Hussein A, Adel M, El-Mesery M, Abbas K, Ali A, Abulseoud O (2018) l-Carnitine Modulates Epileptic Seizures in Pentylene-tetrazole-Kindled Rats via Suppression of Apoptosis and Autophagy and Upregulation of Hsp70. *Brain Sci* 8:45.
- Ishimoto T, Nakamichi N, Hosotani H, Masuo Y, Sugiura T, Kato Y (2014) Organic cation transporter-mediated ergothioneine uptake in mouse neural progenitor cells suppresses proliferation and promotes differentiation into neurons. *PLoS One* 9.
- Ishimoto T, Nakamichi N, Nishijima H, Masuo Y, Kato Y (2018) Carnitine/Organic Cation Transporter OCTN1 Negatively Regulates Activation in Murine Cultured Microglial Cells. *Neurochem Res* 43:107–119.
- Kärkkäinen O, Lankinen MA, Vitale M, Jokkala J, Leppänen J, Koistinen V, Lehtonen M, Giacco R, Rosa-Sibakov N, Micard V, Rivellese AAA, Schwab U, Mykkänen H, Uusitupa M, Kolehmainen M, Riccardi G, Poutanen K, Auriola S, Hanhineva K (2018) Diets rich in whole grains increase betainized compounds associated with glucose metabolism. *Am J Clin Nutr* 108:971–979.
- Kato Y, Kubo Y, Iwata D, Kato S, Sudo T, Sugiura T, Kagaya T, Wakayama T, Hirayama A, Sugimoto M, Sugihara K, Kaneko S, Soga T, Asano M, Tonuta M, Matsui T, Wada M,

- Tsuji A (2010) Gene knockout and metabolome analysis of carnitine/organic cation transporter OCTN1. *Pharm Res* 27:832–840.
- Koch H, Weber YG (2019) The glucose transporter type 1 (Glut1) syndromes. *Epilepsy Behav* 91:90–93.
- Kumar M, Kumar P (2017) Protective effect of spermine against pentylenetetrazole kindling epilepsy induced comorbidities in mice. *Neurosci Res* 120:8–17.
- Magalhães PHM, Moraes HT, Athie MC, Secolin R, Lopes-cendes I (2019) *Epilepsy & Behavior* New avenues in molecular genetics for the diagnosis and application of therapeutics to the epilepsies. *Epilepsy Behav*.
- Mangalam A, Poisson L, Nemutlu E, Datta I, Denic A, Dzeja P, Rodriguez M, Rattan R, Giri S (2013) Profile of Circulatory Metabolites in an Animal Model of Multiple Sclerosis using Global Metabolomics. *J Clin Cell Immunol* 04.
- Masuo Y, Ohba Y, Yamada K, Al-Shammari AH, Seba N, Nakamichi N, Ogihara T, Kunishima M, Kato Y (2018) Combination Metabolomics Approach for Identifying Endogenous Substrates of Carnitine/Organic Cation Transporter OCTN1. *Pharm Res* 35.
- Matsuda Y, Ozawa N, Shinozaki T, Suzuki K, Kawano Y, Ohtsu I, Tatebayashi Y (2020) Ergothioneine, a metabolite of the gut bacterium *Lactobacillus reuteri*, protects against

stress-induced sleep disturbances. *bioRxiv*:1–11.

Mattison KA, Butler KM, Inglis GAS, Dayan O, Boussidan H, Bhambhani V, Philbrook B, da Silva C, Alexander JJ, Kanner BI, Escayg A (2018) SLC6A1 variants identified in epilepsy patients reduce γ -aminobutyric acid transport. *Epilepsia* 59:e135–e141.

Mizoguchi H, Nakade J, Tachibana M, Ibi D, Someya E, Koike H, Kamei H, Nabeshima T, Itohara S, Takuma K, Sawada M, Sato J, Yamada K (2011) Matrix metalloproteinase-9 contributes to kindled seizure development in pentylenetetrazole-treated mice by converting pro-BDNF to mature BDNF in the hippocampus. *J Neurosci* 31:12963–12971.

Morimoto K, Fahnstock M, Racine RJ (2004) Kindling and status epilepticus models of epilepsy: Rewiring the brain. *Prog Neurobiol* 73:1–60.

Nakamichi N, Nakao S, Nishiyama M, Takeda Y, Ishimoto T, Masuo Y, Matsumoto S, Suzuki M, Kato Y (2020) Oral administration of the food derived hydrophilic antioxidant ergothioneine enhances object recognition memory in mice. *Curr Mol Pharmacol* 13:1–15.

Nakamichi N, Nakayama K, Ishimoto T, Masuo Y, Wakayama T, Sekiguchi H, Sutoh K, Usumi K, Iseki S, Kato Y (2016) Food-derived hydrophilic antioxidant ergothioneine is distributed to the brain and exerts antidepressant effect in mice. *Brain Behav* 6.

Nakamichi N, Taguchi T, Hosotani H, Wakayama T, Shimizu T, Sugiura T, Iseki S, Kato Y

(2012) Functional expression of carnitine/organic cation transporter OCTN1 in mouse brain neurons: Possible involvement in neuronal differentiation. *Neurochem Int* 61:1121–1132.

Nina H, Lizer MH, Kidd RS (2011) Evaluation of Genetic Variations in Organic Cationic Transporter 3 in Depressed and Nondepressed Subjects. *ISRN Pharmacol* 2011.

Pearson-smith JN, Patel M (2017) Metabolic Dysfunction and Oxidative Stress in Epilepsy. :1–13.

Pelteková VD, Wintle RF, Rubin LA, Amos CI, Huang Q, Gu X, Newman B, Van Oene M, Cescon D, Greenberg G, Griffiths AM, St. George-Hyslop PH, Siminovitch KA (2004) Functional variants of OCTN cation transporter genes are associated with Crohn disease. *Nat Genet* 36:471–475.

Picot MC, Baldy-Moulinier M, Daurès JP, Dujols P, Crespel A (2008) The prevalence of epilepsy and pharmaco-resistant epilepsy in adults: A population-based study in a Western European country. *Epilepsia* 49:1230–1238.

Plecko B, Hikel C, Korenke GC, Schmitt B, Baumgartner M, Baumeister F, Jakobs C, Struys E, Erwa W, Stöckler-Ipsiroglu S (2005) Pihcolic acid as a diagnostic marker of pyridoxine-dependent epilepsy. *Neuropediatrics* 36:200–205.

- Plecko B, Stöckler - Ipsiroglu S, Paschke E, Erwa W, Struys EA, Jakobs C (2000) Pipecolic acid elevation in plasma and cerebrospinal fluid of two patients with pyridoxine - dependent epilepsy. *Ann Neurol* 48:121–125.
- Pochini L, Scalise M, Galluccio M, Indiveri C (2012a) Regulation by physiological cations of acetylcholine transport mediated by human OCTN1 (SLC22A4). Implications in the non-neuronal cholinergic system. *Life Sci* 91:1013–1016.
- Pochini L, Scalise M, Galluccio M, Pani G, Siminovitch KA, Indiveri C (2012b) The human OCTN1 (SLC22A4) reconstituted in liposomes catalyzes acetylcholine transport which is defective in the mutant L503F associated to the Crohn's disease. *Biochim Biophys Acta - Biomembr* 1818:559–565.
- Servillo L, D'Onofrio N, Giovane A, Casale R, Cautela D, Ferrari G, Castaldo D, Balestrieri ML (2018) The betaine profile of cereal flours unveils new and uncommon betaines. *Food Chem* 239:234–241.
- Servillo L, Giovane A, Balestrieri ML, Ferrari G, Cautela D, Castaldo D (2012) Occurrence of pipecolic acid and pipecolic acid betaine (homostachydrine) in Citrus genus plants. *J Agric Food Chem* 60:315–321.
- Shimizu T, Masuo Y, Takahashi S, Nakamichi N, Kato Y (2015) Organic cation transporter Octn1-mediated uptake of food-derived antioxidant ergothioneine into infiltrating

- macrophages during intestinal inflammation in mice. *Drug Metab Pharmacokinet* 30:231–239.
- Song T-Y, Chen C-L, Liao J-W, Ou H-C, Tsai M-S (2010) Ergothioneine protects against neuronal injury induced by cisplatin both in vitro and in vivo. *Food Chem Toxicol* 48:3492–3499.
- Song TY, Lin HC, Chen CL, Wu JH, Liao JW, Hu ML (2014) Ergothioneine and melatonin attenuate oxidative stress and protect against learning and memory deficits in C57BL/6J mice treated with D-galactose. In: *Free Radical Research*, pp 1049–1060. Informa Healthcare.
- Takagi T, Bungo T, Tachibana T, Saito E-S, Saito S, Yamasaki I, Tomonaga S, Denbow DM, Furuse M (2003) Intracerebroventricular administration of GABA-A and GABA-B receptor antagonists attenuate feeding and sleeping-like behavior induced by L-pipecolic acid in neonatal chicks. *J Neurosci Res* 73:270–275.
- Takahama K, Miyata T, Okano Y, Kataoka M, Hitoshi T, Kasé Y (1982) Potentiation of phenobarbital-induced anticonvulsant activity by pipecolic acid. *Eur J Pharmacol* 81:327–331.
- Tamai I, Ohashi R, Nezu JI, Sai Y, Kobayashi D, Oku A, Shimane M, Tsuji A (2000) Molecular and functional characterization of organic cation/carnitine transporter

family in mice. *J Biol Chem* 275:40064–40072.

Tamai I, Yabuuchi H, Nezu JI, Sai Y, Oku A, Shimane M, Tsuji A (1997) Cloning and characterization of a novel human pH-dependent organic cation transporter, OCTN1. *FEBS Lett* 419:107–111.

Taubert D, Grimberg G, Stenzel W, Schömig E (2007) Identification of the Endogenous Key Substrates of the Human Organic Cation Transporter OCT2 and Their Implication in Function of Dopaminergic Neurons Raible D, ed. *PLoS One* 2:e385.

Thomas RH, Berkovic SF (2014) The hidden genetics of epilepsy - A clinically important new paradigm. *Nat Rev Neurol* 10:283–292.

Tian N, Boring M, Kobau R, Zack MM, Croft JB (2018) Active Epilepsy and Seizure Control in Adults — United States, 2013 and 2015. *MMWR Morb Mortal Wkly Rep* 67:437–442.

Toh DSL, Cheung FSG, Murray M, Pern TK, Lee EJD, Zhou F (2013) Functional Analysis of Novel Variants in the Organic Cation/Ergothioneine Transporter 1 Identified in Singapore Populations. *Mol Pharm* 10:2509–2516.

Tunón H, Thorsell W, Bohlin L (1994) Mosquito repelling activity of compounds occurring in *Achillea millefolium* L. (asteraceae). *Econ Bot* 48:111–120.

Tuomainen M, Kärkkäinen O, Leppänen J, Auriola S, Lehtonen M, Savolainen MJ, Hermansen K, Risérus U, Åkesson B, Thorsdottir I, Kolehmainen M, Uusitupa M,

- Poutanen K, Schwab U, Hanhineva K (2019) Quantitative assessment of betainized compounds and associations with dietary and metabolic biomarkers in the randomized study of the healthy Nordic diet (SYSDIET). *Am J Clin Nutr* 110:1108–1118.
- Urban T, Brown C, Castro R, Shah N, Mercer R, Huang Y, Brett C, Burchard E, Giacomini K (2008) Effects of Genetic Variation in the Novel Organic Cation Transporter, OCTN1, on the Renal Clearance of Gabapentin. *Clin Pharmacol Ther* 83:416–421.
- Urban TJ, Yang C, Lagpacan LL, Brown C, Castro RA, Taylor TR, Huang CC, Stryke D, Johns SJ, Kawamoto M, Carlson EJ, Ferrin TE, Burchard EG, Giacomini KM (2007) Functional effects of protein sequence polymorphisms in the organic cation/ergothioneine transporter OCTN1 (SLC22A4). *Pharmacogenet Genomics* 17:773–782.
- Wiehler G, Marion L (1958) (—)-HOMOSTACHYDRINE, A NEW ALKALOID ISOLATED FROM THE SEEDS OF MEDICAGO SATIVA L. GRIMM. *Can J Chem* 36:339–343.
- Wood K V., Stringham KJ, Smith DL, Volenec JJ, Hendershot KL, Jackson KA, Rich PJ, Yang WJ, Rhodes D (1991) Betaines of alfalfa: Characterization by fast atom bombardment and desorption chemical ionization mass spectrometry. *Plant Physiol* 96:892–897.
- Wultsch T, Grimberg ÆG, Schmitt ÆA, Painsipp ÆE, Wetzstein H, Frauke ÆA,

Breitenkamp S, Gru \AA ED, Lesch \AA EK, Gerlach \AA EM, Reif \AA EA (2009) Decreased anxiety in mice lacking the organic cation transporter 3. :689–697.

Yang J, Yan B, Zhao B, Fan Y, He X, Yang L, Ma Q, Zheng J, Wang W, Bai L, Zhu F, Ma X (2020) Assessing the Causal Effects of Human Serum Metabolites on 5 Major Psychiatric Disorders. *Schizophr Bull*:1–10.

Yang NC, Lin HC, Wu JH, Ou HC, Chai YC, Tseng CY, Liao JW, Song TY (2012) Ergothioneine protects against neuronal injury induced by β -amyloid in mice. *Food Chem Toxicol* 50:3902–3911.

Yung-Feng Chang, Hargest V, Jing-Shyong Chen (1988) Modulation of benzodiazepine by lysine and pipercolic acid on pentylenetetrazol-induced seizures. *Life Sci* 43:1177–1188.

Fig.1

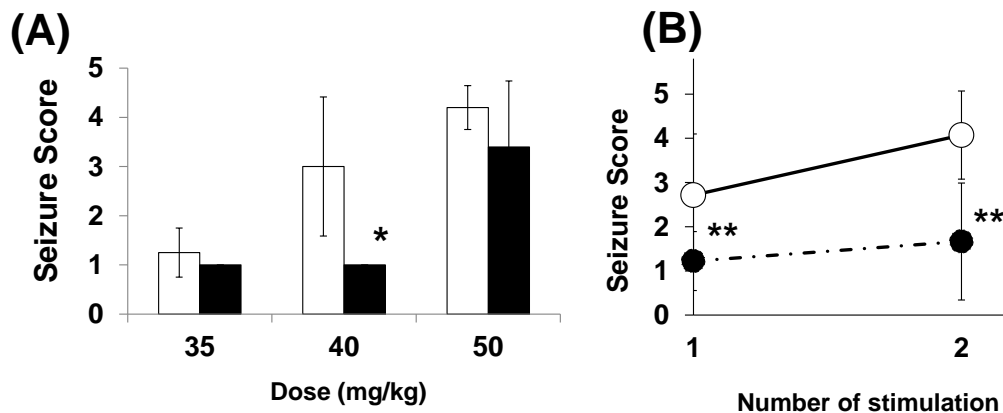


Fig. 1 Difference in PTZ-induced acute seizure between wild-type and *Octn1*^{-/-}

Octn1^{-/-}

(A) Wild-type and *Octn1*^{-/-} *Octn1*^{-/-} mice were administered a single intraperitoneal injection of PTZ at a dose of 35, 40, and 50 mg/kg. Open column shows wild-type and closed column shows *Octn1*^{-/-} mice. Each mouse was observed for 20 min after administration, and severity of seizure was evaluated according to following criteria: Stage 0: No behavioral change; Stage 1: Hypoactivity and immobility; Stage 2: Two or more isolated, myoclonic jerks; Stage 3: Generalized clonic convulsions, with preservation of righting reflex; Stage 4: Generalized clonic or tonic-clonic convulsions with loss of righting reflex; Stage 5: Death. Each value represents the mean \pm S.D.

(n=4-5) *, Significant different from wild-type ($p < 0.05$).

(B) Wild-type and *Octn1*^{-/-} *Octn1*^{-/-} mice were administered PTZ at a dose of 45

mg/kg twice with 48 h interval. Seizure score was evaluated in a same manner as the single PTZ administration study after each injection. Each value represents the mean \pm S.D. (n=9-14) **, Significantly different from wild-type (p<0.01).

Fig.2

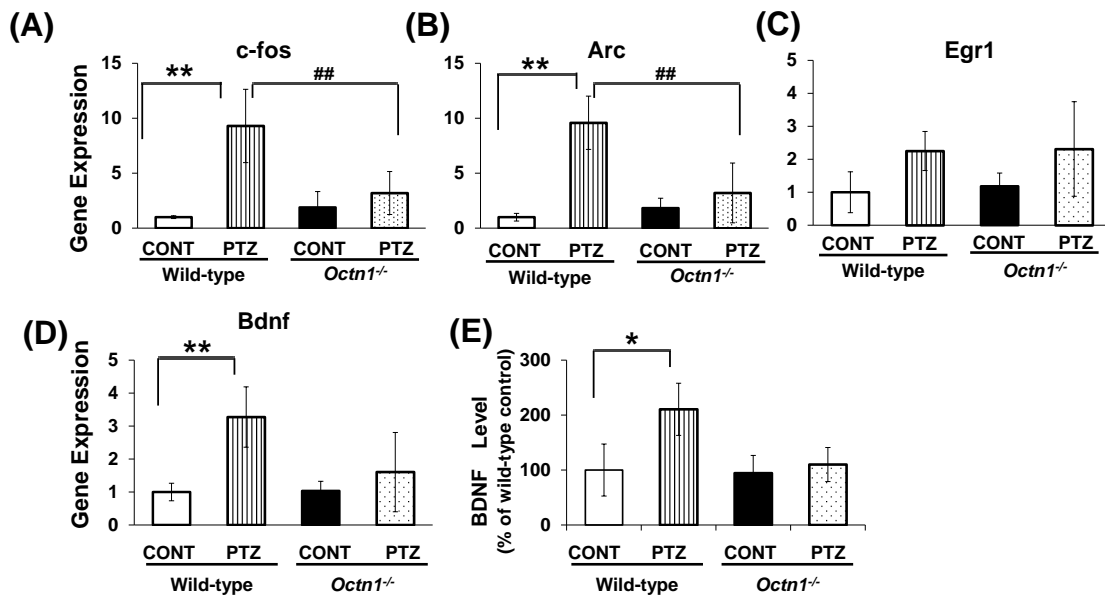


Fig. 2 mRNA expression of genes and protein related to neuronal excitability in hippocampus after PTZ treatment

(A-D) Wild-type and *Octn1*^{-/-} mice were administered saline or PTZ at a dose of 45 mg/kg twice with 48 h interval. Two hours after second PTZ injection, hippocampus was collected for RT-PCR, and mRNA expression of neuronal excitation-related genes were evaluated. Open column shows wild-type with saline, stripe column shows wild-type with PTZ, closed column shows *Octn1*^{-/-} with saline, and dot column shows *Octn1*^{-/-} with PTZ. Expression of mRNA was normalized to that of housekeeping gene 36B4. Each value represents the mean \pm S.D. (n=3-8) **; Significantly different from wild-type control (p < 0.01). ##; Significantly different from PTZ treated wild-type (p < 0.01).

(E) Mice were administered PTZ at a dose of 45 mg/kg twice with 48 h interval. Four hours after second PTZ injection, hippocampus was collected for ELISA, and expression of BDNF protein was measured. Each value represents the mean \pm S.D. (n=3-4) *, Significantly different from wild-type ($p < 0.05$).

Fig.3

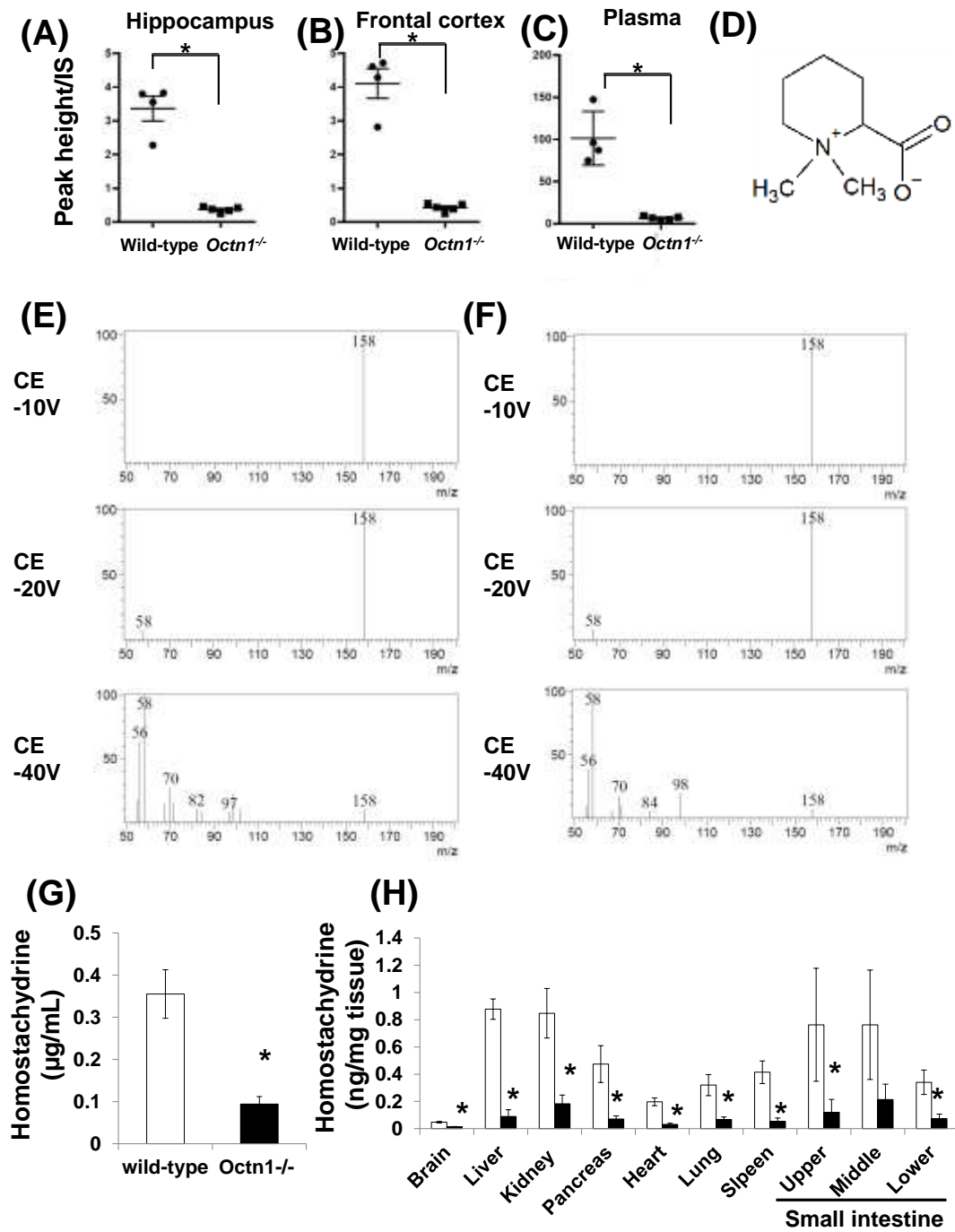


Fig. 3 Identification of homostachydrine as an in vivo substrate of OCTN1

Wild-type and *Octn1*^{-/-} mice were kept in the same cage for one week. Lysates of hippocampus, cortex, and plasma were subjected to LC-TOF-MS, identifying one ion peak at m/z 158.118

(A-C) m/z 158.118 was significantly lower in hippocampus (A), frontal cortex (B), and plasma (C) of *Octn1*^{-/-}. Each point represents each mouse. *; p<0.05 significantly different from wild-type mice.

(D) Structure of homostachydrine

(E-F) Product ion scanning against m/z 158.00 was performed in chemically synthesized homostachydrine (D) and plasma sample (E) with various collision energy from -10 to -40 V.

(G-H) Homostachydrine concentration in plasma (F) and various tissues (G) of wild-type and *Octn1*^{-/-} mice. Each value represents the mean ± S.D. (n=3-4) *; Significantly different from wild-type (p < 0.05).

Fig.4

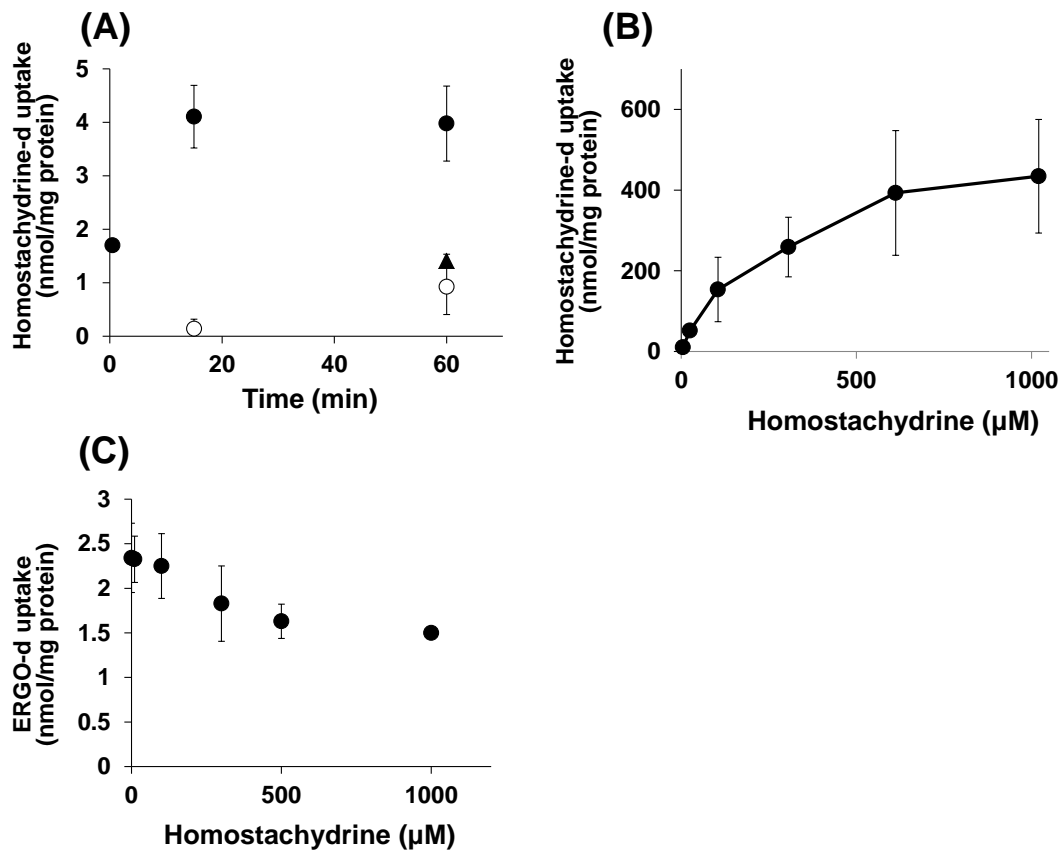


Fig.4 hOCTN1-mediated homostachydrine uptake in HEK293/hOCTN1 cells

(A) HEK293/hOCTN1 and HEK293/mock cells were incubated with the buffer containing 10 μM homostachydrine-d with or without 500 μM ERGO at 37°C. Cells were then washed with ice-cold buffer, and uptake of homostachydrine-d in the cells was measured by LC-MS/MS. Open circle shows HEK293/mock with homostachydrine, closed circle shows HEK293/hOCTN1 with homostachydrine, closed triangle shows HEK293/hOCTN1 with homostachydrine and ERGO. Each

value represents the mean \pm S.D. (n = 3)

(B) HEK293/hOCTN1 cells were incubated with the buffer containing various concentration of homostachydrine-d for 15 s at 37 °C , and uptake of homostachydrine-d was measured. Each value represents the mean \pm S.D. (n = 3)

(C) HEK293/hOCTN1 cells were incubated with the buffer containing ERGO-d and various concentration of homostachydrine for 5 min at 37 °C . Each points represents the mean \pm S.D. (n = 3)

Fig.5

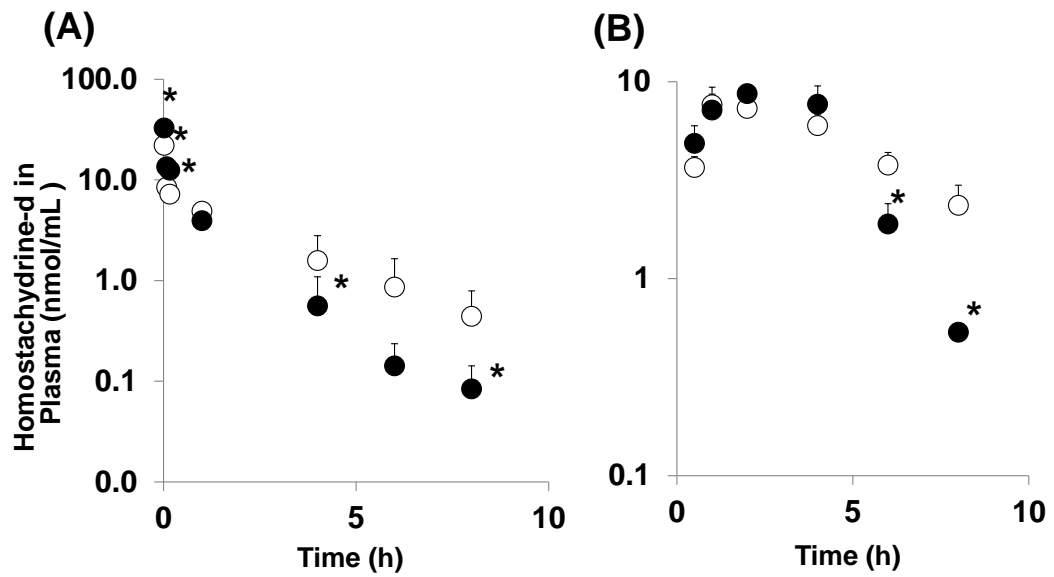


Fig.5 Plasma concentration profile of homostachydrine-d after intravenous

(A) and oral (B) administration

Homostachydrine-d was intravenously (A) and orally (B) administered to wild-type and *Octn1*^{-/-} mice at a dose of 1 and 3 mg/kg, respectively. Plasma homostachydrine-d concentration was measured by LC-MS/MS. Each circle represents the mean \pm S.D. (n = 3 - 5), *; Significantly different from wild-type (p < 0.05).

Table 1 Pharmacokinetic parameters of homostachydrine^a

		Dose	C _{max}	AUC	T _{1/2}	CL _{tot}	Vd ₀	Vd _{ss}	BA
		mg/kg	µg/mL	µg/mg · hr	hr	L/hr/kg	L/kg	L/kg	%
Wild-type	i.v.	1	-	3.58 ±1.29	2.15 ± 0.26	0.307 ± 0.098	0.332 ± 0.140	0.649 ± 0.144	77.8
	p.o.	3	1.29 ± 0.25	8.35 ± 1.16	3.05 ± 0.75	-	-	-	
<i>Octn1</i> ^{-/-}	i.v.	1	-	2.91 ± 0.87	1.70 ± 0.51	0.368 ± 0.103	0.204 ± 0.033	0.346 ± 0.058*	77.3
	p.o.	3	1.42 ± 0.16	6.74 ± 1.01	1.05 ± 0.08*	-	-	-	

a: Mean ± S.D. (n = 5 and 3 for intravenous and oral administration, respectively).

*; significantly difference from wild-type (p<0.05)

Table 2 Urinary excretion of homostachydrine-d^{a)}

		Homostachydrine-d	Cephalexin
i.v.	wild-type	71.4 ± 14.2	49.8 ± 19.8
	<i>Octn1</i> ^{-/-}	69.8 ± 12.7	51.9 ± 8.2
p.o.	wild-type	65.3 ± 6.5	58.2 ± 10.9
	<i>Octn1</i> ^{-/-}	52.2 ± 4.4	48.1 ± 6.8*

a) Mean ± S.D. (n = 5 and 3 for wild-type and *Octn1*^{-/-}, respectively).

*; Significantly different from wild-type (p<0.05)

Fig.6

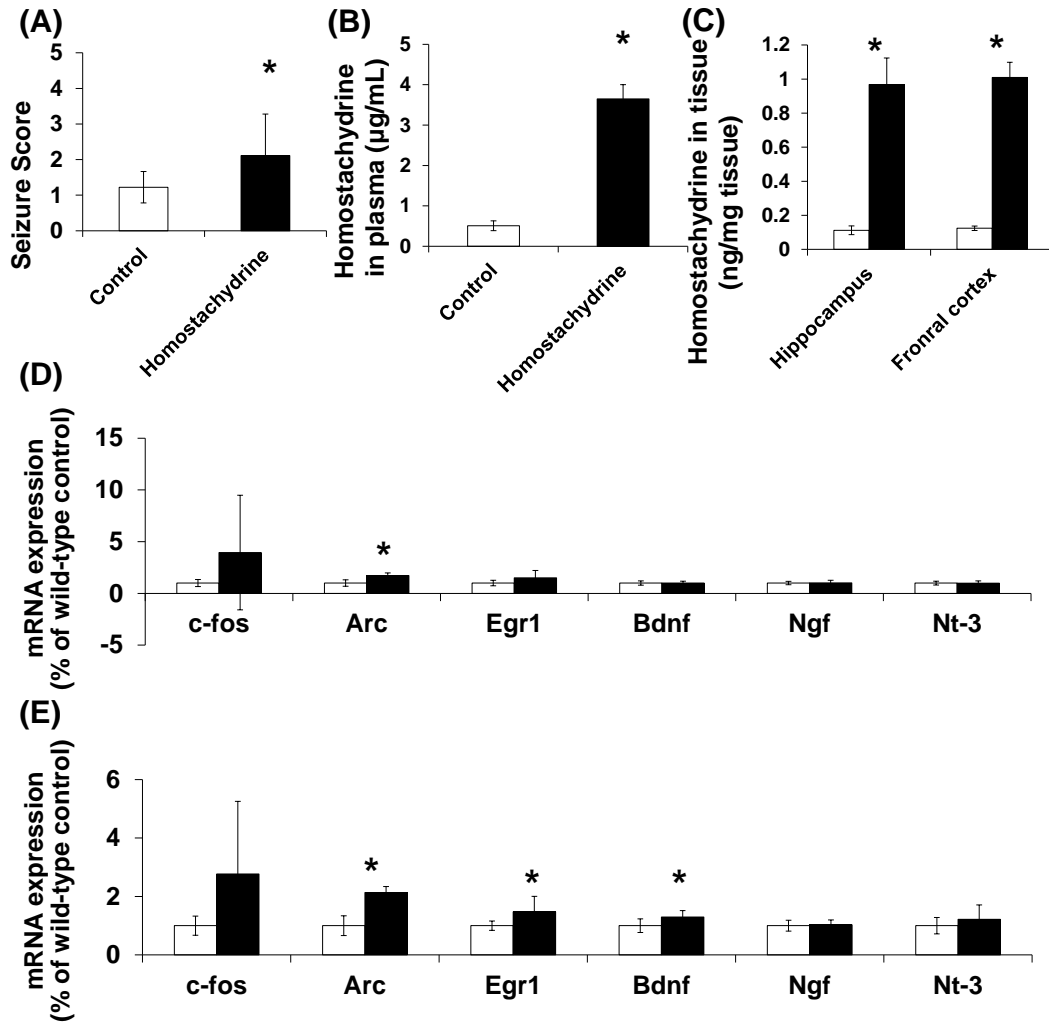


Fig. 6 Stimulative effect of homostachydrine on PTZ-induced acute seizure

(A) Mice were intravenously administered 50 mg/kg homostachydrine, followed by intraperitoneal administration of 40 mg/kg PTZ at 4 h after the homostachydrine administration. Mice were then observed for 20 min, and seizure severity was evaluated. Each value represents the mean \pm S.D. (n = 9) *;Significantly different

from control ($p < 0.05$).

(B-C) After the observation, hippocampus (C) and frontal cortex (D) was collected , and mRNA expression of neuronal excitation-related genes were evaluated. Open

column shows control and closed column shows homostachydrine-treated group.

Each value represents the mean \pm S.D. (n = 9) *; Significantly different from control

($p < 0.05$).

Fig.7

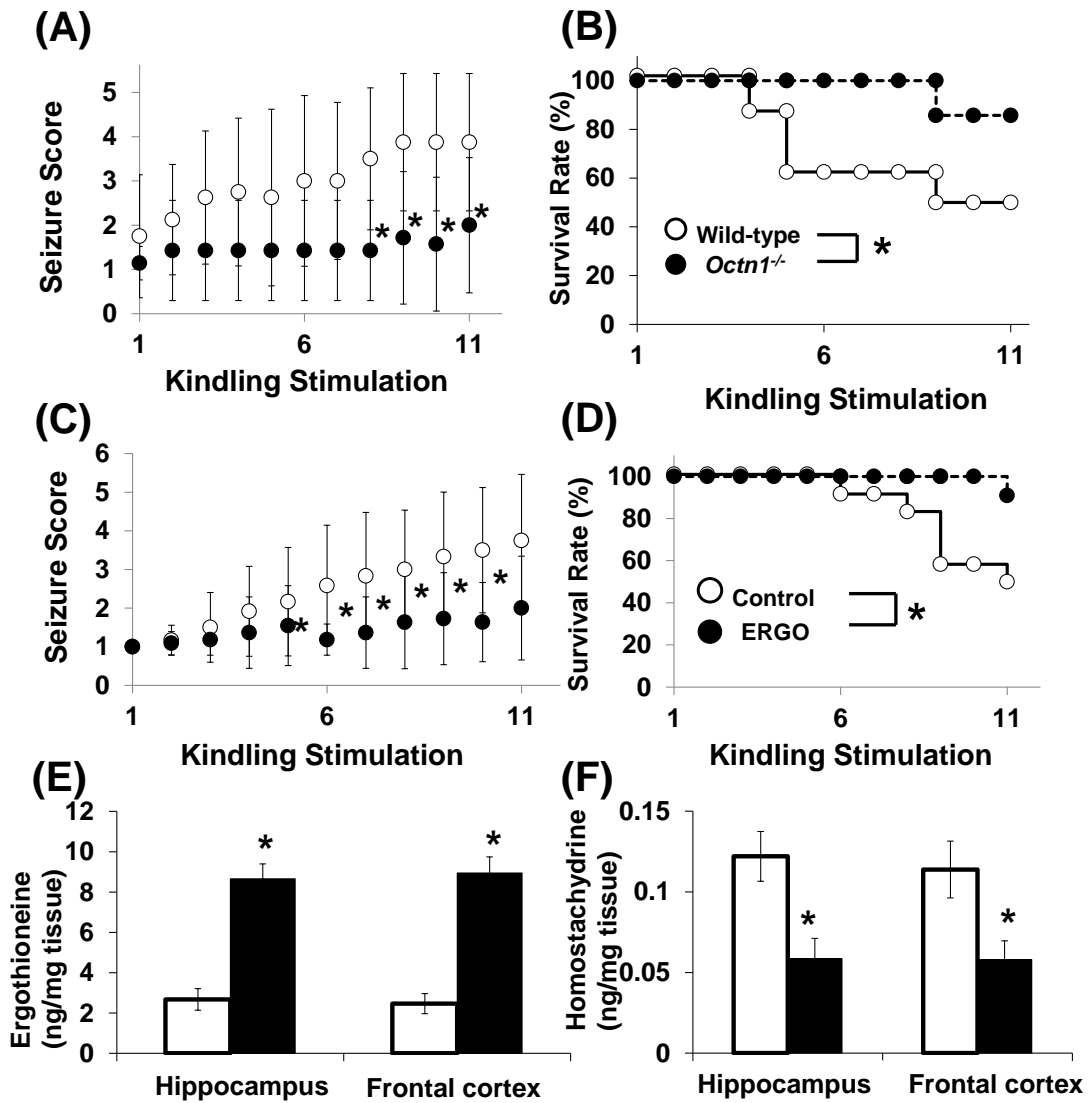


Fig.7 Effect of OCTN1 and ERGO on chronic PTZ administration

(A-B) Wild-type and *Octn1*^{-/-} mice were administered PTZ at a dose of 35 mg/kg intraperitoneally total 11 times with 48 h interval. Mice were observed for 20 min after each administration to evaluate seizure severity (A). When mouse died during chronic administration, the score of the corresponding mouse was regarded five in

the subsequent trial. Survival rate was also recorded (B). Open circle shows wild-type and closed circle shows *Octn1*^{-/-} mice. Each value represents the mean \pm S.D. (n = 7 - 8) *; Significantly different from wild-type (p < 0.05).

(C-F) Mice were administered water or ERGO at a dose of 50 mg/kg orally every day for one week. At day 8, PTZ administration was started while daily ERGO administration was continued. Open circle shows control and closed circle shows ERGO-treated group. Mice were observed for 20 min after each PTZ administration to evaluate seizure severity (C). Survival rate was also recorded (D). After 11th administration of PTZ, hippocampus and frontal cortex were collected, and concentration of ERGO (E) and homostachydrine (F) was measured using LC-MS/MS. Each value represents the mean \pm S.D. (n = 3 - 6) *; Significantly different from control (p < 0.05).

謝辞

本研究に関して、種々の有益な御指導と御助言ならびに御協力戴きました金沢大学医薬保健研究域（薬学系）分子薬物治療学研究室 加藤 将夫 教授に厚く感謝の意を表します。

また、本研究に関して、終始御懇篤なる御指導・御鞭撻を賜りました金沢大学医薬保健研究域（薬学系）分子薬物治療学研究室 中道 範隆 准教授（現高崎健康福祉大学教授）に謹んで謝意を表します。

さらに、本研究に関して、御指導と御助言を戴きました金沢大学医薬保健研究域（薬学系）分子薬物治療学研究室 増尾 友佑 助教に深く感謝の意を表します。

また、本研究に関して、ご指導を頂きました金沢大学医薬保健研究域（薬学系）荒川 大 助教に感謝致します。

また、本研究に関して、共同研究ならびに御助言をいただきました金沢大学医薬保健研究域（薬学系）機能性分子合成学 吉村 智之 准教授に深く感謝致します。

また、日々の研究生生活において、有益な討論を行って頂きました分子薬物治療学研究室の諸氏に感謝致します。さらに、研究を滞りなく遂行できるよう御協力頂いた石田 利佳 技術員に感謝致します。

そして、本研究に関わる実験の遂行のために用いた数多くの動物たちに深く感謝する

とともに、御冥福をお祈り致します。

最後に、有意義な学生生活を送る上で経済的、精神的に支えて戴いた両親並びに妹
弟に深く感謝致します。

参考論文

金沢大学大学院医薬保健学総合研究科
創薬科学専攻
分子薬物治療学研究室

西山 美沙

Homostachydrine is a Xenobiotic Substrate of OCTN1/SLC22A4 and Potentially Sensitizes Pentylentetrazole-Induced Seizures in Mice

Misa Nishiyama, Noritaka Nakamichi, Tomoyuki Yoshimura, Yusuke Masuo, Tomoe Komori, Takahiro Ishimoto, Jun-ichi Matsuo, et al.

Neurochemical Research

ISSN 0364-3190

Volume 45

Number 11

Neurochem Res (2020) 45:2664-2678

DOI 10.1007/s11064-020-03118-8

Your article is protected by copyright and all rights are held exclusively by Springer Science+Business Media, LLC, part of Springer Nature. This e-offprint is for personal use only and shall not be self-archived in electronic repositories. If you wish to self-archive your article, please use the accepted manuscript version for posting on your own website. You may further deposit the accepted manuscript version in any repository, provided it is only made publicly available 12 months after official publication or later and provided acknowledgement is given to the original source of publication and a link is inserted to the published article on Springer's website. The link must be accompanied by the following text: "The final publication is available at link.springer.com".



Homostachydrine is a Xenobiotic Substrate of OCTN1/SLC22A4 and Potentially Sensitizes Pentylentetrazole-Induced Seizures in Mice

Misa Nishiyama¹ · Noritaka Nakamichi^{1,2} · Tomoyuki Yoshimura¹ · Yusuke Masuo¹ · Tomoe Komori¹ · Takahiro Ishimoto¹ · Jun-ichi Matsuo¹ · Yukio Kato¹

Received: 23 July 2020 / Revised: 10 August 2020 / Accepted: 15 August 2020 / Published online: 26 August 2020
© Springer Science+Business Media, LLC, part of Springer Nature 2020

Abstract

Understanding of the underlying mechanism of epilepsy is desired since some patients fail to control their seizures. The carnitine/organic cation transporter OCTN1/SLC22A4 is expressed in brain neurons and transports food-derived antioxidant ergothioneine (ERGO), L-carnitine, and spermine, all of which may be associated with epilepsy. This study aimed to clarify the possible association of this transporter with epileptic seizures. In both pentylentetrazole (PTZ)-induced acute seizure and kindling models, *ocnt1* gene knockout mice (*ocnt1*^{-/-}) showed lower seizure scores compared with wild-type mice. Up-regulation of the epilepsy-related genes, *c-fos* and *Arc*, and the neurotrophic factor BDNF following PTZ administration was observed in the hippocampus of wild-type, but not *ocnt1*^{-/-} mice. To find the OCTN1 substrate associated with the seizure, untargeted metabolomics analysis using liquid chromatography–quadrupole time-of-flight mass spectrometry was conducted on extracts from the hippocampus, frontal cortex, and plasma of both strains, leading to the identification of a plant alkaloid homostachydrine as a compound present in a lower concentration in *ocnt1*^{-/-} mice. OCTN1-mediated uptake of deuterium-labeled homostachydrine was confirmed in OCTN1-transfected HEK293 cells, suggesting that this compound is a substrate of OCTN1. Homostachydrine administration increased PTZ-induced acute seizure scores and the expression of *Arc* in the hippocampus and that of *Arc*, *Egr1*, and BDNF in the frontal cortex. Conversely, administration of the OCTN1 substrate/inhibitor ERGO inhibited PTZ-induced kindling and reduced the plasma homostachydrine concentration. Thus, these results suggest that OCTN1 is at least partially associated with PTZ-induced seizures, which is potentially deteriorated by treatment with homostachydrine, a newly identified food-derived OCTN1 substrate.

Keywords Epilepsy · Ergothioneine · Metabolomics · Pentylentetrazole · Seizure · Slc22a4

Introduction

Epilepsy is characterized by recurrent seizures or loss of consciousness caused by abnormal cerebral excitation. Excitatory and inhibitory balance is mainly regulated by glutamatergic and GABAergic signaling in the brain. Genetic analyses have revealed that various genes are involved in the onset and development of epilepsy [1]. In addition,

dysfunction of some transporters such as the GABA transporter GAT-1 and the glucose transporter GLUT1 causes excitatory and inhibitory imbalance [2, 3]. However, the etiology of epilepsy has remained largely unclear. Since around 20% of epilepsy patients fail to achieve adequate seizure control using current anticonvulsants, and uncontrollable seizures lead to job limitation and decreased life-expectancy, further investigation of mechanisms of epilepsy is desirable [4].

The carnitine/organic cation transporter OCTN1/SLC22A4 is expressed in various organs, including the brain, kidneys, and the small intestine [5, 6]. The OCTN1 transports different organic cations and zwitterions including food-derived compounds such as ergothioneine (ERGO) and stachydrine, endogenous compounds such as acetylcholine, spermine, and L-carnitine, as well as several therapeutic agents although carnitine was proposed

✉ Noritaka Nakamichi
nakamichi@takasaki-u.ac.jp

¹ Faculty of Pharmacy, Institute of Medical, Pharmaceutical and Health Sciences, Kanazawa University, Kanazawa 920-1192, Japan

² Faculty of Pharmacy, Takasaki University of Health and Welfare, 60 Nakaorui-machi, Takasaki, Gunma 370-0033, Japan

to be a weak substrate of OCTN1 [5–9]. Among them, ERGO was proven to be an *in vivo* substrate, at least in rodents, with its concentration observed under the detection limit in *octn1* gene knockout (*octn1*^{-/-}) mice [8, 10]. In the brain, OCTN1 is localized in neural stem cells, neurons, and microglia. It regulates neuronal differentiation, neuronal maturation, and microglial activation *in vitro*, with its substrate ERGO being at least partially involved in such regulation [11–13]. However, the pathophysiological roles of OCTN1 remain unknown.

Oxidative stress is associated with the etiology and progression of epilepsy [14]. Some antioxidants such as α -tocopherol and melatonin ameliorate seizures in humans [15, 16]. ERGO is an antioxidant present in the bodies of rodents and humans due to its ingestion through the daily diet [17]. In addition, other OCTN1 substrates such as spermine and L-carnitine also show anti-seizure effects in rodents [18, 19]. Mutation of the acetylcholine transporter causes autosomal dominant nocturnal frontal lobe epilepsy in humans [20]. Thus, OCTN1 may be associated with the etiology or the progression of epilepsy through the regulation of exposure to these compounds in the brain. However, the relationship between OCTN1 and epilepsy remains unclear.

In this study, we aimed to clarify the possible involvement of OCTN1 in epileptic seizures. First, the experimental epilepsy model was established with repeated administration of GABA receptor antagonist pentylenetetrazole (PTZ) in *octn1*^{-/-} mice. Since the *octn1*^{-/-} mice showed much lower seizure scores compared with wild-type mice, the untargeted metabolomics analysis was performed to identify OCTN1 substrates that contribute to the differential phenotypes between the two strains. The plant alkaloid homostachydrine was identified as a novel OCTN1 substrate, which potentially worsens PTZ-induced seizures. Finally, the ameliorating effects of ERGO and *octn1* gene knockout on PTZ-induced kindling were investigated.

Experimental Procedures

Materials

Pentylenetetrazole was purchased from Sigma–Aldrich Inc. (St. Louis, MO, USA), ERGO was kindly provided by Yuki-guni Maitake Co., Ltd (Minamiuonuma, Japan). Deuterium-labeled ERGO (ERGO-d₉) was kindly supplied by TETRAHEDRON (Paris, France).

Synthesis of Homostachydrine and Deuterium-Labeled Homostachydrine (Homostachydrine-d₆)

Homostachydrine and homostachydrine-d₆ were synthesized from pipercolic acid by treatment of iodomethane or

deuterated iodomethane and KHCO₃, according to the literature [21]. The resulting homostachydrine was identified by ¹H-NMR and electrospray ionization mass spectrometry (*m/z* = 157). The homostachydrine-d₆ product was identified using ¹H-NMR.

Animals

Seven- to nine-week-old male mice were used. The *octn1*^{-/-} mice were backcrossed into a C57BL/6 J background [12]. Wild-type and *octn1*^{-/-} mice were maintained with free access to food and water.

PTZ-Induced Acute Seizures

PTZ dissolved in saline was intraperitoneally administered in mice at doses of 35, 40, or 50 mg/kg. Each mouse was then placed in a plastic cage and observed for 20 min. Seizure severity was evaluated primarily based on previously reported criteria [22], but stage 5 (death) was also included in this study, and the highest score observed within 20 min was monitored (stage 0: no behavioral change; stage 1: hypoactivity and immobility; stage 2: two or more isolated myoclonic jerks; stage 3: generalized clonic convulsions with preservation of righting reflex; stage 4: generalized tonic–clonic seizure with loss of righting reflex; stage 5: death). For PCR and ELISA analyses, PTZ at 45 mg/kg was administered twice with a 48-h interval, and the hippocampus was collected at 2 or 4 h after the second PTZ administration, respectively. The fore part of the cortex, excluding the thalamus, was collected as the frontal cortex. To examine the effect of homostachydrine on PTZ-induced seizures, homostachydrine was intravenously administered at 50 mg/kg in wild-type mice under isoflurane anesthesia. Four hours later, PTZ at 40 mg/kg was intraperitoneally administered, and the seizure score was evaluated as described above. After 20 min observation, the plasma, hippocampus, and frontal cortex were collected for measurement of homostachydrine concentration and mRNA expression.

RT-PCR

The total RNA was extracted from the resected tissues from PTZ-treated wild-type and *octn1*^{-/-} mice by using RNeasy plus (Takara Bio, Shiga, Japan), followed by synthesis and amplification of cDNA as described previously [8, 10]. The sequences of the primers were as follows: *c-fos* forward, GGGACAGCCTTTCCTACTACC and reverse, TTGGCACTAGAGACGGACAG; *Arc* forward, GAGTTCCTTAGCC TGTTCCGGA and reverse, GCTCGGCACTTACCAATCT; *Egr1* forward, AGCCTTCGCTCACTCCACTATCC and reverse, GCGGCTGGGTTTGATGAGTTGG; *Bdnf* forward, GCGGCAGATAAAAAGACTGC and reverse, TCA

GTTGGCCTTTGGATACC; *Ngf* forward, TCTATACTG GCCGCAGTGAG and reverse, GGACATTGCTATCTG TGTACGG; *Nt-3* forward, GGAGGAAACGCTATGCAG AA and reverse, GTCACCCACAGGCTCTCACT; *36B4* forward, ACTGGTCTAGGACCCGAGAAG and reverse, TCCCACCTTGTCTCCAGTCT. The expression levels of mRNA were normalized to the *36B4* housekeeping gene.

ELISA

The isolated hippocampus (10 mg) was mixed with 100 μ L of extraction buffer (50 mM ammonium acetate, 1 M NaCl, and 0.1% Triton X-100 adjusted at pH 4.0 with acetate), followed by sonication on ice using a Handy Sonic UR20-P sonicator (Tommy Seiko, Tokyo, Japan). Homogenates were centrifuged at 21,500 \times *g* for 30 min at 4 °C. The BDNF concentration in the supernatant was measured using a mature BDNF rapid ELISA kit (Biosensis, Thebarton, Australia).

Untargeted Metabolomics Analysis Using Liquid Chromatography–Quadrupole Time-of-Flight Mass Spectrometry (LC-QTOFMS)

Wild-type and *octn1*^{-/-} mice were maintained in the same cage for 1 week. After overnight fasting, the hippocampus, frontal cortex, and plasma were collected. Plasma samples were mixed with five times the volume of methanol, including gabapentin, as an internal standard. The hippocampus and frontal cortex were mixed with five and six times its volume, respectively, of methanol, including gabapentin. Then, tissues were homogenized using a Precellys 24 homogenizer (Bertin Technologies, Montigny-le-Bretonneux, France) using zirconia silica beads at 1.2 mm (Biomedical Science, Tokyo, Japan). The homogenate samples were centrifuged at 21,500 \times *g* for 10 min at 4 °C to precipitate proteins. The supernatant (30 μ L) was then mixed with 120 μ L acetonitrile, and the mixture was again centrifuged. The supernatant was subjected to LC-QTOFMS analysis, which included accurate parent ion scanning with time-of-flight mass spectrometry using an Acquity UPLC system coupled with Xevo G2 QTOFMS (Waters, Milford, MA). The mobile phases were (A) 0.1% formic acid and 10 mM ammonium acetate in 20% acetonitrile solution, and (B) 0.1% formic acid and 10 mM ammonium acetate in 95% acetonitrile solution. The gradient elution (flow rate, 0.4 mL/min) was performed as follows: 0–0.5 min, 1% A/99% B; 0.5–6.5 min, 1% A/99% B to 50% A/50% B; 6.5–7.5 min, 50% A/50% B to 70% A/30% B; 7.5–8.5 min, 70% A/30% B; 8.5–9.0 min, 70% A/30% B to 1% A/99% B; 9.0–13.5 min, 1% A/99% B using an ACQUITY UPLC BEH Amide column (Waters). QTOFMS was operated in positive mode with electrospray ionization, and MS data (50–600 Da) were acquired in a centroid format. Chromatographic and spectral data were deconvoluted

by MarkerLynx software (Waters) to generate a multivariate data matrix. The threshold was set as follows; 2000 for the hippocampus, 1700 for the frontal cortex, and 400 for plasma samples. The peaks with signal intensity less than the threshold, and those observed in fewer than four of six samples were removed as noise. Peak height was divided by the height of gabapentin, and the average was calculated. The average values in *octn1*^{-/-} that were two times higher or less than half that in wild-type mice with a statistically significant difference were chosen. Finally, the peak shape was visually checked, and signals showing appropriate peak shape were selected. The accurate masses of the parent and product were compared with the online METLIN database (<https://metlin.scripps.edu>) and the Human Metabolome Database (<https://www.hmdb.ca/>).

Product Ion Scanning

Synthesized homostachydrine and mouse plasma samples were mixed with MeOH and centrifuged twice at 21,500 \times *g* for 10 min at 4 °C. Supernatants were subjected to product ion scanning using high-performance liquid chromatography–tandem quadrupole mass spectrometry (LC-TQMS), which consisted of a Nexera X2 LC system coupled with an LCMS-8040 (Shimadzu, Kyoto, Japan). Parent mass was set at *m/z* of 158.00, and the product ion was scanned at *m/z* of 50,200. The collision energy was 10, 20, or 40 V. The mobile phases were (A) 0.1% formic acid and 10 mM ammonium acetate in 20% acetonitrile solution, and (B) 0.1% formic acid and 10 mM ammonium acetate in 95% acetonitrile solution. Gradient elution (flow rate, 0.4 mL/min) was performed as follows: 0–0.5 min, 1% A/99% B; 0.5–3.5 min, 1% A/99% B to 15% A/85% B; 3.5–4.5 min; 15% A/85% B to 35% A/65% B; 4.5–4.8 min; 35% A/65% B to 60% A/40% B; 4.8–5.8 min; 60% A/40% B; 5.8–6.0 min; 60% A/40% B to 1% A/99% B; 6.0–8.0 min; 1% A/99% B, using an ACQUITY UPLC BEH Amide column.

Measurement of Homostachydrine Concentration

After fasting overnight, plasma and tissues were collected and mixed with MeOH containing gabapentin (internal standard). Tissues were then homogenized. After vortexing, the samples were centrifuged twice at 21,500 \times *g* for 10 min at 4 °C. The supernatant was subjected to LC-TQMS analysis, as described below.

Uptake of Homostachydrine-d₆ and ERGO-d₉ in HEK293 Cells Transfected with Human OCTN1

HEK293 cells transfected with human *OCTN1* gene (HEK293/OCTN1) were seeded onto poly-L-lysine-coated 4-well plates at a density of 3.8 \times 10⁴ cells/cm². After 72 h,

the medium was replaced with transport buffer and pre-incubated for 10 min at 37 °C as described previously [8, 10]. The buffer was then replaced with fresh one containing 10 μ M homostachydrine- d_6 to initiate transport. To analyze the concentration-dependent uptake of homostachydrine, transport buffer contained a mixture of homostachydrine- d_6 and homostachydrine at 5–1000 μ M. The Michaelis constant (K_m) and maximum velocity (V_{max}) values were estimated by fitting to Michaelis–Menten equation using GraphPad Prism (GraphPad Software, San Diego, CA). To analyze inhibition of uptake of ERGO by homostachydrine, transport buffer containing 1 μ M ERGO- d_9 with various concentrations of homostachydrine was used. At designated times, the cells were washed and collected with 300 μ L of water using a cell scraper, followed by sonication to destroy cell membranes [8, 10]. Samples were mixed with acetonitrile containing gabapentin (internal standard) and centrifuged twice at 21,500 \times g for 10 min at 4 °C. The supernatant was subjected to LC-TQMS analysis, as described below.

Plasma Concentration Profile of Homostachydrine

After fasting overnight, homostachydrine- d_6 dissolved in saline was intravenously and orally administered at doses of 1 and 3 mg/kg, respectively. Blood was collected at designed times and centrifuged to obtain plasma. The plasma samples were deproteinated with MeOH, including gabapentin, and centrifuged twice at 21,500 \times g for 10 min at 4 °C. Then the supernatant was subjected to LC-TQMS analysis as described below. Pharmacokinetic parameters were calculated using moment analysis.

Urinary Excretion of Homostachydrine- d_6

Mice were maintained in a metabolic cage for 24 h for habituation. Homostachydrine- d_6 was then administered, and urine collection was initiated. As a control study, 50 μ mol/kg of cephalexin was dissolved in the same solution as homostachydrine- d_6 and simultaneously administered with homostachydrine- d_6 . Urine was collected at 24 and 48 h after the initiation of urine collection. The samples were then diluted 100 times with water and deproteinated with MeOH, including gabapentin or verapamil. After centrifugation, the supernatant was subjected to LC-TQMS analysis, as shown below.

Measurement of Homostachydrine, ERGO, and Cephalexin by LC-TQMS

The amounts of homostachydrine, homostachydrine- d_6 , ERGO- d_9 , and cephalexin were measured using LC-TQMS. The mobile phases were (A) 0.1% formic acid and 10 mM ammonium acetate in 20% acetonitrile solution, and (B)

0.1% formic acid and 10 mM ammonium acetate in 95% acetonitrile solution. The gradient elution (flow rate, 0.4 mL/min) for homostachydrine and homostachydrine- d_6 was performed as follows: 0–0.5 min, 1% A/99% B; 0.5–3.5 min, 1% A/99% B to 15% A/85% B; 3.5–4.5 min; 15% A/85% B to 35% A/65% B; 4.5–4.8 min; 35% A/65% B to 60% A/40% B; 4.8–5.8 min; 60% A/40% B; 5.8–6.0; 60% A/40% B to 1% A/99% B; 6.0–8.0 min; 1% A/99% B, using an ACQUITY UPLC BEH Amide column. For ERGO- d_9 measurement, gradient elution was performed as follows: 0–0.5 min; 1% A/99% B; 0.5–1.5 min, 1% A/99% B to 25% A/85% B; 1.5–6.3 min, 25% A/85% B; 6.3–7.0 min, 25% A/85% B to 60% A/40% B; 7.0–8.0 min, 60% A/40% B; 8.0–8.2 min, 60% A/40% B to 1% A/99% B; 8.2–11.5 min, 1% A/99% B. For cephalexin measurement the mobile phases were (A) 0.1% formic acid and (B) 0.1% formic acid in acetonitrile. Gradient elution was performed as follows: 0–0.3 min, 99% A/1% B; 0.3–2.8 min, 99% A/1% B to 5% A/95% B; 2.8–3.4 min, 5% A/95% B; 3.4–4.5 min, 5% A/95% B to 99% A/1% B, on a Cosmosil C18-MS-II packed column (Nacalai Tesque, Kyoto, Japan). The MRM transitions of the molecular and product ions were as follows: homostachydrine, m/z 158.0 > 58.0; homostachydrine- d_6 , m/z 164.00 > 64.15; ERGO, m/z 230.00 > 127.10; ERGO- d_9 , m/z 239.15 > 127.00; cephalexin, m/z 348.00 > 157.90, gabapentin (internal standard for homostachydrine, homostachydrine- d_6 , and ERGO- d_9), m/z 172.05 > 154.15; and verapamil (internal standard for cephalexin), m/z 455.20 > 165.05.

Kindling Induced by Repeated Administration of PTZ

PTZ at 35 mg/kg was intraperitoneally administered every other day for a total of eleven times, and seizure severity was evaluated after each injection based on the same criteria as that used for PTZ-induced acute seizure. When the mouse died during the repeated administration, the score for the corresponding mouse was regarded as five in the subsequent PTZ administration. To analyze the effect of coadministration of ERGO, 50 mg/kg ERGO or vehicle (water) alone was orally administered every day to 7-week-old wild-type mice under isoflurane anesthesia. On the 8th day, PTZ administration was initiated, while daily ERGO administration was continued. To minimize the effect of anesthesia used for oral administration, ERGO was administered after PTZ administration. After 11 injections of PTZ, the hippocampus and frontal cortex from the surviving mice were collected to measure the concentration of ERGO and homostachydrine.

Statistics

Data are expressed as the mean \pm S.D. The statistical significance of differences was determined using Student's *t*-test or one-way ANOVA with Tukey–Kramer test. The survival rate was evaluated using the Kaplan–Meier test. A *p*-value of <0.05 was regarded as denoting a significant difference.

Results

Deletion of the *Octn1* Gene Reduces PTZ-Induced Acute Seizures

To investigate the possible association of OCTN1 with PTZ-induced acute seizures, a single intraperitoneal injection of PTZ was administered to wild-type and *octn1*^{-/-} mice, and seizure severity was evaluated. Seizure scores in wild-type mice increased in a dose-dependent manner, whereas *octn1*^{-/-} mice showed significantly lower seizure scores after administration of 40 mg/kg of PTZ compared with wild-type mice (Fig. 1a). The seizure score was not different between the two strains at 35 and 50 mg/kg of PTZ. To confirm this difference, PTZ at 45 mg/kg was administered twice in both strains, and *octn1*^{-/-} mice consistently showed lower seizure scores after each injection (Fig. 1b).

Up-Regulation of Epilepsy-Related Genes was not Observed in *octn1*^{-/-} Mice

To further confirm the association of OCTN1 with PTZ-induced acute seizure, changes in expression of epilepsy-related genes were examined in the hippocampus of the

two strains after PTZ administration. Expression of the neuronal excitation marker genes *c-fos* and *Arc* was primarily increased in PTZ-treated wild-type mice compared to the saline-treated group (Fig. 2a, b). Meanwhile, the up-regulation of *c-fos* and *Arc* by PTZ administration was not observed in *octn1*^{-/-} (Fig. 2a, b). No significant difference was observed in the expression of the neuronal excitation marker *Egr1* among the four groups (Fig. 2c). The expression of BDNF was also measured by PCR and ELISA as BDNF is related to the epilepsy development [23]. The expression of BDNF mRNA and protein increased in PTZ-treated wild-type mice compared with the saline-treated group, whereas such up-regulation was not observed in *octn1*^{-/-} mice (Fig. 2d, e). Thus, a deficiency of OCTN1 may alleviate PTZ-induced seizures through the suppression of neuronal excitation in the brain.

Identification of the OCTN1 Substrate Using Untargeted Metabolomics Analysis

OCTN1 is involved in the uptake of various types of substrates into cells. Therefore, we hypothesized that OCTN1 transport some substrates that deteriorate PTZ-induced acute seizure and that loss in the substrates in *octn1*^{-/-} might lead to the reduced PTZ-induced seizures in this strain. To identify OCTN1 substrates in the brain, untargeted metabolomics analysis was conducted in the brain and plasma. After automatic picking, 2,599, 2,676, and 1,697 ion peaks were detected in the hippocampus, frontal cortex, and plasma, respectively. After correcting for noise, 463, 424, and 186 peaks remained in the hippocampus, frontal cortex, and plasma, respectively. Among them, five, three, and three peaks showed more than two-fold difference between

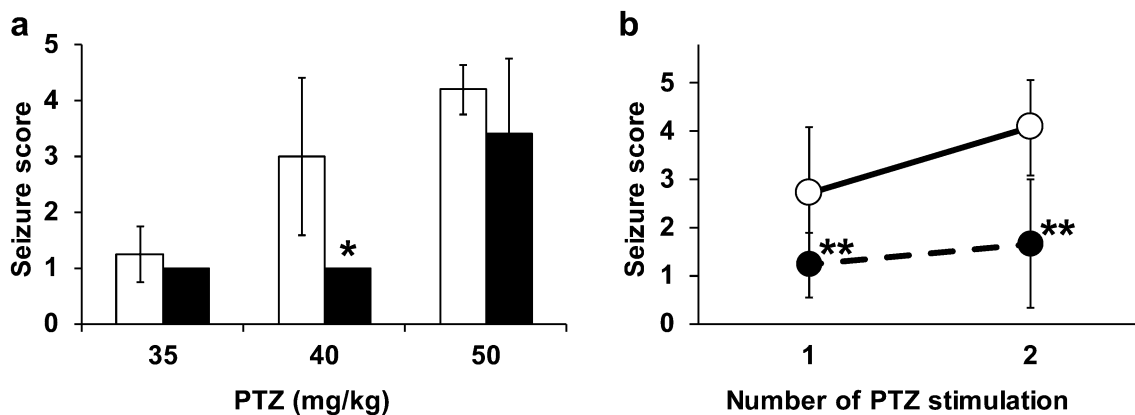


Fig. 1 Differences in PTZ-induced acute seizures in wild-type versus *octn1*^{-/-} mice. **a** Wild-type and *octn1*^{-/-} mice received a single intraperitoneal injection of PTZ (35, 40, or 50 mg/kg). Each mouse was observed for 20 min after administration, and the seizure severity was evaluated according to the criteria shown in the experimental procedures. The open column shows wild-type mice, and the closed

column shows *octn1*^{-/-} mice. Each value represents the mean \pm SD ($n=4-5$). * $p<0.05$, significant difference from wild-type mice. **b** Wild-type and *octn1*^{-/-} mice received intraperitoneal injections of PTZ (45 mg/kg) twice within 48 h. Seizure scores were evaluated after each injection. Each value represents the mean \pm SD ($n=9-14$). ** $p<0.01$, significant difference from wild-type mice

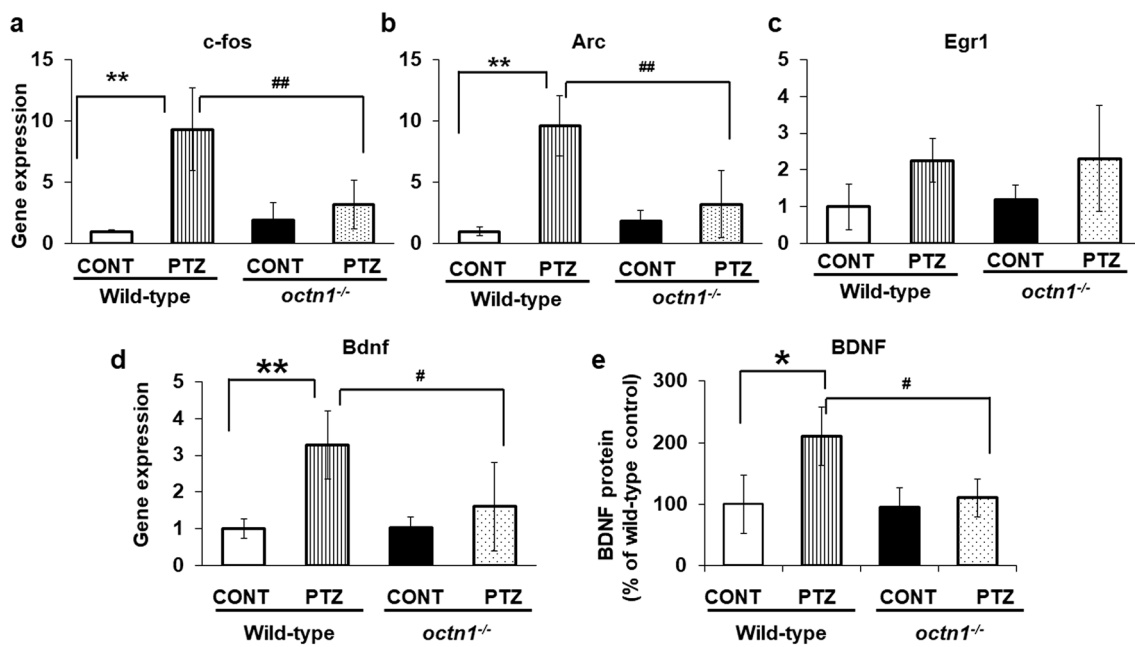


Fig. 2 Expression of epilepsy-related genes in the hippocampus after PTZ treatment. **a–d** PTZ (45 mg/kg) was intraperitoneally administered twice within a 48-h interval, and 2 h after the second PTZ injection the hippocampus was collected for RT-PCR analysis for neuronal excitation-related genes. The open columns show wild-type mice treated with saline; the striped columns show wild-type mice treated with PTZ. The closed columns show *octn1*^{-/-} mice treated with saline, and the dotted columns show *octn1*^{-/-} mice treated with PTZ. The expression of mRNA was normalized to that of the house-

keeping gene *36B4*. Each value represents the mean \pm SD ($n=3-8$). ** $p < 0.01$, significant difference from wild-type controls. ## $p < 0.01$, significant difference from PTZ-treated wild-type mice. **e** 4 h after the second PTZ injection, the hippocampus was collected, homogenized, and centrifuged for ELISA of the supernatant to measure the expression of BDNF protein. Each value represents the mean \pm SD ($n=3-4$). * $p < 0.05$, significant difference from wild-type mice. # $p < 0.05$, significant difference from wild-type mice

wild-type and *octn1*^{-/-} mice, and confirmation of peak shape resulted in four, two, and two peaks in the hippocampus, frontal cortex, and plasma. Among them, only m/z 158 was detected in all three samples at the same retention time (Fig. 3a–c). According to its precursor and product ions, m/z 158 was identified to be homostachydrine. Then, a product ion scan was conducted for both synthesized homostachydrine and a plasma sample from wild-type mice, confirming that m/z 158 is homostachydrine (Fig. 3d) since common product ions, m/z 56, 58, 70, and 84 were detected (Fig. 3e, f). The homostachydrine concentration was then measured in plasma and each tissue from wild-type and *octn1*^{-/-} mice using LC-TQMS. The homostachydrine concentration in *octn1*^{-/-} was significantly lower in the plasma and all tissues except the middle section of the small intestine (Fig. 3g, h).

Human OCTN1-Mediated Transport of Homostachydrine

To examine whether OCTN1 directly transports homostachydrine, an uptake assay was conducted in HEK293/OCTN1 cells. Homostachydrine- d_6 was also synthesized to investigate the disposition of homostachydrine, and incubated with these cell lines for the detection of uptake

of this compound. Homostachydrine- d_6 was taken up by HEK293/OCTN1 cells in a time-dependent manner, and the uptake was reduced in the presence of ERGO (Fig. 4a). Uptake of homostachydrine- d_6 was not detected at 30 s but was detected at 15 and 60 min, and this uptake was much lower than that observed in HEK293/OCTN1 cells (Fig. 4a). Uptake increased almost linearly until 15 s (Fig. 4a inset), and concentration-dependent uptake observed at this incubation period showed saturation of OCTN1-mediated uptake of homostachydrine (Fig. 4b), with K_m and V_{max} values of 310 μ M and 28.3 nmol/mg protein/15 s, respectively. Next, we evaluated the inhibition potential of homostachydrine for ERGO- d_6 uptake. Our results showed that the uptake of ERGO- d_6 was inhibited in the presence of homostachydrine, albeit incompletely (Fig. 4c).

Disposition of Homostachydrine In Vivo

To further evaluate the interaction of homostachydrine with OCTN1, the pharmacokinetics of homostachydrine- d_6 was examined. The doses (1 and 3 mg/kg) of homostachydrine- d_6 was chosen to observe plasma concentration of homostachydrine- d_6 less than that of homostachydrine (Fig. 3g) to avoid saturation of OCTN1 since the purpose of this study was

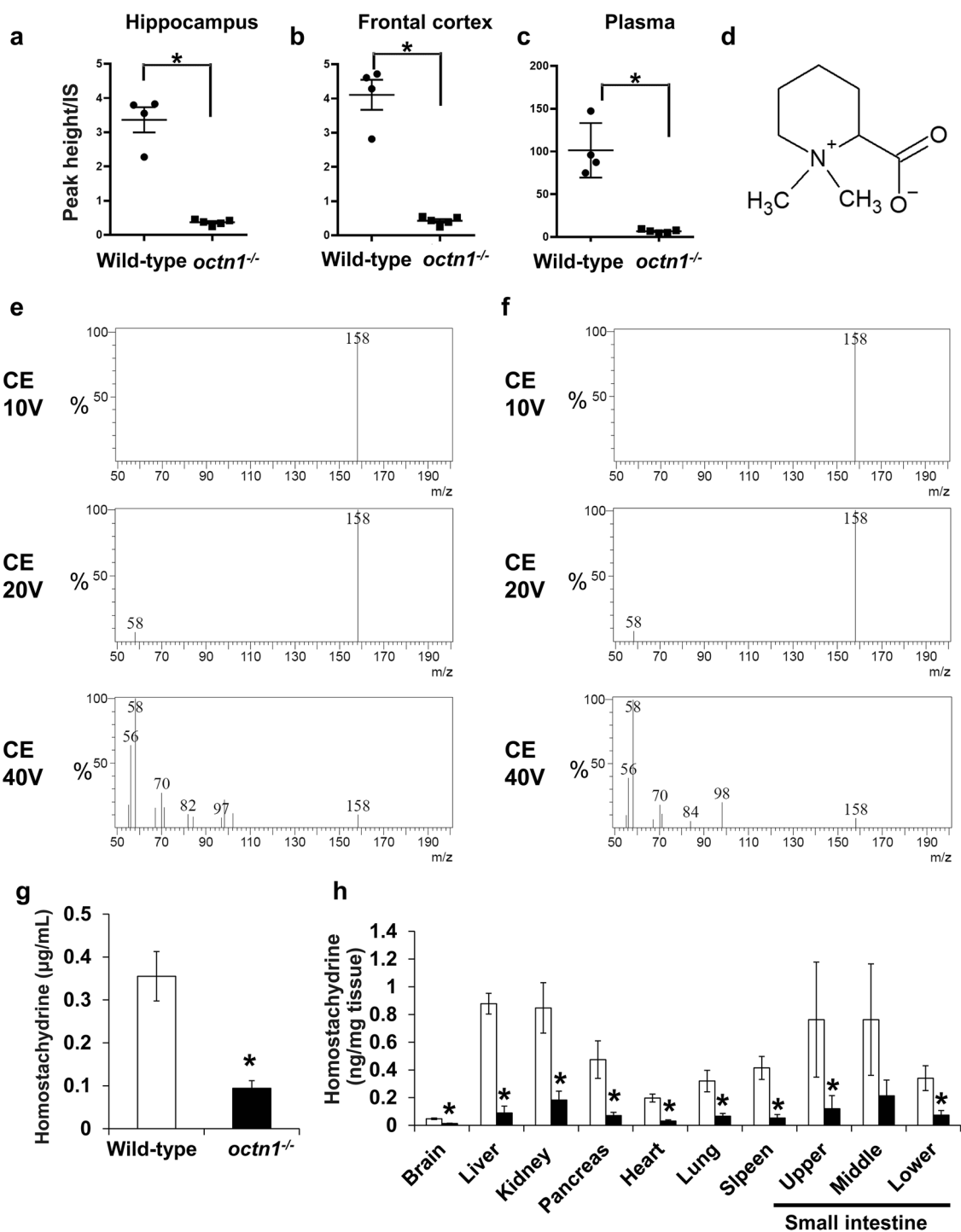


Fig. 3 Identification of homostachydrine as a candidate for the *in vivo* substrate of OCTN1. **a–c** Lysates of the hippocampus, cortex, and plasma were subjected to LC-TOFMS, and an ion peak at *m/z* 158 was identified, which was commonly a lower signal in the hippocampus (**a**), frontal cortex (**b**), and plasma (**c**) of *octn1*^{-/-} mice compared with wild-type mice. Each point represents each mouse. **p* < 0.05, significant difference from wild-type mice. **d** The chemical structure of homostachydrine. **e** and **f** Production scanning against

m/z 158 was performed for chemically synthesized homostachydrine (**e**) and plasma samples of wild-type mice (**f**) with various collision energies from - 10 to - 40 V. **g**, **h** The homostachydrine concentration in the plasma (**g**) and various tissues (**h**) of wild-type (open bars) and *octn1*^{-/-} mice (closed bars) was measured using LC-TQMS. Each value represents the mean ± SD (*n* = 3–4). **p* < 0.05, significant difference from wild-type mice

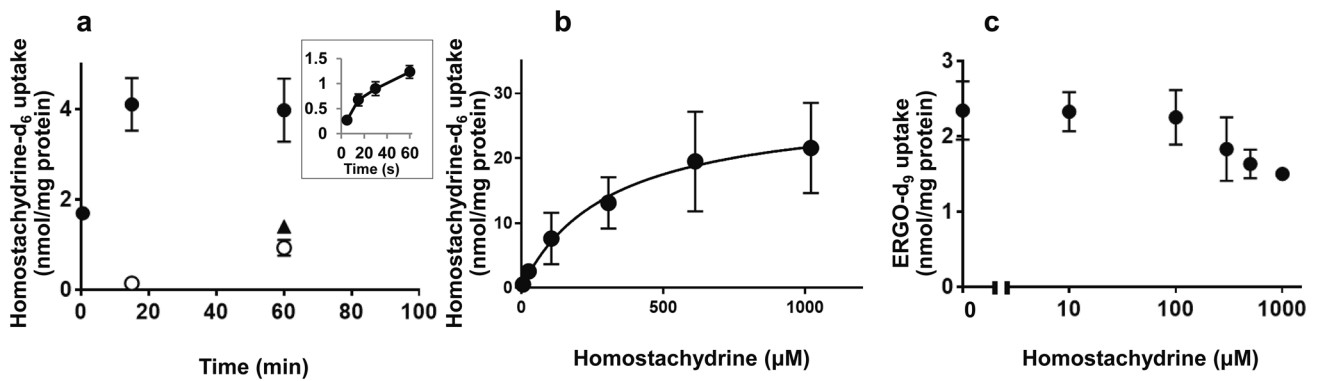


Fig. 4 The interaction of homostachydrine with human OCTN1. **a** HEK293 cells transfected with human OCTN1 gene (HEK293/OCTN1) and vector alone (HEK293/mock) were incubated with homostachydrine- d_6 (10 μ M) in the presence or absence of ERGO (500 μ M), and the uptake of homostachydrine- d_6 was measured by LC-TQMS. Closed circles and triangles indicate HEK293/OCTN1 cells without and with ERGO, whereas the open circles indicate HEK293/mock cells without ERGO. The inset represents the early-phase uptake of homostachydrine- d_6 in HEK293/OCTN1 cells. Each value represents the mean \pm SD (n=3). **b** HEK293/OCTN1 cells

were incubated with various concentrations of homostachydrine for 15 s, and the uptake was measured by LC-TQMS. The uptake of homostachydrine- d_6 in HEK293/mock cells was below detection limits, and therefore, the uptake represents OCTN1-mediated uptake. Each value represents the mean \pm SD (n=3). **c** HEK293/OCTN1 cells were incubated with ERGO- d_9 in the presence of various concentrations of homostachydrine for 5 min, and the uptake of ERGO- d_9 was measured using LC-TQMS. Each point represents the mean \pm SD (n=3)

to understand the role of OCTN1 in disposition of homostachydrine. After intravenous administration, the homostachydrine- d_6 concentration in the plasma of *octn1*^{-/-} mice was higher at the early phase (~ 10 min), but exhibited more rapid elimination until 8 h after administration, showing a lower plasma concentration after 4 h compared to wild-type mice (Fig. 5a). Such rapid elimination of homostachydrine- d_6 in the plasma of *octn1*^{-/-} mice was also confirmed at the terminal phase after oral administration. The plasma concentration of homostachydrine- d_6 in *octn1*^{-/-} after 6 h was lower than that of wild-type mice (Fig. 5). The maximum concentration (C_{max}) after oral administration and bioavailability were almost similar between the two strains,

suggesting that gastrointestinal absorption of homostachydrine may not be affected by OCTN1 (Table 1). Conversely, the half-life at the terminal phase and distribution volume in *octn1*^{-/-} were higher than those in wild-type mice, suggesting the involvement of OCTN1 in the distribution and elimination phases (Table 1). The smaller distribution volume in *octn1*^{-/-} could indicate limited tissue uptake of this compound and might be compatible with lower tissue concentration in *octn1*^{-/-} (Fig. 3h). The total clearance in *octn1*^{-/-} mice tended to be higher than wild-type mice (Table 1).

Fig. 5 Plasma concentration profile of homostachydrine- d_6 after iv and po administration. Homostachydrine- d_6 was intravenously (a) and orally (b) administered at a dose of 1 and 3 mg/kg, respectively, and the plasma concentration of homostachydrine- d_6 was measured by LC-TQMS. Open and closed circles showed wild-type and *octn1*^{-/-} mice, respectively. Each circle represents the mean \pm SD (n=3–5). *p < 0.05, significant difference from wild-type mice

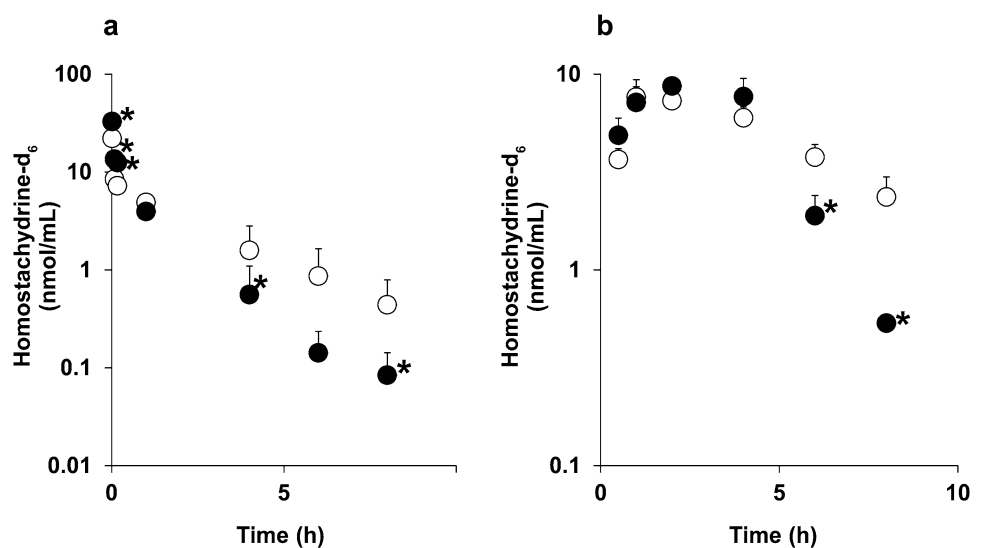


Table 1 Pharmacokinetic parameters of homostachydrine-d₆

	Dose (mg/kg)	C _{max} ^a (µg/mL)	AUC (µg/mg h)	T _{1/2} ^b (h)	CL _{tot} ^c (L/h/kg)	V ₀ ^d (L/kg)	Vd _{ss} ^e (L/kg)	F ^f (%)
Wild-type								
	i.v. 1	–	3.58 ± 1.29	2.15 ± 0.26	0.307 ± 0.098	0.332 ± 0.140	0.649 ± 0.144	77.8
	p.o. 3	1.29 ± 0.25	8.35 ± 1.16	3.05 ± 0.75	–	–	–	
<i>octn1</i> ^{-/-}								
	i.v. 1	–	2.91 ± 0.87	1.70 ± 0.51	0.368 ± 0.103	0.204 ± 0.033	0.346 ± 0.058*	77.3
	p.o. 3	1.42 ± 0.16	6.74 ± 1.01	1.05 ± 0.08*	–	–	–	

Mean ± SD (n = 5 and 3 for intravenous and oral administration, respectively)

*Significantly difference from wild-type (p < 0.05)

^aMaximum concentration

^bHalf-life at the terminal phase

^cTotal body clearance

^dInitial-phase distribution volume

^eSteady-state distribution volume

^fBioavailability

Table 2 Urinary excretion of homostachydrine-d₆

	Homostachydrine-d ₆ ^a	Cephalexin ^b
i.v.		
Wild-type	71.4 ± 14.2	49.8 ± 19.8
<i>octn1</i> ^{-/-}	69.8 ± 12.7	51.9 ± 8.2
p.o.		
<i>octn1</i> ^{-/-}	52.2 ± 4.4*	48.1 ± 6.8

Urinary excretion was recovered for 48 h after the administration and expressed as % of dose (Mean ± SD, n = 5 and 3 for wild-type and *octn1*^{-/-} mice, respectively)

*Significantly different from wild-type mice (p < 0.05)

^aDose of homostachydrine-d₆ was 1 and 3 mg/kg for i.v. and p.o., respectively

^bDose of cephalexin was 50 µmol/kg

Homostachydrine is Mainly Excreted in the Urine

To investigate the excretory route of homostachydrine, urine was collected for 48 h after intravenous and oral administration of homostachydrine-d₆ (Table 2). Approximately 70% of the dose was excreted in the urine after intravenous administration in both strains, and this was comparable or slightly higher than the urinary recovery of cephalexin (Table 2), which is known to be mainly eliminated by urinary excretion in rodents. Urinary excretion of homostachydrine-d₆ after oral administration tended to be slightly lower (50–65% of the dose) than that after intravenous administration in both strains (Table 2), and this finding would be compatible with incomplete gastrointestinal absorption (bioavailability ~ 80%, Table 1).

Homostachydrine Deteriorates PTZ-Induced Acute Seizures

To investigate whether homostachydrine deteriorates PTZ-induced acute seizures, homostachydrine was administered intravenously 4 h before PTZ administration in wild-type mice. The severity of PTZ-induced seizures was elevated in the homostachydrine-treated group compared with the saline-treated control group (Fig. 6a). After 20 min of observation, the plasma and brain were collected, and the homostachydrine concentration was measured (Fig. 6b, c). The homostachydrine concentration in plasma of the homostachydrine-treated group was around seven times higher than that in the PTZ only group (Fig. 6b). The homostachydrine concentration in the hippocampus and frontal cortex of the homostachydrine-treated group was also much higher than that in the control group (Fig. 6c). The expression of *Arc* in the hippocampus of the homostachydrine-treated group was significantly increased compared with the control group (Fig. 6d). The expressions of *Arc*, *Egr1*, and *Bdnf* in the frontal cortex of the homostachydrine-treated group were also up-regulated compared with the control group (Fig. 6e). The expression of *c-fos* in the homostachydrine-treated group tended to be increased compared with the control group in both brain tissues (Fig. 6d, e).

Gene Knockout of *octn1* and Repeated Administration of ERGO Inhibits PTZ-Induced Kindling

PTZ-induced kindling is regarded as an acquired epilepsy model that can be used to evaluate epileptogenesis, whereas PTZ-induced acute seizure is regarded as an epileptic

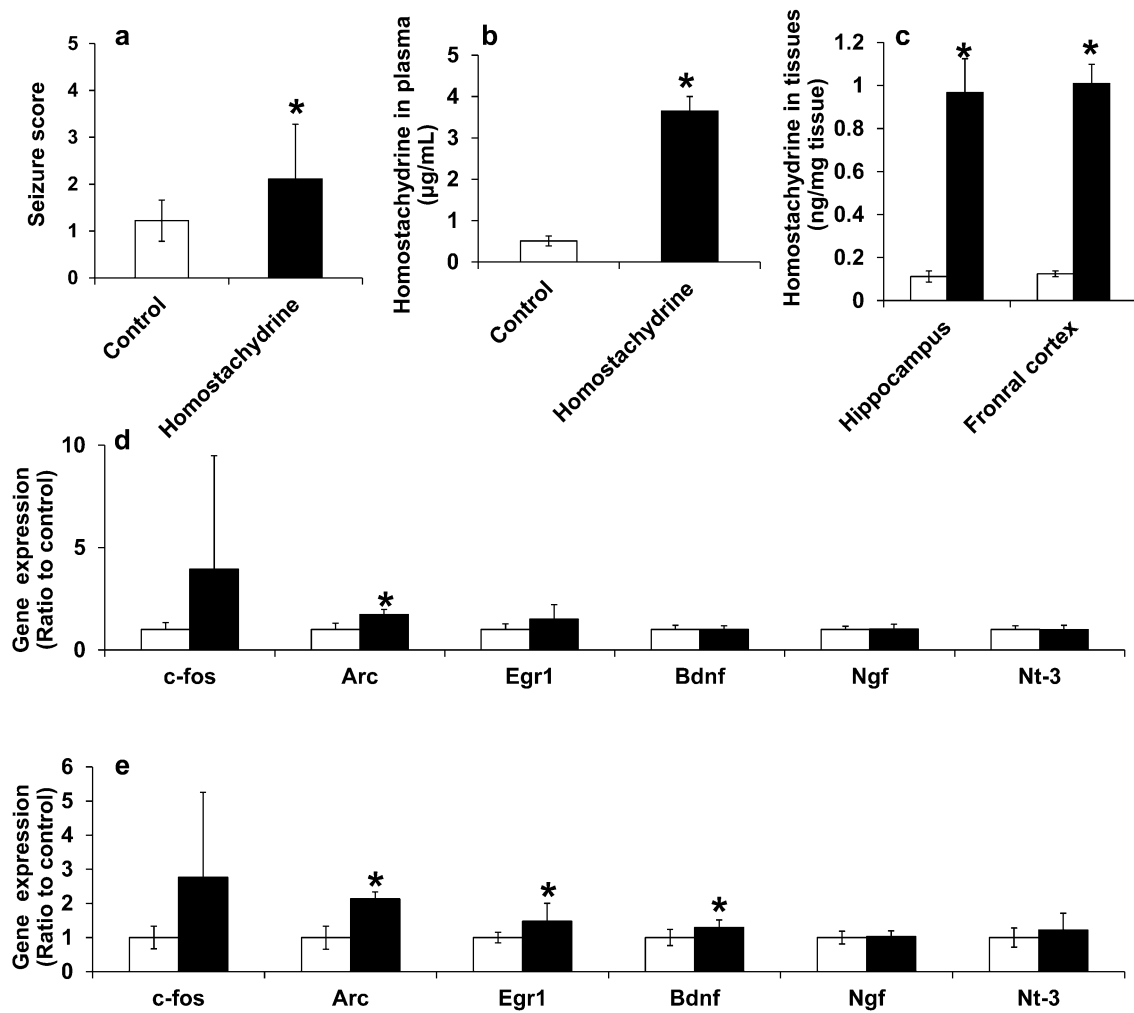


Fig. 6 The stimulating effect of homostachydrine on PTZ-induced acute seizures. **a** Homostachydrine (50 mg/kg) was intravenously administered, followed by intraperitoneal administration of PTZ (40 mg/kg) 4 h after homostachydrine administration in wild-type mice. Each mouse was then observed for 20 min after treatment, and seizure scores were evaluated. Each value represents the mean \pm SD (n=9) *p < 0.05, significant difference from control. **b, c** After seizure scores were recorded, the plasma (**b**) and brains (**c**) were collected, and homostachydrine concentrations were measured by

LC-TQMS. Open columns showed controls, and closed columns showed the homostachydrine-treated group. Each value represents the mean \pm SD (n=9) *p < 0.05, significant difference from controls. **d, e** After the seizure score observation, the hippocampus (**d**) and frontal cortex (**e**) were collected, and mRNA expression of epilepsy-related genes was evaluated. Closed and open columns showed homostachydrine-treated and control groups, respectively. Each value represents the mean \pm SD (n=9) and was normalized to the control value. *p < 0.05, significant difference from control

seizure model [24]. Effect of OCTN1 on epileptogenesis was next examined using a PTZ-induced kindling model. The seizure scores resulting from the repeated administration of PTZ at a sub-convulsive dose in wild-type mice was gradually increased, whereas that in *octn1*^{-/-} was minimally changed, and the scores in *octn1*^{-/-} mice were significantly lower than that in wild-type mice after the 8th kindling stimulation (Fig. 7a). The survival rate after the final kindling stimulation in wild-type mice was 50%, whereas that in *octn1*^{-/-} mice was 86%, and the rate in *octn1*^{-/-} mice was significantly higher than that in wild-type mice (Fig. 7b). Next, we investigated the effect of inhibiting

homostachydrine transport by OCTN1 on PTZ-induced kindling. ERGO was used to inhibit OCTN1 since OCTN1-specific inhibitor has not yet been clarified. The seizure scores following repeated PTZ stimulation in the ERGO-treated group was minimally changed like that in the *octn1*^{-/-} group. Furthermore, the score in the ERGO-treated group was significantly lower than that in the wild-type group after the 6th kindling stimulation (Fig. 7c). The survival rate after the final kindling stimulation in the control group was 50%, whereas that in the ERGO-treated group was 91%, and the rate in the ERGO-treated group was significantly higher (Fig. 7d).

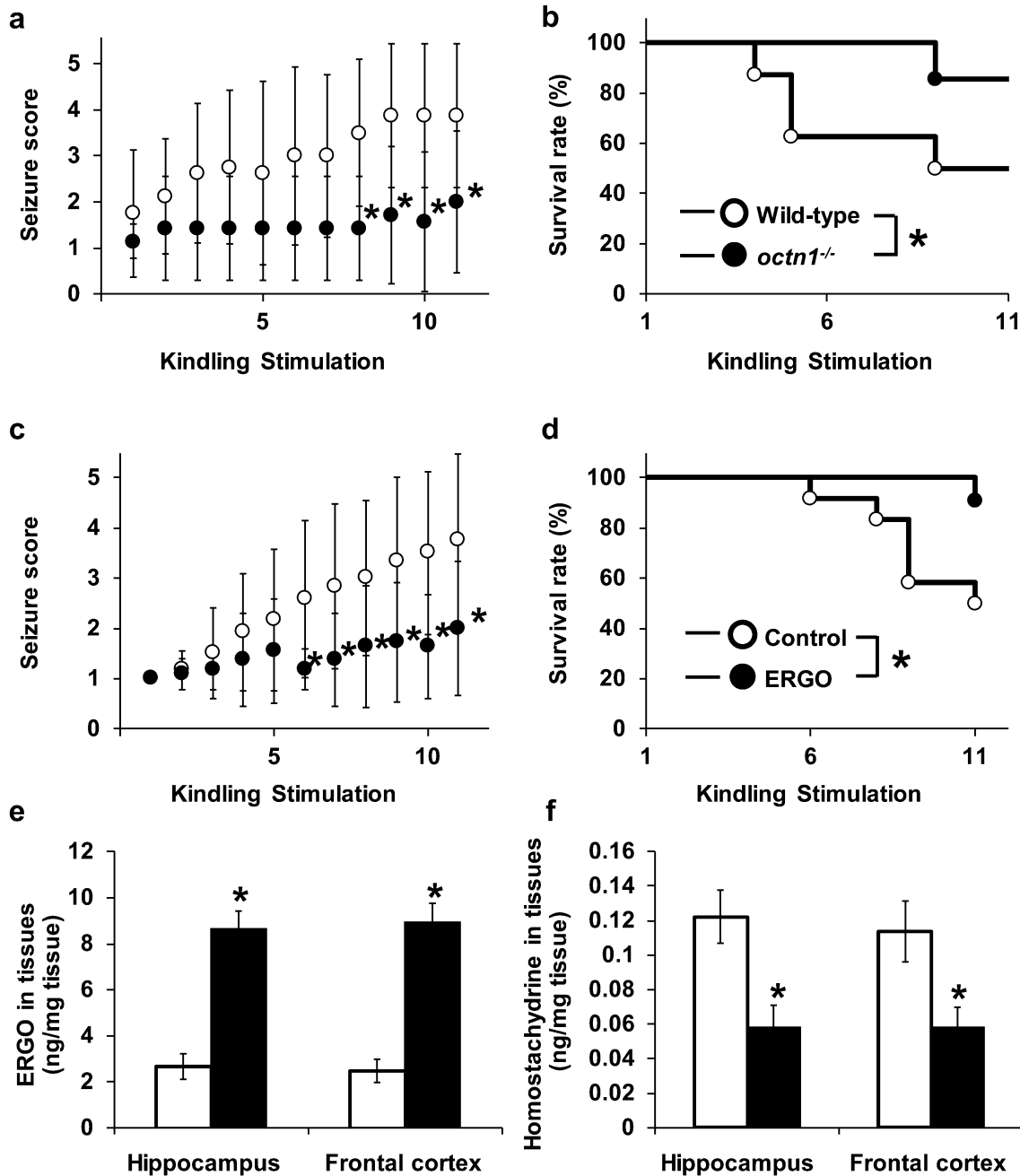


Fig. 7 The effect of *octn1* gene knockout and ERGO administration on PTZ-induced kindling. **a, b** PTZ (35 mg/kg) was intraperitoneally administered 11 times within a 48-h interval. Each mouse was then observed for 20 min after administration, and seizure scores (**a**) and survival rates (**b**) were evaluated. Open and closed circles showed wild-type and *octn1*^{-/-} mice, respectively. Each value represents the mean ± SD (n = 7–8) *p < 0.05, significant difference from wild-type mice. **c–f** ERGO (50 mg/kg) or vehicle (water) was orally administered every day for 1 week. On day 8, the intraperitoneal administra-

tion of PTZ (35 mg/kg) was initiated, while daily ERGO administration was continued. Closed and open circles showed ERGO-treated and control groups, respectively. Each mouse was then observed for 20 min after administration, and seizure scores (**c**) and survival rates (**d**) were evaluated. After the 11th administration of PTZ, the concentration of ERGO (**e**) and homostachydrine (**f**) in the hippocampus and frontal cortex was measured using LC-TQMS. Each value represents the mean ± SD (n = 3–6). *p < 0.05, significant difference from control

ERGO and homostachydrine concentrations in the brain were measured in surviving mice after the final PTZ administration. ERGO concentrations in the hippocampus and

frontal cortex in the ERGO-treated group were significantly higher than those in the control group (Fig. 7e). In contrast, homostachydrine concentrations in the two brain tissues

from the ERGO-treated group were substantially lower than those in the control group (Fig. 7f). These results suggest that the inhibition of OCTN1 may suppress not only epileptic seizures but also the acquisition of epilepsy through the decline of homostachydrine concentrations in the brain.

Discussion

This study demonstrated that OCTN1 deficiency inhibits PTZ-induced seizures and excitation of brain neurons in mice (Figs. 1, 2). Since OCTN1 transports the antioxidant ERGO and anti-seizure compounds such as L-carnitine and spermine [8, 10], we predicted that seizure scores in *octn1*^{-/-} mice would be increased compared with wild-type mice. However, the opposite result was observed. In our preliminary studies, the PTZ concentration in the whole brain and extracellular fluid (assessed by microdialysis) was measured 30 min after intraperitoneal PTZ administration (50 mg/kg), but no differences between wild-type and *octn1*^{-/-} mice were observed (data not shown). Therefore, the differences in seizure scores between the two strains may not be the result of the pharmacokinetic alteration of PTZ effects. We then hypothesized that OCTN1 transports unknown substrates which deteriorates PTZ-induced seizures, since both transporters accept a variety of compounds as substrates.

To clarify putative substrates involved in PTZ-induced acute seizure, untargeted metabolomics analysis was performed, and homostachydrine was identified as a candidate OCTN1 substrate in vivo (Figs. 3, 4). Homostachydrine is one alkaloid contained in the *Citrus* genus, alfalfa, and rye [21, 25, 26]. Homostachydrine is putatively synthesized from pipercolic acid in plants [27], whereas biosynthesis in animals and humans has not yet been reported. Thus, it is assumed that animals acquire homostachydrine from daily food intake, as in the case of the typical OCTN1 substrate ERGO.

After intravenous and oral administration, homostachydrine in plasma was rapidly eliminated in *octn1*^{-/-} mice compared with wild-type mice (Fig. 5). In contrast, the maximum concentration after oral administration and bioavailability was almost the same between the two strains (Table 1), suggesting that OCTN1 is mainly involved in the elimination of this compound, but not the primary transporter for its gastrointestinal absorption. OCTN1 is expressed on the apical membranes of proximal renal tubules and involved in the reabsorption of ERGO in the kidney, which at least partially explains why ERGO is present in plasma and almost all tissues of wild-type, but not *octn1*^{-/-} mice [10]. When we consider that ~70% of an administered dose was eliminated into the urine after intravenous administration (Table 2), the rapid elimination of homostachydrine in *octn1*^{-/-} mice (Fig. 5) can be similarly

explained by a deficiency in renal reabsorption of this compound in the kidney. This hypothesis is supported by the lower renal concentration in *octn1*^{-/-} mice compared with wild-type mice (Fig. 3g). Recovery of homostachydrine-d₆ into the urine was similar in the two strains (Table 2), but this may be caused by chronic urine sampling (~48 h) which may result in minimizing the effect of the excretion rate on recovery or the contribution of another transporter(s) besides OCTN1 in the renal handling of this compound.

Homostachydrine deteriorated PTZ-induced acute seizures in wild-type mice (Fig. 6). Plasma concentrations of homostachydrine are reportedly associated with schizophrenia and attention deficit hyperactivity disorder in humans [28]. In addition, the plasma concentration of homostachydrine was increased in experimental autoimmune encephalitis in mice [29]. However, the pathophysiological activity of homostachydrine has not yet been clarified in those studies. In contrast, the present study, for the first time, reported that homostachydrine exhibits stimulatory effects on PTZ-induced acute seizures. Pipercolic acid, a precursor of homostachydrine in plants, has a similar structure to homostachydrine and was reported to exacerbate epilepsy and experimental seizure models, although its proposed effect was controversial. Patients with pyridoxine-dependent seizures showed increased pipercolic acid concentrations in the plasma and cerebrospinal fluid [30]. In addition, intraperitoneal administration of high doses of pipercolic acid deteriorated PTZ-induced seizures [31]. Conversely, intracerebroventricular administration of low doses of pipercolic acid inhibited PTZ-induced seizures [31]. These reports suggest that pipercolic acid elicits contradictory seizure-related effects depending on its brain concentration. However, our study did not detect such contradictory effects of homostachydrine, though further investigations are warranted. Pipercolic acid is a modulator of GABAergic transmission and stimulates GABA release and inhibits GABA uptake [32]. Although there have been no reports regarding the effect of homostachydrine on GABAergic transmission, further investigation of the possible association of this compound with GABA homeostasis should be conducted to explain its deteriorating effects on seizures.

The deteriorating effect of homostachydrine (50 mg/kg) on PTZ-induced seizure was observed at much higher plasma and brain concentration (Fig. 6b, c) compared with the background level (Fig. 3g, h). Therefore, the effect of homostachydrine at lower dose would be much more helpful to understand its exact role in the body, but was not examined in the present study since effect of the background level of homostachydrine cannot be neglected. Further studies by constructing homostachydrine-free mice are needed to know its exact role in the body.

Plasma concentrations of homostachydrine in healthy volunteers were reported to be around 7.0 ng/mL [33], whereas

in mice after overnight fasting plasma concentrations averaged 0.35 µg/mL (Fig. 3g). Thus, homostachydrine concentrations in humans could be much lower than in mice. In humans, however, homostachydrine concentration in plasma is affected by dietary intake [34], as strict sodium restriction and a healthy Nordic diet has been shown to increase homostachydrine concentrations by 1.47- and 1.41-fold, respectively [35]. In addition, homostachydrine is present in plants that are used as herbal medicine such as *Medicago sativa* (alfalfa) and *Achillea millefolium* [26, 36]. Therefore, consuming homostachydrine-rich foods or herbal medicines may increase exposure to homostachydrine in humans. In addition, brain concentrations of homostachydrine seem to be highly dependent on the *octn1* (Fig. 3a–c, h). In contrast, SNPs in the *OCTN1* in humans profoundly affect the transport activity of gene products for specific substrates. The L503F SNP in the *OCTN1* gene is prominent in Caucasians (allele frequency: 0.458), whereas the I306T SNP is prominent in both Caucasians and the Japanese [37, 38]. Transport activity for ERGO and organic cations such as tetraethylammonium and metformin in L503F is higher compared with wild-type *OCTN1*, whereas that for L-carnitine and gabapentin in L503F is lower [38, 39]. Conversely, transport activity for ERGO is almost the same for either SNP, but is lower for gabapentin in the I306T variant compared with wild-type [38]. Thus, the genetic background may affect the exposure of homostachydrine to the brain, and further studies on plasma homostachydrine concentrations in humans and its association with food or medicine consumption are required to clarify whether homostachydrine affects seizure or not.

The PTZ-induced kindling model has been used to examine epileptogenesis, the process of transformation from a normal to an epileptic brain. In the PTZ-induced kindling model, sub-convulsive doses of PTZ are repeatedly administered to mice, and the brain is sensitized to stimulation. Since common phenotypes such as neuronal loss and mossy fiber sprouting are observed in the brain of both kindled mice and epilepsy patients [24], the PTZ-kindling model is regarded as the premium epilepsy model. In our study, *octn1*^{-/-} mice exhibited lower seizure scores and higher survival rates compared with wild-type mice in the PTZ-induced kindling model (Fig. 7a, b), suggesting that *OCTN1* may be associated with epileptogenesis as well as seizures. In addition, repeated oral administration of the *OCTN1* substrate/inhibitor ERGO exhibited inhibitory effects on PTZ-induced kindling (Fig. 7). ERGO is a diet-derived antioxidant and is synthesized in fungi or gut bacteria [40]. Administration of ERGO protected neurons from damage caused by cisplatin and β-amyloid via its antioxidant effects [41, 42]. Since the dose of ERGO in the present study was higher than previous reports, a portion of the anti-kindling effects (Fig. 7) may be due to antioxidant effects. However, homostachydrine concentrations in the brain were decreased

in the ERGO-treated group (Fig. 7f). This result implies that the protective effects of ERGO in PTZ-induced kindling may be at least partially caused by the inhibition of *OCTN1*, thereby reducing brain concentrations of homostachydrine or other endogenous substrates. If we consider the potential inhibition of *OCTN1* by ERGO treatment, our findings regarding *octn1* gene knockout (Fig. 7a, b) and ERGO treatment (Fig. 7c, d) in the PTZ-induced kindling model suggest the possibility that *OCTN1* inhibition may improve epileptic seizure or development of epilepsy. Since *octn1*^{-/-} mice show no distinct phenotype under normal conditions, the inhibition of *OCTN1* should not cause serious side-effects. Thus, the utility of *OCTN1* inhibitors as potential anti-epileptic compounds may require further examination. Another antioxidant, melatonin, also showed anti-seizure effects in animals and humans [16]. Melatonin is a dietary supplement food, and treatment with melatonin is considered relatively safe, although headache and sleepiness were reported in a study of insomnia treatment [43]. Conversely, side-effects were not reported following a 1-week treatment with ERGO in humans [44]. ERGO exhibits an extremely long half-life in humans and mice [10, 44], whereas the elimination of melatonin is much more rapid, with a half-life of 30 to 120 min [45]. Therefore, the anti-seizure activity of ERGO is promising and requires further examination.

In conclusion, this study showed that a deficiency of *OCTN1* inhibits PTZ-induced seizures. A newly identified *OCTN1* substrate, homostachydrine, may behave as a seizure-deteriorating compound in the brain. *OCTN1* substrate and inhibitor ERGO decreases homostachydrine concentrations in the brain and inhibits PTZ-induced kindling. These findings indicate the necessity for further investigation of whether *OCTN1* or its typical substrate and inhibitor ERGO is associated with epilepsy, and whether *OCTN1* represents a suitable target for anti-epileptic drugs in the future.

Author Contributions Conceptualization: MN, NN, YK. Methodology: NN, TY, YM, YK. Analysis and investigation: MN, TY, TK, YM. Writing—original draft preparation: MN, TK, TY. Writing, review, and editing: NN, TI, YK. Funding acquisition: NN, YK. Resources: YK. Supervision: NN, JM, YK.

Funding Grants-in-Aid for Scientific Research to Noritaka Nakamichi (No. 19K07126) and Yukio Kato (No. 15H04664) from the Ministry of Education, Culture, Sports, Science, and Technology of Japan, and grant by the Hoansha Foundation (Osaka, Japan) to Yukio Kato.

Data Availability The datasets used or analyzed during this study are available from the corresponding author upon reasonable request.

Compliance with Ethical Standards

Conflict of interest The authors declare that they have no competing interest.

Ethical Approval Experiments were performed according to the Guidelines for the Care and Use of Laboratory Animals at Kanazawa University. All protocols were approved by the Institutional Animal Care and Use Committee of Kanazawa University.

References

- Wang J, Lin Z-J, Liu L et al (2017) Epilepsy-associated genes. *Seizure* 44:11–20. <https://doi.org/10.1016/j.seizure.2016.11.030>
- Mattison KA, Butler KM, Inglis GAS et al (2018) SLC6A1 variants identified in epilepsy patients reduce γ -aminobutyric acid transport. *Epilepsia* 59:e135–e141. <https://doi.org/10.1111/epi.14531>
- Koch H, Weber YG (2019) The glucose transporter type 1 (Glut1) syndromes. *Epilepsy Behav* 91:90–93. <https://doi.org/10.1016/j.yebeh.2018.06.010>
- Tian N, Boring M, Kobau R et al (2018) Active epilepsy and seizure control in adults—United States, 2013 and 2015. *Morb Mortal Wkly Rep* 67:437–442. <https://doi.org/10.15585/mmwr.mm6715a1>
- Gründemann D, Harlfinger S, Golz S et al (2005) Discovery of the ergothioneine transporter. *Proc Natl Acad Sci USA* 102:5256–5261. <https://doi.org/10.1073/pnas.0408624102>
- Tamai I, Ohashi R, Nezu JI et al (2000) Molecular and functional characterization of organic cation/carnitine transporter family in mice. *J Biol Chem* 275:40064–40072. <https://doi.org/10.1074/jbc.M005340200>
- Bacher P, Giersiefer S, Bach M et al (2009) Substrate discrimination by ergothioneine transporter SLC22A4 and carnitine transporter SLC22A5: gain-of-function by interchange of selected amino acids. *Biochim Biophys Acta* 1788:2594–2602. <https://doi.org/10.1016/j.bbame.2009.09.019>
- Masuo Y, Ohba Y, Yamada K et al (2018) Combination metabolomics approach for identifying endogenous substrates of carnitine/organic cation transporter OCTN1. *Pharm Res* 35:224. <https://doi.org/10.1007/s11095-018-2507-1>
- Pochini L, Scalise M, Galluccio M et al (2012) The human OCTN1 (SLC22A4) reconstituted in liposomes catalyzes acetylcholine transport which is defective in the mutant L503F associated to the Crohn's disease. *Biochim Biophys Acta - Biomembr* 1818:559–565. <https://doi.org/10.1016/j.bbame.2011.12.014>
- Kato Y, Kubo Y, Iwata D et al (2010) Gene knockout and metabolome analysis of carnitine/organic cation transporter OCTN1. *Pharm Res* 27:832–840. <https://doi.org/10.1007/s11095-010-0076-z>
- Ishimoto T, Nakamichi N, Hosotani H et al (2014) Organic cation transporter-mediated ergothioneine uptake in mouse neural progenitor cells suppresses proliferation and promotes differentiation into neurons. *PLoS ONE* 9:e89434. <https://doi.org/10.1371/journal.pone.0089434>
- Ishimoto T, Nakamichi N, Nishijima H et al (2018) Carnitine/organic cation transporter OCTN1 negatively regulates activation in murine cultured microglial cells. *Neurochem Res* 43:107–119. <https://doi.org/10.1007/s11064-017-2350-5>
- Nakamichi N, Nakao S, Nishiyama M et al (2020) Oral administration of the food derived hydrophilic antioxidant ergothioneine enhances object recognition memory in mice. *Curr Mol Pharmacol* 13:1121–1132. <https://doi.org/10.2174/1874467213666200212102710>
- Pearson-Smith J, Patel M (2017) Metabolic dysfunction and oxidative stress in epilepsy. *Int J Mol Sci* 18:2365. <https://doi.org/10.3390/ijms18112365>
- Mehvari J, Motlagh F, Najafi M et al (2016) Effects of Vitamin E on seizure frequency, electroencephalogram findings, and oxidative stress status of refractory epileptic patients. *Adv Biomed Res* 5:36. <https://doi.org/10.4103/2277-9175.178780>
- Banach M, Gurdziel E, Jędrych M, Borowicz KK (2011) Melatonin in experimental seizures and epilepsy. *Pharmacol Rep* 63:1–11. [https://doi.org/10.1016/S1734-1140\(11\)70393-0](https://doi.org/10.1016/S1734-1140(11)70393-0)
- Halliwel B, Cheah IK, Tang RMY (2018) Ergothioneine – a diet-derived antioxidant with therapeutic potential. *FEBS Lett* 592:3357–3366
- Kumar M, Kumar P (2017) Protective effect of spermine against pentylenetetrazole kindling epilepsy induced comorbidities in mice. *Neurosci Res* 120:8–17. <https://doi.org/10.1016/j.neurosci.2017.02.003>
- Hussein A, Adel M, El-Mesery M et al (2018) L-carnitine modulates epileptic seizures in pentylenetetrazole-kindled rats via suppression of apoptosis and autophagy and upregulation of Hsp70. *Brain Sci* 8:45. <https://doi.org/10.3390/brainsci8030045>
- Becchetti A, Aracri P, Meneghini S et al (2015) The role of nicotinic acetylcholine receptors in autosomal dominant nocturnal frontal lobe epilepsy. *Front Physiol* 6:22. <https://doi.org/10.3389/fphys.2015.00022>
- Servillo L, Giovane A, Balestrieri ML et al (2012) Occurrence of pipercolic acid and pipercolic acid betaine (Homostachydrine) in citrus genus plants. *J Agric Food Chem* 60:315–321. <https://doi.org/10.1021/jf204286r>
- Claycomb RJ, Hewett SJ, Hewett JA (2011) Prophylactic, prandial rofecoxib treatment lacks efficacy against acute PTZ-induced seizure generation and kindling acquisition. *Epilepsia* 52:273–283. <https://doi.org/10.1111/j.1528-1167.2010.02889.x>
- Binder DK, Croll SD, Gall CM, Scharfman HE (2001) BDNF and epilepsy: too much of a good thing? *Trends Neurosci* 24:47–53. [https://doi.org/10.1016/S0166-2236\(00\)01682-9](https://doi.org/10.1016/S0166-2236(00)01682-9)
- Morimoto K, Fahnestock M, Racine RJ (2004) Kindling and status epilepticus models of epilepsy: rewiring the brain. *Prog Neurobiol* 73:1–60. <https://doi.org/10.1016/j.pneurobio.2004.03.009>
- Servillo L, D'Onofrio N, Giovane A et al (2018) The betaine profile of cereal flours unveils new and uncommon betaines. *Food Chem* 239:234–241. <https://doi.org/10.1016/j.foodchem.2017.06.111>
- Wood KV, Stringham KJ, Smith DL et al (1991) Betaines of alfalfa: characterization by fast atom bombardment and desorption chemical ionization mass spectrometry. *Plant Physiol* 96:892–897. <https://doi.org/10.1104/pp.96.3.892>
- Essery JM, McCaldint DJ, Marion L (1962) The biogenesis of stachydrine. *Phytochemistry* 1:209–213. [https://doi.org/10.1016/S0031-9422\(00\)82824-1](https://doi.org/10.1016/S0031-9422(00)82824-1)
- Yang J, Yan B, Zhao B et al (2020) Assessing the causal effects of human serum metabolites on 5 major psychiatric disorders. *Schizophr Bull* 46:804–813. <https://doi.org/10.1093/schbul/sbz138>
- Mangalam A, Poisson L, Nemutlu E et al (2013) Profile of circulatory metabolites in a relapsing-remitting animal model of multiple sclerosis using global metabolomics. *J Clin Cell Immunol* 4:1000150. <https://doi.org/10.4172/2155-9899.1000150>
- Plecko B, Stöckler-Ipsiroglu S, Paschke E et al (2000) Pipercolic acid elevation in plasma and cerebrospinal fluid of two patients with pyridoxine-dependent epilepsy. *Ann Neurol* 48:121–125. [https://doi.org/10.1002/1531-8249\(200007\)48:1<121::AID-ANA20>3.0.CO;2-V](https://doi.org/10.1002/1531-8249(200007)48:1<121::AID-ANA20>3.0.CO;2-V)
- Chang Y-F, Hargest V, Chen J-S (1988) Modulation of benzodiazepine by lysine and pipercolic acid on pentylenetetrazol-induced seizures. *Life Sci* 43:1177–1188. [https://doi.org/10.1016/0024-3205\(88\)90207-X](https://doi.org/10.1016/0024-3205(88)90207-X)
- Gutiérrez MC, Delgado-Coello BA (1989) Influence of pipercolic acid on the release and uptake of [3 H]GABA from brain slices of

- mouse cerebral cortex. *Neurochem Res* 14:405–408. <https://doi.org/10.1007/BF00964852>
33. Tuomainen M, Kärkkäinen O, Leppänen J et al (2019) Quantitative assessment of betainized compounds and associations with dietary and metabolic biomarkers in the randomized study of the healthy Nordic diet (SYSDIET). *Am J Clin Nutr* 110:1108–1118. <https://doi.org/10.1093/ajcn/nqz179>
 34. Kärkkäinen O, Lankinen MA, Vitale M et al (2018) Diets rich in whole grains increase betainized compounds associated with glucose metabolism. *Am J Clin Nutr* 108:971–979. <https://doi.org/10.1093/ajcn/nqy169>
 35. Derkach A, Sampson J, Joseph J et al (2017) Effects of dietary sodium on metabolites: the Dietary Approaches to Stop Hypertension (DASH)–Sodium Feeding Study. *Am J Clin Nutr* 106:1131–1141. <https://doi.org/10.3945/ajcn.116.150136>
 36. Tunón H, Thorsell W, Bohlin L (1994) Mosquito repelling activity of compounds occurring in *Achillea millefolium* L. (asteraceae). *Econ Bot* 48:111–120. <https://doi.org/10.1007/BF02908196>
 37. Urban TJ, Yang C, Lagpacan LL et al (2007) Functional effects of protein sequence polymorphisms in the organic cation/ergothioneine transporter OCTN1 (SLC22A4). *Pharmacogenet Genomics* 17:773–782. <https://doi.org/10.1097/FPC.0b013e3281c6d08e>
 38. Futatsugi A, Masuo Y, Kawabata S et al (2016) L503F variant of carnitine/organic cation transporter 1 efficiently transports metformin and other biguanides. *J Pharm Pharmacol* 68:1160–1169. <https://doi.org/10.1111/jphp.12574>
 39. Peltekova VD, Wintle RF, Rubin LA et al (2004) Functional variants of OCTN cation transporter genes are associated with Crohn disease. *Nat Genet* 36:471–475. <https://doi.org/10.1038/ng1339>
 40. Genghof DS (1970) Biosynthesis of ergothioneine and hercynine by fungi and actinomycetales. *J Bacteriol* 103:475–478. <https://doi.org/10.1128/JB.103.2.475-478.1970>
 41. Song T-Y, Chen C-L, Liao J-W et al (2010) Ergothioneine protects against neuronal injury induced by cisplatin both in vitro and in vivo. *Food Chem Toxicol* 48:3492–3499. <https://doi.org/10.1016/j.fct.2010.09.030>
 42. Yang N-C, Lin H-C, Wu J-H et al (2012) Ergothioneine protects against neuronal injury induced by β -amyloid in mice. *Food Chem Toxicol* 50:3902–3911. <https://doi.org/10.1016/j.fct.2012.08.021>
 43. Boeve BF, Silber MH, Ferman TJ (2003) Melatonin for treatment of REM sleep behavior disorder in neurologic disorders: results in 14 patients. *Sleep Med* 4:281–284. [https://doi.org/10.1016/S1389-9457\(03\)00072-8](https://doi.org/10.1016/S1389-9457(03)00072-8)
 44. Cheah IK, Tang RMY, Yew TSZ et al (2017) Administration of pure ergothioneine to healthy human subjects: uptake, metabolism, and effects on biomarkers of oxidative damage and inflammation. *Antioxid Redox Signal* 26:193–206. <https://doi.org/10.1089/ars.2016.6778>
 45. Harpsøe NG, Andersen LPH, Gögenur I, Rosenberg J (2015) Clinical pharmacokinetics of melatonin: a systematic review. *Eur J Clin Pharmacol* 71:901–909. <https://doi.org/10.1007/s00228-015-1873-4>

Publisher's Note Springer Nature remains neutral with regard to jurisdictional claims in published maps and institutional affiliations.

副論文

金沢大学大学院医薬保健学総合研究科
創薬科学専攻
分子薬物治療学研究室

西山 美沙

RESEARCH ARTICLE

Oral Administration of the Food-derived Hydrophilic Antioxidant Ergothioneine Enhances Object Recognition Memory in Mice

Noritaka Nakamichi¹, Shunsuke Nakao¹, Misa Nishiyama¹, Yuka Takeda¹, Takahiro Ishimoto¹, Yusu-
suke Masuo¹, Satoshi Matsumoto², Makoto Suzuki² and Yukio Kato^{1,*}

¹Faculty of Pharmacy, Institute of Medical, Pharmaceutical and Health Sciences, Kanazawa University, Kanazawa 920-1192, Japan; ²L•S Corporation Co. Ltd., 3-10-1 Ningyocho-Nihonbashi, Chuo-ku, Tokyo 103-0013, Japan

Abstract: Background: The enhancement of learning and memory through food-derived ingredients is of great interest to healthy individuals as well as those with diseases. Ergothioneine (ERGO) is a hydrophilic antioxidant highly contained in edible golden oyster mushrooms (*Pleurotus cornucopiae* var. *citrinopileatus*), and systemically absorbed by its specific transporter, carnitine/organic cation transporter OCTN1/SLC22A4.

Objective: This study aims to examine the possible enhancement of object recognition memory by oral administration of ERGO in normal mice.

Method: Novel object recognition test, spatial recognition test, LC-MS/MS, Golgi staining, neuronal culture, western blotting, immunocytochemistry, and quantitative RT-PCR were utilized.

Result: After oral administration of ERGO (at a dose of 1–50 mg/kg) three times per week for two weeks in ICR mice, the novel object recognition test revealed a longer exploration time for the novel object than for the familiar object. After oral administration of ERGO, the spatial recognition test also revealed a longer exploration time for the spatially moved object than the unmoved one in mice fed ERGO-free diet. The discrimination index was significantly higher in the ERGO-treated group than the control in both behavioral tests. ERGO administration led to an increase in its concentration in the plasma and hippocampus. The systemic concentration reached was relevant to those found in humans after oral ERGO administration. Golgi staining revealed that ERGO administration increased the number of matured spines in the hippocampus. Exposure of cultured hippocampal neurons to ERGO elevated the expression of the synapse formation marker, synapsin I. This elevation of synapsin I was inhibited by the tropomyosin receptor kinase inhibitor, K252a. Treatment with ERGO also increased the expression of neurotrophin-3 and -5, and phosphorylated mammalian target of rapamycin in hippocampal neurons.

Conclusion: Oral intake of ERGO may enhance object recognition memory at its plasma concentration achievable in humans, and this enhancement effect could occur, at least in part, through the promotion of neuronal maturation in the hippocampus.

Keywords: Ergothioneine, Object recognition memory, Neuronal maturation, Hippocampus, Neurotrophin, Organic cation transporter.

1. INTRODUCTION

Dysfunction of learning and memory due to neuronal disorders causes dementia, resulting in an extremely lowered quality of life in patients. There are 50 million dementia patients worldwide [1], and the treatment of dementia is an urgent issue. However, despite the clinical application of several therapeutic agents for the treatment of dementia, such as

inhibitors of cholinesterase and the *N*-methyl-D-aspartate receptor [2, 3], there are no fundamental therapeutic drugs for recovering the neurons that are lost during brain disorders. Some patients are insensitive to the current clinically available drugs [2]. In addition, the administration of cholinesterase inhibitors sometimes causes several adverse events, such as gastrointestinal or mental disorders [2, 4]. Therefore, the development of drugs with a novel mechanism of action and minimal adverse effects is desirable.

Food-derived ingredients that improve recognition function through the enhancement of brain function would also be a promising tool for the treatment of dementia and may

* Address correspondence to this author at the Faculty of Pharmacy, Institute of Medical, Pharmaceutical and Health Sciences, Kanazawa University, Kakuma-machi, Kanazawa 920-1192, Japan; Tel/Fax: +81-76-234-4465; E-mail: ykato@p.kanazawa-u.ac.jp

help to clarify novel mechanisms of action for the drug development. Food-derived ingredients that have an antioxidant effect and/or promotive effect on neuronal maturation and neurogenesis may improve learning and memory ability. For example, intake of antioxidant polyphenol catechin and resveratrol, which are found in high levels in green tea and red grapes, respectively, improves the decline in spatial memory provoked by the suppression of spine reduction in aged mice [5, 6]. Intake of carotenoid astaxanthin, which is found in salmon roe, enhances neurogenesis and spatial memory in normal mice [7]. However, over-intake of resveratrol inhibits neurogenesis and reduces the learning and memory ability [8]. The astaxanthin intake required to improve learning and memory in mice may cause several adverse events, such as hepatic impairment [9]. Thus, it would be desirable to improve the pharmacokinetic properties to gain efficient activity of learning and memory with minimal toxicity at the clinically relevant amount of ingestion.

Ergothioneine (ERGO) is an antioxidant that is abundantly found in certain edible mushrooms, including golden oyster mushrooms (*Pleurotus cornucopiae* var. *citrinopileatus*), meat, and grains. ERGO is synthesized by fungi and mycobacteria, but not by mammals. Thus, ERGO is ingested from daily food and is present at a concentration range of μM to sub mM in the blood and organs of humans and mice [10, 11]. The hydrophilic nature of ERGO hinders its membrane permeation, however, it is actively transported across membranes by the specific transporter carnitine/organic cation transporter (OCTN1/SLC22A4), which was identified by the metabolomics approach [12]. ERGO is orally absorbed mainly through this transporter [13]. The concentration of ERGO in any of the organs of *octn1* gene knockout mice is below the detection limit [11], indicating the fundamental role of this transporter in the distribution of ERGO. ERGO can enter the brain by crossing the blood-brain barrier [14]. Thus, this antioxidant appears to have the beneficial pharmacokinetic properties of a candidate for the improvement of brain function. In fact, ERGO shows protective effects against the neuronal damage provoked by H_2O_2 , β -amyloid, and cisplatin [15-17]. Exposure of cultured neural stem cells to ERGO promotes cellular differentiation into neurons, through an unidentified mechanism that is distinct from its antioxidant activity [18]. Oral ingestion of a diet that includes ERGO actually promotes hippocampal neurogenesis and exerts an antidepressant-like effect in mice [14]. In addition to these beneficial effects of exogenous administration of ERGO in experimental animals, recent clinical studies have indicated that the systemic concentration of ERGO is reduced in older adults (0.8–1.4 μM in serum of older subjects) [19], patients with Parkinson's disease [20], and in people with mild cognitive impairment (0.1–0.2 $\mu\text{g}/\text{mg}$ hemoglobin in whole blood) [21]. These findings imply that ERGO may play a role in the maintenance of normal brain function. However, though ERGO is known to improve the decline of learning and memory ability in senescent model mice [22], the effect of ERGO on learning and memory under normal (untreated) conditions has not yet been clarified.

In the present study, we investigated whether orally administered ERGO can enhance the learning and memory ability of normal mice. For such purposes, both the novel object recognition test (NORT) and the spatial recognition test (SRT) were performed after the oral administration of ERGO. To support such an effect on brain function, the gastrointestinal absorption and hippocampal distribution of ERGO were also examined. The promotion of neuronal maturation by ERGO, through the induction of neurotrophic factors, was also demonstrated as the possible underlying mechanism.

2. MATERIALS AND METHODS

2.1. Materials

ERGO was kindly provided by Yukiguni Maitake Co. Ltd. (Minamiuonuma, Japan). L-(+)-Ergothioneine-d9 was kindly provided by TETRAHEDRON (Romainville, France). ISOGEN, MultiScribe™ Reverse Transcriptase, and THUNDERBIRD SYBR qPCR Mix were purchased from Nippon Gene (Tokyo, Japan), Biosystems (Foster City, CA, USA), and TOYOBO (Osaka, Japan), respectively. ERGO-free feed (basal diet®) was obtained from TestDiet (St. Louis, MO, USA) and contained less than 0.01 μg ERGO/g chow [23]. All other chemicals and reagents, of the highest purity available, were purchased from commercial sources.

2.2. Animals

Male ICR mice for *in vivo* experiments and female pregnant ICR mice for neuronal culture were purchased from Sankyo Labo Service Co. (Toyama, Japan). Male mice fed control diet were regarded as “normal mice”. Male ICR mice at the age of 3 weeks were also purchased from Sankyo Labo Service and fed ERGO-free diet. These mice were regarded as “ERGO-free mice”. These ERGO-free mice were prepared with an aim to clearly observe pharmacological effect of ERGO exogenously administered since ERGO exists in the body of normal mice that were not administered ERGO due to ingestion from the daily diet which includes ERGO [11, 14]. Mice were housed in pathogen-free conditions at a controlled temperature (21–25 °C) under a 12 h light/dark cycle. The lights remained on from 8:00 to 20:00. Food and water were available *ad libitum*. Total number of normal mice used for behavioral tests, measurement of ERGO concentration, and Golgi staining was 70, 24, and 19, respectively, whereas that of ERGO-free mice used for behavioral tests and measurement of ERGO concentration was 48 and 32, respectively.

2.3. Behavioral Tests in Normal and ERGO-free Mice

ERGO was dissolved in autoclaved pure water and orally administered to normal mice at the age of 5 weeks at 0, 1, 5, 20, or 50 mg/kg on experimental days 0, 2, 4, 7, 9, and 11 by gavage (Supplementary Fig. S1A). The number of mice administered 0, 1, 5, 20, and 50 mg/kg ERGO was 14, 15, 14, 13, and 14, respectively. ERGO was orally administered to ERGO-free mice at the age of 6 weeks at 0, 5, 20, or 50 mg/kg on experimental days 0, 2, 4, 7, 9, and 11 by gavage

(Supplementary Fig. S1A). The number of mice administered 0, 5, 20, and 50 mg/kg ERGO was 12. On experimental day 14, NORT was first performed: each mouse was individually placed in an acrylic chamber (45 × 45 × 45 cm) without any objects and was allowed to explore for 10 min. On the next day, each mouse was placed in the same chamber with two identical objects located on a diagonal line. Animals were allowed to explore the chamber for five minutes (Supplementary Fig. S2). The time spent exploring each object was recorded. Twenty-four hours later, one of the objects was replaced by a novel object of a different shape at the same location in the chamber. Each mouse was allowed to explore the chamber under these conditions for five minutes. The exploration time for each object was recorded. The discrimination index was calculated as [(novel object exploration time/ total exploration time) – (familiar object exploration time/ total exploration time) × 100] (Table 1).

The SRT was conducted on the day after the final NORT day (Supplementary Fig. S1A): each mouse was individually placed in an acrylic chamber without any objects and allowed to explore for 10 min. On the next day, each mouse was placed in the same chamber with two identical objects located on a diagonal line. Animals were allowed to explore the chamber for five minutes (Supplementary Fig. S3). The time spent exploring each object was recorded. One hour later, one of the objects was moved, and each mouse was allowed to explore the chamber under these conditions for five minutes. The exploration time for each object was recorded. The discrimination index was calculated as [(moved object exploration time/ total exploration time) – (unmoved object exploration time/ total exploration time) × 100] (Table 1).

2.4. Measurement of ERGO Concentration

Repeated oral administration of ERGO at 0, 1, 5, 20, 50, or 100 mg/kg was performed in a separate set of normal mice at the age of 5 weeks, in the similar schedule to the behavioral tests. In these mice, the plasma was collected on experimental days 0, 7, 14, and 19 (Fig. S1A). Similarly, administration of ERGO was also performed in another set of mice at the age of 5 weeks in which the hippocampus was collected on experimental day 14. These experiments were performed to examine oral absorption and brain distribution of ERGO in mice. On the other hand, plasma and hippocampal samples were obtained in the same mice used for behavioral tests on the experimental day 19 (Supplementary Fig. S1A) to confirm reduction in basal level of ERGO and systemic absorption of ERGO in ERGO-free mice. All samples were preserved at –80 °C before the determination of ERGO concentration. Hippocampal samples were weighed, and portions were homogenized in 2 volumes of distilled water. Plasma and hippocampus homogenates were diluted 5- and 250-fold with water, respectively, deproteinized with methanol, and subjected to LC-MS/MS after centrifugation. The LC-MS/MS system was based on the LCMS-8040 model (Shimadzu, Kyoto, Japan). Chromatography was performed by means of step-gradient elution (flow rate, 0.4 mL/min) as follows: 0–0.5 min: 5% A/95% B; 0.5–3.5 min: 5% A/95% B to 70% A/30% B; 3.5–5.5 min: 70% A/30%

B; 5.5–5.6 min: 70% A/30% B to 5% A/95% B; 5.6–8 min: 5% A/95% B (A, water containing 0.1% formic acid; B, acetonitrile-containing 0.1% formic acid), using a Luna 3.0 μm HILIC column (200 Å, 150 × 2.0 mm; Phenomenex, Torrance, CA) at 40 °C. L-(+)-Ergothioneine-d9 was used as the internal standard.

2.5. Golgi Staining

Mice were purchased at the age of 5 weeks, 0 or 50 mg/kg ERGO was orally administered on experimental days 0, 2, 4, 7, 9, and 11 (Fig. S1B). Golgi staining was performed according to the recommended procedure of the FD Rapid GolgiStain Kit (PK401; FD Neuro Technologies, Columbia, MD, USA). On experimental day 14, mice were decapitated under anesthesia by pentobarbital, and brains were removed. Brains were put into the recommended solution and kept at room temperature in the dark for two weeks, followed by further incubation for 72 h in another solution. Brains were embedded in TFM (Triangle Biomedical Sciences, Durham, NC, USA), and coronal slices were cut at the thickness of 100 μm using a cryostat. The sections were placed on gelatin coated glass slides (Matsunami Glass, Osaka, Japan), dried overnight, washed with pure water, and immersed in the recommended solution for 10 min. The sections were washed with phosphate-buffered saline (PBS), sequentially immersed in 50, 75, and 90% ethanol, and then dehydrated in 100% ethanol, followed by 100% xylene. The sections were then coverslipped using Permount (Sigma-Aldrich, St. Louis, MO, USA) and observed with BZ9000 fluorescence microscope (Keyence, Osaka, Japan). Two to four neurons from the hippocampal dentate gyrus were randomly selected from each mouse for spine analysis. A total of nine to 10 neurons were analyzed in each group. Quantification of spines was performed using NIH ImageJ software. Spines were classified into 3 groups: mushroom, filopodia/thin, and stubby. Mushroom spines were characterized by a big head that was more than three times larger than its neck. Filopodia/thin spines were characterized by the absence of a head or the presence of a head that was not big. Stubby spines were characterized by their short and round appearance.

2.6. Neuronal Culture

Primary hippocampal neuronal cultures were performed according to the methods described by Nakamichi *et al.* [24], with minor modifications. In brief, hippocampi from 15-day-old embryonic ICR mice were dissected and incubated with 0.25% trypsin in PBS containing 28 mM glucose at 37°C for 20 min. Cells were mechanically dissociated using a 1,000-μL pipette tip in culture medium and plated at a density of 5×10^4 cells/cm² on plastic dishes that were coated with 7.5 μg/ml poly-L-lysine. Hippocampal neurons were cultured in Neurobasal™ media (Thermo Fisher Scientific, Waltham, MA, USA) that was supplemented with 100 U/mL penicillin, 100 μg/mL streptomycin, B-27 supplement, 0.5 mM glutamine, and 25 μM glutamate from 0 to 3 days *in vitro* (DIV) at 37°C in a humidified 5% CO₂ incubator (Fig. S1C). At three DIV, half of the culture medium was replaced with Neurobasal™ media supplemented with B-27

Table 1. Discrimination index in novel object recognition (NORT) and spatial recognition tests (SRT).

Discrimination index		ERGO (mg/kg) ^a				
		0	1	5	20	50
Normal mice	NORT ^b	1.83 ± 4.02	16.6 ± 5.6	16.3 ± 4.2	18.8 ± 3.6*	16.8 ± 4.6
	SRT ^c	1.63 ± 4.25	5.91 ± 6.18	10.5 ± 7.7	15.5 ± 6.5	24.9 ± 6.7*
ERGO-free mice	NORT ^b	-2.88 ± 7.55	- ^d	22.5 ± 4.0*	23.6 ± 3.4*	28.5 ± 4.3*
	SRT ^c	4.61 ± 4.38	- ^d	18.5 ± 5.0	18.9 ± 4.1	34.5 ± 3.4*

a) Orally administered in normal mice on days 0, 2, 4, 7, 9, and 11

b) Performed at three days after the last ERGO administration

c) Performed at six days after the last ERGO administration

d) Not performed

* Significant difference from the corresponding control values ($P < 0.05$)

supplement, 100 U/mL penicillin, 100 µg/mL streptomycin, and 0.5 mM glutamine, and cells were incubated for a further three days. At six DIV, the culture medium was replaced with NeurobasalTM media supplemented with 100 U/mL penicillin, 100 µg/mL streptomycin, and 0.5 mM glutamine. From 6 to 9 or 12 DIV, the cells were treated with 0, 5, 50, and 500 µM ERGO (Fig. S1C). For the inhibition study, 10 or 100 nM tropomyosin receptor kinase (Trk) inhibitor K252a dissolved in NeurobasalTM media that was supplemented with 100 U/mL penicillin, 100 µg/mL streptomycin, 0.5 mM glutamine, and 25 µM glutamate was added to the medium at six DIV and incubated for 20 min. The medium was then replaced with NeurobasalTM media that was supplemented with 100 U/mL penicillin, 100 µg/mL streptomycin, 0.5 mM glutamine, and 25 µM glutamate, and cells were incubated until 12 DIV (Fig. S1C).

2.7. Western Blot Analysis

Western blot analysis was performed according to the methods of Nakamichi *et al.* [25], with minor modifications. Hippocampal neurons were seeded at 5.0×10^4 cells/cm² on 12 well plastic dishes, cultured for 12 days, and washed twice with ice-cold PBS. Cells were centrifuged at 4°C for 5 min at 15,000 g after cell harvesting. Pellets thus obtained were suspended and sonicated in 20 mM Tris-HCl buffer (pH 7.5) containing 1 mM EDTA, 1 mM EGTA, 10 mM sodium fluoride, 10 mM sodium β-glycerophosphate, 10 mM sodium pyrophosphate, 1 mM sodium orthovanadate, and 1 µg/mL of various protease inhibitors [(p-amidinophenyl)methanesulfonyl fluoride, leupeptin, anti-pain, and benzamidin]. The suspensions were added at a volume ratio of 4:1 to 10 mM Tris-HCl buffer (pH 6.8) containing 10% glycerol, 2% sodium dodecylsulfate, 0.01% bromophenol blue, and 5% mercaptoethanol, and mixed at room temperature for one hour. The protein concentration was determined using a Bio-Rad Protein Assay Kit. The concentration of polyacrylamide gel was 7.5% for the detection of βIII-tubulin, microtubule-associated protein 2 (MAP2), and synapsin I, or 12.5% for the detection of mammalian target of rapamycin (mTOR), p-mTOR, S6K1, p-S6K1 (Ser371), p-S6K1 (Thr389), 4EBP1, and p-4EBP1. Each aliquot of 10 µg proteins was loaded on to a polyacrylamide

gel for electrophoresis at a constant current of 60 mA/2 plates for 100 min at room temperature, using a wide-mini-slab size PAGE system (Sima Biotech, Chiba, Japan), followed by blotting to a polyvinylidene fluoride membrane that was previously treated with 100% methanol. The membrane was blocked with a 2% bovine serum albumin (BSA) solution at 4°C overnight. The membrane was then reacted with antibodies against βIII-tubulin (1:10,000), MAP2 (1:10,000), Synapsin I (1:10,000), or β-actin (1:50,000) and diluted with buffer containing 0.2% BSA at room temperature for two hours while shaking [18], or reacted with antibodies against mTOR (1:1,000), p-mTOR (1:1,000), S6K1 (1:500), p-S6K1 (Ser371) (1:500), p-S6K1 (Thr389) (1:500), 4EBP1 (1:500), or p-4EBP1 (1:500) and diluted with Can Get Signal[®] at room temperature for two hours while shaking [26]. The membrane was then washed and reacted with an anti-mouse IgG (1:10,000–50,000) or anti-rabbit IgG (1: 2,000–10,000), diluted with 0.2% BSA or Can Get Signal[®]. Proteins reactive with these antibodies were detected with the aid of ECLTM detection reagents using a lumino image analyzer (LAS-4000; FUJIFILM, Tokyo, Japan). Densitometric determination was performed using ImageJ software.

2.8. Immunocytochemical Analysis

Hippocampal neurons were seeded at 1.25×10^4 cells/cm² on 12 well plastic dishes and cultured for 12 days. Neurons were washed with PBS, then fixed with 4% paraformaldehyde for 20 min at room temperature, and incubated for 30 min in blocking solution (3% BSA and 0.2% Triton X-100 in PBS) at room temperature. Cells were then incubated overnight in 10-times-diluted blocking solution containing antiserum against MAP2 (1:1,000) or an antibody against synapsin I (1:2,000) at 4°C, washed with PBS, and reacted with Alexa Fluor series-conjugated secondary antibodies (1:2,000) for one hour at room temperature. The cells were rinsed again with PBS, treated with mounting medium that contained DAPI, and observed under a confocal laser scanning microscope (LSM710) with a 63× objective. Five fields per well were chosen at random for analysis, and only non-clustered neurons were evaluated. The data were obtained from four wells in each preparation. To minimize

bias, neurons were evaluated blindly without the knowledge of the sample condition. Five neurons were analyzed from each well for the measurement of the number of synapsin I-positive puncta/10 μm neurite length, total neurite length, number of neurites, and Sholl analysis. Measurement of neurite length, total number of neurites, and Sholl analysis were conducted using the Simple neurite tracer plug-in [27] on Fiji, an open-source platform for biological-image analysis [28]. Sholl analysis was carried out at a 3.36 μm interval to a maximum radius of 137.2 μm . The area under the curve (AUC) was calculated using the trapezoidal rule for each Sholl profile.

2.9. Quantitative RT-PCR

Hippocampal neurons were seeded at 5.0×10^4 cells/cm² on 12 well plastic dishes and cultured for nine days. The total RNA was extracted from cultured cells according to the manufacturer's protocol of ISOGEN. cDNA was synthesized with oligo (dT)₁₂₋₁₈ primers, deoxynucleotide triphosphate mix, RT buffer, and MultiScribe Reverse Transcriptase, and amplified on Mx3005P (Agilent Technologies, Santa Clara, CA, USA) using a reaction mixture containing cDNA with the relevant forward and reverse primers and the THUNDERBIRD SYBR qPCR Mix. PCR reactions were initiated by template denaturation at 95°C for 15 min, followed by 40 cycles of amplification (denaturation at 95°C for 10 s, and primer annealing and extension at 60°C for 30 s). Relative quantification of expression levels of the target genes was determined by the delta-delta Ct method using transcripts of acidic ribosomal phosphoprotein P0 (36B4) as the internal standard. The sequences of the primers (5' to 3') were as follows: nerve growth factor (NGF) forward, TCTA-TACTGGCCGCAGTGAG and reverse, GGACATTGC-TATCTGTGTACGG; brain-derived neurotrophic factor (BDNF) forward, GCGGCAGATAAAAAGACTGC and reverse, TCAGTTGGCCTTTGGATACC; NT3 forward, GGAGGAAACGCTATGCAGAA and reverse, TTCTCT-GAGGCCGTGAAGTT; NT-5 forward, CCAAGTT-GAGGAAAACAA and reverse, TCCTCCGGGA-GAACTCCTAT; 36B4 forward, ACTGGTCTAGGACCC-GAGAAG and reverse, TCCCACCTTGTCTCCAGTCT.

2.10. Statistical Analysis

Data are expressed as the mean \pm S.E.M. The statistical significance of differences was determined by means of Student's t-test or one-way or repeated measures ANOVA, using Excel or IBM SPSS Statistics (Chicago, IL, USA), followed by the appropriate post-hoc tests. $P < 0.05$ was regarded as denoting a significant difference.

3. RESULTS

3.1. Enhancement of Object Recognition and Object Location Memory by Oral Administration of ERGO

To investigate whether oral intake of ERGO enhances the learning and memory ability under normal conditions, the experimental schedule in NORT was first constructed using mice that had not been exposed to ERGO treatment (Fig.

S2). The exploration time for the novel object was significantly longer than that for the familiar one under the condition that retention time was set to be three hours, whereas the exploration time was not different between the novel and familiar objects under the condition that retention time was set to 24 h (Fig. S2). This suggests that mice cannot recognize a difference between the novel and familiar object after a 24 h retention time. Thus, the enhancement effect of ERGO on object recognition memory was next observed under the condition that retention time was set to 24 h. ERGO was orally administered at 0–50 mg/kg three times per week for two weeks, and then NORT was performed (Fig. S1A). In retention trials, the exploration time for the novel object was significantly longer than that for the familiar object in normal mice administered 1–50 mg/kg ERGO, whereas the exploration time for the two objects was similar in normal mice that had not been treated with ERGO (Fig. 1A). The similar results were obtained in ERGO-free mice (Fig. 1B). The discrimination index at each dose was calculated to compare object recognition ability. The discrimination index was significantly higher in normal mice exposed to ERGO at a dose of 20 mg/kg than in the control group (Table 1). The discrimination index was significantly higher in ERGO-free mice exposed to ERGO at a dose of 5 mg/kg or higher dose than in the control group (Table 1). These results suggest that oral administration of ERGO enhances the object recognition memory under normal conditions in mice.

Next, the possible enhancement effect of oral administration of ERGO on object location memory was investigated using the SRT. In mice that were not exposed to ERGO treatment, the exploration time for the moved object was significantly longer than that for the unmoved object when measurement time was set to 10 min, whereas the exploration time was minimally different between the moved and unmoved objects when the measurement time was set to five minutes (Fig. S3). Thus, the enhancement effect of ERGO on object location memory was next examined under the condition that measurement time was five minutes. In retention trials, the exploration time for the moved object tended to be longer than that for the unmoved object in normal mice that were treated with 50 mg/kg ERGO (Fig. 1C). The exploration time for the moved object was significantly longer than that for the unmoved object in ERGO-free mice administered 5 or 50 mg/kg ERGO, whereas the exploration time for the two objects was similar in ERGO-free mice that had not been treated with ERGO (Fig. 1D). The discrimination index at each dose was calculated to compare spatial recognition ability. The discrimination index was significantly higher in normal and ERGO-free mice exposed to ERGO at a dose of 50 mg/kg than in the control group (Table 1). This suggests that oral administration of ERGO may also enhance object location memory under normal conditions in mice.

3.2. Plasma and Hippocampal Concentration of ERGO after Oral Administration

To support the findings that oral administration of ERGO has an enhancement effect on learning and memory ability

ty, we examined the gastrointestinal absorption and distribution to the hippocampus of ERGO following oral administration. During and after oral administration of ERGO (1–100 mg/kg) three times per week for two weeks, the plasma concentration profile of ERGO was measured. The plasma concentration of ERGO was remarkably higher in the mice that were treated with 100 mg/kg ERGO than in the control group from days 7 to 19 (Fig. 2A). In the group treated with 50 mg/kg ERGO, the plasma concentration of ERGO tended to be higher than that in the control on day 7 and this difference reached significance on day 14 (Fig. 2A). In the group treated with 20 mg/kg ERGO, the plasma concentration of ERGO also tended to be higher than that in the control group on day 14 (Fig. 2A). Meanwhile, the hippocampal concentration of ERGO on day 14 in the group treated with ERGO was also measured and showed a dose-dependent increase (Fig. 2B). The hippocampal concentration of ERGO in the group treated with ERGO at 20 mg/kg or more was significantly higher than that in the control group (Fig. 2B). The plasma and hippocampal concentrations of ERGO were also increased in a dose-dependent manner in ERGO-free mice (Table S1). These results indicate that orally administered ERGO is absorbed from the gastrointestinal tract and distributed to the hippocampus, after passing through the blood-brain barrier. These results support the finding that

learning and memory ability is enhanced after oral administration of ERGO and suggest that this may result from the action of ERGO being distributed to the hippocampus.

3.3. Promotive Effect of ERGO on Neuronal Maturation in the Hippocampal Dentate Gyrus

Neuronal maturation was next examined as a possible mechanism of action for the learning and memory enhancement observed after oral administration of ERGO. Golgi staining demonstrated that neurons with numerous neurites existed in the hippocampal dentate gyrus of the control group (Fig. 3A). Furthermore, morphological observation of the neurites revealed the existence of at least three types of spines (mushroom, filopodia/thin, and stubby; (Fig. 3B). In the dentate gyrus of mice that were orally administered 50 mg/kg ERGO three times per week for two weeks, there appeared to be more mushroom type spines than in the control group (Fig. 3C). Quantification of the number of each type of spines in each condition revealed that the population of mushroom type spines in the ERGO-treated group was significantly higher than that observed in the control group (Fig. 3D). These results suggest that oral administration of ERGO may promote neuronal maturation in the hippocampal dentate gyrus.

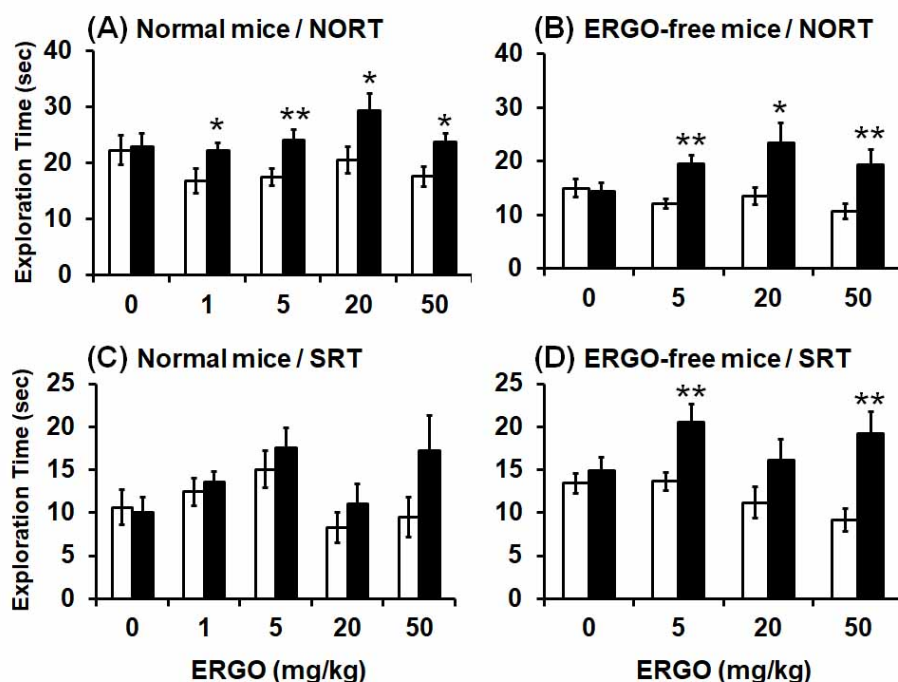


Fig. (1). Effect of oral administration of ERGO on object recognition and object location memory under normal conditions. Normal (A, C) and ERGO-free (B, D) mice were orally administered ERGO at 0, 1, 5, 20, or 50 mg/kg on days 0, 2, 4, 7, 9, and 11. Three and six days after the final ERGO administration, NORT (A, B) and SRT (C, D) were conducted, respectively, and the exploration time was measured. The white and black columns in panels (A) and (B) display the exploration time for the familiar and novel objects, respectively. The white and black columns in panels (C) and (D) show the exploration time for the unmoved and moved objects, respectively. Each value represents the mean \pm S.E.M. (n = 12–15). * Significant difference from the control ($P < 0.05$); ** Significant difference from the control ($P < 0.01$)

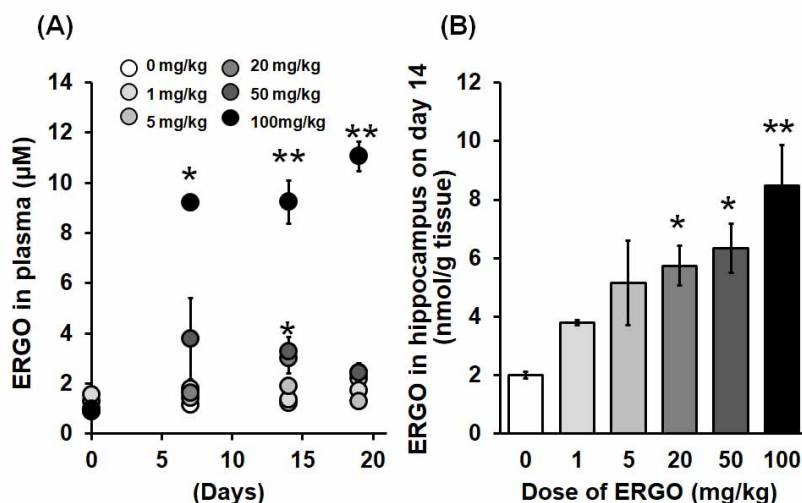


Fig. (2). ERGO concentration in the plasma (A) and hippocampus (B) after oral administration of ERGO. Mice were orally administered 0, 1, 5, 20, 50, or 100 mg/kg ERGO on days 0, 2, 4, 7, 9, and 11. Plasma samples were collected on days 0, 7, 14, and 19, and hippocampal samples were collected on day 14. The ERGO concentration was then measured by LC-MS/MS. Each value represents the mean ± S.E.M. (n = 3–6). * Significant difference from the values obtained in mice not treated with ERGO ($P < 0.05$); ** Significant difference the values obtained in mice not treated with ERGO ($P < 0.01$)

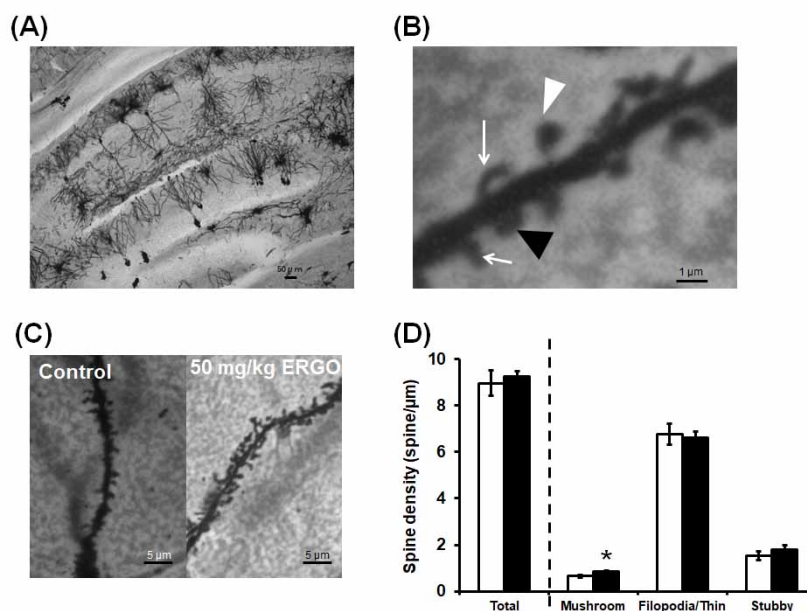


Fig. (3). Effect of oral administration of ERGO on spine morphology in the hippocampal dentate gyrus. Mice were orally administered 0 or 50 mg/kg ERGO on days 0, 2, 4, 7, 9, and 11. On day 14, the brain was collected for Golgi staining. Neurons in the hippocampal dentate gyrus were observed, and spines were classified. (A) A representative image of Golgi staining in the hippocampus of the control group. Scale bar: 50 µm. (B) Examples of the three classifications of spines in the control group. The white triangle indicates the mushroom-type spine, the white arrows indicate the filopodia/thin-type spines, and the black triangle indicates the stubby-type spine. Scale bar: 1 µm. (C) Representative images of dendritic branches in the hippocampal dentate gyrus of control mice and mice treated ERGO. Scale bar: 5 µm. (D) The quantitative results of spine morphological analysis in control mice (white) and mice treated with ERGO (black). Nine to 10 neurons from three mice were analyzed in each group. Each value represents the mean ± S.E.M. (n = 9–10). * Significant difference from the control group ($P < 0.05$).

3.4. Promotive Effect of ERGO on Cellular Maturation in Primary Cultured Hippocampal Neurons

To further investigate the promotive effect of ERGO on neuronal maturation, the expression of neuronal maturation-related markers was examined through quantitative PCR and Western blotting in primary cultured hippocampal neurons. The expression of mRNA for β III-tubulin and synapsin I was significantly higher in the hippocampal neurons that were exposed to 50 or 500 μ M ERGO than in the control group (Fig. 4A). Exposure of hippocampal neurons to 5–500 μ M ERGO also elevated the protein expression of β III-tubulin and synapsin I in a concentration-dependent manner (Fig. 4B, C). To confirm that exposure to ERGO increased the expression of these neuronal markers through a mechanism distinct from its neuroprotective effect, the protective effect of ERGO was also examined under the same culture condition. No significant difference was observed in

the number of Hoechst- and propidium iodide (PI)-positive cells between the control and ERGO-treated groups (Fig. S4). This result indicates a minimal protective effect of ERGO under this experimental condition. Meanwhile, exposure to ERGO minimally affected the expression of MAP2 at both the mRNA and protein level (Fig. 4). In cultured hippocampal neurons, more synapsin I-positive puncta per neurite were observed in the group exposed to 500 μ M ERGO than in the control group (Fig. 5A, B). However, ERGO exposure appeared to minimally affect neurite length (Fig. 5C) and the number of neurites per cell (Fig. 5D). However, the number of neurite intersections was significantly higher in the groups that were exposure to 50 and 500 μ M ERGO than in the control group (Fig. 5E, F). These results suggest that ERGO may promote synapse formation by increasing the number of neurite intersections in hippocampal neurons, supporting a promotive effect of ERGO on neuronal maturation.

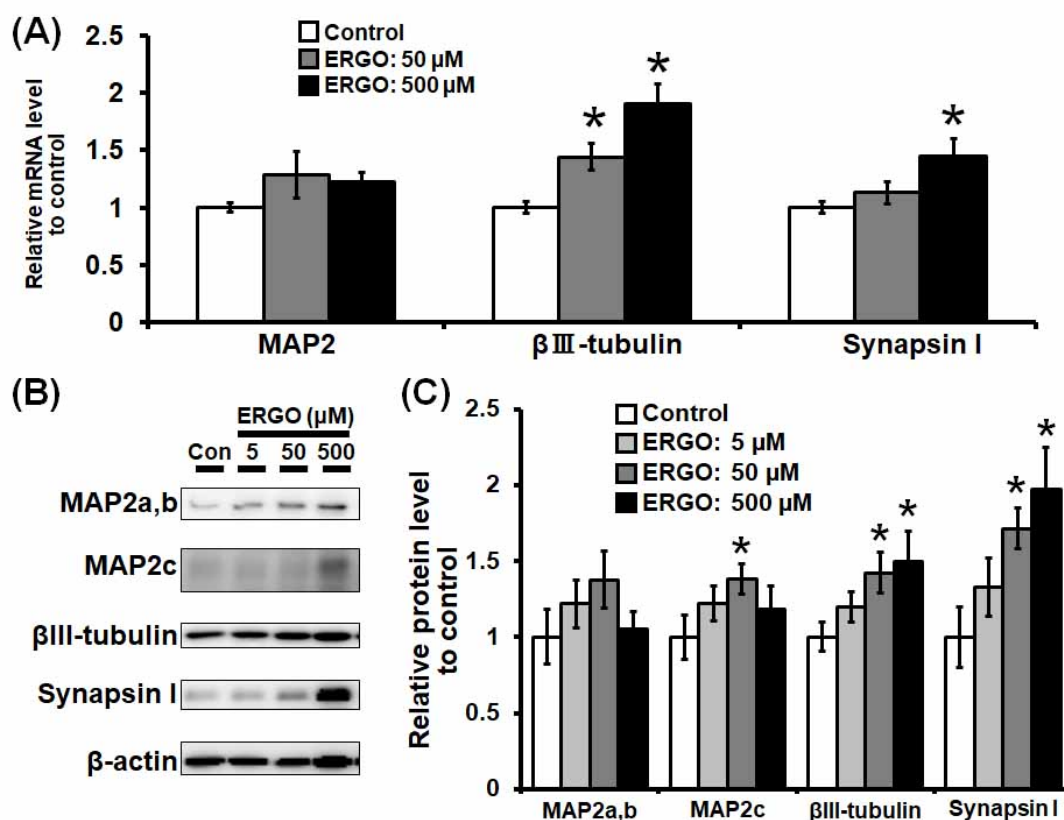


Fig. (4). Effect of ERGO on the expression of neuronal maturation markers in primary cultured hippocampal neurons. Hippocampal neurons were cultured in neurobasal medium supplemented with B-27 for six days, followed by further culture in neurobasal medium without B-27 in either the absence (white columns) or presence (gray or black columns) of ERGO until experimental day 12. (A) The total RNA was extracted from neurons cultured for 9 days for quantitative RT-PCR analysis. Data were normalized by the expression level of 36B4 mRNA and expressed as relative values to the corresponding control obtained in the absence of ERGO. The mRNA expression of MAP2, β III-tubulin, and synapsin I was evaluated in the control group and in mice treated with ERGO at 50 and 500 μ M. Each value represents the mean \pm S.E.M. ($n = 9$). (B, C) Neurons cultured for 12 days were homogenized, followed by SDS-PAGE for immunoblotting using antibodies against MAP2, β III-tubulin, and synapsin I. In panel (B), typical immunoblots were shown. In panel (C), data were normalized by the expression level of β -actin and expressed as relative values to the corresponding control obtained in the absence of ERGO. Each value represents the mean \pm S.E.M. ($n = 8-11$). * Significant difference from the control ($P < 0.05$).

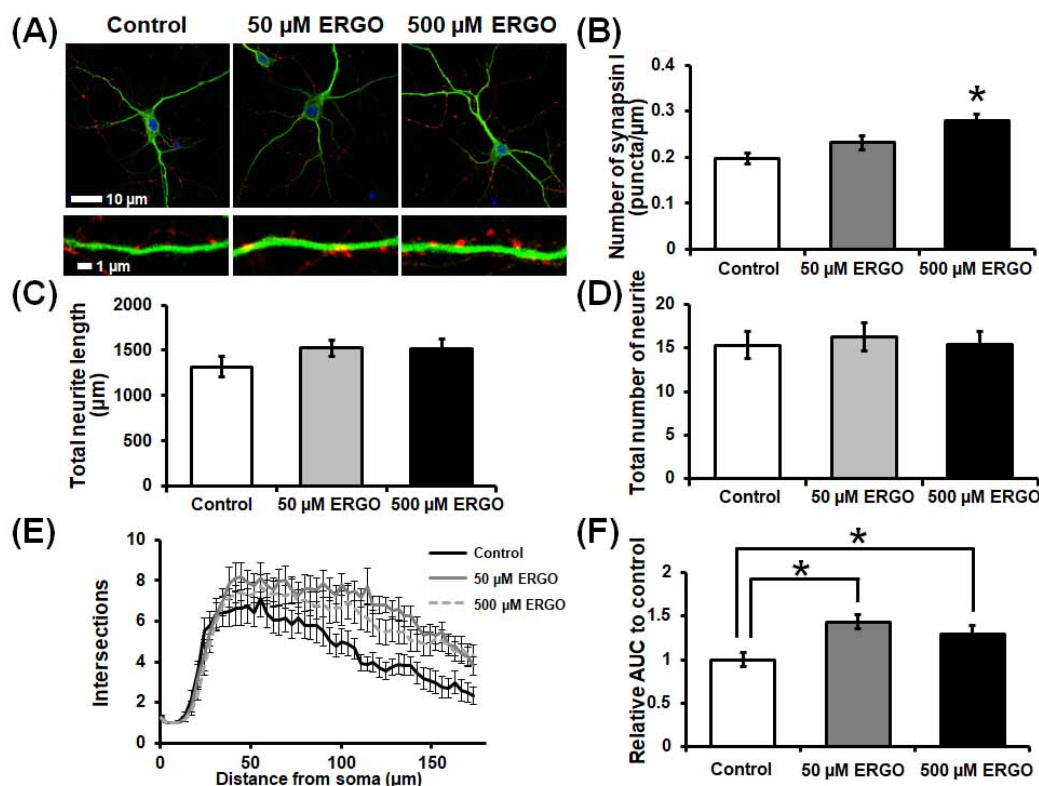


Fig. (5). Effect of ERGO on synapse formation and neurite outgrowth in primary cultured hippocampal neurons. Hippocampal neurons were cultured in neurobasal medium supplemented with B-27 for six days, followed by further culture in neurobasal medium without B-27 in either the absence (white columns) or presence (gray or black columns) of ERGO until experimental day 12. (A) Primary hippocampal neurons were fixed with 4% paraformaldehyde, followed by immunocytochemical detection of neuronal marker MAP2 (green), synapse marker synapsin I (red), and nuclear marker DAPI (blue). Scale bars: 1 (lower panel) or 10 μm (upper panel). The merged images are shown. (B) The number of puncta that were positive for synapsin I were counted by using ImageJ software and normalized by the length of neurites. Each value represents the mean \pm S.E.M. ($n = 15\text{--}20$). (C–F) The length (C) and number (D) of neurites per cell were measured. Sholl analysis was also carried out using simple neurite tracer plug-in on Fiji (E), and the AUC was calculated using the trapezoidal rule for each Sholl profile (F). Twenty neurons in each group were analyzed. Each value represents the mean \pm S.E.M. ($n = 20$). * Significant difference from the control ($P < 0.05$).

3.5. Induction of Neurotrophic Factors and Activation of mTORC1 Signaling by ERGO

To further investigate the mechanism underlying the promotion of neuronal maturation by ERGO, the possible induction of the expression of neurotrophic factors by ERGO was examined in cultured hippocampal neurons. The expression of mRNA for NT3 and NT5 was higher in the ERGO-treated group than in the control group (Fig. 6A). This ERGO-induced increase in the expression of NT3 and NT5 mRNA was concentration-dependent (Fig. 6A). However, the expression of NGF mRNA was slightly lower in the group exposed to 500 μM ERGO than in the control (Fig. 6A). Additionally, the mRNA expression of BDNF was minimally changed by ERGO (Fig. 6A). Next, the effect of inhibitor of Trk, which is the receptor for NT3 and NT5, on the expression of synapsin I was examined. The increase in the gene product of synapsin I that was provoked by ERGO was significantly suppressed in the presence of the Trk inhibitor

K252a at a concentration of 100 μM (Fig. 6B, C). This suggests the possible involvement of Trk signaling in the effects of ERGO.

Because ERGO is an amino acid and is incorporated into the intracellular space by the transporter OCTN1, the possible activation of the intracellular amino acid sensor mTORC1 signaling by ERGO was examined in cultured hippocampal neurons. In rodents, three isoforms of 4EBP1 are detected: α is the least phosphorylated form, β is an intermediate form, and γ is a hyperphosphorylated isoform [29]. The expression of phosphorylated mTOR and its downstream effector, 4EBP1, in hippocampal neurons was higher in the group exposed to ERGO than in the control group, whereas the phosphorylation of S6K1 was minimally changed by ERGO (Fig. 7). These results suggest that ERGO may promote cellular maturation at least in part through the induction of the neurotrophic factors NT3 and NT5, and activation of the Trk/mTORC1 signaling pathway in hippocampal neurons.

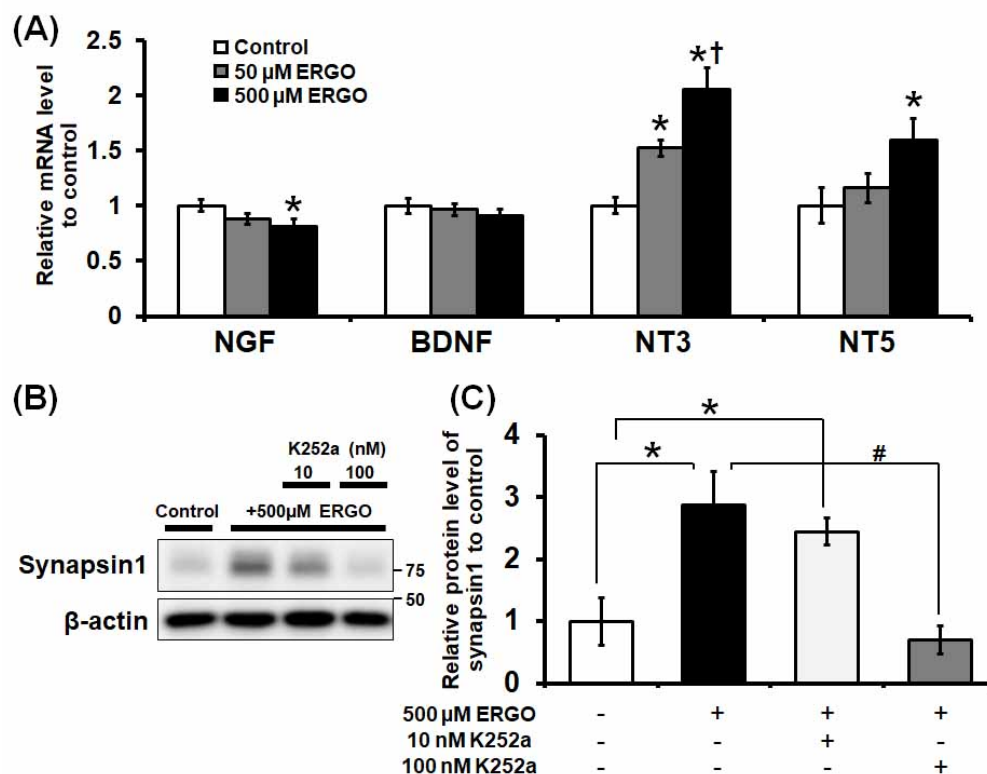


Fig. (6). Involvement of neurotrophic factor signaling in ERGO-induced neuronal maturation in cultured hippocampal neurons.

Hippocampal neurons were cultured in neurobasal medium supplemented with B-27 for six days, followed by further culture in neurobasal medium without B-27 in either the absence (white columns) or presence (gray or black columns) of ERGO until experimental day 9 or 12. (A) The total RNA was extracted from neurons cultured for 9 days for quantitative RT-PCR analysis. Data were normalized by the expression level of 36B4 mRNA and expressed as relative values to the corresponding control obtained in the absence of ERGO. Each value represents the mean \pm S.E.M. ($n = 9$). (B, C) Neurons that were cultured for six days were exposed to the Trk inhibitor, K252a (10 or 100 nM), for 20 min and further cultured in either the absence (white columns) or presence (gray or black columns) of 500 μ M ERGO until experimental day 12. Cultured neurons were then homogenized, followed by SDS-PAGE for immunoblotting using an antibody against MAP2, β III-tubulin, and synapsin I. In panel (B), typical immunoblots are shown. In panel (C), data were normalized by the expression level of β -actin and expressed as relative values to the corresponding control obtained in the absence of ERGO. Each value represents the mean \pm S.E.M. ($n = 8-11$). * Significant difference from the control obtained in the absence of ERGO ($P < 0.05$); † Significant difference from the value obtained in neurons treated with 50 μ M of ERGO ($P < 0.05$); # Significant difference from the values obtained in the presence of ERGO alone ($P < 0.05$).

4. DISCUSSION

The present study demonstrated that the food-derived ingredient ERGO is distributed to the hippocampus through the blood-brain barrier after oral administration, and that ERGO may enhance learning and memory ability at least in part through the promotion of neuronal maturation in the hippocampus. It is noteworthy that the NORT results indicated a significant effect of ERGO at 5 mg/kg (Fig. 1A, Table 1), while both the NORT and SRT results indicated a promotive effect of ERGO at 20 or 50 mg/kg (Table 1). This dose of ERGO yielded a systemic concentration of 3–4 μ M (Fig. 2A). This ERGO concentration is clinically relevant since Cheah *et al.* recently reported a pharmacokinetic study of orally administered ERGO in healthy volunteers, which indicated that the plasma concentration of ERGO was 1 μ M at the basal level and 2–3 μ M after repeated daily oral adminis-

tration of ERGO at a dose of 25 mg/body [21]. Thus, the enhancement effect of ERGO on brain function may be advantageous in terms of its clinical application.

Because ERGO is ingested from the daily diet, ERGO exists in the plasma and hippocampus in normal mice that were not administered ERGO (Fig. 2). Nevertheless, exogenously administered ERGO displayed an enhancement effect on the learning and memory ability (Fig. 1, Table 1). The ERGO concentration in the hippocampus after oral administration for two weeks showed a significant increase at a dose of 20 mg/kg or than (Fig. 2B), whereas, the discrimination index for the NORT in the group that was exposed to ERGO at a dose of 20 mg/kg was significantly higher than in the control group. The discrimination index for the SRT tended to be higher in the group exposed to 20 mg/kg ERGO than in the control group (Table 1). These results support the

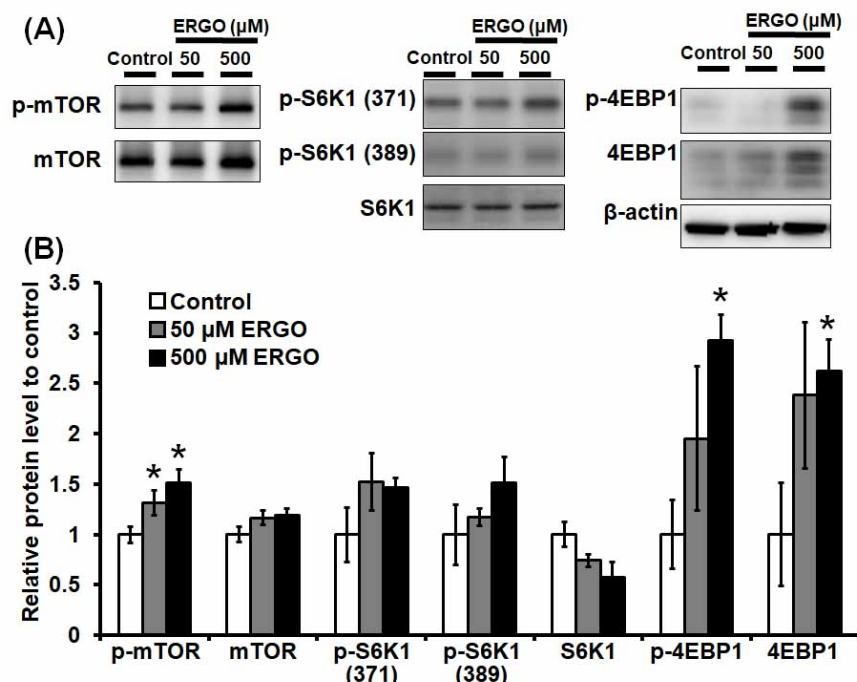


Fig. (7). Activation of the mTOR signaling pathway by ERGO in cultured hippocampal neurons.

Hippocampal neurons were cultured in neurobasal medium supplemented with B-27 for six days, followed by further culture in neurobasal medium without B-27 in either the absence (white columns) or presence (gray or black columns) of ERGO until experimental day 12. Cultured neurons were homogenized, followed by SDS-PAGE for immunoblotting using antibodies against p-mTOR, mTOR, p-S6K1 (Ser371), p-S6K1 (Thr389), S6K1, p-4EBP1, 4EBP1, and β-actin. In panel (A), typical immunoblots are shown. In panel (B), data were normalized by the protein level of β-actin and expressed as relative values to the corresponding control. Each value represents the mean ± S.E.M. (n = 4–12). * Significant difference from the control ($P < 0.05$).

theory that ERGO may be incorporated in the hippocampus and may exert an enhancing effect on learning and memory. This hypothesis is also supported by the previous finding that OCTN1, which actively transports ERGO into the intracellular space, is expressed in both neurons [24] and neural stem cells [18]. Neural stem cells are abundantly present in the hippocampus. Additionally, exposure to ERGO leads to the uptake of ERGO in cultured neural stem cells and promotes cellular differentiation into neurons [18]. Learning and memory ability are improved by the promotion of neurogenesis in the hippocampus [30], whereas spatial memory declines when hippocampal neurogenesis is inhibited [31], suggesting that there is a potential association between hippocampal neurogenesis and brain function. The oral intake of a diet containing ERGO promotes neurogenesis in the murine hippocampus [14], further supporting a role of ERGO in the enhancement of learning and memory ability, at least in part through promotion of neurogenesis and neuronal maturation. Expression of the uptake transporter OCTN1 for ERGO in neurons and neural stem cells would be advantageous for ERGO to exert its biological activity in the brain since the concentration of ERGO in the hippocampus after 14 days of oral ERGO administration at 5–20 mg/kg was 5–6 μM, which is 2–3 times higher than that in plasma (2–3 μM) if we assume that the specific gravity of the hippocampal tissue is 1.

It is noteworthy that ERGO enhanced object recognition memory under normal conditions (Fig. 1, Table 1). Improvement of the learning and memory ability in dementia is an urgent social problem. Therefore, compounds that improve the impaired learning and memory ability in aged and/or brain-damaged animals have been extensively researched. In fact, it has been reported that curcumin and acetyl-L-carnitine both improve the impaired learning and memory ability in aged animals [32, 33]. However, limited reports are available on compounds that exert an enhancement effect on learning and memory under normal conditions. Advanced learning and memory abilities are advantageous for successful living in human society, which consists of diverse and advanced social tasks [34, 35]. The compounds that can be taken from daily diet and exert an enhancement effect on learning and memory could possess a prophylactic activity against dementia. Therefore, improvement of brain function through the daily diet is of great interest to healthy people as well as diseased people. Oral administration of ERGO exerted an improvement in learning and memory in the healthy condition (Fig. 1, Table 1). Because ERGO is a food-derived compound, improvement of brain function may be expected by its daily ingestion. Krill phosphatidylserine and certain types of nucleotide are also known as compounds that exert enhancement effects on the learning and memory ability in normal animals [36, 37]. However, limited informa-

tion is available regarding the clinical relevance of the dose required for such enhancement effect. Additionally, the mechanism controlling the systemic exposure of these compounds is mostly unknown, whereas the exposure of ERGO in the body is principally governed by OCTN1 [11, 13]. Mice were used at the age of 5 weeks in the present study. Further studies using aged mice are required to consider the prevention of dementia.

In the present study, the promotion of neuronal maturation, such as synapse formation, by ERGO was demonstrated in hippocampal neurons (Figs. 3, 4, 5). This may also be associated with the enhancement effect of ERGO on learning and memory, since neuronal activity in the hippocampus plays a crucial role in learning and memory, and synapse formation is essential for neuronal activity. This may also imply that the neuronal maturation that is provoked by ERGO may exert an enhancement effect not only on learning and memory, but also on other brain functions. The antidepressant effect of ERGO has already been demonstrated through oral administration in mice [14]. Antidepressants, such as fluoxetine and agomelatine, also exhibit a promotive effect on neuronal maturation and neurogenesis [38, 39]. Exposure to ERGO increased the expression of NT3 and NT5 in hippocampal neurons (Fig. 6). These neurotrophic factors caused neurite outgrowth [40, 41]. Administration of NT3 improves memory impairment in adult rats with damaged basal forebrain cholinergic neurons [42]. Furthermore, administration of NT5 also improves memory impairment in aged rats [43]. Thus, the induction of these neurotrophic factors may be at least partially associated with the enhancing effect of ERGO on learning and memory ability.

The transporter, OCTN1, is ubiquitously expressed in almost all of the bodily organs, at least in mice. This expression profile is compatible with the existence of ERGO in those organs, including brain, at the μM to sub mM range in wild-type mice, while ERGO is absent in the *octn1* gene knockout mice [11]. Exogenous administration of ERGO improved brain function in the present study (Fig. 1, Table 1). Similar beneficial effects of ERGO have also been observed in the peripheral organs. Administration of ERGO yields a protective effect against ischemia-reperfusion injury in the heart, small intestine, and liver [11, 44-46] and suppresses liver fibrosis [23], acute lesions in the lung [47], and skin aging [48]. These results support the existence of potential pharmacological activities of ERGO in various organs in the body, implying that it is a potential target of novel therapeutic agents for diseased conditions. However, the molecular mechanism(s) of ERGO, other than its antioxidant activity, that may underlie such pharmacological activities are largely unknown. In the present study, activation of the Trk/mTOR-C1 signaling pathway was proposed in hippocampal neurons (Figs. 6, 7). Yoshida *et al.* recently proposed that ERGO has immune-enhancing properties, through the potentiation of the toll-like receptor signaling pathway [49]. Further clarification of the mechanisms that underlie the action of ERGO will clarify its potential as a therapeutic target.

CONCLUSION

The food-derived hydrophilic amino acid, ERGO, is distributed to the hippocampus after oral administration and may enhance learning and memory abilities, at least in part, through the promotion of neuronal maturation in the hippocampus in normal mice. This pharmacological effect of ERGO in the brain is observed at a plasma ERGO concentration achievable in humans. Although further clarification of the mechanisms that underlie the action of ERGO, considering its safety, based on the ingestion of ERGO as a food ingredient for many years, and the transporter-mediated gastrointestinal absorption of ERGO followed by its uptake into brain parenchymal cells, this compound may be a unique target for improving brain function in normal subjects.

LIST OF ABBREVIATIONS

AUC	=	Area under the curve
BDNF	=	Brain-derived neurotrophic factor
BSA	=	Bovine serum albumin
DIV	=	Days <i>in vitro</i>
ERGO	=	Ergothioneine
MAP2	=	Microtubule-associated protein 2
NGF	=	Nerve growth factor
mTOR	=	Mammalian target of rapamycin
NORT	=	Novel object recognition test
NT	=	Neurotrophin
PBS	=	Phosphate-buffered saline
PI	=	Propidium iodide
SRT	=	Spatial recognition test
Trk	=	Tropomyosin receptor kinase
36B4	=	Acidic ribosomal phosphoprotein P0

ETHICS APPROVAL AND CONSENT TO PARTICIPATE

All animal procedures used in the present work were approved by the Kanazawa University Animal Care Committee (approval number: AP-183968).

HUMAN AND ANIMAL RIGHTS

All animal experiments were carried out in accordance with the NC3Rs ARRIVE guidelines. The animals were cared for in strict compliance with the guidelines outlined in the National Institutes of Health Guide for the Care and Use of Laboratory Animals.

CONSENT FOR PUBLICATION

Not applicable.

AVAILABILITY OF DATA AND MATERIALS

The datasets used and/or analysed during the current study are available from the corresponding author on reasonable request.

FUNDING

This work was partially supported by Grants-in-Aid for Scientific Research to NN (No. 19K07126) and YK (No. 15H04664) from the Ministry of Education, Culture, Sports, Science, and Technology of Japan, and by the Hoansha Foundation (Osaka, Japan) to YK

CONFLICT OF INTEREST

The author declares no conflict of interest, financial or otherwise.

ACKNOWLEDGEMENTS

The authors would like to thank Dr. Akihiro Tanaka in Yukiguni Maitake Co. Ltd. and Dr. Jean-Claude Yadan in TETRAHEDRON for their kind arrangement in providing ergothioneine. The authors would also like to thank Ms. Moe Mitamura at the Kanazawa University for technical assistance.

SUPPLEMENTARY MATERIAL

Supplementary material is available on the publisher's web site along with the published article.

REFERENCES

- [1] World Health Organization. *Dementia: Key facts.*, <http://www.who.int/news-room/fact-sheets/detail/dementia>
- [2] Briggs, R.; Kennelly, S.P.; O'Neill, D. Drug treatments in Alzheimer's disease. *Clin. Med. (Lond.)*, **2016**, *16*(3), 247-253. [<http://dx.doi.org/10.7861/clinmedicine.16-3-247>] [PMID: 27251914]
- [3] Weller, J.; Budson, A. Current understanding of Alzheimer's disease diagnosis and treatment. *F1000Res*, **2018**, *7* F1000 Faculty Rev-1161 [<http://dx.doi.org/10.12688/f1000research.14506.1>]
- [4] Venäläinen, O.; Bell, J.S.; Kirkpatrick, C.M.; Nishtala, P.S.; Liew, D.; Iiomäki, J. Adverse Drug Reactions Associated With Cholinesterase Inhibitors-Sequence Symmetry Analyses Using Prescription Claims Data. *J. Am. Med. Dir. Assoc.*, **2017**, *18*(2), 186-189. [<http://dx.doi.org/10.1016/j.jamda.2016.11.002>] [PMID: 28043802]
- [5] Li, Q.; Zhao, H.F.; Zhang, Z.F.; Liu, Z.G.; Pei, X.R.; Wang, J.B.; Cai, M.Y.; Li, Y. Long-term administration of green tea catechins prevents age-related spatial learning and memory decline in C57BL/6 J mice by regulating hippocampal cyclic amp-response element binding protein signaling cascade. *Neuroscience*, **2009**, *159*(4), 1208-1215. [<http://dx.doi.org/10.1016/j.neuroscience.2009.02.008>] [PMID: 19409206]
- [6] Kodali, M.; Parihar, V.K.; Hattiangady, B.; Mishra, V.; Shuai, B.; Shetty, A.K. Resveratrol prevents age-related memory and mood dysfunction with increased hippocampal neurogenesis and microvasculature, and reduced glial activation. *Sci. Rep.*, **2015**, *5*, 8075. [<http://dx.doi.org/10.1038/srep08075>] [PMID: 25627672]
- [7] Yook, J.S.; Okamoto, M.; Rakwal, R.; Shibato, J.; Lee, M.C.; Matsui, T.; Chang, H.; Cho, J.Y.; Soya, H. Astaxanthin supplementation enhances adult hippocampal neurogenesis and spatial memory in mice. *Mol. Nutr. Food Res.*, **2016**, *60*(3), 589-599. [<http://dx.doi.org/10.1002/mnfr.201500634>] [PMID: 26643409]
- [8] Park, H.R.; Kong, K.H.; Yu, B.P.; Mattson, M.P.; Lee, J. Resveratrol inhibits the proliferation of neural progenitor cells and hippocampal neurogenesis. *J. Biol. Chem.*, **2012**, *287*(51), 42588-42600. [<http://dx.doi.org/10.1074/jbc.M112.406413>] [PMID: 23105098]
- [9] Edwards, J.A.; Bellion, P.; Beilstein, P.; Rumbeli, R.; Schierle, J. Review of genotoxicity and rat carcinogenicity investigations with astaxanthin. *Regul. Toxicol. Pharmacol.*, **2016**, *75*, 5-19. [<http://dx.doi.org/10.1016/j.yrtph.2015.12.009>] [PMID: 26713891]
- [10] Kato, Y.; Kubo, Y.; Iwata, D.; Kato, S.; Sudo, T.; Sugiura, T.; Kagaya, T.; Wakayama, T.; Hirayama, A.; Sugimoto, M.; Sugihara, K.; Kaneko, S.; Soga, T.; Asano, M.; Tomita, M.; Matsui, T.; Wada, M.; Tsuji, A. Gene knockout and metabolome analysis of carnitine/organic cation transporter OCTN1. *Pharm. Res.*, **2010**, *27*(5), 832-840. [<http://dx.doi.org/10.1007/s11095-010-0076-z>] [PMID: 20224991]
- [11] Halliwell, B.; Cheah, I.K.; Tang, R.M.Y. Ergothioneine - a diet-derived antioxidant with therapeutic potential. *FEBS Lett.*, **2018**, *592*(20), 3357-3366. [<http://dx.doi.org/10.1002/1873-3468.13123>] [PMID: 29851075]
- [12] Gründemann, D.; Harlfinger, S.; Golz, S.; Geerts, A.; Lazar, A.; Berkels, R.; Jung, N.; Rubbert, A.; Schömig, E. Discovery of the ergothioneine transporter. *Proc. Natl. Acad. Sci. USA*, **2005**, *102*(14), 5256-5261. [<http://dx.doi.org/10.1073/pnas.0408624102>] [PMID: 15795384]
- [13] Sugiura, T.; Kato, S.; Shimizu, T.; Wakayama, T.; Nakamichi, N.; Kubo, Y.; Iwata, D.; Suzuki, K.; Soga, T.; Asano, M.; Iseki, S.; Tamai, I.; Tsuji, A.; Kato, Y. Functional expression of carnitine/organic cation transporter OCTN1/SLC22A4 in mouse small intestine and liver. *Drug Metab. Dispos.*, **2010**, *38*(10), 1665-1672. [<http://dx.doi.org/10.1124/dmd.110.032763>] [PMID: 20601551]
- [14] Nakamichi, N.; Nakayama, K.; Ishimoto, T.; Masuo, Y.; Wakayama, T.; Sekiguchi, H.; Sutoh, K.; Usumi, K.; Iseki, S.; Kato, Y. Food-derived hydrophilic antioxidant ergothioneine is distributed to the brain and exerts antidepressant effect in mice. *Brain Behav.*, **2016**, *6*(6)e00477 [<http://dx.doi.org/10.1002/brb3.477>] [PMID: 27134772]
- [15] Aruoma, O.I.; Spencer, J.P.; Mahmood, N. Protection against oxidative damage and cell death by the natural antioxidant ergothioneine. *Food Chem. Toxicol.*, **1999**, *37*(11), 1043-1053. [[http://dx.doi.org/10.1016/S0278-6915\(99\)00098-8](http://dx.doi.org/10.1016/S0278-6915(99)00098-8)] [PMID: 10566875]
- [16] Song, T.Y.; Chen, C.L.; Liao, J.W.; Ou, H.C.; Tsai, M.S. Ergothioneine protects against neuronal injury induced by cisplatin both in vitro and in vivo. *Food Chem. Toxicol.*, **2010**, *48*(12), 3492-3499. [<http://dx.doi.org/10.1016/j.fct.2010.09.030>] [PMID: 20932872]
- [17] Yang, N.C.; Lin, H.C.; Wu, J.H.; Ou, H.C.; Chai, Y.C.; Tseng, C.Y.; Liao, J.W.; Song, T.Y. Ergothioneine protects against neuronal injury induced by β -amyloid in mice. *Food Chem. Toxicol.*, **2012**, *50*(11), 3902-3911. [<http://dx.doi.org/10.1016/j.fct.2012.08.021>] [PMID: 22921351]
- [18] Ishimoto, T.; Nakamichi, N.; Hosotani, H.; Masuo, Y.; Sugiura, T.; Kato, Y. Organic cation transporter-mediated ergothioneine uptake in mouse neural progenitor cells suppresses proliferation and promotes differentiation into neurons. *PLoS One*, **2014**, *9*(2)e89434 [<http://dx.doi.org/10.1371/journal.pone.0089434>] [PMID: 24586778]
- [19] Sotgia, S.; Zinellu, A.; Mangoni, A.A.; Pintus, G.; Attia, J.; Carru, C.; McEvoy, M. Clinical and biochemical correlates of serum L-ergothioneine concentrations in community-dwelling middle-aged and older adults. *PLoS One*, **2014**, *9*(1)e84918 [<http://dx.doi.org/10.1371/journal.pone.0084918>] [PMID: 24392160]
- [20] Hatano, T.; Saiki, S.; Okuzumi, A.; Mohney, R.P.; Hattori, N. Identification of novel biomarkers for Parkinson's disease by metabolomic technologies. *J. Neurol. Neurosurg. Psychiatry*, **2016**, *87*(3), 295-301. [<http://dx.doi.org/10.1136/jnnp-2014-309676>] [PMID: 25795009]
- [21] Cheah, I.K.; Feng, L.; Tang, R.M.Y.; Lim, K.H.C.; Halliwell, B. Ergothioneine levels in an elderly population decrease with age and incidence of cognitive decline; a risk factor for neurodegeneration? *Biochem. Biophys. Res. Commun.*, **2016**, *478*(1), 162-167. [<http://dx.doi.org/10.1016/j.bbrc.2016.07.074>] [PMID: 27444382]
- [22] Song, T.Y.; Lin, H.C.; Chen, C.L.; Wu, J.H.; Liao, J.W.; Hu, M.L.

- Ergothioneine and melatonin attenuate oxidative stress and protect against learning and memory deficits in C57BL/6J mice treated with D-galactose. *Free Radic. Res.*, **2014**, *48*(9), 1049-1060. [http://dx.doi.org/10.3109/10715762.2014.920954] [PMID: 24797165]
- [23] Tang, Y.; Masuo, Y.; Sakai, Y.; Wakayama, T.; Sugiura, T.; Hara-da, R.; Futatsugi, A.; Komura, T.; Nakamichi, N.; Sekiguchi, H.; Sutoh, K.; Usumi, K.; Iseki, S.; Kaneko, S.; Kato, Y. Localization of xenobiotic transporter OCTN1/SLC22A4 in hepatic stellate cells and its protective role in liver fibrosis. *J. Pharm. Sci.*, **2016**, *105*(5), 1779-1789. [http://dx.doi.org/10.1016/j.xphs.2016.02.023] [PMID: 27020986]
- [24] Nakamichi, N.; Taguchi, T.; Hosotani, H.; Wakayama, T.; Shimizu, T.; Sugiura, T.; Iseki, S.; Kato, Y. Functional expression of carnitine/organic cation transporter OCTN1 in mouse brain neurons: possible involvement in neuronal differentiation. *Neurochem. Int.*, **2012**, *61*(7), 1121-1132. [http://dx.doi.org/10.1016/j.neuint.2012.08.004] [PMID: 22944603]
- [25] Nakamichi, N.; Kambe, Y.; Oikawa, H.; Ogura, M.; Takano, K.; Tamaki, K.; Inoue, M.; Hinoi, E.; Yoneda, Y. Protection by exogenous pyruvate through a mechanism related to monocarboxylate transporters against cell death induced by hydrogen peroxide in cultured rat cortical neurons. *J. Neurochem.*, **2005**, *93*(1), 84-93. [http://dx.doi.org/10.1111/j.1471-4159.2005.02999.x] [PMID: 15773908]
- [26] Ishimoto, T.; Masuo, Y.; Kato, Y.; Nakamichi, N. Ergothioneine-induced neuronal differentiation is mediated through activation of S6K1 and neurotrophin 4/5-TrkB signaling in murine neural stem cells. *Cell. Signal.*, **2019**, *53*, 269-280. [http://dx.doi.org/10.1016/j.cellsig.2018.10.012] [PMID: 30359715]
- [27] Longair, M.H.; Baker, D.A.; Armstrong, J.D. Simple Neurite Tracer: open source software for reconstruction, visualization and analysis of neuronal processes. *Bioinformatics*, **2011**, *27*(17), 2453-2454. [http://dx.doi.org/10.1093/bioinformatics/btr390] [PMID: 21727141]
- [28] Schindelin, J.; Arganda-Carreras, I.; Frise, E.; Kaynig, V.; Longair, M.; Pietzsch, T.; Preibisch, S.; Rueden, C.; Saalfeld, S.; Schmid, B.; Tinevez, J.Y.; White, D.J.; Hartenstein, V.; Eliceiri, K.; Tomancak, P.; Cardona, A. Fiji: an open-source platform for biological-image analysis. *Nat. Methods*, **2012**, *9*(7), 676-682. [http://dx.doi.org/10.1038/nmeth.2019] [PMID: 22743772]
- [29] Lin, T.A.; Kong, X.; Saltiel, A.R.; Blackshear, P.J.; Lawrence, J.C., Jr Control of PHAS-I by insulin in 3T3-L1 adipocytes. Synthesis, degradation, and phosphorylation by a rapamycin-sensitive and mitogen-activated protein kinase-independent pathway. *J. Biol. Chem.*, **1995**, *270*(31), 18531-18538. [http://dx.doi.org/10.1074/jbc.270.31.18531] [PMID: 7629182]
- [30] Bruel-Jungerman, E.; Laroche, S.; Rampon, C. New neurons in the dentate gyrus are involved in the expression of enhanced long-term memory following environmental enrichment. *Eur. J. Neurosci.*, **2005**, *21*(2), 513-521. [http://dx.doi.org/10.1111/j.1460-9568.2005.03875.x] [PMID: 15673450]
- [31] Winocur, G.; Wojtowicz, J.M.; Sekeres, M.; Snyder, J.S.; Wang, S. Inhibition of neurogenesis interferes with hippocampus-dependent memory function. *Hippocampus*, **2006**, *16*(3), 296-304. [http://dx.doi.org/10.1002/hipo.20163] [PMID: 16411241]
- [32] Goo, M.J.; Choi, S.M.; Kim, S.H.; Ahn, B.O. Protective effects of acetyl-L-carnitine on neurodegenerative changes in chronic cerebral ischemia models and learning-memory impairment in aged rats. *Arch. Pharm. Res.*, **2012**, *35*(1), 145-154. [http://dx.doi.org/10.1007/s12272-012-0116-9] [PMID: 22297753]
- [33] Yu, S.Y.; Zhang, M.; Luo, J.; Zhang, L.; Shao, Y.; Li, G. Curcumin ameliorates memory deficits via neuronal nitric oxide synthase in aged mice. *Prog. Neuropsychopharmacol. Biol. Psychiatry*, **2013**, *45*, 47-53. [http://dx.doi.org/10.1016/j.pnpbp.2013.05.001] [PMID: 23665290]
- [34] Batty, G.D.; Deary, I.J. Early life intelligence and adult health. *BMJ*, **2004**, *329*(7466), 585-586. [http://dx.doi.org/10.1136/bmj.329.7466.585] [PMID: 15361422]
- [35] Gottfredson, L.S. Life, Death, and Intelligence. *J. Cogn. Educ. Psychol.*, **2004**, *4*(1), 23-46. [http://dx.doi.org/10.1891/194589504787382839]
- [36] Sato, N.; Murakami, Y.; Nakano, T.; Sugawara, M.; Kawakami, H.; Idota, T.; Nakajima, I. Effects of dietary nucleotides on lipid metabolism and learning ability of rats. *Biosci. Biotechnol. Biochem.*, **1995**, *59*(7), 1267-1271. [http://dx.doi.org/10.1271/bbb.59.1267] [PMID: 7670187]
- [37] Lee, B.; Sur, B.J.; Han, J.J.; Shim, I.; Her, S.; Lee, H.J.; Hahn, D.H. Krill phosphatidylserine improves learning and memory in Morris water maze in aged rats. *Prog. Neuropsychopharmacol. Biol. Psychiatry*, **2010**, *34*(6), 1085-1093. [http://dx.doi.org/10.1016/j.pnpbp.2010.05.031] [PMID: 20677367]
- [38] Marcussen, A.B.; Flagstad, P.; Kristjansen, P.E.; Johansen, F.F.; Englund, U. Increase in neurogenesis and behavioural benefit after chronic fluoxetine treatment in Wistar rats. *Acta Neurol. Scand.*, **2008**, *117*(2), 94-100. [PMID: 18184344]
- [39] Rainer, Q.; Xia, L.; Guilloux, J.P.; Gabriel, C.; Mocaër, E.; Hen, R.; Enhamre, E.; Gardier, A.M.; David, D.J. Beneficial behavioural and neurogenic effects of agomelatine in a model of depression/anxiety. *Int. J. Neuropsychopharmacol.*, **2012**, *15*(3), 321-335. [http://dx.doi.org/10.1017/S1461145711000356] [PMID: 21473810]
- [40] Rabacchi, S.A.; Kruk, B.; Hamilton, J.; Carney, C.; Hoffman, J.R.; Meyer, S.L.; Springer, J.E.; Baird, D.H. BDNF and NT4/5 promote survival and neurite outgrowth of pontocerebellar mossy fiber neurons. *J. Neurobiol.*, **1999**, *40*(2), 254-269. [http://dx.doi.org/10.1002/(SICI)1097-4695(199908)40:2<254::AID-NEU11>3.0.CO;2-4] [PMID: 10413455]
- [41] Hechler, D.; Boato, F.; Nitsch, R.; Hendrix, S. Differential regulation of axon outgrowth and reinnervation by neurotrophin-3 and neurotrophin-4 in the hippocampal formation. *Exp. Brain Res.*, **2010**, *205*(2), 215-221. [http://dx.doi.org/10.1007/s00221-010-2355-7] [PMID: 20640412]
- [42] Lee, Y.S.; Danandeh, A.; Baratta, J.; Lin, C.Y.; Yu, J.; Robertson, R.T. Neurotrophic factors rescue basal forebrain cholinergic neurons and improve performance on a spatial learning test. *Exp. Neurol.*, **2013**, *249*, 178-186. [http://dx.doi.org/10.1016/j.expneurol.2013.08.012] [PMID: 24017996]
- [43] Fischer, W.; Sirevaag, A.; Wiegand, S.J.; Lindsay, R.M.; Björklund, A. Reversal of spatial memory impairments in aged rats by nerve growth factor and neurotrophins 3 and 4/5 but not by brain-derived neurotrophic factor. *Proc. Natl. Acad. Sci. USA*, **1994**, *91*(18), 8607-8611. [http://dx.doi.org/10.1073/pnas.91.18.8607] [PMID: 8078930]
- [44] Arduini, A.; Eddy, L.; Hochstein, P. The reduction of ferryl myoglobin by ergothioneine: a novel function for ergothioneine. *Arch. Biochem. Biophys.*, **1990**, *281*(1), 41-43. [http://dx.doi.org/10.1016/0003-9861(90)90410-Z] [PMID: 2383023]
- [45] Bedirli, A.; Sakrak, O.; Muhtaroglu, S.; Soyuer, I.; Guler, I.; Riza Erdogan, A.; Sozuer, E.M. Ergothioneine pretreatment protects the liver from ischemia-reperfusion injury caused by increasing hepatic heat shock protein 70. *J. Surg. Res.*, **2004**, *122*(1), 96-102. [http://dx.doi.org/10.1016/j.jss.2004.06.016] [PMID: 15522321]
- [46] Sakrak, O.; Kerem, M.; Bedirli, A.; Pasaoglu, H.; Akyurek, N.; Ofloglu, E.; Gültekin, F.A. Ergothioneine modulates proinflammatory cytokines and heat shock protein 70 in mesenteric ischemia and reperfusion injury. *J. Surg. Res.*, **2008**, *144*(1), 36-42. [http://dx.doi.org/10.1016/j.jss.2007.04.020] [PMID: 17603080]
- [47] Repine, J.E.; Elkins, N.D. Effect of ergothioneine on acute lung injury and inflammation in cytokine insufflated rats. *Prev. Med.*, **2012**, *54*(Suppl.), S79-S82. [http://dx.doi.org/10.1016/j.yjmed.2011.12.006] [PMID: 22197759]
- [48] Obayashi, K.; Kurihara, K.; Okano, Y.; Masaki, H.; Yarosh, D.B.

L-Ergothioneine scavenges superoxide and singlet oxygen and suppresses TNF-alpha and MMP-1 expression in UV-irradiated human dermal fibroblasts. *J. Cosmet. Sci.*, **2005**, *56*(1), 17-27. [http://dx.doi.org/10.1111/j.0142-5463.2005.00265_2.x] [PMID: 15744438]

[49] Yoshida, S.; Shime, H.; Funami, K.; Takaki, H.; Matsumoto, M.;

Kasahara, M.; Seya, T. The anti-oxidant ergothioneine augments the immunomodulatory function of TLR agonists by direct action on macrophages. *PLoS One*, **2017**, *12*(1)e0169360 [<http://dx.doi.org/10.1371/journal.pone.0169360>] [PMID: 28114402]

Hydrolyzed Salmon Milt Extract Enhances Object Recognition and Location Memory Through an Increase in Hippocampal Cytidine Nucleoside Levels in Normal Mice

Noritaka Nakamichi,¹ Shunsuke Nakao,¹ Yusuke Masuo,¹ Ayaka Koike,¹ Naoto Matsumura,¹ Misa Nishiyama,¹ Aya Hasan Al-Shammari,¹ Hirotaka Sekiguchi,² Keita Sutoh,² Koji Usumi,² and Yukio Kato¹

¹Faculty of Pharmacy, Institute of Medical, Pharmaceutical and Health Sciences, Kanazawa University, Kanazawa, Japan.

²Life Science Institute Co., Ltd., Tokyo, Japan.

ABSTRACT Salmon milt extract contains high levels of nucleic acids and has antioxidant potential. Although salmon milt extract is known to improve impaired brain function in animal models with brain disease, its effects on learning and memory ability in healthy subjects is unknown. The purpose of the present study was to clarify the effect of hydrolyzed salmon milt extract (HSME) on object recognition and object location memory under normal conditions. A diet containing 2.5% HSME induced normal mice to devote more time to exploring novel and moved objects than in exploring familiar and unmoved objects, as observed during novel object recognition and spatial recognition tests, respectively. A diet containing 2.5% nucleic acid fraction purified from HSME also induced similar effects, as measured by the same behavioral tests. This suggests that the nucleic acids may be a functional component contributing to the effects of HSME on brain function. Quantitative polymerase chain reaction analysis revealed that gene expression of the markers for brain parenchymal cells, including neural stem cells, astrocytes, oligodendrocytes, and microglia, in the hippocampi of mice on an HSME diet was higher than that in mice on a control diet. Oral administration of HSME increased concentrations of cytosine, cytidine, and deoxycytidine in the hippocampus. Overall, ingestion of HSME may enhance object recognition and object location memory under normal conditions in mice, at least, in part, via the activation of brain parenchymal cells. Our results thus indicate that dietary intake of this easily ingestible food might enhance brain function in healthy individuals.

KEYWORDS: • amino acids • brain parenchymal cells • hydrolyzed salmon milt extract • nucleic acids • object location memory • object recognition memory

INTRODUCTION

LEARNING AND MEMORY are brain functions involved in the acquisition of information essential for animal survival. Impairment in the abilities of learning and memory resulting from brain injury or neurodegenerative disorders leads to a considerable decrease in the quality of life. Therefore, many studies have been performed with the aim of recovering learning and memory abilities that have been degraded by brain lesions or neurodegeneration. Learning and memory impairments are generally improved by compounds with antioxidant properties and/or those that promote neurogenesis and synaptic plasticity.^{1–3}

Under normal conditions of mental health and intellect, on the contrary, humans are able to learn and memorize various information unrelated to survival, but essential to the construction of a sophisticated and diversified society.

Possession of high learning and memory ability is advantageous in pursuing a successful social life. Indeed, the intelligence quotient has been reported to be highly correlated with health and wealth.^{4,5} Despite these benefits, however, limited information is available regarding compounds that enhance learning and memory ability in healthy animals, which is in contrast to extensive research on compounds that improve these abilities after brain injury.

Salmon milt extract is produced by removing fluids and lipids from salmon milt, and mainly contains protein and deoxynucleotides. It is used as an ingredient in health food, and can be easily assimilated. The components of salmon milt extract are further hydrolyzed to obtain small, water-soluble molecules by treatment with hydrolases, including proteases and nucleases. The resultant substance is known as hydrolyzed salmon milt extract (HSME). The deoxynucleotides abundantly contained in salmon milt extract not only form genetic material but also contribute to the improvement of brain function.

Oral ingestion of a diet supplemented with nucleotides has been reported to enhance learning and memory ability in rats as assessed by the water-filled multiple T-maze test and

Manuscript received 10 July 2018. Revision accepted 9 January 2019.

Address correspondence to: Yukio Kato, PhD, Faculty of Pharmacy, Institute of Medical, Pharmaceutical and Health Sciences, Kanazawa University, Kakuma-machi, Kanazawa 920-1192, Japan, E-mail: ykato@p.kanazawa-u.ac.jp

passive avoidance test.⁶ Dietary nucleotides and nucleosides have also been found to improve impaired abilities related to learning and memory in aged, memory-deficient mice and in senescence-accelerated mice as assessed by the passive avoidance test.^{7,8} Furthermore, oral administration of the purine nucleoside guanosine promotes hippocampal neuronal differentiation and exerts an antidepressant-like effect in mice.⁹

In addition, various components contained in salmon milt extract are known to exhibit protective effects against brain impairment. For example, oral ingestion of nucleoprotein extracted from salmon milt suppresses dopaminergic neuronal death and motor deficiency in mice models of Parkinson's disease induced by 1-methyl-4-phenyl-1, 2, 3, 6-tetrahydropyridine (MPTP),¹⁰ and inhibits neuronal death induced by brain ischemia in mice hippocampi.¹¹ Thus, salmon milt extract is a promising candidate for treatment of brain injury or degeneration as a food-derived ingredient exhibiting beneficial effects on learning and memory. However, its effect on learning and memory under normal conditions cannot be easily predicted owing to limited research on enhancement of brain function in healthy individuals.

In the present study, to examine the effect of salmon milt extract on learning and memory under normal conditions, a diet supplemented with HSME was fed to healthy mice. Novel object recognition test (NORT) and spatial recognition test (SRT) were performed to appraise learning and memory. The effects of diets supplemented with nucleic acid fraction (NAF) of HSME or with a mixture of amino acids (AAM) contained in HSME were also studied to identify the functional components of HSME.

MATERIALS AND METHODS

Materials

HSME consisted of salmon milt water solubilized by nuclease and protease as described previously,¹² and contained oligo- and mononucleotides, nucleosides, bases, peptides, and amino acids. NAF was a DNA sodium salt produced from salmon milt extract,¹³ which was then hydrolyzed by nuclease. AAM was a mixture of 18 authentic amino acids in the ratio in which they are found in HSME. HSME, NAF, and AAM were provided by Life Science Institute Co. Ltd (Tokyo, Japan) and Foday's Co. Ltd (Tokyo, Japan). ISOGEN, MultiScribe™ Reverse Transcriptase, and THUNDERBIRD SYBR qPCR Mix were purchased from Nippon Gene (Tokyo, Japan), Biosystems (Foster City, CA, USA), and TOYOBO (Osaka, Japan), respectively. All other chemicals and reagents were of the highest purity available and were purchased from commercial sources.

Animals

Male Institute of Cancer Research (ICR) mice were used for *in vivo* analyses of behavior, measurement of nucleic acid concentration, and gene expression, and pregnant ICR mice were used for *in vitro* analysis using neural stem cell culture. These ICR mice were purchased from Sankyo Labo

Service Co. (Tokyo, Japan). Mice were housed under pathogen-free conditions at a controlled temperature (21–25°C) and were subjected to a 12 h light per dark cycle. The lights remained on from 8:00 to 20:00, and food and water were available *ad libitum*. The animals were cared for in strict compliance with the guidelines outlined in the National Institutes of Health Guide for the Care and Use of Laboratory Animals. All animal procedures used in this work were approved by the Kanazawa University Animal Care Committee (Permit Number: AP-132875).

Behavioral tests in mice

The experimental schedule is summarized in Supplementary Figure S1. The mice were purchased at the age of 4 weeks and fed control diets for 1 week. Then, they were randomly divided into four groups based on diet. The four groups of mice were fed a control diet (PicoLab Rodent Diet 20®; PMI Nutrition International, Brentwood, MO), a control diet containing 2.5% (w/w) HSME, NAF, or AAM, respectively, for 2 weeks. The body weights of mice from the control and HSME groups were measured every week, whereas those of mice from the NAF and AAM groups were measured on experimental day 14. To perform NORT, each mouse was individually placed in an acrylic chamber (45 × 45 × 45 cm) and allowed to explore for 10 min. The next day, each mouse was placed in the chamber with two similar objects located on a diagonal line, and allowed to explore for 5 min. Following a 24 h period, one of the objects was replaced by a new one at the same position in the chamber, and each mouse was allowed to explore for 5 min. Exploration time for each object was recorded. Discrimination index was calculated as follows: (novel object exploration time/total exploration time) – (familiar object exploration time/total exploration time) × 100.

SRT was conducted on the following day. Each mouse was individually placed in an acrylic chamber and allowed to explore for 10 min. The next day, each mouse was placed in the chamber with two similar objects located on a diagonal line and allowed to explore for 5 min. After 1 h, one of the objects was displaced, and each mouse was allowed to explore for 5 min. Exploration time devoted to each object was recorded. Discrimination index was calculated as follows: (moved object exploration time/total exploration time) – (unmoved object exploration time/total exploration time) × 100.

Measurement of nucleic acid concentration in the forebrain and hippocampus

For detailed information, see Measurement of Nucleic Acid Concentration in the Forebrain and Hippocampus section in Supplementary Data.

Quantitative reverse transcription-polymerase chain reaction

For detailed information, see Quantitative reverse transcription-polymerase chain reaction section in Supplementary Data.

Neural stem cell culture

For detailed information, see Neural Stem Cell Culture section in Supplementary Data.

MTT assay

For detailed information, see MTT Assay section in Supplementary Data.

Adenosine triphosphate assay

Adenosine triphosphate (ATP) assay was performed in primary cultured neural stem cells according to the standard procedure of the ATP assay kit ATPlite™ (PerkinElmer, Waltham, MA).

Statistical analysis

Data are expressed as means \pm standard error of the mean. The statistical significance of differences was determined using Student's *t*-test or one-way analysis of variance, followed by Dunnett's multiple comparison tests for the appropriate *post hoc* analysis. $P < .05$ was regarded as indicative of significant difference.

RESULTS

Nucleoside composition of HSME and NAF is shown in Table 1. Approximately 32% and 69% of HSME and NAF, respectively, consisted of mono- or oligodeoxynucleotides (Table 1). Gel filtration analysis revealed that mono-, di-, tri-, and tetranucleotides were present in both HSME and NAF (Supplementary Fig. S2). The amino acid composition of HSME is shown in Table 2. Approximately 48% of HSME was made up of amino acids, and of this, 40% was arginine (Table 2).

To clarify the effect of HSME on learning and memory ability, NORT and SRT were performed. The body weights of the mice on the HSME diet showed similar changes as did those of the mice on the control diet (Fig. 1A). To clarify the effect of diet containing HSME on object recognition memory, NORT was performed under the condition in which normal mice ingested with the control diet cannot

distinguish the novel object from the familiar one. The exploration time devoted to the novel object was significantly longer than the time devoted to the familiar one in mice on the HSME-supplemented diet, whereas it was similar for both novel and familiar objects in mice on control diet (Fig. 2A). SRT was performed under the condition in which normal mice ingested with the control diet cannot distinguish the moved object from the unmoved one, with an aim to clarify the effect of diet containing HSME on object location memory in normal mice. The exploration time devoted to the moved object was significantly longer than that devoted to the unmoved one in mice on the HSME-supplemented diet, whereas it was similar for both objects in mice on control diet (Fig. 2B). These results suggest that oral ingestion of HSME under normal conditions of health may enhance object recognition and object location memory in mice. Discrimination index for NORT in mice on the HSME-supplemented diet was significantly higher than that in mice on control diet (Table 3). To clarify the component responsible for the improvement in brain function induced by HSME, two components of the substance were prepared for analysis. HSME was fractionated, and the nucleic acid portion was separated out as NAF. AAM was prepared by mixing authentic amino acids in the ratios in which they are present in HSME (Table 2). Body weights of 14 days following the commencement of the experimental diets were similar among mice on the control, HSME, NAF, and AAM diets (Fig. 1B). The effect of NAF on exploration times assessed by both NORT and SRT was similar to that of HSME (Fig. 2A, B), and discrimination indices for both NORT and SRT in mice that were given NAF were significantly higher than in mice that were on control diet (Table 3). AAM had effects on exploration time (Fig. 2A) and discrimination index (Table 3) as assessed by NORT.

To verify that the enhancement in learning and memory seen upon oral ingestion of HSME is indeed provoked by nucleic acids, the concentrations of several nucleic acids in the hippocampus, a region of the forebrain closely associated with learning and memory abilities, and in the remainder of the forebrain were measured using liquid chromatography-tandem mass spectrometry, following oral administration of HSME. Concentrations of cytosine and cytidine in both the

TABLE 1. NUCLEOSIDE COMPOSITION OF HYDROLYZED SALMON MILT EXTRACT AND NUCLEIC ACID FRACTION

	HSME		NAF	
	Oligo- and monodeoxynucleotides (g/100 g) ^a	Monodeoxynucleotides (g/100 g) ^b	Oligo- and monodeoxynucleotides (g/100 g) ^a	Monodeoxynucleotides (g/100 g) ^b
dAMP	8.78	3.93	17.0	10.1
dTMP	10.3	1.83	23.4	6.42
dGMP	6.74	1.96	14.2	6.66
dCMP	6.39	2.51	14.6	8.01

^aContent of each monodeoxynucleotide was measured after hydrolysis of the samples. Therefore, the amount represents the sum of oligo- and monodeoxynucleotides.

^bContent of each monodeoxynucleotide was measured before hydrolysis of the samples. Therefore, the amount represents monodeoxynucleotides alone.

dAMP, deoxyadenosine monophosphate; dCMP, deoxycytidine monophosphate; dGMP, deoxyguanosine monophosphate; dTMP, deoxythymidine monophosphate; HSME, hydrolyzed salmon milt extract; NAF, nucleic acid fraction.

TABLE 2. AMINO ACID COMPOSITION OF HYDROLYZED SALMON MILT EXTRACT

Arg 18.70	Lys 2.60	His 0.67	Phe 0.87	Tyr 0.85	Leu 1.90	Ile 1.22	Met 0.58	Val 2.11	Ala 1.93
Gly 4.09	Pro 2.67	Gln 3.30	Ser 2.54	Thr 1.23	Asp 2.10	Trp 0.20	Cys ^a 0.23	Total 47.8	

Unit is g/100 g of HSME.

^aCysteine was measured as cystine.

hippocampus and the rest of the forebrain in mice administered HSME were significantly higher than in mice administered the vehicle alone (Fig. 3). In addition, concentrations of deoxycytidine in the hippocampus of mice administered HSME were significantly higher than in mice administered the vehicle alone (Fig. 3). Hippocampal thymidine concentration was slightly, but significantly, higher in mice administered HSME than in the control group mice (Fig. 3). Plasma concentration profiles were also measured (Supplementary Fig. S3), and concentration of cytosine, deoxycytidine, and thymidine in mice administered HSME tended to be higher than that in mice administered the vehicle alone, although experimental variation was relatively large possibly due to the effect of any homeostatic regulation.

To understand the mechanisms underlying the enhancement of object recognition and object location memory by dietary HSME, gene expression of the neuronal maturation markers, and the markers for brain parenchymal cells found in the hippocampus was investigated. In our preliminary study, expressions of all the marker genes examined in the present study were almost identical between control and HSME groups at 2 weeks following the start of the experimental diet (data not shown). Therefore, we thought that the change in gene expression of these markers may be induced within 1 week following the start of the experimental diet, and gene expression of these markers was examined at 2, 4, and 6 days following the start of the experimental diet. Gene expression of the neural stem cell marker nestin, astro-

cyte marker glial fibrillary acidic protein, microglia marker CD11b, oligodendrocyte marker myelin basic protein (MBP)-1 and -2, and undifferentiated proliferative cell marker sex determining region Y-box 2 (SOX2) at 2 days following the start of the experimental diet in mice fed HSME was significantly higher than in mice on control diet (Fig. 4). On the contrary, expressions of these marker genes were almost identical in all groups at 4 and 6 days following the start of the experimental diet (Fig. 4).

Furthermore, to verify that HSME and NAF directly influence brain parenchymal cells, the effect of HSME and NAF on cellular proliferation in cultured neural stem cells was investigated. Exposure of cultured neural stem cells to 10 μg/mL of HSME and NAF, and the positive control forskolin at 10 μM significantly increased MTT reduction activity (Fig. 5A). HSME, NAF, and forskolin also increased cellular ATP level (Fig. 5B). These results suggest that HSME and NAF promote cellular proliferation in neural stem cells. Moreover, oral ingestion of HSME may enhance learning and memory abilities, at least in part, through the direct action in brain parenchymal cells. It should be noted that dose dependency was minimally observed for the promotive effect of HSME and NAF on the cellular proliferation (Fig. 5). Although exact reason for the minimal dose dependency is unknown, HSME and NAF are the mixture of various compounds, and some of which may exhibit suppressive effect at higher concentrations of HSME and NAF on the cellular proliferation.

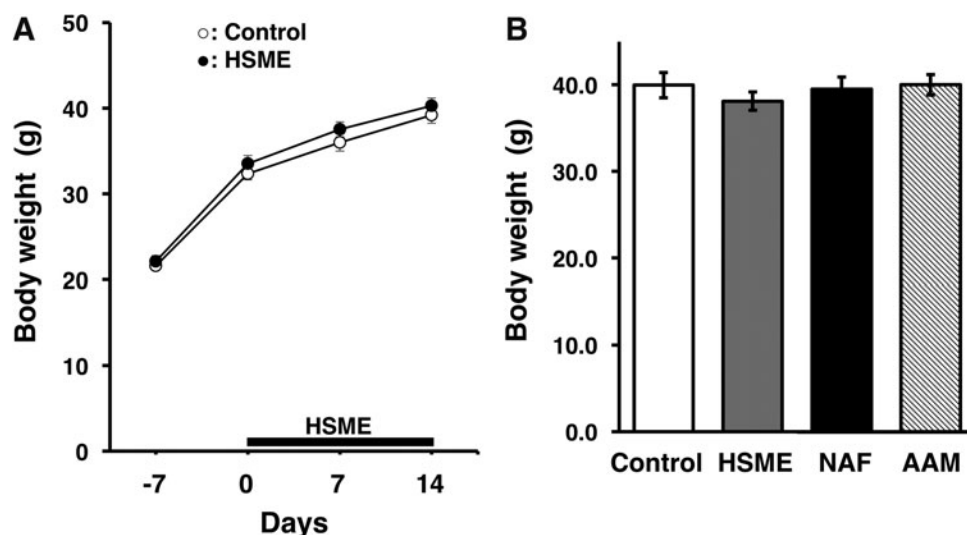


FIG. 1. Effect of ingestion of HSME, NAF, and AAM on body weight in mice. Mice were fed a control diet or a control diet supplemented with 2.5% (w/w) of HSME, NAF, or AAM for 2 weeks. (A) Body weights of mice fed the control diet (white) or the diet containing HSME (black) were measured on days 7, 0, 7, and 14. (B) Body weights of mice fed control diet (white), or the diet containing HSME (gray), NAF (black), or AAM (diagonal) were measured on day 14. Each value represents the mean ± SEM (n=6). AAM, mixture of amino acids; HSME, hydrolyzed salmon milt extract; NAF, nucleic acid fraction; SEM, standard error of the mean.

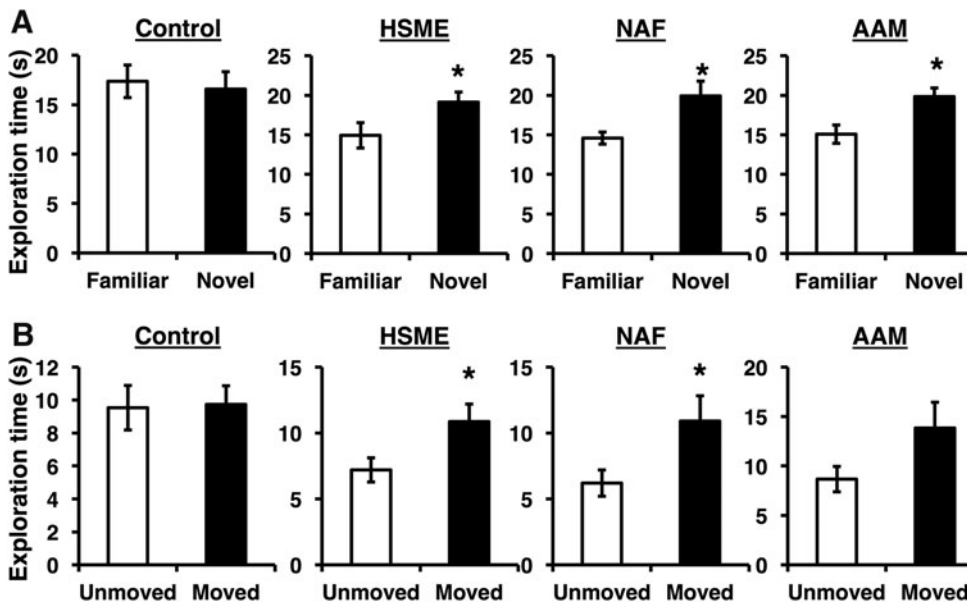


FIG. 2. Effect of ingestion of HSME, NAF, and AAM on object recognition and object location memory. Mice were fed a control diet or a control diet supplemented with 2.5% (w/w) of HSME, NAF, or AAM (A) and NORT (A) and SRT (B) were conducted. In (A), white and black columns show exploration time devoted to familiar and novel objects, respectively. In (B), white and black columns show exploration time devoted to the unmoved and moved object, respectively. Each value represents the mean \pm SEM ($n=10-15$). *Significant difference relative to the corresponding control values ($P < .05$). NORT, novel object recognition test; SRT, spatial recognition test.

DISCUSSION

The present findings indicate that oral ingestion of salmon milt extract enhances object recognition and object location memory in healthy mice (Fig. 2 and Table 3). Salmon milt extract contains an abundance of nucleic acids and can be made available as a nutritional ingredient. That is, it can be easily assimilated from the daily diet. This makes it even more noteworthy that brain function in healthy mice can be enhanced by this easily available food ingredient.

NAF could be one of the functional components in HSME, since both object recognition and object location memory in mice, assessed as exploration time devoted to novel and moved objects, respectively, upon oral ingestion of this fraction, were enhanced to a degree similar to that in mice on an HSME-supplemented diet (Fig. 2). Discrimination index after ingestion of NAF was significantly increased in both studies, a tendency that was also observed after ingestion of HSME (Table 3). In addition, exposure of neural stem cells to NAF as well as HSME increased cellular proliferation (Fig. 5). NAF used in the present study contained mono- and oligonucleotides (Table 1 and Supplementary Fig. S2). Oral ingestion of the mononucleoside uridine has been previously reported to enhance learning and memory ability through improvement of lipid metabo-

lism in the cerebral cortex of rats and in the brain of gerbils.^{6,14} However, the dietary intake of nucleotides and nucleosides has been reported to improve memory function in aged, memory-deficient mice, and not in normal mice.^{7,8} In the present study, the dietary intake of HSME and NAF was shown to improve learning and memory function in normal mice (Fig. 2). It should be noted that both substances contained not only mononucleotides but also oligonucleotides as major components (Supplementary Fig. S2), but little information is available on the direct effect of this latter component on learning and memory ability in normal mice.

The concentrations of several nucleic acids such as cytosine, cytidine, deoxycytidine, and thymidine in the hippocampus and in the remaining part of forebrain were elevated upon oral administration of HSME (Fig. 3), supporting the hypothesis that the nucleic acid component of HSME played a role in the enhancement of brain function. In the present study, the concentration of each nucleic acid was directly measured, and to our knowledge, this is the first report on changes in each nucleic acid component in the hippocampus upon oral administration of food ingredients containing high proportions of nucleic acids. Due to the limitation of the study design, however, further studies are required to know whether the elevation of these nucleic acids directly represents the ingestion of nucleic acids in HSME or reflects any indirect phenomenon due to homeostatic regulation. Although the exact component responsible for the improvement in brain function is still unknown, energy-independent equilibrative nucleoside transporters (ENTs), which recognize nucleosides as endogenous substrates, are known to be expressed in brain capillary epithelial cells.¹⁵ It is plausible that nucleosides such as cytidine and deoxycytidine might be distributed to the brain across the blood-brain barrier via the transporter after oral ingestion. Administration of cytidine diphosphorylcholine, which is a precursor of cytidine and uridine, raises the

TABLE 3. DISCRIMINATION INDEX ASSESSED IN NOVEL OBJECT RECOGNITION TEST AND SPATIAL RECOGNITION TEST

	Control	HSME	NAF	AAM
Discrimination index				
NORT	-3.01 ± 5.38	$13.9 \pm 3.3^*$	$13.2 \pm 5.0^*$	$14.3 \pm 4.8^*$
SRT	2.91 ± 4.74	20.3 ± 4.5	$26.9 \pm 8.5^*$	20.7 ± 7.5

*Significant difference relative to the corresponding control values ($P < .05$).

AAM, mixture of amino acids; NORT, novel object recognition test; SRT, spatial recognition test.

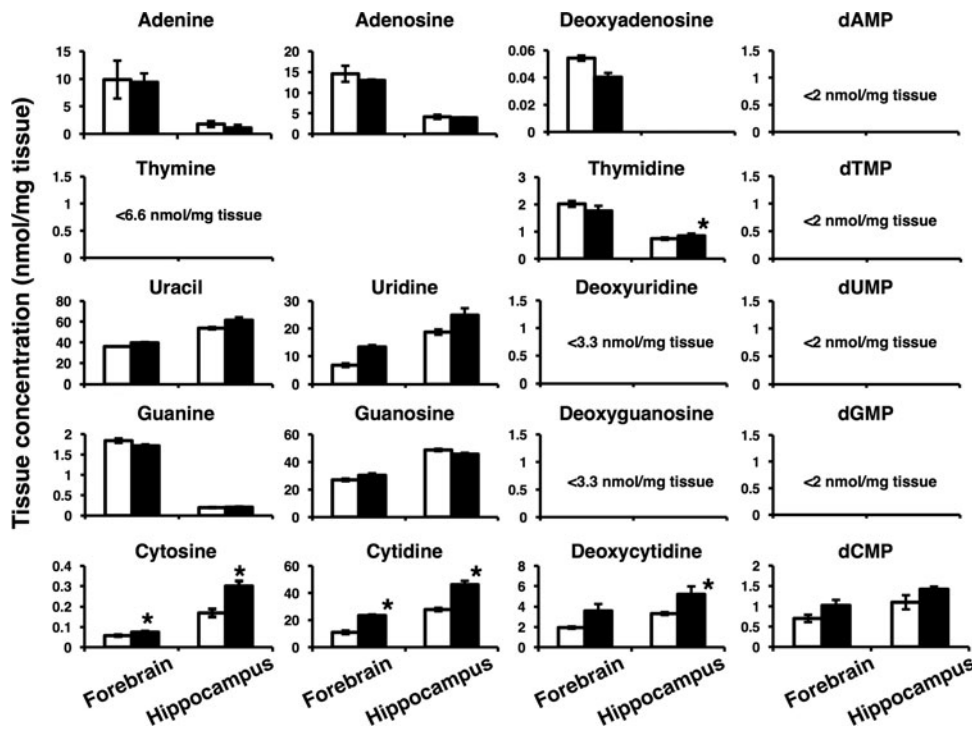


FIG. 3. Concentration of nucleobases, nucleosides, deoxynucleosides, and deoxynucleotides in the hippocampus and in the remaining part of the forebrain in mice upon oral administration of HSME. Mice were orally administered saline or 2 g HSME per kg of body weight. The forebrain was collected at 24 h following administration, and hippocampus was isolated from the forebrain. *White* and *black* columns show the saline and HSME groups, respectively. Concentration of each nucleic acid was measured using liquid chromatography-tandem mass spectrometry. Each value represents the mean \pm SEM ($n=3$). *Significant difference relative to the corresponding control values ($P<.05$). dAMP, deoxyadenosine monophosphate; dCMP, deoxycytidine monophosphate; dGMP, deoxyguanosine monophosphate; dTMP, deoxythymidine monophosphate.

plasma concentration of cytidine and uridine and improves memory function in memory-impaired rats and humans.^{16–18} Taken together, enhancement of learning and memory induced by oral ingestion of HSME might be caused, at least in part, by the increase in levels of certain nucleic acids in the brain. It is interesting to note that elevation of brain levels of nucleic acids upon oral administration of HSME was selectively observed in the cases of cytosine, cytidine, and deoxycytidine (Fig. 3), even though all nucleosides were present at almost evenly distributed levels in HSME (Table 1), and ENTs nonselectively recognize nucleo-

sides.¹⁹ Hossain *et al.* recently postulated a promotive effect of dietary cytidine monophosphate on the growth of fishes in early stages that might contribute to their high rate of cellular replication.²⁰ It is also possible that the nucleosides are unevenly supplied to the brain by oral administration of nucleic acid ingredients, and levels of both cytosine and deoxycytidine might be relatively easily elevated compared with those of other nucleosides (Fig. 3).

AAM contained glutamate and aspartate (Table 2), both of which are agonists of the *N*-methyl-D-aspartate (NMDA) receptor and play an important role in synaptic plasticity.^{21,22}

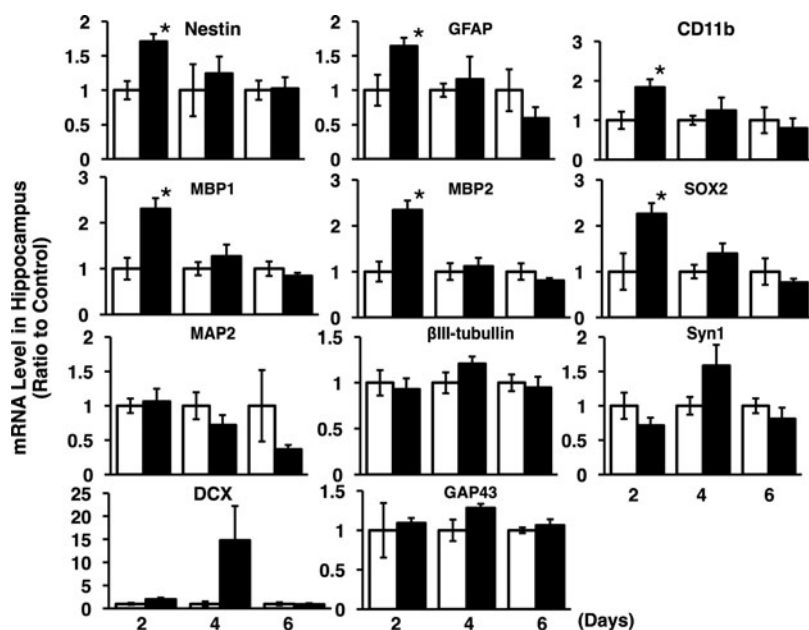


FIG. 4. Effect of ingestion of HSME on expression in the hippocampus of the marker genes for neuronal maturation and brain parenchymal cells. Mice were fed a control diet or a control diet supplemented with 2.5% HSME for 6 days. Hippocampus was collected on days 2, 4, and 6. Total RNA was extracted from the tissue for quantitative reverse transcription-polymerase chain reaction analysis. *White* and *black* columns show the control and HSME groups, respectively. Data were normalized to the expression level of 36B4 and expressed as relative to the corresponding controls. Each value represents the mean \pm SEM ($n=4-8$). MAP2 and GAP43 stand for microtubule-associated protein 2 and growth associated protein 43, respectively. *Significant difference relative to the corresponding control values ($P<.05$).

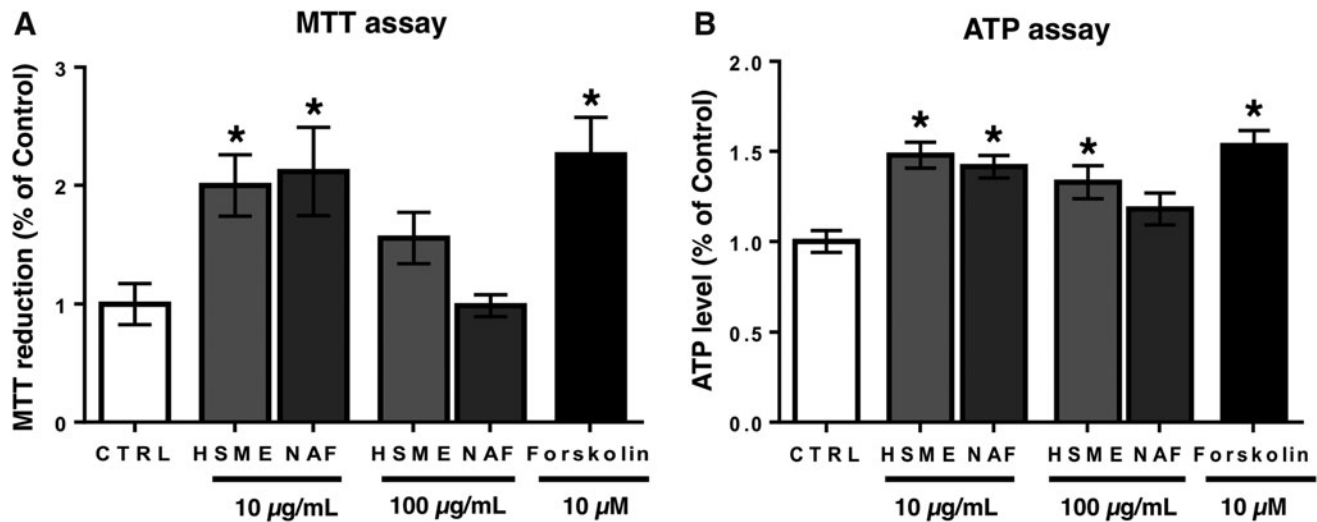


FIG. 5. Effect of HSME and NAF on cellular proliferation in primary cultured neural stem cells. Cortical neural stem cells were exposed to HSME, NAF, or forskolin at the indicated concentrations. Mitochondrial activity and ATP concentration were measured by MTT (A) and ATP (B) assay, respectively. Each value represents the mean \pm SEM ($n=8$). *Significant difference relative to the corresponding control values ($P<.05$). ATP, adenosine triphosphate.

This fraction also contained essential amino acids such as leucine (Table 2), which is an activator of mammalian target of rapamycin signaling and plays an important role in neuronal maturation.^{23,24} However, these hydrophilic amino acids are already present in endogenous plasma and/or brain, so it is unclear whether their concentration is elevated upon oral ingestion of AAM. Meanwhile, learning and memory abilities were increased by oral ingestion of AAM (Fig. 2 and Table 3). Improvement of blood flow to the brain must also be considered as a possible mechanism underlying the enhancement of brain function induced by AAM.

Gene expression of the markers for proliferative brain parenchymal cells was increased 2 days after oral ingestion of HSME was begun (Fig. 4), suggesting that orally ingested HSME activates the proliferative brain parenchymal cells such as glial cells and neural stem cells. The activated glial cells are known to release neurotrophic factors that promote neuronal differentiation and maturation. Furthermore, gene expression of the synapse marker synapsin I (Syn1) and the immature neuron marker doublecortin (DCX) showed an increasing trend at 4 days following the start of the experimental diet (Fig. 4). Based on the increasing trend in the levels of neuronal markers that occur after activation of glial cells, it can be speculated that HSME may promote neuronal differentiation and maturation through the release of neurotrophic factors by glial cells. A previous report found that oral administration of guanosine promoted neuronal differentiation in the hippocampi of mice.¹¹ In other studies, ATP and adenosine were found to promote neuronal differentiation and synaptic plasticity through the activation of the purinergic signaling pathway in cultured neural cells.^{25,26} Activation of NMDA receptor by its agonists, such as glutamate and aspartate, has also been found to promote neuronal differentiation and maturation in cultured neural cells.^{22,27,28} Thus, multiple mechanisms may be involved in

the enhancement of learning and memory upon oral ingestion of HSME.

Astaxanthin and the flavonoid nobiletin are known as food ingredients that enhance brain function in normal animals. Astaxanthin enhances brain function through antioxidant activity and the promotion of neurogenesis.^{29,30} Salmon milt extract also possesses antioxidant activity¹² and induces enhancement through the promotion of neurogenesis, leading to increased learning and memory ability (Fig. 2 and Table 3). Contrarily, nobiletin activates extracellular signal-regulated kinase and protein kinase A signaling.³¹ This flavonoid enhances object recognition memory, but not object location memory.³² The mechanism underlying its enhancement of learning and memory ability may be different from that associated with the effects caused by salmon milt ingestion.

In conclusion, oral ingestion of HSME elevates the concentrations of nucleic acids, including cytosine, cytidine, deoxycytidine, and thymidine in the hippocampus, and may enhance learning and memory abilities, at least in part, through the activation of brain parenchymal cells in normal mice. The easily available and ingestible food ingredient, salmon milt extract, could thus potentially be used as a “brain food” that enhances brain function in healthy people.

ACKNOWLEDGMENTS

The authors thank Ms. Moe Mitamura in Kanazawa University for technical assistance. This work was partially supported by Grants-in-Aid for Scientific Research to N.N. (No. 16K08266) and Y.K. (No. 17K19482) from the Ministry of Education, Culture, Sports, Science, and Technology, Japan.

AUTHOR DISCLOSURE STATEMENT

No competing financial interests exist.

SUPPLEMENTARY MATERIAL

Supplementary Data
 Supplementary Figure S1
 Supplementary Figure S2
 Supplementary Figure S3
 Supplementary Table S1

REFERENCES

- Song TY, Lin HC, Chen CL, *et al.*: Ergothioneine and melatonin attenuate oxidative stress and protect against learning and memory deficits in C57BL/6J mice treated with D-galactose. *Free Radic Res* 2014;48:1049–1060.
- Zhou X, Zhang F, Hu X, *et al.*: Inhibition of inflammation by astaxanthin alleviates cognition deficits in diabetic mice. *Physiol Behav* 2015;151:412–420.
- Bick SK, Eskandar EN: Neuromodulation for restoring memory. *Neurosurg Focus* 2016;40:E5.
- Dama MS: Cognitive ability correlates positively with son birth and predicts cross-cultural variation of the offspring sex ratio. *Naturwissenschaften* 2013;100:559–569.
- Gottfredson LS: Life, death, and intelligence. *J Cogn Educ Psychol* 2004;4:23–46.
- Sato N, Murakami Y, Nakano T, *et al.*: Effects of dietary nucleotides on lipid metabolism and learning ability of rats. *Biosci Biotechnol Biochem* 1995;59:1267–1271.
- Chen TH, Huang HP, Matsumoto Y, *et al.*: Effects of dietary nucleoside-nucleotide mixture on memory in aged and young memory deficient mice. *Life Sci* 1996;59:PL325–PL330.
- Chen TH, Wang MF, Liang YF, *et al.*: A nucleoside-nucleotide mixture may reduce memory deterioration in old senescence-accelerated mice. *J Nutr* 2000;130:3085–3089.
- Bettio LE, Neis VB, Pazini FL, *et al.*: The antidepressant-like effect of chronic guanosine treatment is associated with increased hippocampal neuronal differentiation. *Eur J Neurosci* 2016;43:1006–1015.
- Kiriyama K, Ohtaki H, Kobayashi N, *et al.*: A nucleoprotein-enriched diet suppresses dopaminergic neuronal cell loss and motor deficit in mice with MPTP-induced Parkinson's disease. *J Mol Neurosci* 2015;55:803–811.
- Matsunaga M, Ohtaki H, Takaki A, *et al.*: Nucleoprotamine diet derived from salmon soft roe protects mouse hippocampal neurons from delayed cell death after transient forebrain ischemia. *Neurosci Res* 2003;47:269–276.
- Kojima-Yuasa A, Goto M, Yoshikawa E, *et al.*: Protective effects of hydrolyzed nucleoproteins from salmon milt against ethanol-induced liver injury in rats. *Mar Drugs* 2016;14:E232.
- Mitarai M, Sekido H, Ueda S, *et al.*: Effect of dietary DNA from Chum salmon milt on endurance running capacity of mice. *J Jpn Soc Food Sci Technol* 2008;62:1–26 (in Japanese).
- Holguin S, Martinez J, Chow C, Wurtman R: Dietary uridine enhances the improvement in learning and memory produced by administering DHA to gerbils. *FASEB J* 2008;22:3938–3946.
- Uchida Y, Ohtsuki S, Katsukura Y, *et al.*: Quantitative targeted absolute proteomics of human blood-brain barrier transporters and receptors. *J Neurochem* 2011;117:333–345.
- Teather LA, Wurtman RJ: Dietary CDP-choline supplementation prevents memory impairment caused by impoverished environmental conditions in rats. *Learn Mem* 2005;12:39–43.
- Cotroneo AM, Castagna A, Putignano S, *et al.*: Effectiveness and safety of citicoline in mild vascular cognitive impairment: The IDEALE study. *Clin Interv Aging* 2013;8:131–137.
- Fioravanti M, Yanagi M: Cytidinediphosphocholine (CDP-choline) for cognitive and behavioural disturbances associated with chronic cerebral disorders in the elderly. *Cochrane Database Syst Rev* 2005;2:CD000269.
- Young JD, Yao SY, Baldwin JM, Cass CE, Baldwin SA: The human concentrative and equilibrative nucleoside transporter families, SLC28 and SLC29. *Mol Aspects Med* 2013;34:529–547.
- Hossain MS, Koshio S, Ishikawa M, Yokohama S, Sony NM: Dietary cytidine monophosphate enhances the growth, blood characteristics, innate and adaptive immune functions and stress resistance of juvenile red sea bream, *Pagrus major*. *Aquaculture* 2017;473:366–374.
- Balazs D, Csillag A, Gerber G: L-aspartate effects on single neurons and interactions with glutamate in striatal slice preparation from chicken brain. *Brain Res* 2012;1474:1–7.
- Park H, Han KS, Seo J, *et al.*: Channel-mediated astrocytic glutamate modulates hippocampal synaptic plasticity by activating postsynaptic NMDA receptors. *Mol Brain* 2015;8:7.
- Hay N, Sonenberg N: Upstream and downstream of mTOR. *Genes Dev* 2004;18:1926–1945.
- Ishizuka Y, Kakiya N, Nawa H, Takei N: Leucine induces phosphorylation and activation of p70S6K in cortical neurons via the system L amino acid transporter. *J Neurochem* 2008;106:934–942.
- Delic J, Zimmermann H: Nucleotides affect neurogenesis and dopaminergic differentiation of mouse fetal midbrain-derived neural precursor cells. *Purinergic Signal* 2010;6:417–428.
- Marin-Vicente C, Guerrero-Valero M, Nielsen ML, *et al.*: ATP enhances neuronal differentiation of PC12 cells by activating PKC α interactions with cytoskeletal proteins. *J Proteome Res* 2011;10:529–540.
- Yoneyama M, Nakamichi N, Fukui M, *et al.*: Promotion of neuronal differentiation through activation of N-methyl-D-aspartate receptors transiently expressed by undifferentiated neural progenitor cells in fetal rat neocortex. *J Neurosci Res* 2008;86:2392–2402.
- Jansson LC, Akerman KE: The role of glutamate and its receptors in the proliferation, migration, differentiation and survival of neural progenitor cells. *J Neural Transm (Vienna)* 2014;121:819–836.
- Liu X, Osawa T: Astaxanthin protects neuronal cells against oxidative damage and is a potent candidate for brain food. *Forum Nutr* 2009;61:129–135.
- Yook JS, Okamoto M, Rakwal R, *et al.*: Astaxanthin supplementation enhances adult hippocampal neurogenesis and spatial memory in mice. *Mol Nutr Food Res* 2016;60:589–599.
- Kawahata I, Yoshida M, Sun W, *et al.*: Potent activity of nobiletin-rich Citrus reticulata peel extract to facilitate cAMP/PKA/ERK/CREB signaling associated with learning and memory in cultured hippocampal neurons: Identification of the substances responsible for the pharmacological action. *J Neural Transm (Vienna)* 2013;120:1397–1409.
- Kang J, Shin JW, Kim YR, *et al.*: Nobiletin improves emotional and novelty recognition memory but not spatial referential memory. *J Nat Med* 2017;71:181–189.

参考論文

金沢大学大学院医薬保健学総合研究科
創薬科学専攻
分子薬物治療学研究室

西山 美沙



Homostachydrine is a Xenobiotic Substrate of OCTN1/SLC22A4 and Potentially Sensitizes Pentylentetrazole-Induced Seizures in Mice

Misa Nishiyama¹ · Noritaka Nakamichi^{1,2} · Tomoyuki Yoshimura¹ · Yusuke Masuo¹ · Tomoe Komori¹ · Takahiro Ishimoto¹ · Jun-ichi Matsuo¹ · Yukio Kato¹

Received: 23 July 2020 / Revised: 10 August 2020 / Accepted: 15 August 2020 / Published online: 26 August 2020
© Springer Science+Business Media, LLC, part of Springer Nature 2020

Abstract

Understanding of the underlying mechanism of epilepsy is desired since some patients fail to control their seizures. The carnitine/organic cation transporter OCTN1/SLC22A4 is expressed in brain neurons and transports food-derived antioxidant ergothioneine (ERGO), L-carnitine, and spermine, all of which may be associated with epilepsy. This study aimed to clarify the possible association of this transporter with epileptic seizures. In both pentylentetrazole (PTZ)-induced acute seizure and kindling models, *ocnt1* gene knockout mice (*ocnt1*^{-/-}) showed lower seizure scores compared with wild-type mice. Up-regulation of the epilepsy-related genes, *c-fos* and *Arc*, and the neurotrophic factor BDNF following PTZ administration was observed in the hippocampus of wild-type, but not *ocnt1*^{-/-} mice. To find the OCTN1 substrate associated with the seizure, untargeted metabolomics analysis using liquid chromatography–quadrupole time-of-flight mass spectrometry was conducted on extracts from the hippocampus, frontal cortex, and plasma of both strains, leading to the identification of a plant alkaloid homostachydrine as a compound present in a lower concentration in *ocnt1*^{-/-} mice. OCTN1-mediated uptake of deuterium-labeled homostachydrine was confirmed in OCTN1-transfected HEK293 cells, suggesting that this compound is a substrate of OCTN1. Homostachydrine administration increased PTZ-induced acute seizure scores and the expression of *Arc* in the hippocampus and that of *Arc*, *Egr1*, and BDNF in the frontal cortex. Conversely, administration of the OCTN1 substrate/inhibitor ERGO inhibited PTZ-induced kindling and reduced the plasma homostachydrine concentration. Thus, these results suggest that OCTN1 is at least partially associated with PTZ-induced seizures, which is potentially deteriorated by treatment with homostachydrine, a newly identified food-derived OCTN1 substrate.

Keywords Epilepsy · Ergothioneine · Metabolomics · Pentylentetrazole · Seizure · Slc22a4

Introduction

Epilepsy is characterized by recurrent seizures or loss of consciousness caused by abnormal cerebral excitation. Excitatory and inhibitory balance is mainly regulated by glutamatergic and GABAergic signaling in the brain. Genetic analyses have revealed that various genes are involved in the onset and development of epilepsy [1]. In addition,

dysfunction of some transporters such as the GABA transporter GAT-1 and the glucose transporter GLUT1 causes excitatory and inhibitory imbalance [2, 3]. However, the etiology of epilepsy has remained largely unclear. Since around 20% of epilepsy patients fail to achieve adequate seizure control using current anticonvulsants, and uncontrollable seizures lead to job limitation and decreased life-expectancy, further investigation of mechanisms of epilepsy is desirable [4].

The carnitine/organic cation transporter OCTN1/SLC22A4 is expressed in various organs, including the brain, kidneys, and the small intestine [5, 6]. The OCTN1 transports different organic cations and zwitterions including food-derived compounds such as ergothioneine (ERGO) and stachydrine, endogenous compounds such as acetylcholine, spermine, and L-carnitine, as well as several therapeutic agents although carnitine was proposed

✉ Noritaka Nakamichi
nakamichi@takasaki-u.ac.jp

¹ Faculty of Pharmacy, Institute of Medical, Pharmaceutical and Health Sciences, Kanazawa University, Kanazawa 920-1192, Japan

² Faculty of Pharmacy, Takasaki University of Health and Welfare, 60 Nakaorui-machi, Takasaki, Gunma 370-0033, Japan

to be a weak substrate of OCTN1 [5–9]. Among them, ERGO was proven to be an *in vivo* substrate, at least in rodents, with its concentration observed under the detection limit in *octn1* gene knockout (*octn1*^{-/-}) mice [8, 10]. In the brain, OCTN1 is localized in neural stem cells, neurons, and microglia. It regulates neuronal differentiation, neuronal maturation, and microglial activation *in vitro*, with its substrate ERGO being at least partially involved in such regulation [11–13]. However, the pathophysiological roles of OCTN1 remain unknown.

Oxidative stress is associated with the etiology and progression of epilepsy [14]. Some antioxidants such as α -tocopherol and melatonin ameliorate seizures in humans [15, 16]. ERGO is an antioxidant present in the bodies of rodents and humans due to its ingestion through the daily diet [17]. In addition, other OCTN1 substrates such as spermine and L-carnitine also show anti-seizure effects in rodents [18, 19]. Mutation of the acetylcholine transporter causes autosomal dominant nocturnal frontal lobe epilepsy in humans [20]. Thus, OCTN1 may be associated with the etiology or the progression of epilepsy through the regulation of exposure to these compounds in the brain. However, the relationship between OCTN1 and epilepsy remains unclear.

In this study, we aimed to clarify the possible involvement of OCTN1 in epileptic seizures. First, the experimental epilepsy model was established with repeated administration of GABA receptor antagonist pentylenetetrazole (PTZ) in *octn1*^{-/-} mice. Since the *octn1*^{-/-} mice showed much lower seizure scores compared with wild-type mice, the untargeted metabolomics analysis was performed to identify OCTN1 substrates that contribute to the differential phenotypes between the two strains. The plant alkaloid homostachydrine was identified as a novel OCTN1 substrate, which potentially worsens PTZ-induced seizures. Finally, the ameliorating effects of ERGO and *octn1* gene knockout on PTZ-induced kindling were investigated.

Experimental Procedures

Materials

Pentylenetetrazole was purchased from Sigma–Aldrich Inc. (St. Louis, MO, USA), ERGO was kindly provided by Yuki-guni Maitake Co., Ltd (Minamiuonuma, Japan). Deuterium-labeled ERGO (ERGO-d₉) was kindly supplied by TETRAHEDRON (Paris, France).

Synthesis of Homostachydrine and Deuterium-Labeled Homostachydrine (Homostachydrine-d₆)

Homostachydrine and homostachydrine-d₆ were synthesized from pipercolic acid by treatment of iodomethane or

deuterated iodomethane and KHCO₃, according to the literature [21]. The resulting homostachydrine was identified by ¹H-NMR and electrospray ionization mass spectrometry (*m/z* = 157). The homostachydrine-d₆ product was identified using ¹H-NMR.

Animals

Seven- to nine-week-old male mice were used. The *octn1*^{-/-} mice were backcrossed into a C57BL/6 J background [12]. Wild-type and *octn1*^{-/-} mice were maintained with free access to food and water.

PTZ-Induced Acute Seizures

PTZ dissolved in saline was intraperitoneally administered in mice at doses of 35, 40, or 50 mg/kg. Each mouse was then placed in a plastic cage and observed for 20 min. Seizure severity was evaluated primarily based on previously reported criteria [22], but stage 5 (death) was also included in this study, and the highest score observed within 20 min was monitored (stage 0: no behavioral change; stage 1: hypoactivity and immobility; stage 2: two or more isolated myoclonic jerks; stage 3: generalized clonic convulsions with preservation of righting reflex; stage 4: generalized tonic–clonic seizure with loss of righting reflex; stage 5: death). For PCR and ELISA analyses, PTZ at 45 mg/kg was administered twice with a 48-h interval, and the hippocampus was collected at 2 or 4 h after the second PTZ administration, respectively. The fore part of the cortex, excluding the thalamus, was collected as the frontal cortex. To examine the effect of homostachydrine on PTZ-induced seizures, homostachydrine was intravenously administered at 50 mg/kg in wild-type mice under isoflurane anesthesia. Four hours later, PTZ at 40 mg/kg was intraperitoneally administered, and the seizure score was evaluated as described above. After 20 min observation, the plasma, hippocampus, and frontal cortex were collected for measurement of homostachydrine concentration and mRNA expression.

RT-PCR

The total RNA was extracted from the resected tissues from PTZ-treated wild-type and *octn1*^{-/-} mice by using RNeasy plus (Takara Bio, Shiga, Japan), followed by synthesis and amplification of cDNA as described previously [8, 10]. The sequences of the primers were as follows: *c-fos* forward, GGGACAGCCTTTCCTACTACC and reverse, TTGGCACTAGAGACGGACAG; *Arc* forward, GAGTTCCTAGCC TGTTCCGGA and reverse, GCTCGGCACTTACCAATCT; *Egr1* forward, AGCCTTCGCTCACTCCACTATCC and reverse, GCGGCTGGGTTTGATGAGTTGG; *Bdnf* forward, GCGGCAGATAAAAAGACTGC and reverse, TCA

GTTGGCCTTTGGATACC; *Ngf* forward, TCTATACTG GCCGCAGTGAG and reverse, GGACATTGCTATCTG TGTACGG; *Nt-3* forward, GGAGGAAACGCTATGCAG AA and reverse, GTCACCCACAGGCTCTCACT; *36B4* forward, ACTGGTCTAGGACCCGAGAAG and reverse, TCCCACCTTGTCTCCAGTCT. The expression levels of mRNA were normalized to the *36B4* housekeeping gene.

ELISA

The isolated hippocampus (10 mg) was mixed with 100 μ L of extraction buffer (50 mM ammonium acetate, 1 M NaCl, and 0.1% Triton X-100 adjusted at pH 4.0 with acetate), followed by sonication on ice using a Handy Sonic UR20-P sonicator (Tommy Seiko, Tokyo, Japan). Homogenates were centrifuged at 21,500 \times g for 30 min at 4 °C. The BDNF concentration in the supernatant was measured using a mature BDNF rapid ELISA kit (Biosensis, Thebarton, Australia).

Untargeted Metabolomics Analysis Using Liquid Chromatography–Quadrupole Time-of-Flight Mass Spectrometry (LC-QTOFMS)

Wild-type and *octn1*^{-/-} mice were maintained in the same cage for 1 week. After overnight fasting, the hippocampus, frontal cortex, and plasma were collected. Plasma samples were mixed with five times the volume of methanol, including gabapentin, as an internal standard. The hippocampus and frontal cortex were mixed with five and six times its volume, respectively, of methanol, including gabapentin. Then, tissues were homogenized using a Precellys 24 homogenizer (Bertin Technologies, Montigny-le-Bretonneux, France) using zirconia silica beads at 1.2 mm (Biomedical Science, Tokyo, Japan). The homogenate samples were centrifuged at 21,500 \times g for 10 min at 4 °C to precipitate proteins. The supernatant (30 μ L) was then mixed with 120 μ L acetonitrile, and the mixture was again centrifuged. The supernatant was subjected to LC-QTOFMS analysis, which included accurate parent ion scanning with time-of-flight mass spectrometry using an Acquity UPLC system coupled with Xevo G2 QTOFMS (Waters, Milford, MA). The mobile phases were (A) 0.1% formic acid and 10 mM ammonium acetate in 20% acetonitrile solution, and (B) 0.1% formic acid and 10 mM ammonium acetate in 95% acetonitrile solution. The gradient elution (flow rate, 0.4 mL/min) was performed as follows: 0–0.5 min, 1% A/99% B; 0.5–6.5 min, 1% A/99% B to 50% A/50% B; 6.5–7.5 min, 50% A/50% B to 70% A/30% B; 7.5–8.5 min, 70% A/30% B; 8.5–9.0 min, 70% A/30% B to 1% A/99% B; 9.0–13.5 min, 1% A/99% B using an ACQUITY UPLC BEH Amide column (Waters). QTOFMS was operated in positive mode with electrospray ionization, and MS data (50–600 Da) were acquired in a centroid format. Chromatographic and spectral data were deconvoluted

by MarkerLynx software (Waters) to generate a multivariate data matrix. The threshold was set as follows; 2000 for the hippocampus, 1700 for the frontal cortex, and 400 for plasma samples. The peaks with signal intensity less than the threshold, and those observed in fewer than four of six samples were removed as noise. Peak height was divided by the height of gabapentin, and the average was calculated. The average values in *octn1*^{-/-} that were two times higher or less than half that in wild-type mice with a statistically significant difference were chosen. Finally, the peak shape was visually checked, and signals showing appropriate peak shape were selected. The accurate masses of the parent and product were compared with the online METLIN database (<https://metlin.scripps.edu>) and the Human Metabolome Database (<https://www.hmdb.ca/>).

Product Ion Scanning

Synthesized homostachydrine and mouse plasma samples were mixed with MeOH and centrifuged twice at 21,500 \times g for 10 min at 4 °C. Supernatants were subjected to product ion scanning using high-performance liquid chromatography–tandem quadrupole mass spectrometry (LC-TQMS), which consisted of a Nexera X2 LC system coupled with an LCMS-8040 (Shimadzu, Kyoto, Japan). Parent mass was set at m/z of 158.00, and the product ion was scanned at m/z of 50,200. The collision energy was 10, 20, or 40 V. The mobile phases were (A) 0.1% formic acid and 10 mM ammonium acetate in 20% acetonitrile solution, and (B) 0.1% formic acid and 10 mM ammonium acetate in 95% acetonitrile solution. Gradient elution (flow rate, 0.4 mL/min) was performed as follows: 0–0.5 min, 1% A/99% B; 0.5–3.5 min, 1% A/99% B to 15% A/85% B; 3.5–4.5 min; 15% A/85% B to 35% A/65% B; 4.5–4.8 min; 35% A/65% B to 60% A/40% B; 4.8–5.8 min; 60% A/40% B; 5.8–6.0 min; 60% A/40% B to 1% A/99% B; 6.0–8.0 min; 1% A/99% B, using an ACQUITY UPLC BEH Amide column.

Measurement of Homostachydrine Concentration

After fasting overnight, plasma and tissues were collected and mixed with MeOH containing gabapentin (internal standard). Tissues were then homogenized. After vortexing, the samples were centrifuged twice at 21,500 \times g for 10 min at 4 °C. The supernatant was subjected to LC-TQMS analysis, as described below.

Uptake of Homostachydrine-d₆ and ERGO-d₉ in HEK293 Cells Transfected with Human OCTN1

HEK293 cells transfected with human *OCTN1* gene (HEK293/OCTN1) were seeded onto poly-L-lysine-coated 4-well plates at a density of 3.8 \times 10⁴ cells/cm². After 72 h,

the medium was replaced with transport buffer and pre-incubated for 10 min at 37 °C as described previously [8, 10]. The buffer was then replaced with fresh one containing 10 μ M homostachydrine- d_6 to initiate transport. To analyze the concentration-dependent uptake of homostachydrine, transport buffer contained a mixture of homostachydrine- d_6 and homostachydrine at 5–1000 μ M. The Michaelis constant (K_m) and maximum velocity (V_{max}) values were estimated by fitting to Michaelis–Menten equation using GraphPad Prism (GraphPad Software, San Diego, CA). To analyze inhibition of uptake of ERGO by homostachydrine, transport buffer containing 1 μ M ERGO- d_9 with various concentrations of homostachydrine was used. At designated times, the cells were washed and collected with 300 μ L of water using a cell scraper, followed by sonication to destroy cell membranes [8, 10]. Samples were mixed with acetonitrile containing gabapentin (internal standard) and centrifuged twice at 21,500 \times g for 10 min at 4 °C. The supernatant was subjected to LC-TQMS analysis, as described below.

Plasma Concentration Profile of Homostachydrine

After fasting overnight, homostachydrine- d_6 dissolved in saline was intravenously and orally administered at doses of 1 and 3 mg/kg, respectively. Blood was collected at designed times and centrifuged to obtain plasma. The plasma samples were deproteinated with MeOH, including gabapentin, and centrifuged twice at 21,500 \times g for 10 min at 4 °C. Then the supernatant was subjected to LC-TQMS analysis as described below. Pharmacokinetic parameters were calculated using moment analysis.

Urinary Excretion of Homostachydrine- d_6

Mice were maintained in a metabolic cage for 24 h for habituation. Homostachydrine- d_6 was then administered, and urine collection was initiated. As a control study, 50 μ mol/kg of cephalexin was dissolved in the same solution as homostachydrine- d_6 and simultaneously administered with homostachydrine- d_6 . Urine was collected at 24 and 48 h after the initiation of urine collection. The samples were then diluted 100 times with water and deproteinated with MeOH, including gabapentin or verapamil. After centrifugation, the supernatant was subjected to LC-TQMS analysis, as shown below.

Measurement of Homostachydrine, ERGO, and Cephalexin by LC-TQMS

The amounts of homostachydrine, homostachydrine- d_6 , ERGO- d_9 , and cephalexin were measured using LC-TQMS. The mobile phases were (A) 0.1% formic acid and 10 mM ammonium acetate in 20% acetonitrile solution, and (B)

0.1% formic acid and 10 mM ammonium acetate in 95% acetonitrile solution. The gradient elution (flow rate, 0.4 mL/min) for homostachydrine and homostachydrine- d_6 was performed as follows: 0–0.5 min, 1% A/99% B; 0.5–3.5 min, 1% A/99% B to 15% A/85%B; 3.5–4.5 min; 15% A/85% B to 35% A/65% B; 4.5–4.8 min; 35% A/65% B to 60% A/40% B; 4.8–5.8 min; 60% A/40% B; 5.8–6.0; 60% A/40% B to 1% A/99% B; 6.0–8.0 min; 1% A/99% B, using an ACQUITY UPLC BEH Amide column. For ERGO- d_9 measurement, gradient elution was performed as follows; 0–0.5 min; 1% A/99% B; 0.5–1.5 min, 1% A/99% B to 25% A/85% B; 1.5–6.3 min, 25% A/85% B; 6.3–7.0 min, 25% A/85% B to 60% A/40% B; 7.0–8.0 min, 60% A/40% B; 8.0–8.2 min, 60% A/40% B to 1% A/99% B; 8.2–11.5 min, 1% A/99% B. For cephalexin measurement the mobile phases were (A) 0.1% formic acid and (B) 0.1% formic acid in acetonitrile. Gradient elution was performed as follows: 0–0.3 min, 99% A/1% B; 0.3–2.8 min, 99% A/1% B to 5% A/95% B; 2.8–3.4 min, 5% A/95% B; 3.4–4.5 min, 5% A/95% B to 99% A/1% B, on a Cosmosil C18-MS-II packed column (Nacalai Tesque, Kyoto, Japan). The MRM transitions of the molecular and product ions were as follows: homostachydrine, m/z 158.0 > 58.0; homostachydrine- d_6 , m/z 164.00 > 64.15; ERGO, m/z 230.00 > 127.10; ERGO- d_9 , m/z 239.15 > 127.00; cephalexin, m/z 348.00 > 157.90, gabapentin (internal standard for homostachydrine, homostachydrine- d_6 , and ERGO- d_9), m/z 172.05 > 154.15; and verapamil (internal standard for cephalexin), m/z 455.20 > 165.05.

Kindling Induced by Repeated Administration of PTZ

PTZ at 35 mg/kg was intraperitoneally administered every other day for a total of eleven times, and seizure severity was evaluated after each injection based on the same criteria as that used for PTZ-induced acute seizure. When the mouse died during the repeated administration, the score for the corresponding mouse was regarded as five in the subsequent PTZ administration. To analyze the effect of coadministration of ERGO, 50 mg/kg ERGO or vehicle (water) alone was orally administered every day to 7-week-old wild-type mice under isoflurane anesthesia. On the 8th day, PTZ administration was initiated, while daily ERGO administration was continued. To minimize the effect of anesthesia used for oral administration, ERGO was administered after PTZ administration. After 11 injections of PTZ, the hippocampus and frontal cortex from the surviving mice were collected to measure the concentration of ERGO and homostachydrine.

Statistics

Data are expressed as the mean \pm S.D. The statistical significance of differences was determined using Student's *t*-test or one-way ANOVA with Tukey–Kramer test. The survival rate was evaluated using the Kaplan–Meier test. A *p*-value of <0.05 was regarded as denoting a significant difference.

Results

Deletion of the *Octn1* Gene Reduces PTZ-Induced Acute Seizures

To investigate the possible association of OCTN1 with PTZ-induced acute seizures, a single intraperitoneal injection of PTZ was administered to wild-type and *octn1*^{-/-} mice, and seizure severity was evaluated. Seizure scores in wild-type mice increased in a dose-dependent manner, whereas *octn1*^{-/-} mice showed significantly lower seizure scores after administration of 40 mg/kg of PTZ compared with wild-type mice (Fig. 1a). The seizure score was not different between the two strains at 35 and 50 mg/kg of PTZ. To confirm this difference, PTZ at 45 mg/kg was administered twice in both strains, and *octn1*^{-/-} mice consistently showed lower seizure scores after each injection (Fig. 1b).

Up-Regulation of Epilepsy-Related Genes was not Observed in *octn1*^{-/-} Mice

To further confirm the association of OCTN1 with PTZ-induced acute seizure, changes in expression of epilepsy-related genes were examined in the hippocampus of the

two strains after PTZ administration. Expression of the neuronal excitation marker genes *c-fos* and *Arc* was primarily increased in PTZ-treated wild-type mice compared to the saline-treated group (Fig. 2a, b). Meanwhile, the up-regulation of *c-fos* and *Arc* by PTZ administration was not observed in *octn1*^{-/-} (Fig. 2a, b). No significant difference was observed in the expression of the neuronal excitation marker *Egr1* among the four groups (Fig. 2c). The expression of BDNF was also measured by PCR and ELISA as BDNF is related to the epilepsy development [23]. The expression of BDNF mRNA and protein increased in PTZ-treated wild-type mice compared with the saline-treated group, whereas such up-regulation was not observed in *octn1*^{-/-} mice (Fig. 2d, e). Thus, a deficiency of OCTN1 may alleviate PTZ-induced seizures through the suppression of neuronal excitation in the brain.

Identification of the OCTN1 Substrate Using Untargeted Metabolomics Analysis

OCTN1 is involved in the uptake of various types of substrates into cells. Therefore, we hypothesized that OCTN1 transport some substrates that deteriorate PTZ-induced acute seizure and that loss in the substrates in *octn1*^{-/-} might lead to the reduced PTZ-induced seizures in this strain. To identify OCTN1 substrates in the brain, untargeted metabolomics analysis was conducted in the brain and plasma. After automatic picking, 2,599, 2,676, and 1,697 ion peaks were detected in the hippocampus, frontal cortex, and plasma, respectively. After correcting for noise, 463, 424, and 186 peaks remained in the hippocampus, frontal cortex, and plasma, respectively. Among them, five, three, and three peaks showed more than two-fold difference between

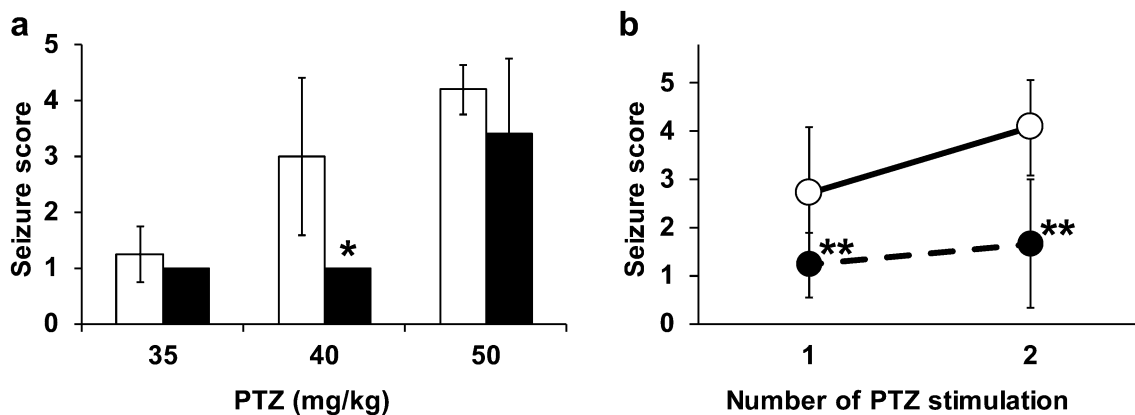


Fig. 1 Differences in PTZ-induced acute seizures in wild-type versus *octn1*^{-/-} mice. **a** Wild-type and *octn1*^{-/-} mice received a single intraperitoneal injection of PTZ (35, 40, or 50 mg/kg). Each mouse was observed for 20 min after administration, and the seizure severity was evaluated according to the criteria shown in the experimental procedures. The open column shows wild-type mice, and the closed

column shows *octn1*^{-/-} mice. Each value represents the mean \pm SD (*n*=4–5). **p*<0.05, significant difference from wild-type mice. **b** Wild-type and *octn1*^{-/-} mice received intraperitoneal injections of PTZ (45 mg/kg) twice within 48 h. Seizure scores were evaluated after each injection. Each value represents the mean \pm SD (*n*=9–14). ***p*<0.01, significant difference from wild-type mice

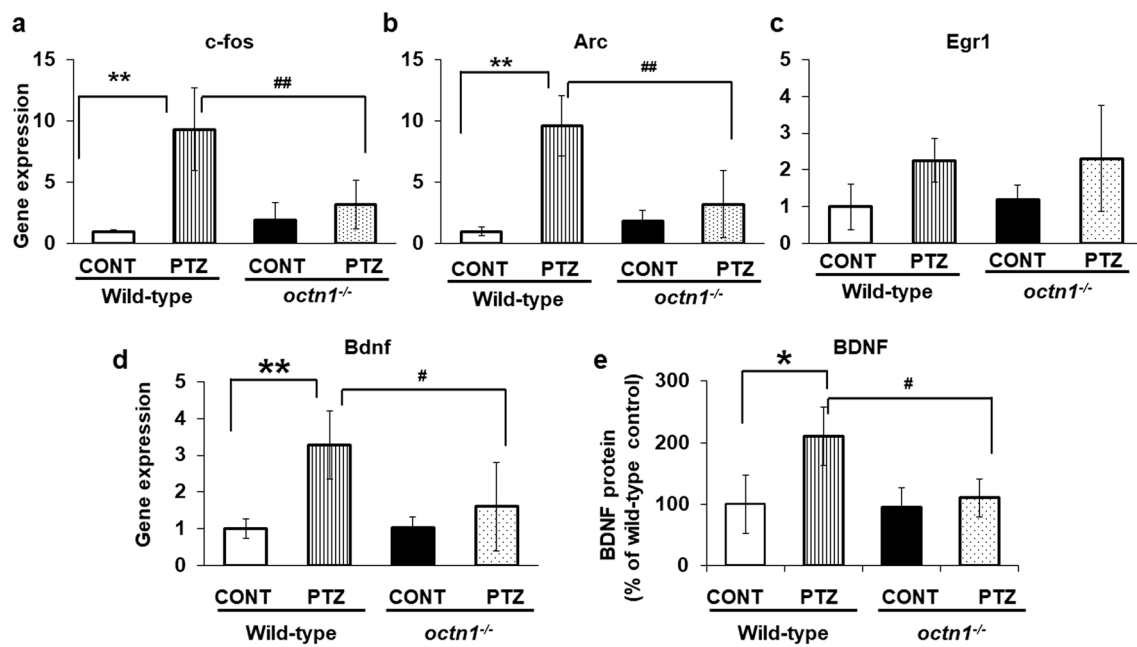


Fig. 2 Expression of epilepsy-related genes in the hippocampus after PTZ treatment. **a–d** PTZ (45 mg/kg) was intraperitoneally administered twice within a 48-h interval, and 2 h after the second PTZ injection the hippocampus was collected for RT-PCR analysis for neuronal excitation-related genes. The open columns show wild-type mice treated with saline; the striped columns show wild-type mice treated with PTZ. The closed columns show *octn1*^{-/-} mice treated with saline, and the dotted columns show *octn1*^{-/-} mice treated with PTZ. The expression of mRNA was normalized to that of the house-

keeping gene *36B4*. Each value represents the mean ± SD (n=3–8). **p<0.01, significant difference from wild-type controls. ##p<0.01, significant difference from PTZ-treated wild-type mice. **e** 4 h after the second PTZ injection, the hippocampus was collected, homogenized, and centrifuged for ELISA of the supernatant to measure the expression of BDNF protein. Each value represents the mean ± SD (n=3–4). *p<0.05, significant difference from wild-type mice. #p<0.05, significant difference from wild-type mice

wild-type and *octn1*^{-/-} mice, and confirmation of peak shape resulted in four, two, and two peaks in the hippocampus, frontal cortex, and plasma. Among them, only m/z 158 was detected in all three samples at the same retention time (Fig. 3a–c). According to its precursor and product ions, m/z 158 was identified to be homostachydrine. Then, a product ion scan was conducted for both synthesized homostachydrine and a plasma sample from wild-type mice, confirming that m/z 158 is homostachydrine (Fig. 3d) since common product ions, m/z 56, 58, 70, and 84 were detected (Fig. 3e, f). The homostachydrine concentration was then measured in plasma and each tissue from wild-type and *octn1*^{-/-} mice using LC-TQMS. The homostachydrine concentration in *octn1*^{-/-} was significantly lower in the plasma and all tissues except the middle section of the small intestine (Fig. 3g, h).

Human OCTN1-Mediated Transport of Homostachydrine

To examine whether OCTN1 directly transports homostachydrine, an uptake assay was conducted in HEK293/OCTN1 cells. Homostachydrine-d₆ was also synthesized to investigate the disposition of homostachydrine, and incubated with these cell lines for the detection of uptake

of this compound. Homostachydrine-d₆ was taken up by HEK293/OCTN1 cells in a time-dependent manner, and the uptake was reduced in the presence of ERGO (Fig. 4a). Uptake of homostachydrine-d₆ was not detected at 30 s but was detected at 15 and 60 min, and this uptake was much lower than that observed in HEK293/OCTN1 cells (Fig. 4a). Uptake increased almost linearly until 15 s (Fig. 4a inset), and concentration-dependent uptake observed at this incubation period showed saturation of OCTN1-mediated uptake of homostachydrine (Fig. 4b), with Km and Vmax values of 310 μM and 28.3 nmol/mg protein/15 s, respectively. Next, we evaluated the inhibition potential of homostachydrine for ERGO-d₉ uptake. Our results showed that the uptake of ERGO-d₉ was inhibited in the presence of homostachydrine, albeit incompletely (Fig. 4c).

Disposition of Homostachydrine In Vivo

To further evaluate the interaction of homostachydrine with OCTN1, the pharmacokinetics of homostachydrine-d₆ was examined. The doses (1 and 3 mg/kg) of homostachydrine-d₆ was chosen to observe plasma concentration of homostachydrine-d₆ less than that of homostachydrine (Fig. 3g) to avoid saturation of OCTN1 since the purpose of this study was

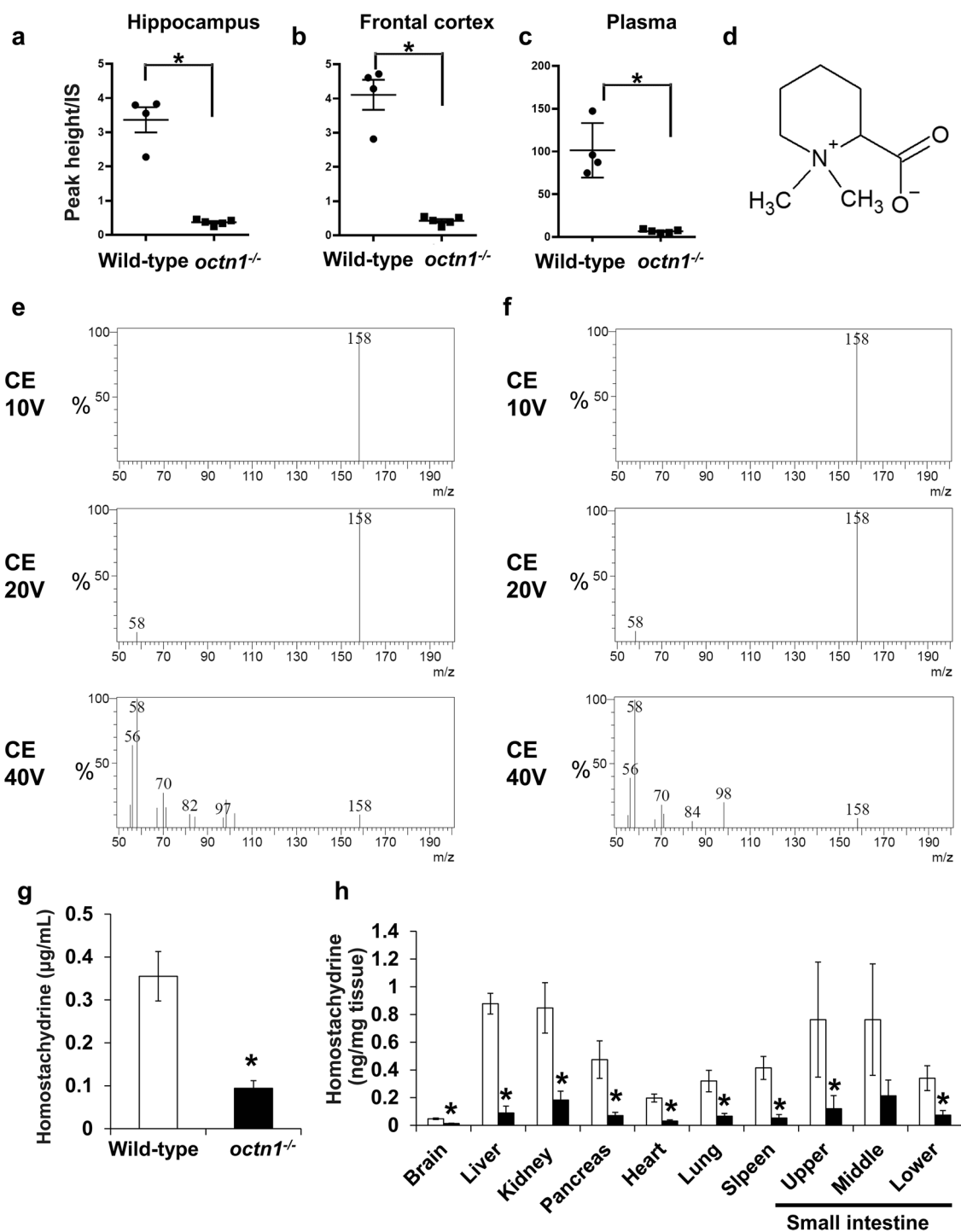


Fig. 3 Identification of homostachydrine as a candidate for the *in vivo* substrate of OCTN1. **a–c** Lysates of the hippocampus, cortex, and plasma were subjected to LC-TOFMS, and an ion peak at *m/z* 158 was identified, which was commonly a lower signal in the hippocampus (**a**), frontal cortex (**b**), and plasma (**c**) of *octn1*^{-/-} mice compared with wild-type mice. Each point represents each mouse. **p*<0.05, significant difference from wild-type mice. **d** The chemical structure of homostachydrine. **e** and **f** Production scanning against

m/z 158 was performed for chemically synthesized homostachydrine (**e**) and plasma samples of wild-type mice (**f**) with various collision energies from -10 to -40 V. **g, h** The homostachydrine concentration in the plasma (**g**) and various tissues (**h**) of wild-type (open bars) and *octn1*^{-/-} mice (closed bars) was measured using LC-TQMS. Each value represents the mean ± SD (*n*=3–4). **p*<0.05, significant difference from wild-type mice

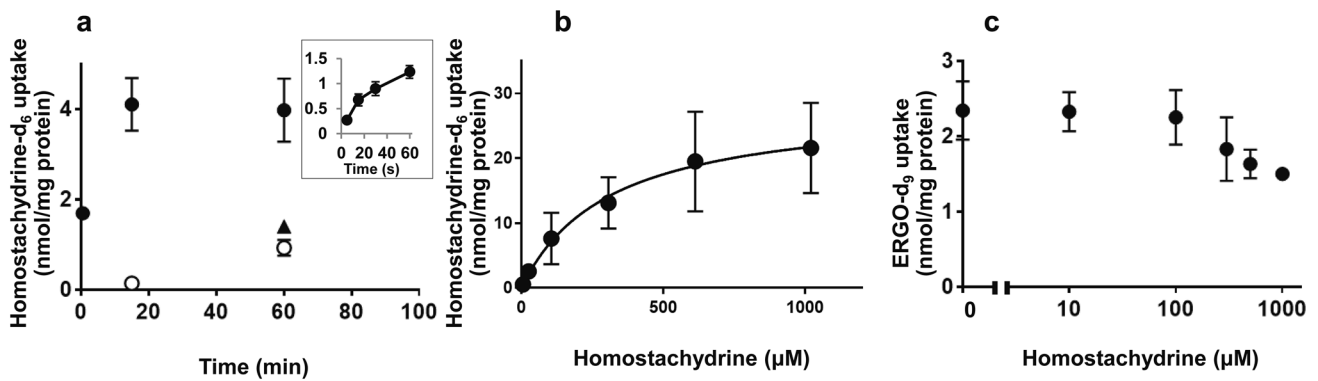


Fig. 4 The interaction of homostachydrine with human OCTN1. **a** HEK293 cells transfected with human OCTN1 gene (HEK293/OCTN1) and vector alone (HEK293/mock) were incubated with homostachydrine- d_6 (10 μ M) in the presence or absence of ERGO (500 μ M), and the uptake of homostachydrine- d_6 was measured by LC-TQMS. Closed circles and triangles indicate HEK293/OCTN1 cells without and with ERGO, whereas the open circles indicate HEK293/mock cells without ERGO. The inset represents the early-phase uptake of homostachydrine- d_6 in HEK293/OCTN1 cells. Each value represents the mean \pm SD (n=3). **b** HEK293/OCTN1 cells

were incubated with various concentrations of homostachydrine for 15 s, and the uptake was measured by LC-TQMS. The uptake of homostachydrine- d_6 in HEK293/mock cells was below detection limits, and therefore, the uptake represents OCTN1-mediated uptake. Each value represents the mean \pm SD (n=3). **c** HEK293/OCTN1 cells were incubated with ERGO- d_9 in the presence of various concentrations of homostachydrine for 5 min, and the uptake of ERGO- d_9 was measured using LC-TQMS. Each point represents the mean \pm SD (n=3)

to understand the role of OCTN1 in disposition of homostachydrine. After intravenous administration, the homostachydrine- d_6 concentration in the plasma of *octn1*^{-/-} mice was higher at the early phase (~ 10 min), but exhibited more rapid elimination until 8 h after administration, showing a lower plasma concentration after 4 h compared to wild-type mice (Fig. 5a). Such rapid elimination of homostachydrine- d_6 in the plasma of *octn1*^{-/-} mice was also confirmed at the terminal phase after oral administration. The plasma concentration of homostachydrine- d_6 in *octn1*^{-/-} after 6 h was lower than that of wild-type mice (Fig. 5). The maximum concentration (C_{max}) after oral administration and bioavailability were almost similar between the two strains,

suggesting that gastrointestinal absorption of homostachydrine may not be affected by OCTN1 (Table 1). Conversely, the half-life at the terminal phase and distribution volume in *octn1*^{-/-} were higher than those in wild-type mice, suggesting the involvement of OCTN1 in the distribution and elimination phases (Table 1). The smaller distribution volume in *octn1*^{-/-} could indicate limited tissue uptake of this compound and might be compatible with lower tissue concentration in *octn1*^{-/-} (Fig. 3h). The total clearance in *octn1*^{-/-} mice tended to be higher than wild-type mice (Table 1).

Fig. 5 Plasma concentration profile of homostachydrine- d_6 after iv and po administration. Homostachydrine- d_6 was intravenously (a) and orally (b) administered at a dose of 1 and 3 mg/kg, respectively, and the plasma concentration of homostachydrine- d_6 was measured by LC-TQMS. Open and closed circles showed wild-type and *octn1*^{-/-} mice, respectively. Each circle represents the mean \pm SD (n=3–5). *p < 0.05, significant difference from wild-type mice

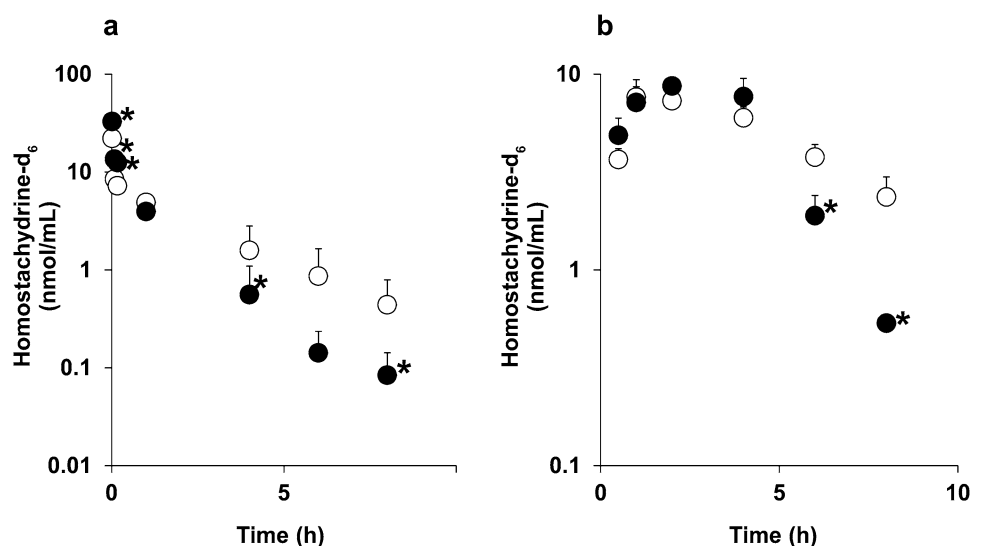


Table 1 Pharmacokinetic parameters of homostachydrine-d₆

	Dose (mg/kg)	C _{max} ^a (µg/mL)	AUC (µg/mg h)	T _{1/2} ^b (h)	CL _{tot} ^c (L/h/kg)	V ₀ ^d (L/kg)	Vd _{ss} ^e (L/kg)	F ^f (%)
Wild-type								
i.v.	1	–	3.58 ± 1.29	2.15 ± 0.26	0.307 ± 0.098	0.332 ± 0.140	0.649 ± 0.144	77.8
p.o.	3	1.29 ± 0.25	8.35 ± 1.16	3.05 ± 0.75	–	–	–	–
<i>octn1</i> ^{-/-}								
i.v.	1	–	2.91 ± 0.87	1.70 ± 0.51	0.368 ± 0.103	0.204 ± 0.033	0.346 ± 0.058*	77.3
p.o.	3	1.42 ± 0.16	6.74 ± 1.01	1.05 ± 0.08*	–	–	–	–

Mean ± SD (n = 5 and 3 for intravenous and oral administration, respectively)

*Significantly difference from wild-type (p < 0.05)

^aMaximum concentration

^bHalf-life at the terminal phase

^cTotal body clearance

^dInitial-phase distribution volume

^eSteady-state distribution volume

^fBioavailability

Table 2 Urinary excretion of homostachydrine-d₆

	Homostachydrine-d ₆ ^a	Cephalexin ^b
i.v.		
Wild-type	71.4 ± 14.2	49.8 ± 19.8
<i>octn1</i> ^{-/-}	69.8 ± 12.7	51.9 ± 8.2
p.o.		
<i>octn1</i> ^{-/-}	52.2 ± 4.4*	48.1 ± 6.8

Urinary excretion was recovered for 48 h after the administration and expressed as % of dose (Mean ± SD, n = 5 and 3 for wild-type and *octn1*^{-/-} mice, respectively)

*Significantly different from wild-type mice (p < 0.05)

^aDose of homostachydrine-d₆ was 1 and 3 mg/kg for i.v. and p.o., respectively

^bDose of cephalexin was 50 µmol/kg

Homostachydrine is Mainly Excreted in the Urine

To investigate the excretory route of homostachydrine, urine was collected for 48 h after intravenous and oral administration of homostachydrine-d₆ (Table 2). Approximately 70% of the dose was excreted in the urine after intravenous administration in both strains, and this was comparable or slightly higher than the urinary recovery of cephalexin (Table 2), which is known to be mainly eliminated by urinary excretion in rodents. Urinary excretion of homostachydrine-d₆ after oral administration tended to be slightly lower (50–65% of the dose) than that after intravenous administration in both strains (Table 2), and this finding would be compatible with incomplete gastrointestinal absorption (bioavailability ~ 80%, Table 1).

Homostachydrine Deteriorates PTZ-Induced Acute Seizures

To investigate whether homostachydrine deteriorates PTZ-induced acute seizures, homostachydrine was administered intravenously 4 h before PTZ administration in wild-type mice. The severity of PTZ-induced seizures was elevated in the homostachydrine-treated group compared with the saline-treated control group (Fig. 6a). After 20 min of observation, the plasma and brain were collected, and the homostachydrine concentration was measured (Fig. 6b, c). The homostachydrine concentration in plasma of the homostachydrine-treated group was around seven times higher than that in the PTZ only group (Fig. 6b). The homostachydrine concentration in the hippocampus and frontal cortex of the homostachydrine-treated group was also much higher than that in the control group (Fig. 6c). The expression of *Arc* in the hippocampus of the homostachydrine-treated group was significantly increased compared with the control group (Fig. 6d). The expressions of *Arc*, *Egr1*, and *Bdnf* in the frontal cortex of the homostachydrine-treated group were also up-regulated compared with the control group (Fig. 6e). The expression of *c-fos* in the homostachydrine-treated group tended to be increased compared with the control group in both brain tissues (Fig. 6d, e).

Gene Knockout of *octn1* and Repeated Administration of ERGO Inhibits PTZ-Induced Kindling

PTZ-induced kindling is regarded as an acquired epilepsy model that can be used to evaluate epileptogenesis, whereas PTZ-induced acute seizure is regarded as an epileptic

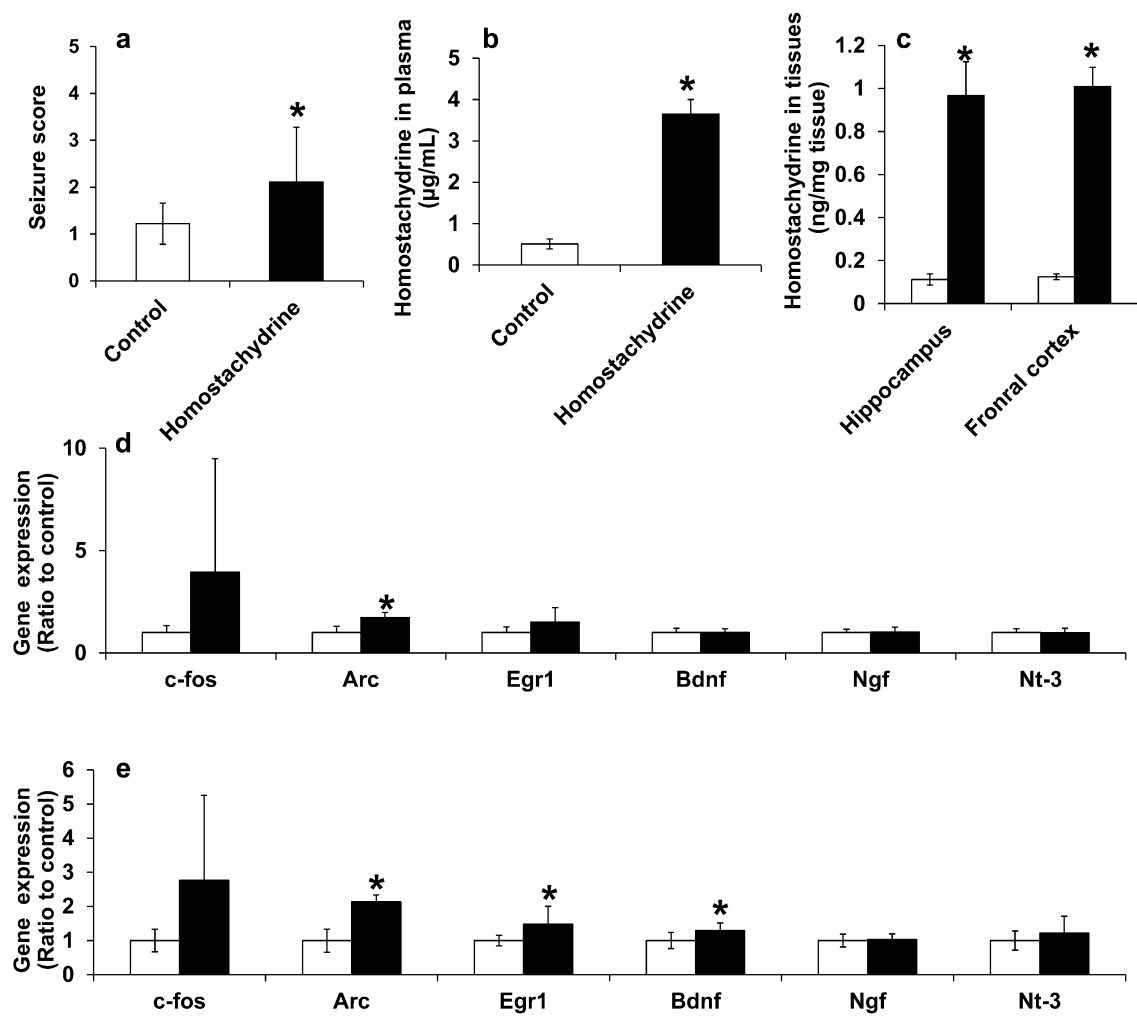


Fig. 6 The stimulating effect of homostachydrine on PTZ-induced acute seizures. **a** Homostachydrine (50 mg/kg) was intravenously administered, followed by intraperitoneal administration of PTZ (40 mg/kg) 4 h after homostachydrine administration in wild-type mice. Each mouse was then observed for 20 min after treatment, and seizure scores were evaluated. Each value represents the mean ± SD (n=9) *p < 0.05, significant difference from control. **b, c** After seizure scores were recorded, the plasma (**b**) and brains (**c**) were collected, and homostachydrine concentrations were measured by

LC-TQMS. Open columns showed controls, and closed columns showed the homostachydrine-treated group. Each value represents the mean ± SD (n=9) *p < 0.05, significant difference from controls. **d, e** After the seizure score observation, the hippocampus (**d**) and frontal cortex (**e**) were collected, and mRNA expression of epilepsy-related genes was evaluated. Closed and open columns showed homostachydrine-treated and control groups, respectively. Each value represents the mean ± SD (n=9) and was normalized to the control value. *p < 0.05, significant difference from control

seizure model [24]. Effect of OCTN1 on epileptogenesis was next examined using a PTZ-induced kindling model. The seizure scores resulting from the repeated administration of PTZ at a sub-convulsive dose in wild-type mice was gradually increased, whereas that in *octn1*^{-/-} was minimally changed, and the scores in *octn1*^{-/-} mice were significantly lower than that in wild-type mice after the 8th kindling stimulation (Fig. 7a). The survival rate after the final kindling stimulation in wild-type mice was 50%, whereas that in *octn1*^{-/-} mice was 86%, and the rate in *octn1*^{-/-} mice was significantly higher than that in wild-type mice (Fig. 7b). Next, we investigated the effect of inhibiting

homostachydrine transport by OCTN1 on PTZ-induced kindling. ERGO was used to inhibit OCTN1 since OCTN1-specific inhibitor has not yet been clarified. The seizure scores following repeated PTZ stimulation in the ERGO-treated group was minimally changed like that in the *octn1*^{-/-} group. Furthermore, the score in the ERGO-treated group was significantly lower than that in the wild-type group after the 6th kindling stimulation (Fig. 7c). The survival rate after the final kindling stimulation in the control group was 50%, whereas that in the ERGO-treated group was 91%, and the rate in the ERGO-treated group was significantly higher (Fig. 7d).

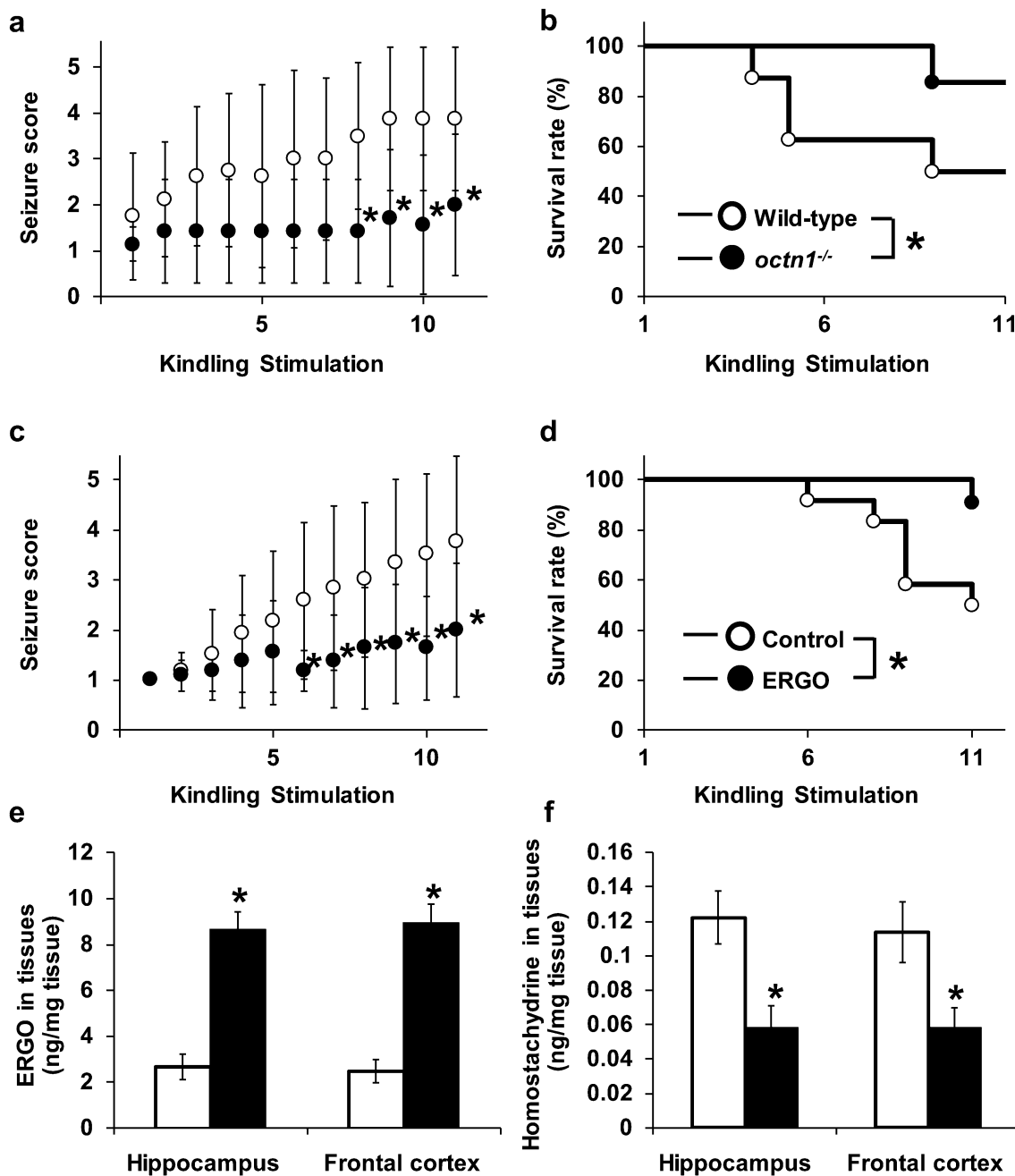


Fig. 7 The effect of *octn1* gene knockout and ERGO administration on PTZ-induced kindling. **a, b** PTZ (35 mg/kg) was intraperitoneally administered 11 times within a 48-h interval. Each mouse was then observed for 20 min after administration, and seizure scores (**a**) and survival rates (**b**) were evaluated. Open and closed circles showed wild-type and *octn1*^{-/-} mice, respectively. Each value represents the mean \pm SD ($n=7-8$). * $p<0.05$, significant difference from wild-type mice. **c-f** ERGO (50 mg/kg) or vehicle (water) was orally administered every day for 1 week. On day 8, the intraperitoneal administra-

tion of PTZ (35 mg/kg) was initiated, while daily ERGO administration was continued. Closed and open circles showed ERGO-treated and control groups, respectively. Each mouse was then observed for 20 min after administration, and seizure scores (**c**) and survival rates (**d**) were evaluated. After the 11th administration of PTZ, the concentration of ERGO (**e**) and homostachydrine (**f**) in the hippocampus and frontal cortex was measured using LC-TQMS. Each value represents the mean \pm SD ($n=3-6$). * $p<0.05$, significant difference from control

ERGO and homostachydrine concentrations in the brain were measured in surviving mice after the final PTZ administration. ERGO concentrations in the hippocampus and

frontal cortex in the ERGO-treated group were significantly higher than those in the control group (Fig. 7e). In contrast, homostachydrine concentrations in the two brain tissues

from the ERGO-treated group were substantially lower than those in the control group (Fig. 7f). These results suggest that the inhibition of OCTN1 may suppress not only epileptic seizures but also the acquisition of epilepsy through the decline of homostachydrine concentrations in the brain.

Discussion

This study demonstrated that OCTN1 deficiency inhibits PTZ-induced seizures and excitation of brain neurons in mice (Figs. 1, 2). Since OCTN1 transports the antioxidant ERGO and anti-seizure compounds such as L-carnitine and spermine [8, 10], we predicted that seizure scores in *octn1*^{-/-} mice would be increased compared with wild-type mice. However, the opposite result was observed. In our preliminary studies, the PTZ concentration in the whole brain and extracellular fluid (assessed by microdialysis) was measured 30 min after intraperitoneal PTZ administration (50 mg/kg), but no differences between wild-type and *octn1*^{-/-} mice were observed (data not shown). Therefore, the differences in seizure scores between the two strains may not be the result of the pharmacokinetic alteration of PTZ effects. We then hypothesized that OCTN1 transports unknown substrates which deteriorates PTZ-induced seizures, since both transporters accept a variety of compounds as substrates.

To clarify putative substrates involved in PTZ-induced acute seizure, untargeted metabolomics analysis was performed, and homostachydrine was identified as a candidate OCTN1 substrate in vivo (Figs. 3, 4). Homostachydrine is one alkaloid contained in the *Citrus* genus, alfalfa, and rye [21, 25, 26]. Homostachydrine is putatively synthesized from pipercolic acid in plants [27], whereas biosynthesis in animals and humans has not yet been reported. Thus, it is assumed that animals acquire homostachydrine from daily food intake, as in the case of the typical OCTN1 substrate ERGO.

After intravenous and oral administration, homostachydrine in plasma was rapidly eliminated in *octn1*^{-/-} mice compared with wild-type mice (Fig. 5). In contrast, the maximum concentration after oral administration and bioavailability was almost the same between the two strains (Table 1), suggesting that OCTN1 is mainly involved in the elimination of this compound, but not the primary transporter for its gastrointestinal absorption. OCTN1 is expressed on the apical membranes of proximal renal tubules and involved in the reabsorption of ERGO in the kidney, which at least partially explains why ERGO is present in plasma and almost all tissues of wild-type, but not *octn1*^{-/-} mice [10]. When we consider that ~70% of an administered dose was eliminated into the urine after intravenous administration (Table 2), the rapid elimination of homostachydrine in *octn1*^{-/-} mice (Fig. 5) can be similarly

explained by a deficiency in renal reabsorption of this compound in the kidney. This hypothesis is supported by the lower renal concentration in *octn1*^{-/-} mice compared with wild-type mice (Fig. 3g). Recovery of homostachydrine-d₆ into the urine was similar in the two strains (Table 2), but this may be caused by chronic urine sampling (~48 h) which may result in minimizing the effect of the excretion rate on recovery or the contribution of another transporter(s) besides OCTN1 in the renal handling of this compound.

Homostachydrine deteriorated PTZ-induced acute seizures in wild-type mice (Fig. 6). Plasma concentrations of homostachydrine are reportedly associated with schizophrenia and attention deficit hyperactivity disorder in humans [28]. In addition, the plasma concentration of homostachydrine was increased in experimental autoimmune encephalitis in mice [29]. However, the pathophysiological activity of homostachydrine has not yet been clarified in those studies. In contrast, the present study, for the first time, reported that homostachydrine exhibits stimulatory effects on PTZ-induced acute seizures. Pipercolic acid, a precursor of homostachydrine in plants, has a similar structure to homostachydrine and was reported to exacerbate epilepsy and experimental seizure models, although its proposed effect was controversial. Patients with pyridoxine-dependent seizures showed increased pipercolic acid concentrations in the plasma and cerebrospinal fluid [30]. In addition, intraperitoneal administration of high doses of pipercolic acid deteriorated PTZ-induced seizures [31]. Conversely, intracerebroventricular administration of low doses of pipercolic acid inhibited PTZ-induced seizures [31]. These reports suggest that pipercolic acid elicits contradictory seizure-related effects depending on its brain concentration. However, our study did not detect such contradictory effects of homostachydrine, though further investigations are warranted. Pipercolic acid is a modulator of GABAergic transmission and stimulates GABA release and inhibits GABA uptake [32]. Although there have been no reports regarding the effect of homostachydrine on GABAergic transmission, further investigation of the possible association of this compound with GABA homeostasis should be conducted to explain its deteriorating effects on seizures.

The deteriorating effect of homostachydrine (50 mg/kg) on PTZ-induced seizure was observed at much higher plasma and brain concentration (Fig. 6b, c) compared with the background level (Fig. 3g, h). Therefore, the effect of homostachydrine at lower dose would be much more helpful to understand its exact role in the body, but was not examined in the present study since effect of the background level of homostachydrine cannot be neglected. Further studies by constructing homostachydrine-free mice are needed to know its exact role in the body.

Plasma concentrations of homostachydrine in healthy volunteers were reported to be around 7.0 ng/mL [33], whereas

in mice after overnight fasting plasma concentrations averaged 0.35 µg/mL (Fig. 3g). Thus, homostachydrine concentrations in humans could be much lower than in mice. In humans, however, homostachydrine concentration in plasma is affected by dietary intake [34], as strict sodium restriction and a healthy Nordic diet has been shown to increase homostachydrine concentrations by 1.47- and 1.41-fold, respectively [35]. In addition, homostachydrine is present in plants that are used as herbal medicine such as *Medicago sativa* (alfalfa) and *Achillea millefolium* [26, 36]. Therefore, consuming homostachydrine-rich foods or herbal medicines may increase exposure to homostachydrine in humans. In addition, brain concentrations of homostachydrine seem to be highly dependent on the *octn1* (Fig. 3a–c, h). In contrast, SNPs in the *OCTN1* in humans profoundly affect the transport activity of gene products for specific substrates. The L503F SNP in the *OCTN1* gene is prominent in Caucasians (allele frequency: 0.458), whereas the I306T SNP is prominent in both Caucasians and the Japanese [37, 38]. Transport activity for ERGO and organic cations such as tetraethylammonium and metformin in L503F is higher compared with wild-type OCTN1, whereas that for L-carnitine and gabapentin in L503F is lower [38, 39]. Conversely, transport activity for ERGO is almost the same for either SNP, but is lower for gabapentin in the I306T variant compared with wild-type [38]. Thus, the genetic background may affect the exposure of homostachydrine to the brain, and further studies on plasma homostachydrine concentrations in humans and its association with food or medicine consumption are required to clarify whether homostachydrine affects seizure or not.

The PTZ-induced kindling model has been used to examine epileptogenesis, the process of transformation from a normal to an epileptic brain. In the PTZ-induced kindling model, sub-convulsive doses of PTZ are repeatedly administered to mice, and the brain is sensitized to stimulation. Since common phenotypes such as neuronal loss and mossy fiber sprouting are observed in the brain of both kindled mice and epilepsy patients [24], the PTZ-kindling model is regarded as the premium epilepsy model. In our study, *octn1*^{-/-} mice exhibited lower seizure scores and higher survival rates compared with wild-type mice in the PTZ-induced kindling model (Fig. 7a, b), suggesting that OCTN1 may be associated with epileptogenesis as well as seizures. In addition, repeated oral administration of the OCTN1 substrate/inhibitor ERGO exhibited inhibitory effects on PTZ-induced kindling (Fig. 7). ERGO is a diet-derived antioxidant and is synthesized in fungi or gut bacteria [40]. Administration of ERGO protected neurons from damage caused by cisplatin and β-amyloid via its antioxidant effects [41, 42]. Since the dose of ERGO in the present study was higher than previous reports, a portion of the anti-kindling effects (Fig. 7) may be due to antioxidant effects. However, homostachydrine concentrations in the brain were decreased

in the ERGO-treated group (Fig. 7f). This result implies that the protective effects of ERGO in PTZ-induced kindling may be at least partially caused by the inhibition of OCTN1, thereby reducing brain concentrations of homostachydrine or other endogenous substrates. If we consider the potential inhibition of OCTN1 by ERGO treatment, our findings regarding *octn1* gene knockout (Fig. 7a, b) and ERGO treatment (Fig. 7c, d) in the PTZ-induced kindling model suggest the possibility that OCTN1 inhibition may improve epileptic seizure or development of epilepsy. Since *octn1*^{-/-} mice show no distinct phenotype under normal conditions, the inhibition of OCTN1 should not cause serious side-effects. Thus, the utility of OCTN1 inhibitors as potential anti-epileptic compounds may require further examination. Another antioxidant, melatonin, also showed anti-seizure effects in animals and humans [16]. Melatonin is a dietary supplement food, and treatment with melatonin is considered relatively safe, although headache and sleepiness were reported in a study of insomnia treatment [43]. Conversely, side-effects were not reported following a 1-week treatment with ERGO in humans [44]. ERGO exhibits an extremely long half-life in humans and mice [10, 44], whereas the elimination of melatonin is much more rapid, with a half-life of 30 to 120 min [45]. Therefore, the anti-seizure activity of ERGO is promising and requires further examination.

In conclusion, this study showed that a deficiency of OCTN1 inhibits PTZ-induced seizures. A newly identified OCTN1 substrate, homostachydrine, may behave as a seizure-deteriorating compound in the brain. OCTN1 substrate and inhibitor ERGO decreases homostachydrine concentrations in the brain and inhibits PTZ-induced kindling. These findings indicate the necessity for further investigation of whether OCTN1 or its typical substrate and inhibitor ERGO is associated with epilepsy, and whether OCTN1 represents a suitable target for anti-epileptic drugs in the future.

Author Contributions Conceptualization: MN, NN, YK. Methodology: NN, TY, YM, YK. Analysis and investigation: MN, TY, TK, YM. Writing—original draft preparation: MN, TK, TY. Writing, review, and editing: NN, TI, YK. Funding acquisition: NN, YK. Resources: YK. Supervision: NN, JM, YK.

Funding Grants-in-Aid for Scientific Research to Noritaka Nakamichi (No. 19K07126) and Yukio Kato (No. 15H04664) from the Ministry of Education, Culture, Sports, Science, and Technology of Japan, and grant by the Hoansha Foundation (Osaka, Japan) to Yukio Kato.

Data Availability The datasets used or analyzed during this study are available from the corresponding author upon reasonable request.

Compliance with Ethical Standards

Conflict of interest The authors declare that they have no competing interest.

Ethical Approval Experiments were performed according to the Guidelines for the Care and Use of Laboratory Animals at Kanazawa University. All protocols were approved by the Institutional Animal Care and Use Committee of Kanazawa University.

References

- Wang J, Lin Z-J, Liu L et al (2017) Epilepsy-associated genes. *Seizure* 44:11–20. <https://doi.org/10.1016/j.seizure.2016.11.030>
- Mattison KA, Butler KM, Inglis GAS et al (2018) SLC6A1 variants identified in epilepsy patients reduce γ -aminobutyric acid transport. *Epilepsia* 59:e135–e141. <https://doi.org/10.1111/epi.14531>
- Koch H, Weber YG (2019) The glucose transporter type 1 (Glut1) syndromes. *Epilepsy Behav* 91:90–93. <https://doi.org/10.1016/j.yebeh.2018.06.010>
- Tian N, Boring M, Kobau R et al (2018) Active epilepsy and seizure control in adults—United States, 2013 and 2015. *Morb Mortal Wkly Rep* 67:437–442. <https://doi.org/10.15585/mmwr.mm6715a1>
- Gründemann D, Harlfinger S, Golz S et al (2005) Discovery of the ergothioneine transporter. *Proc Natl Acad Sci USA* 102:5256–5261. <https://doi.org/10.1073/pnas.0408624102>
- Tamai I, Ohashi R, Nezu JI et al (2000) Molecular and functional characterization of organic cation/carnitine transporter family in mice. *J Biol Chem* 275:40064–40072. <https://doi.org/10.1074/jbc.M005340200>
- Bacher P, Giersiefer S, Bach M et al (2009) Substrate discrimination by ergothioneine transporter SLC22A4 and carnitine transporter SLC22A5: gain-of-function by interchange of selected amino acids. *Biochim Biophys Acta* 1788:2594–2602. <https://doi.org/10.1016/j.bbame.2009.09.019>
- Masuo Y, Ohba Y, Yamada K et al (2018) Combination metabolomics approach for identifying endogenous substrates of carnitine/organic cation transporter OCTN1. *Pharm Res* 35:224. <https://doi.org/10.1007/s11095-018-2507-1>
- Pochini L, Scalise M, Galluccio M et al (2012) The human OCTN1 (SLC22A4) reconstituted in liposomes catalyzes acetylcholine transport which is defective in the mutant L503F associated to the Crohn's disease. *Biochim Biophys Acta - Biomembr* 1818:559–565. <https://doi.org/10.1016/j.bbame.2011.12.014>
- Kato Y, Kubo Y, Iwata D et al (2010) Gene knockout and metabolome analysis of carnitine/organic cation transporter OCTN1. *Pharm Res* 27:832–840. <https://doi.org/10.1007/s11095-010-0076-z>
- Ishimoto T, Nakamichi N, Hosotani H et al (2014) Organic cation transporter-mediated ergothioneine uptake in mouse neural progenitor cells suppresses proliferation and promotes differentiation into neurons. *PLoS ONE* 9:e89434. <https://doi.org/10.1371/journal.pone.0089434>
- Ishimoto T, Nakamichi N, Nishijima H et al (2018) Carnitine/organic cation transporter OCTN1 negatively regulates activation in murine cultured microglial cells. *Neurochem Res* 43:107–119. <https://doi.org/10.1007/s11064-017-2350-5>
- Nakamichi N, Nakao S, Nishiyama M et al (2020) Oral administration of the food derived hydrophilic antioxidant ergothioneine enhances object recognition memory in mice. *Curr Mol Pharmacol* 13:1121–1132. <https://doi.org/10.2174/1874467213666200212102710>
- Pearson-Smith J, Patel M (2017) Metabolic dysfunction and oxidative stress in epilepsy. *Int J Mol Sci* 18:2365. <https://doi.org/10.3390/ijms18112365>
- Mehvari J, Motlagh F, Najafi M et al (2016) Effects of Vitamin E on seizure frequency, electroencephalogram findings, and oxidative stress status of refractory epileptic patients. *Adv Biomed Res* 5:36. <https://doi.org/10.4103/2277-9175.178780>
- Banach M, Gurdziel E, Jędrych M, Borowicz KK (2011) Melatonin in experimental seizures and epilepsy. *Pharmacol Rep* 63:1–11. [https://doi.org/10.1016/S1734-1140\(11\)70393-0](https://doi.org/10.1016/S1734-1140(11)70393-0)
- Halliwel B, Cheah IK, Tang RMY (2018) Ergothioneine – a diet-derived antioxidant with therapeutic potential. *FEBS Lett* 592:3357–3366
- Kumar M, Kumar P (2017) Protective effect of spermine against pentylenetetrazole kindling epilepsy induced comorbidities in mice. *Neurosci Res* 120:8–17. <https://doi.org/10.1016/j.neurosci.2017.02.003>
- Hussein A, Adel M, El-Mesery M et al (2018) L-carnitine modulates epileptic seizures in pentylenetetrazole-kindled rats via suppression of apoptosis and autophagy and upregulation of Hsp70. *Brain Sci* 8:45. <https://doi.org/10.3390/brainsci8030045>
- Becchetti A, Aracri P, Meneghini S et al (2015) The role of nicotinic acetylcholine receptors in autosomal dominant nocturnal frontal lobe epilepsy. *Front Physiol* 6:22. <https://doi.org/10.3389/fphys.2015.00022>
- Servillo L, Giovane A, Balestrieri ML et al (2012) Occurrence of pipercolic acid and pipercolic acid betaine (Homostachydrine) in citrus genus plants. *J Agric Food Chem* 60:315–321. <https://doi.org/10.1021/jf204286r>
- Claycomb RJ, Hewett SJ, Hewett JA (2011) Prophylactic, prandial rofecoxib treatment lacks efficacy against acute PTZ-induced seizure generation and kindling acquisition. *Epilepsia* 52:273–283. <https://doi.org/10.1111/j.1528-1167.2010.02889.x>
- Binder DK, Croll SD, Gall CM, Scharfman HE (2001) BDNF and epilepsy: too much of a good thing? *Trends Neurosci* 24:47–53. [https://doi.org/10.1016/S0166-2236\(00\)01682-9](https://doi.org/10.1016/S0166-2236(00)01682-9)
- Morimoto K, Fahnestock M, Racine RJ (2004) Kindling and status epilepticus models of epilepsy: rewiring the brain. *Prog Neurobiol* 73:1–60. <https://doi.org/10.1016/j.pneurobio.2004.03.009>
- Servillo L, D'Onofrio N, Giovane A et al (2018) The betaine profile of cereal flours unveils new and uncommon betaines. *Food Chem* 239:234–241. <https://doi.org/10.1016/j.foodchem.2017.06.111>
- Wood KV, Stringham KJ, Smith DL et al (1991) Betaines of alfalfa: characterization by fast atom bombardment and desorption chemical ionization mass spectrometry. *Plant Physiol* 96:892–897. <https://doi.org/10.1104/pp.96.3.892>
- Essery JM, McCaldint DJ, Marion L (1962) The biogenesis of stachydrine. *Phytochemistry* 1:209–213. [https://doi.org/10.1016/S0031-9422\(00\)82824-1](https://doi.org/10.1016/S0031-9422(00)82824-1)
- Yang J, Yan B, Zhao B et al (2020) Assessing the causal effects of human serum metabolites on 5 major psychiatric disorders. *Schizophr Bull* 46:804–813. <https://doi.org/10.1093/schbul/sbz138>
- Mangalam A, Poisson L, Nemutlu E et al (2013) Profile of circulatory metabolites in a relapsing-remitting animal model of multiple sclerosis using global metabolomics. *J Clin Cell Immunol* 4:1000150. <https://doi.org/10.4172/2155-9899.1000150>
- Plecko B, Stöckler-Ipsiroglu S, Paschke E et al (2000) Pipercolic acid elevation in plasma and cerebrospinal fluid of two patients with pyridoxine-dependent epilepsy. *Ann Neurol* 48:121–125. [https://doi.org/10.1002/1531-8249\(200007\)48:1<121::AID-ANA20>3.0.CO;2-V](https://doi.org/10.1002/1531-8249(200007)48:1<121::AID-ANA20>3.0.CO;2-V)
- Chang Y-F, Hargest V, Chen J-S (1988) Modulation of benzodiazepine by lysine and pipercolic acid on pentylenetetrazol-induced seizures. *Life Sci* 43:1177–1188. [https://doi.org/10.1016/0024-3205\(88\)90207-X](https://doi.org/10.1016/0024-3205(88)90207-X)
- Gutiérrez MC, Delgado-Coello BA (1989) Influence of pipercolic acid on the release and uptake of [3 H]GABA from brain slices of

- mouse cerebral cortex. *Neurochem Res* 14:405–408. <https://doi.org/10.1007/BF00964852>
33. Tuomainen M, Kärkkäinen O, Leppänen J et al (2019) Quantitative assessment of betainized compounds and associations with dietary and metabolic biomarkers in the randomized study of the healthy Nordic diet (SYSDIET). *Am J Clin Nutr* 110:1108–1118. <https://doi.org/10.1093/ajcn/nqz179>
 34. Kärkkäinen O, Lankinen MA, Vitale M et al (2018) Diets rich in whole grains increase betainized compounds associated with glucose metabolism. *Am J Clin Nutr* 108:971–979. <https://doi.org/10.1093/ajcn/nqy169>
 35. Derkach A, Sampson J, Joseph J et al (2017) Effects of dietary sodium on metabolites: the Dietary Approaches to Stop Hypertension (DASH)–Sodium Feeding Study. *Am J Clin Nutr* 106:1131–1141. <https://doi.org/10.3945/ajcn.116.150136>
 36. Tunón H, Thorsell W, Bohlin L (1994) Mosquito repelling activity of compounds occurring in *Achillea millefolium* L. (asteraceae). *Econ Bot* 48:111–120. <https://doi.org/10.1007/BF02908196>
 37. Urban TJ, Yang C, Lagpacan LL et al (2007) Functional effects of protein sequence polymorphisms in the organic cation/ergothioneine transporter OCTN1 (SLC22A4). *Pharmacogenet Genomics* 17:773–782. <https://doi.org/10.1097/FPC.0b013e3281c6d08e>
 38. Futatsugi A, Masuo Y, Kawabata S et al (2016) L503F variant of carnitine/organic cation transporter 1 efficiently transports metformin and other biguanides. *J Pharm Pharmacol* 68:1160–1169. <https://doi.org/10.1111/jphp.12574>
 39. Peltekova VD, Wintle RF, Rubin LA et al (2004) Functional variants of OCTN cation transporter genes are associated with Crohn disease. *Nat Genet* 36:471–475. <https://doi.org/10.1038/ng1339>
 40. Genghof DS (1970) Biosynthesis of ergothioneine and hercynine by fungi and actinomycetales. *J Bacteriol* 103:475–478. <https://doi.org/10.1128/JB.103.2.475-478.1970>
 41. Song T-Y, Chen C-L, Liao J-W et al (2010) Ergothioneine protects against neuronal injury induced by cisplatin both in vitro and in vivo. *Food Chem Toxicol* 48:3492–3499. <https://doi.org/10.1016/j.fct.2010.09.030>
 42. Yang N-C, Lin H-C, Wu J-H et al (2012) Ergothioneine protects against neuronal injury induced by β -amyloid in mice. *Food Chem Toxicol* 50:3902–3911. <https://doi.org/10.1016/j.fct.2012.08.021>
 43. Boeve BF, Silber MH, Ferman TJ (2003) Melatonin for treatment of REM sleep behavior disorder in neurologic disorders: results in 14 patients. *Sleep Med* 4:281–284. [https://doi.org/10.1016/S1389-9457\(03\)00072-8](https://doi.org/10.1016/S1389-9457(03)00072-8)
 44. Cheah IK, Tang RMY, Yew TSZ et al (2017) Administration of pure ergothioneine to healthy human subjects: uptake, metabolism, and effects on biomarkers of oxidative damage and inflammation. *Antioxid Redox Signal* 26:193–206. <https://doi.org/10.1089/ars.2016.6778>
 45. Harpsøe NG, Andersen LPH, Gögenur I, Rosenberg J (2015) Clinical pharmacokinetics of melatonin: a systematic review. *Eur J Clin Pharmacol* 71:901–909. <https://doi.org/10.1007/s00228-015-1873-4>

Publisher's Note Springer Nature remains neutral with regard to jurisdictional claims in published maps and institutional affiliations.

副論文

金沢大学大学院医薬保健学総合研究科
創薬科学専攻
分子薬物治療学研究室

西山 美沙

Hydrolyzed Salmon Milt Extract Enhances Object Recognition and Location Memory Through an Increase in Hippocampal Cytidine Nucleoside Levels in Normal Mice

Noritaka Nakamichi,¹ Shunsuke Nakao,¹ Yusuke Masuo,¹ Ayaka Koike,¹ Naoto Matsumura,¹ Misa Nishiyama,¹ Aya Hasan Al-Shammari,¹ Hirotaka Sekiguchi,² Keita Sutoh,² Koji Usumi,² and Yukio Kato¹

¹Faculty of Pharmacy, Institute of Medical, Pharmaceutical and Health Sciences, Kanazawa University, Kanazawa, Japan.

²Life Science Institute Co., Ltd., Tokyo, Japan.

ABSTRACT Salmon milt extract contains high levels of nucleic acids and has antioxidant potential. Although salmon milt extract is known to improve impaired brain function in animal models with brain disease, its effects on learning and memory ability in healthy subjects is unknown. The purpose of the present study was to clarify the effect of hydrolyzed salmon milt extract (HSME) on object recognition and object location memory under normal conditions. A diet containing 2.5% HSME induced normal mice to devote more time to exploring novel and moved objects than in exploring familiar and unmoved objects, as observed during novel object recognition and spatial recognition tests, respectively. A diet containing 2.5% nucleic acid fraction purified from HSME also induced similar effects, as measured by the same behavioral tests. This suggests that the nucleic acids may be a functional component contributing to the effects of HSME on brain function. Quantitative polymerase chain reaction analysis revealed that gene expression of the markers for brain parenchymal cells, including neural stem cells, astrocytes, oligodendrocytes, and microglia, in the hippocampi of mice on an HSME diet was higher than that in mice on a control diet. Oral administration of HSME increased concentrations of cytosine, cytidine, and deoxycytidine in the hippocampus. Overall, ingestion of HSME may enhance object recognition and object location memory under normal conditions in mice, at least, in part, via the activation of brain parenchymal cells. Our results thus indicate that dietary intake of this easily ingestible food might enhance brain function in healthy individuals.

KEYWORDS: • amino acids • brain parenchymal cells • hydrolyzed salmon milt extract • nucleic acids • object location memory • object recognition memory

INTRODUCTION

LEARNING AND MEMORY are brain functions involved in the acquisition of information essential for animal survival. Impairment in the abilities of learning and memory resulting from brain injury or neurodegenerative disorders leads to a considerable decrease in the quality of life. Therefore, many studies have been performed with the aim of recovering learning and memory abilities that have been degraded by brain lesions or neurodegeneration. Learning and memory impairments are generally improved by compounds with antioxidant properties and/or those that promote neurogenesis and synaptic plasticity.^{1–3}

Under normal conditions of mental health and intellect, on the contrary, humans are able to learn and memorize various information unrelated to survival, but essential to the construction of a sophisticated and diversified society.

Possession of high learning and memory ability is advantageous in pursuing a successful social life. Indeed, the intelligence quotient has been reported to be highly correlated with health and wealth.^{4,5} Despite these benefits, however, limited information is available regarding compounds that enhance learning and memory ability in healthy animals, which is in contrast to extensive research on compounds that improve these abilities after brain injury.

Salmon milt extract is produced by removing fluids and lipids from salmon milt, and mainly contains protein and deoxynucleotides. It is used as an ingredient in health food, and can be easily assimilated. The components of salmon milt extract are further hydrolyzed to obtain small, water-soluble molecules by treatment with hydrolases, including proteases and nucleases. The resultant substance is known as hydrolyzed salmon milt extract (HSME). The deoxynucleotides abundantly contained in salmon milt extract not only form genetic material but also contribute to the improvement of brain function.

Oral ingestion of a diet supplemented with nucleotides has been reported to enhance learning and memory ability in rats as assessed by the water-filled multiple T-maze test and

Manuscript received 10 July 2018. Revision accepted 9 January 2019.

Address correspondence to: Yukio Kato, PhD, Faculty of Pharmacy, Institute of Medical, Pharmaceutical and Health Sciences, Kanazawa University, Kakuma-machi, Kanazawa 920-1192, Japan, E-mail: ykato@p.kanazawa-u.ac.jp

passive avoidance test.⁶ Dietary nucleotides and nucleosides have also been found to improve impaired abilities related to learning and memory in aged, memory-deficient mice and in senescence-accelerated mice as assessed by the passive avoidance test.^{7,8} Furthermore, oral administration of the purine nucleoside guanosine promotes hippocampal neuronal differentiation and exerts an antidepressant-like effect in mice.⁹

In addition, various components contained in salmon milt extract are known to exhibit protective effects against brain impairment. For example, oral ingestion of nucleoprotein extracted from salmon milt suppresses dopaminergic neuronal death and motor deficiency in mice models of Parkinson's disease induced by 1-methyl-4-phenyl-1, 2, 3, 6-tetrahydropyridine (MPTP),¹⁰ and inhibits neuronal death induced by brain ischemia in mice hippocampi.¹¹ Thus, salmon milt extract is a promising candidate for treatment of brain injury or degeneration as a food-derived ingredient exhibiting beneficial effects on learning and memory. However, its effect on learning and memory under normal conditions cannot be easily predicted owing to limited research on enhancement of brain function in healthy individuals.

In the present study, to examine the effect of salmon milt extract on learning and memory under normal conditions, a diet supplemented with HSME was fed to healthy mice. Novel object recognition test (NORT) and spatial recognition test (SRT) were performed to appraise learning and memory. The effects of diets supplemented with nucleic acid fraction (NAF) of HSME or with a mixture of amino acids (AAM) contained in HSME were also studied to identify the functional components of HSME.

MATERIALS AND METHODS

Materials

HSME consisted of salmon milt water solubilized by nuclease and protease as described previously,¹² and contained oligo- and mononucleotides, nucleosides, bases, peptides, and amino acids. NAF was a DNA sodium salt produced from salmon milt extract,¹³ which was then hydrolyzed by nuclease. AAM was a mixture of 18 authentic amino acids in the ratio in which they are found in HSME. HSME, NAF, and AAM were provided by Life Science Institute Co. Ltd (Tokyo, Japan) and Foday's Co. Ltd (Tokyo, Japan). ISOGEN, MultiScribe™ Reverse Transcriptase, and THUNDERBIRD SYBR qPCR Mix were purchased from Nippon Gene (Tokyo, Japan), Biosystems (Foster City, CA, USA), and TOYOBO (Osaka, Japan), respectively. All other chemicals and reagents were of the highest purity available and were purchased from commercial sources.

Animals

Male Institute of Cancer Research (ICR) mice were used for *in vivo* analyses of behavior, measurement of nucleic acid concentration, and gene expression, and pregnant ICR mice were used for *in vitro* analysis using neural stem cell culture. These ICR mice were purchased from Sankyo Labo

Service Co. (Tokyo, Japan). Mice were housed under pathogen-free conditions at a controlled temperature (21–25°C) and were subjected to a 12 h light per dark cycle. The lights remained on from 8:00 to 20:00, and food and water were available *ad libitum*. The animals were cared for in strict compliance with the guidelines outlined in the National Institutes of Health Guide for the Care and Use of Laboratory Animals. All animal procedures used in this work were approved by the Kanazawa University Animal Care Committee (Permit Number: AP-132875).

Behavioral tests in mice

The experimental schedule is summarized in Supplementary Figure S1. The mice were purchased at the age of 4 weeks and fed control diets for 1 week. Then, they were randomly divided into four groups based on diet. The four groups of mice were fed a control diet (PicoLab Rodent Diet 20®; PMI Nutrition International, Brentwood, MO), a control diet containing 2.5% (w/w) HSME, NAF, or AAM, respectively, for 2 weeks. The body weights of mice from the control and HSME groups were measured every week, whereas those of mice from the NAF and AAM groups were measured on experimental day 14. To perform NORT, each mouse was individually placed in an acrylic chamber (45 × 45 × 45 cm) and allowed to explore for 10 min. The next day, each mouse was placed in the chamber with two similar objects located on a diagonal line, and allowed to explore for 5 min. Following a 24 h period, one of the objects was replaced by a new one at the same position in the chamber, and each mouse was allowed to explore for 5 min. Exploration time for each object was recorded. Discrimination index was calculated as follows: (novel object exploration time/total exploration time) – (familiar object exploration time/total exploration time) × 100.

SRT was conducted on the following day. Each mouse was individually placed in an acrylic chamber and allowed to explore for 10 min. The next day, each mouse was placed in the chamber with two similar objects located on a diagonal line and allowed to explore for 5 min. After 1 h, one of the objects was displaced, and each mouse was allowed to explore for 5 min. Exploration time devoted to each object was recorded. Discrimination index was calculated as follows: (moved object exploration time/total exploration time) – (unmoved object exploration time/total exploration time) × 100.

Measurement of nucleic acid concentration in the forebrain and hippocampus

For detailed information, see Measurement of Nucleic Acid Concentration in the Forebrain and Hippocampus section in Supplementary Data.

Quantitative reverse transcription-polymerase chain reaction

For detailed information, see Quantitative reverse transcription-polymerase chain reaction section in Supplementary Data.

Neural stem cell culture

For detailed information, see Neural Stem Cell Culture section in Supplementary Data.

MTT assay

For detailed information, see MTT Assay section in Supplementary Data.

Adenosine triphosphate assay

Adenosine triphosphate (ATP) assay was performed in primary cultured neural stem cells according to the standard procedure of the ATP assay kit ATPlite™ (PerkinElmer, Waltham, MA).

Statistical analysis

Data are expressed as means \pm standard error of the mean. The statistical significance of differences was determined using Student's *t*-test or one-way analysis of variance, followed by Dunnett's multiple comparison tests for the appropriate *post hoc* analysis. *P* < .05 was regarded as indicative of significant difference.

RESULTS

Nucleoside composition of HSME and NAF is shown in Table 1. Approximately 32% and 69% of HSME and NAF, respectively, consisted of mono- or oligodeoxynucleotides (Table 1). Gel filtration analysis revealed that mono-, di-, tri-, and tetranucleotides were present in both HSME and NAF (Supplementary Fig. S2). The amino acid composition of HSME is shown in Table 2. Approximately 48% of HSME was made up of amino acids, and of this, 40% was arginine (Table 2).

To clarify the effect of HSME on learning and memory ability, NORT and SRT were performed. The body weights of the mice on the HSME diet showed similar changes as did those of the mice on the control diet (Fig. 1A). To clarify the effect of diet containing HSME on object recognition memory, NORT was performed under the condition in which normal mice ingested with the control diet cannot

distinguish the novel object from the familiar one. The exploration time devoted to the novel object was significantly longer than the time devoted to the familiar one in mice on the HSME-supplemented diet, whereas it was similar for both novel and familiar objects in mice on control diet (Fig. 2A). SRT was performed under the condition in which normal mice ingested with the control diet cannot distinguish the moved object from the unmoved one, with an aim to clarify the effect of diet containing HSME on object location memory in normal mice. The exploration time devoted to the moved object was significantly longer than that devoted to the unmoved one in mice on the HSME-supplemented diet, whereas it was similar for both objects in mice on control diet (Fig. 2B). These results suggest that oral ingestion of HSME under normal conditions of health may enhance object recognition and object location memory in mice. Discrimination index for NORT in mice on the HSME-supplemented diet was significantly higher than that in mice on control diet (Table 3). To clarify the component responsible for the improvement in brain function induced by HSME, two components of the substance were prepared for analysis. HSME was fractionated, and the nucleic acid portion was separated out as NAF. AAM was prepared by mixing authentic amino acids in the ratios in which they are present in HSME (Table 2). Body weights of 14 days following the commencement of the experimental diets were similar among mice on the control, HSME, NAF, and AAM diets (Fig. 1B). The effect of NAF on exploration times assessed by both NORT and SRT was similar to that of HSME (Fig. 2A, B), and discrimination indices for both NORT and SRT in mice that were given NAF were significantly higher than in mice that were on control diet (Table 3). AAM had effects on exploration time (Fig. 2A) and discrimination index (Table 3) as assessed by NORT.

To verify that the enhancement in learning and memory seen upon oral ingestion of HSME is indeed provoked by nucleic acids, the concentrations of several nucleic acids in the hippocampus, a region of the forebrain closely associated with learning and memory abilities, and in the remainder of the forebrain were measured using liquid chromatography-tandem mass spectrometry, following oral administration of HSME. Concentrations of cytosine and cytidine in both the

TABLE 1. NUCLEOSIDE COMPOSITION OF HYDROLYZED SALMON MILT EXTRACT AND NUCLEIC ACID FRACTION

	HSME		NAF	
	Oligo- and monodeoxynucleotides (g/100 g) ^a	Monodeoxynucleotides (g/100 g) ^b	Oligo- and monodeoxynucleotides (g/100 g) ^a	Monodeoxynucleotides (g/100 g) ^b
dAMP	8.78	3.93	17.0	10.1
dTMP	10.3	1.83	23.4	6.42
dGMP	6.74	1.96	14.2	6.66
dCMP	6.39	2.51	14.6	8.01

^aContent of each monodeoxynucleotide was measured after hydrolysis of the samples. Therefore, the amount represents the sum of oligo- and monodeoxynucleotides.

^bContent of each monodeoxynucleotide was measured before hydrolysis of the samples. Therefore, the amount represents monodeoxynucleotides alone.

dAMP, deoxyadenosine monophosphate; dCMP, deoxycytidine monophosphate; dGMP, deoxyguanosine monophosphate; dTMP, deoxythymidine monophosphate; HSME, hydrolyzed salmon milt extract; NAF, nucleic acid fraction.

TABLE 2. AMINO ACID COMPOSITION OF HYDROLYZED SALMON MILT EXTRACT

Arg 18.70	Lys 2.60	His 0.67	Phe 0.87	Tyr 0.85	Leu 1.90	Ile 1.22	Met 0.58	Val 2.11	Ala 1.93
Gly 4.09	Pro 2.67	Gln 3.30	Ser 2.54	Thr 1.23	Asp 2.10	Trp 0.20	Cys ^a 0.23	Total 47.8	

Unit is g/100 g of HSME.

^aCysteine was measured as cystine.

hippocampus and the rest of the forebrain in mice administered HSME were significantly higher than in mice administered the vehicle alone (Fig. 3). In addition, concentrations of deoxycytidine in the hippocampus of mice administered HSME were significantly higher than in mice administered the vehicle alone (Fig. 3). Hippocampal thymidine concentration was slightly, but significantly, higher in mice administered HSME than in the control group mice (Fig. 3). Plasma concentration profiles were also measured (Supplementary Fig. S3), and concentration of cytosine, deoxycytidine, and thymidine in mice administered HSME tended to be higher than that in mice administered the vehicle alone, although experimental variation was relatively large possibly due to the effect of any homeostatic regulation.

To understand the mechanisms underlying the enhancement of object recognition and object location memory by dietary HSME, gene expression of the neuronal maturation markers, and the markers for brain parenchymal cells found in the hippocampus was investigated. In our preliminary study, expressions of all the marker genes examined in the present study were almost identical between control and HSME groups at 2 weeks following the start of the experimental diet (data not shown). Therefore, we thought that the change in gene expression of these markers may be induced within 1 week following the start of the experimental diet, and gene expression of these markers was examined at 2, 4, and 6 days following the start of the experimental diet. Gene expression of the neural stem cell marker nestin, astro-

cyte marker glial fibrillary acidic protein, microglia marker CD11b, oligodendrocyte marker myelin basic protein (MBP)-1 and -2, and undifferentiated proliferative cell marker sex determining region Y-box 2 (SOX2) at 2 days following the start of the experimental diet in mice fed HSME was significantly higher than in mice on control diet (Fig. 4). On the contrary, expressions of these marker genes were almost identical in all groups at 4 and 6 days following the start of the experimental diet (Fig. 4).

Furthermore, to verify that HSME and NAF directly influence brain parenchymal cells, the effect of HSME and NAF on cellular proliferation in cultured neural stem cells was investigated. Exposure of cultured neural stem cells to 10 μg/mL of HSME and NAF, and the positive control forskolin at 10 μM significantly increased MTT reduction activity (Fig. 5A). HSME, NAF, and forskolin also increased cellular ATP level (Fig. 5B). These results suggest that HSME and NAF promote cellular proliferation in neural stem cells. Moreover, oral ingestion of HSME may enhance learning and memory abilities, at least in part, through the direct action in brain parenchymal cells. It should be noted that dose dependency was minimally observed for the promotive effect of HSME and NAF on the cellular proliferation (Fig. 5). Although exact reason for the minimal dose dependency is unknown, HSME and NAF are the mixture of various compounds, and some of which may exhibit suppressive effect at higher concentrations of HSME and NAF on the cellular proliferation.

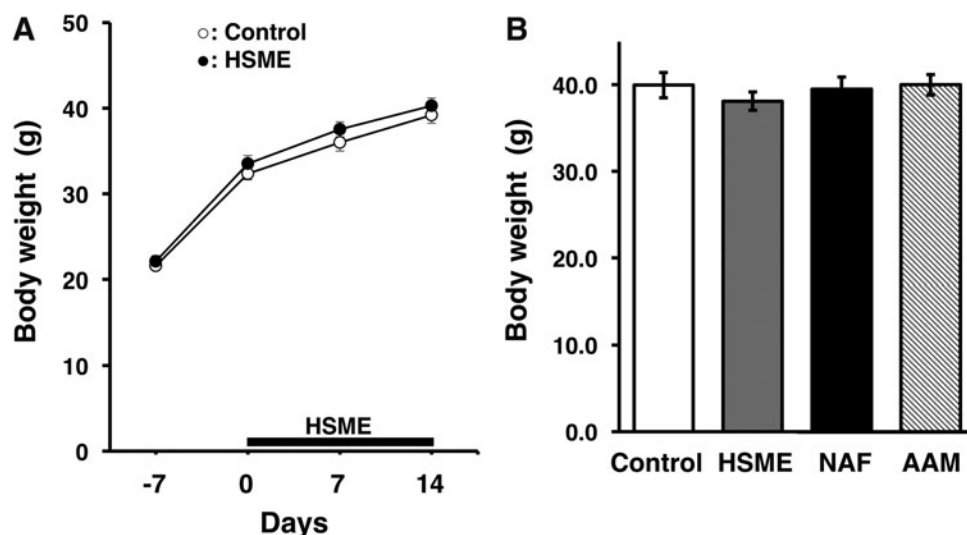


FIG. 1. Effect of ingestion of HSME, NAF, and AAM on body weight in mice. Mice were fed a control diet or a control diet supplemented with 2.5% (w/w) of HSME, NAF, or AAM for 2 weeks. (A) Body weights of mice fed the control diet (white) or the diet containing HSME (black) were measured on days 7, 0, 7, and 14. (B) Body weights of mice fed control diet (white), or the diet containing HSME (gray), NAF (black), or AAM (diagonal) were measured on day 14. Each value represents the mean ± SEM (n=6). AAM, mixture of amino acids; HSME, hydrolyzed salmon milt extract; NAF, nucleic acid fraction; SEM, standard error of the mean.

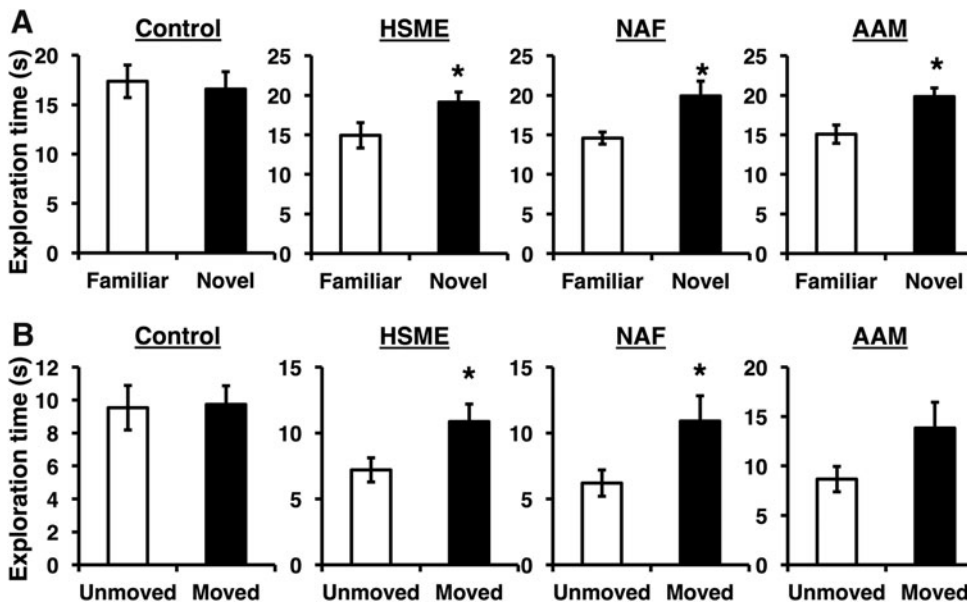


FIG. 2. Effect of ingestion of HSME, NAF, and AAM on object recognition and object location memory. Mice were fed a control diet or a control diet supplemented with 2.5% (w/w) of HSME, NAF, or AAM (A) and NORT (A) and SRT (B) were conducted. In (A), white and black columns show exploration time devoted to familiar and novel objects, respectively. In (B), white and black columns show exploration time devoted to the unmoved and moved object, respectively. Each value represents the mean \pm SEM ($n=10-15$). *Significant difference relative to the corresponding control values ($P < .05$). NORT, novel object recognition test; SRT, spatial recognition test.

DISCUSSION

The present findings indicate that oral ingestion of salmon milt extract enhances object recognition and object location memory in healthy mice (Fig. 2 and Table 3). Salmon milt extract contains an abundance of nucleic acids and can be made available as a nutritional ingredient. That is, it can be easily assimilated from the daily diet. This makes it even more noteworthy that brain function in healthy mice can be enhanced by this easily available food ingredient.

NAF could be one of the functional components in HSME, since both object recognition and object location memory in mice, assessed as exploration time devoted to novel and moved objects, respectively, upon oral ingestion of this fraction, were enhanced to a degree similar to that in mice on an HSME-supplemented diet (Fig. 2). Discrimination index after ingestion of NAF was significantly increased in both studies, a tendency that was also observed after ingestion of HSME (Table 3). In addition, exposure of neural stem cells to NAF as well as HSME increased cellular proliferation (Fig. 5). NAF used in the present study contained mono- and oligonucleotides (Table 1 and Supplementary Fig. S2). Oral ingestion of the mononucleoside uridine has been previously reported to enhance learning and memory ability through improvement of lipid metabo-

lism in the cerebral cortex of rats and in the brain of gerbils.^{6,14} However, the dietary intake of nucleotides and nucleosides has been reported to improve memory function in aged, memory-deficient mice, and not in normal mice.^{7,8} In the present study, the dietary intake of HSME and NAF was shown to improve learning and memory function in normal mice (Fig. 2). It should be noted that both substances contained not only mononucleotides but also oligonucleotides as major components (Supplementary Fig. S2), but little information is available on the direct effect of this latter component on learning and memory ability in normal mice.

The concentrations of several nucleic acids such as cytosine, cytidine, deoxycytidine, and thymidine in the hippocampus and in the remaining part of forebrain were elevated upon oral administration of HSME (Fig. 3), supporting the hypothesis that the nucleic acid component of HSME played a role in the enhancement of brain function. In the present study, the concentration of each nucleic acid was directly measured, and to our knowledge, this is the first report on changes in each nucleic acid component in the hippocampus upon oral administration of food ingredients containing high proportions of nucleic acids. Due to the limitation of the study design, however, further studies are required to know whether the elevation of these nucleic acids directly represents the ingestion of nucleic acids in HSME or reflects any indirect phenomenon due to homeostatic regulation. Although the exact component responsible for the improvement in brain function is still unknown, energy-independent equilibrative nucleoside transporters (ENTs), which recognize nucleosides as endogenous substrates, are known to be expressed in brain capillary epithelial cells.¹⁵ It is plausible that nucleosides such as cytidine and deoxycytidine might be distributed to the brain across the blood-brain barrier via the transporter after oral ingestion. Administration of cytidine diphosphorylcholine, which is a precursor of cytidine and uridine, raises the

TABLE 3. DISCRIMINATION INDEX ASSESSED IN NOVEL OBJECT RECOGNITION TEST AND SPATIAL RECOGNITION TEST

	Control	HSME	NAF	AAM
Discrimination index				
NORT	-3.01 ± 5.38	$13.9 \pm 3.3^*$	$13.2 \pm 5.0^*$	$14.3 \pm 4.8^*$
SRT	2.91 ± 4.74	20.3 ± 4.5	$26.9 \pm 8.5^*$	20.7 ± 7.5

*Significant difference relative to the corresponding control values ($P < .05$).

AAM, mixture of amino acids; NORT, novel object recognition test; SRT, spatial recognition test.

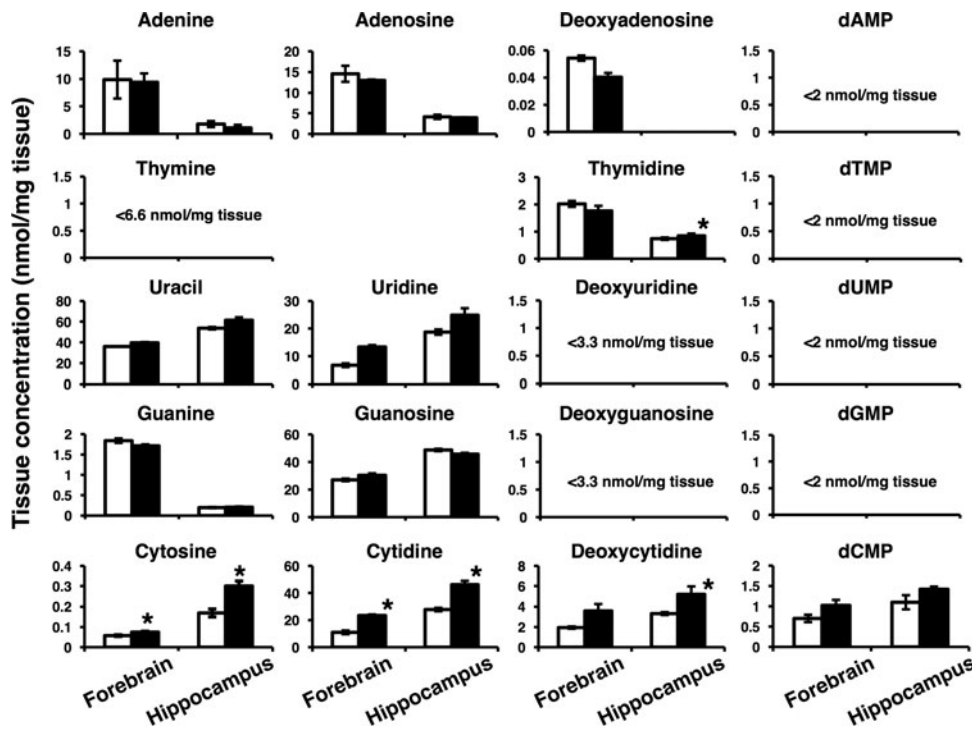


FIG. 3. Concentration of nucleobases, nucleosides, deoxynucleosides, and deoxynucleotides in the hippocampus and in the remaining part of the forebrain in mice upon oral administration of HSME. Mice were orally administered saline or 2 g HSME per kg of body weight. The forebrain was collected at 24 h following administration, and hippocampus was isolated from the forebrain. *White* and *black* columns show the saline and HSME groups, respectively. Concentration of each nucleic acid was measured using liquid chromatography-tandem mass spectrometry. Each value represents the mean \pm SEM ($n=3$). *Significant difference relative to the corresponding control values ($P<.05$). dAMP, deoxyadenosine monophosphate; dCMP, deoxycytidine monophosphate; dGMP, deoxyguanosine monophosphate; dTMP, deoxythymidine monophosphate.

plasma concentration of cytidine and uridine and improves memory function in memory-impaired rats and humans.^{16–18} Taken together, enhancement of learning and memory induced by oral ingestion of HSME might be caused, at least in part, by the increase in levels of certain nucleic acids in the brain. It is interesting to note that elevation of brain levels of nucleic acids upon oral administration of HSME was selectively observed in the cases of cytosine, cytidine, and deoxycytidine (Fig. 3), even though all nucleosides were present at almost evenly distributed levels in HSME (Table 1), and ENTs nonselectively recognize nucleo-

sides.¹⁹ Hossain *et al.* recently postulated a promotive effect of dietary cytidine monophosphate on the growth of fishes in early stages that might contribute to their high rate of cellular replication.²⁰ It is also possible that the nucleosides are unevenly supplied to the brain by oral administration of nucleic acid ingredients, and levels of both cytosine and deoxycytidine might be relatively easily elevated compared with those of other nucleosides (Fig. 3).

AAM contained glutamate and aspartate (Table 2), both of which are agonists of the *N*-methyl-D-aspartate (NMDA) receptor and play an important role in synaptic plasticity.^{21,22}

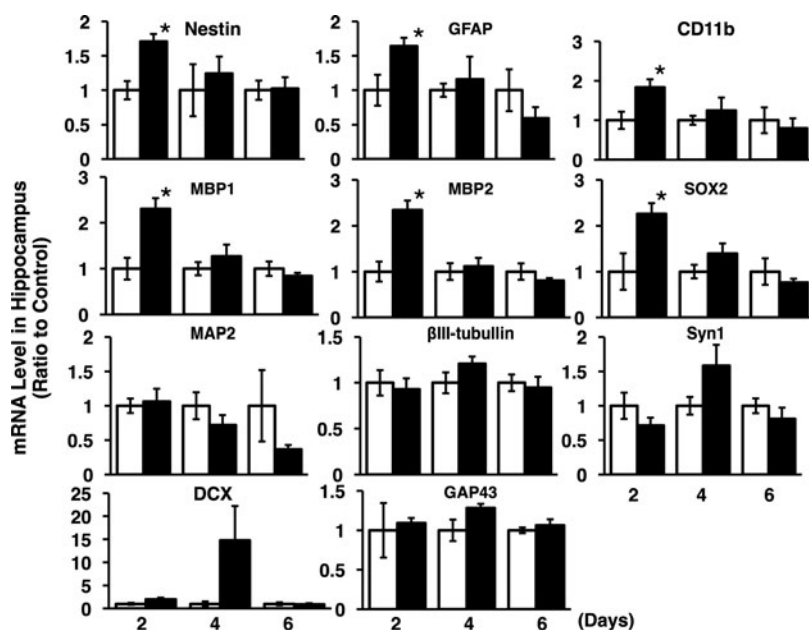


FIG. 4. Effect of ingestion of HSME on expression in the hippocampus of the marker genes for neuronal maturation and brain parenchymal cells. Mice were fed a control diet or a control diet supplemented with 2.5% HSME for 6 days. Hippocampus was collected on days 2, 4, and 6. Total RNA was extracted from the tissue for quantitative reverse transcription-polymerase chain reaction analysis. *White* and *black* columns show the control and HSME groups, respectively. Data were normalized to the expression level of 36B4 and expressed as relative to the corresponding controls. Each value represents the mean \pm SEM ($n=4-8$). MAP2 and GAP43 stand for microtubule-associated protein 2 and growth associated protein 43, respectively. *Significant difference relative to the corresponding control values ($P<.05$).

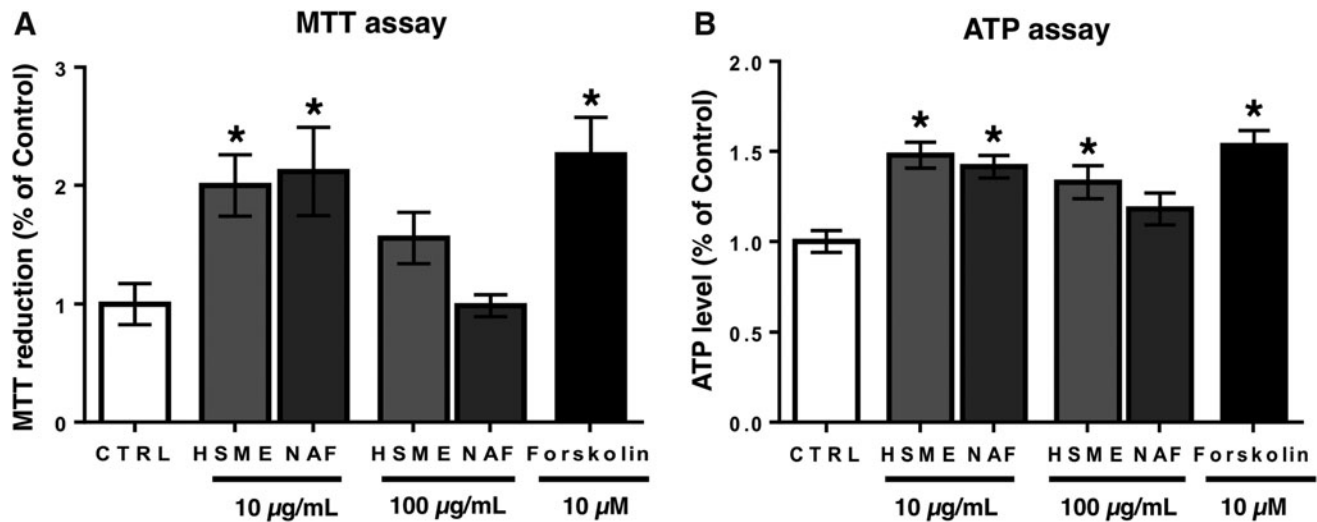


FIG. 5. Effect of HSME and NAF on cellular proliferation in primary cultured neural stem cells. Cortical neural stem cells were exposed to HSME, NAF, or forskolin at the indicated concentrations. Mitochondrial activity and ATP concentration were measured by MTT (A) and ATP (B) assay, respectively. Each value represents the mean \pm SEM ($n=8$). *Significant difference relative to the corresponding control values ($P<.05$). ATP, adenosine triphosphate.

This fraction also contained essential amino acids such as leucine (Table 2), which is an activator of mammalian target of rapamycin signaling and plays an important role in neuronal maturation.^{23,24} However, these hydrophilic amino acids are already present in endogenous plasma and/or brain, so it is unclear whether their concentration is elevated upon oral ingestion of AAM. Meanwhile, learning and memory abilities were increased by oral ingestion of AAM (Fig. 2 and Table 3). Improvement of blood flow to the brain must also be considered as a possible mechanism underlying the enhancement of brain function induced by AAM.

Gene expression of the markers for proliferative brain parenchymal cells was increased 2 days after oral ingestion of HSME was begun (Fig. 4), suggesting that orally ingested HSME activates the proliferative brain parenchymal cells such as glial cells and neural stem cells. The activated glial cells are known to release neurotrophic factors that promote neuronal differentiation and maturation. Furthermore, gene expression of the synapse marker synapsin I (Syn1) and the immature neuron marker doublecortin (DCX) showed an increasing trend at 4 days following the start of the experimental diet (Fig. 4). Based on the increasing trend in the levels of neuronal markers that occur after activation of glial cells, it can be speculated that HSME may promote neuronal differentiation and maturation through the release of neurotrophic factors by glial cells. A previous report found that oral administration of guanosine promoted neuronal differentiation in the hippocampi of mice.¹¹ In other studies, ATP and adenosine were found to promote neuronal differentiation and synaptic plasticity through the activation of the purinergic signaling pathway in cultured neural cells.^{25,26} Activation of NMDA receptor by its agonists, such as glutamate and aspartate, has also been found to promote neuronal differentiation and maturation in cultured neural cells.^{22,27,28} Thus, multiple mechanisms may be involved in

the enhancement of learning and memory upon oral ingestion of HSME.

Astaxanthin and the flavonoid nobiletin are known as food ingredients that enhance brain function in normal animals. Astaxanthin enhances brain function through antioxidant activity and the promotion of neurogenesis.^{29,30} Salmon milt extract also possesses antioxidant activity¹² and induces enhancement through the promotion of neurogenesis, leading to increased learning and memory ability (Fig. 2 and Table 3). Contrarily, nobiletin activates extracellular signal-regulated kinase and protein kinase A signaling.³¹ This flavonoid enhances object recognition memory, but not object location memory.³² The mechanism underlying its enhancement of learning and memory ability may be different from that associated with the effects caused by salmon milt ingestion.

In conclusion, oral ingestion of HSME elevates the concentrations of nucleic acids, including cytosine, cytidine, deoxycytidine, and thymidine in the hippocampus, and may enhance learning and memory abilities, at least in part, through the activation of brain parenchymal cells in normal mice. The easily available and ingestible food ingredient, salmon milt extract, could thus potentially be used as a “brain food” that enhances brain function in healthy people.

ACKNOWLEDGMENTS

The authors thank Ms. Moe Mitamura in Kanazawa University for technical assistance. This work was partially supported by Grants-in-Aid for Scientific Research to N.N. (No. 16K08266) and Y.K. (No. 17K19482) from the Ministry of Education, Culture, Sports, Science, and Technology, Japan.

AUTHOR DISCLOSURE STATEMENT

No competing financial interests exist.

SUPPLEMENTARY MATERIAL

Supplementary Data
 Supplementary Figure S1
 Supplementary Figure S2
 Supplementary Figure S3
 Supplementary Table S1

REFERENCES

- Song TY, Lin HC, Chen CL, *et al.*: Ergothioneine and melatonin attenuate oxidative stress and protect against learning and memory deficits in C57BL/6J mice treated with D-galactose. *Free Radic Res* 2014;48:1049–1060.
- Zhou X, Zhang F, Hu X, *et al.*: Inhibition of inflammation by astaxanthin alleviates cognition deficits in diabetic mice. *Physiol Behav* 2015;151:412–420.
- Bick SK, Eskandar EN: Neuromodulation for restoring memory. *Neurosurg Focus* 2016;40:E5.
- Dama MS: Cognitive ability correlates positively with son birth and predicts cross-cultural variation of the offspring sex ratio. *Naturwissenschaften* 2013;100:559–569.
- Gottfredson LS: Life, death, and intelligence. *J Cogn Educ Psychol* 2004;4:23–46.
- Sato N, Murakami Y, Nakano T, *et al.*: Effects of dietary nucleotides on lipid metabolism and learning ability of rats. *Biosci Biotechnol Biochem* 1995;59:1267–1271.
- Chen TH, Huang HP, Matsumoto Y, *et al.*: Effects of dietary nucleoside-nucleotide mixture on memory in aged and young memory deficient mice. *Life Sci* 1996;59:PL325–PL330.
- Chen TH, Wang MF, Liang YF, *et al.*: A nucleoside-nucleotide mixture may reduce memory deterioration in old senescence-accelerated mice. *J Nutr* 2000;130:3085–3089.
- Bettio LE, Neis VB, Pazini FL, *et al.*: The antidepressant-like effect of chronic guanosine treatment is associated with increased hippocampal neuronal differentiation. *Eur J Neurosci* 2016;43:1006–1015.
- Kiriyama K, Ohtaki H, Kobayashi N, *et al.*: A nucleoprotein-enriched diet suppresses dopaminergic neuronal cell loss and motor deficit in mice with MPTP-induced Parkinson's disease. *J Mol Neurosci* 2015;55:803–811.
- Matsunaga M, Ohtaki H, Takaki A, *et al.*: Nucleoprotamine diet derived from salmon soft roe protects mouse hippocampal neurons from delayed cell death after transient forebrain ischemia. *Neurosci Res* 2003;47:269–276.
- Kojima-Yuasa A, Goto M, Yoshikawa E, *et al.*: Protective effects of hydrolyzed nucleoproteins from salmon milt against ethanol-induced liver injury in rats. *Mar Drugs* 2016;14:E232.
- Mitarai M, Sekido H, Ueda S, *et al.*: Effect of dietary DNA from Chum salmon milt on endurance running capacity of mice. *J Jpn Soc Food Sci Technol* 2008;62:1–26 (in Japanese).
- Holguin S, Martinez J, Chow C, Wurtman R: Dietary uridine enhances the improvement in learning and memory produced by administering DHA to gerbils. *FASEB J* 2008;22:3938–3946.
- Uchida Y, Ohtsuki S, Katsukura Y, *et al.*: Quantitative targeted absolute proteomics of human blood-brain barrier transporters and receptors. *J Neurochem* 2011;117:333–345.
- Teather LA, Wurtman RJ: Dietary CDP-choline supplementation prevents memory impairment caused by impoverished environmental conditions in rats. *Learn Mem* 2005;12:39–43.
- Cotroneo AM, Castagna A, Putignano S, *et al.*: Effectiveness and safety of citicoline in mild vascular cognitive impairment: The IDEALE study. *Clin Interv Aging* 2013;8:131–137.
- Fioravanti M, Yanagi M: Cytidinediphosphocholine (CDP-choline) for cognitive and behavioural disturbances associated with chronic cerebral disorders in the elderly. *Cochrane Database Syst Rev* 2005;2:CD000269.
- Young JD, Yao SY, Baldwin JM, Cass CE, Baldwin SA: The human concentrative and equilibrative nucleoside transporter families, SLC28 and SLC29. *Mol Aspects Med* 2013;34:529–547.
- Hossain MS, Koshio S, Ishikawa M, Yokohama S, Sony NM: Dietary cytidine monophosphate enhances the growth, blood characteristics, innate and adaptive immune functions and stress resistance of juvenile red sea bream, *Pagrus major*. *Aquaculture* 2017;473:366–374.
- Balazs D, Csillag A, Gerber G: L-aspartate effects on single neurons and interactions with glutamate in striatal slice preparation from chicken brain. *Brain Res* 2012;1474:1–7.
- Park H, Han KS, Seo J, *et al.*: Channel-mediated astrocytic glutamate modulates hippocampal synaptic plasticity by activating postsynaptic NMDA receptors. *Mol Brain* 2015;8:7.
- Hay N, Sonenberg N: Upstream and downstream of mTOR. *Genes Dev* 2004;18:1926–1945.
- Ishizuka Y, Kakiya N, Nawa H, Takei N: Leucine induces phosphorylation and activation of p70S6K in cortical neurons via the system L amino acid transporter. *J Neurochem* 2008;106:934–942.
- Delic J, Zimmermann H: Nucleotides affect neurogenesis and dopaminergic differentiation of mouse fetal midbrain-derived neural precursor cells. *Purinergic Signal* 2010;6:417–428.
- Marin-Vicente C, Guerrero-Valero M, Nielsen ML, *et al.*: ATP enhances neuronal differentiation of PC12 cells by activating PKC α interactions with cytoskeletal proteins. *J Proteome Res* 2011;10:529–540.
- Yoneyama M, Nakamichi N, Fukui M, *et al.*: Promotion of neuronal differentiation through activation of N-methyl-D-aspartate receptors transiently expressed by undifferentiated neural progenitor cells in fetal rat neocortex. *J Neurosci Res* 2008;86:2392–2402.
- Jansson LC, Akerman KE: The role of glutamate and its receptors in the proliferation, migration, differentiation and survival of neural progenitor cells. *J Neural Transm (Vienna)* 2014;121:819–836.
- Liu X, Osawa T: Astaxanthin protects neuronal cells against oxidative damage and is a potent candidate for brain food. *Forum Nutr* 2009;61:129–135.
- Yook JS, Okamoto M, Rakwal R, *et al.*: Astaxanthin supplementation enhances adult hippocampal neurogenesis and spatial memory in mice. *Mol Nutr Food Res* 2016;60:589–599.
- Kawahata I, Yoshida M, Sun W, *et al.*: Potent activity of nobiletin-rich Citrus reticulata peel extract to facilitate cAMP/PKA/ERK/CREB signaling associated with learning and memory in cultured hippocampal neurons: Identification of the substances responsible for the pharmacological action. *J Neural Transm (Vienna)* 2013;120:1397–1409.
- Kang J, Shin JW, Kim YR, *et al.*: Nobiletin improves emotional and novelty recognition memory but not spatial referential memory. *J Nat Med* 2017;71:181–189.

RESEARCH ARTICLE

Oral Administration of the Food-derived Hydrophilic Antioxidant Ergothioneine Enhances Object Recognition Memory in Mice

Noritaka Nakamichi¹, Shunsuke Nakao¹, Misa Nishiyama¹, Yuka Takeda¹, Takahiro Ishimoto¹, Yusu-
suke Masuo¹, Satoshi Matsumoto², Makoto Suzuki² and Yukio Kato^{1,*}

¹Faculty of Pharmacy, Institute of Medical, Pharmaceutical and Health Sciences, Kanazawa University, Kanazawa 920-1192, Japan; ²L•S Corporation Co. Ltd., 3-10-1 Ningyocho-Nihonbashi, Chuo-ku, Tokyo 103-0013, Japan

Abstract: Background: The enhancement of learning and memory through food-derived ingredients is of great interest to healthy individuals as well as those with diseases. Ergothioneine (ERGO) is a hydrophilic antioxidant highly contained in edible golden oyster mushrooms (*Pleurotus cornucopiae* var. *citrinopileatus*), and systemically absorbed by its specific transporter, carnitine/organic cation transporter OCTN1/SLC22A4.

Objective: This study aims to examine the possible enhancement of object recognition memory by oral administration of ERGO in normal mice.

Method: Novel object recognition test, spatial recognition test, LC-MS/MS, Golgi staining, neuronal culture, western blotting, immunocytochemistry, and quantitative RT-PCR were utilized.

Result: After oral administration of ERGO (at a dose of 1–50 mg/kg) three times per week for two weeks in ICR mice, the novel object recognition test revealed a longer exploration time for the novel object than for the familiar object. After oral administration of ERGO, the spatial recognition test also revealed a longer exploration time for the spatially moved object than the unmoved one in mice fed ERGO-free diet. The discrimination index was significantly higher in the ERGO-treated group than the control in both behavioral tests. ERGO administration led to an increase in its concentration in the plasma and hippocampus. The systemic concentration reached was relevant to those found in humans after oral ERGO administration. Golgi staining revealed that ERGO administration increased the number of matured spines in the hippocampus. Exposure of cultured hippocampal neurons to ERGO elevated the expression of the synapse formation marker, synapsin I. This elevation of synapsin I was inhibited by the tropomyosin receptor kinase inhibitor, K252a. Treatment with ERGO also increased the expression of neurotrophin-3 and -5, and phosphorylated mammalian target of rapamycin in hippocampal neurons.

Conclusion: Oral intake of ERGO may enhance object recognition memory at its plasma concentration achievable in humans, and this enhancement effect could occur, at least in part, through the promotion of neuronal maturation in the hippocampus.

Keywords: Ergothioneine, Object recognition memory, Neuronal maturation, Hippocampus, Neurotrophin, Organic cation transporter.

1. INTRODUCTION

Dysfunction of learning and memory due to neuronal disorders causes dementia, resulting in an extremely lowered quality of life in patients. There are 50 million dementia patients worldwide [1], and the treatment of dementia is an urgent issue. However, despite the clinical application of several therapeutic agents for the treatment of dementia, such as

inhibitors of cholinesterase and the *N*-methyl-D-aspartate receptor [2, 3], there are no fundamental therapeutic drugs for recovering the neurons that are lost during brain disorders. Some patients are insensitive to the current clinically available drugs [2]. In addition, the administration of cholinesterase inhibitors sometimes causes several adverse events, such as gastrointestinal or mental disorders [2, 4]. Therefore, the development of drugs with a novel mechanism of action and minimal adverse effects is desirable.

Food-derived ingredients that improve recognition function through the enhancement of brain function would also be a promising tool for the treatment of dementia and may

* Address correspondence to this author at the Faculty of Pharmacy, Institute of Medical, Pharmaceutical and Health Sciences, Kanazawa University, Kakuma-machi, Kanazawa 920-1192, Japan; Tel/Fax: +81-76-234-4465; E-mail: ykato@p.kanazawa-u.ac.jp

help to clarify novel mechanisms of action for the drug development. Food-derived ingredients that have an antioxidant effect and/or promotive effect on neuronal maturation and neurogenesis may improve learning and memory ability. For example, intake of antioxidant polyphenol catechin and resveratrol, which are found in high levels in green tea and red grapes, respectively, improves the decline in spatial memory provoked by the suppression of spine reduction in aged mice [5, 6]. Intake of carotenoid astaxanthin, which is found in salmon roe, enhances neurogenesis and spatial memory in normal mice [7]. However, over-intake of resveratrol inhibits neurogenesis and reduces the learning and memory ability [8]. The astaxanthin intake required to improve learning and memory in mice may cause several adverse events, such as hepatic impairment [9]. Thus, it would be desirable to improve the pharmacokinetic properties to gain efficient activity of learning and memory with minimal toxicity at the clinically relevant amount of ingestion.

Ergothioneine (ERGO) is an antioxidant that is abundantly found in certain edible mushrooms, including golden oyster mushrooms (*Pleurotus cornucopiae* var. *citrinopileatus*), meat, and grains. ERGO is synthesized by fungi and mycobacteria, but not by mammals. Thus, ERGO is ingested from daily food and is present at a concentration range of μM to sub mM in the blood and organs of humans and mice [10, 11]. The hydrophilic nature of ERGO hinders its membrane permeation, however, it is actively transported across membranes by the specific transporter carnitine/organic cation transporter (OCTN1/SLC22A4), which was identified by the metabolomics approach [12]. ERGO is orally absorbed mainly through this transporter [13]. The concentration of ERGO in any of the organs of *octn1* gene knockout mice is below the detection limit [11], indicating the fundamental role of this transporter in the distribution of ERGO. ERGO can enter the brain by crossing the blood-brain barrier [14]. Thus, this antioxidant appears to have the beneficial pharmacokinetic properties of a candidate for the improvement of brain function. In fact, ERGO shows protective effects against the neuronal damage provoked by H_2O_2 , β -amyloid, and cisplatin [15-17]. Exposure of cultured neural stem cells to ERGO promotes cellular differentiation into neurons, through an unidentified mechanism that is distinct from its antioxidant activity [18]. Oral ingestion of a diet that includes ERGO actually promotes hippocampal neurogenesis and exerts an antidepressant-like effect in mice [14]. In addition to these beneficial effects of exogenous administration of ERGO in experimental animals, recent clinical studies have indicated that the systemic concentration of ERGO is reduced in older adults (0.8–1.4 μM in serum of older subjects) [19], patients with Parkinson's disease [20], and in people with mild cognitive impairment (0.1–0.2 $\mu\text{g}/\text{mg}$ hemoglobin in whole blood) [21]. These findings imply that ERGO may play a role in the maintenance of normal brain function. However, though ERGO is known to improve the decline of learning and memory ability in senescent model mice [22], the effect of ERGO on learning and memory under normal (untreated) conditions has not yet been clarified.

In the present study, we investigated whether orally administered ERGO can enhance the learning and memory ability of normal mice. For such purposes, both the novel object recognition test (NORT) and the spatial recognition test (SRT) were performed after the oral administration of ERGO. To support such an effect on brain function, the gastrointestinal absorption and hippocampal distribution of ERGO were also examined. The promotion of neuronal maturation by ERGO, through the induction of neurotrophic factors, was also demonstrated as the possible underlying mechanism.

2. MATERIALS AND METHODS

2.1. Materials

ERGO was kindly provided by Yukiguni Maitake Co. Ltd. (Minamiuonuma, Japan). L-(+)-Ergothioneine-d9 was kindly provided by TETRAHEDRON (Romainville, France). ISOGEN, MultiScribe™ Reverse Transcriptase, and THUNDERBIRD SYBR qPCR Mix were purchased from Nippon Gene (Tokyo, Japan), Biosystems (Foster City, CA, USA), and TOYOBO (Osaka, Japan), respectively. ERGO-free feed (basal diet®) was obtained from TestDiet (St. Louis, MO, USA) and contained less than 0.01 μg ERGO/g chow [23]. All other chemicals and reagents, of the highest purity available, were purchased from commercial sources.

2.2. Animals

Male ICR mice for *in vivo* experiments and female pregnant ICR mice for neuronal culture were purchased from Sankyo Labo Service Co. (Toyama, Japan). Male mice fed control diet were regarded as “normal mice”. Male ICR mice at the age of 3 weeks were also purchased from Sankyo Labo Service and fed ERGO-free diet. These mice were regarded as “ERGO-free mice”. These ERGO-free mice were prepared with an aim to clearly observe pharmacological effect of ERGO exogenously administered since ERGO exists in the body of normal mice that were not administered ERGO due to ingestion from the daily diet which includes ERGO [11, 14]. Mice were housed in pathogen-free conditions at a controlled temperature (21–25 °C) under a 12 h light/dark cycle. The lights remained on from 8:00 to 20:00. Food and water were available *ad libitum*. Total number of normal mice used for behavioral tests, measurement of ERGO concentration, and Golgi staining was 70, 24, and 19, respectively, whereas that of ERGO-free mice used for behavioral tests and measurement of ERGO concentration was 48 and 32, respectively.

2.3. Behavioral Tests in Normal and ERGO-free Mice

ERGO was dissolved in autoclaved pure water and orally administered to normal mice at the age of 5 weeks at 0, 1, 5, 20, or 50 mg/kg on experimental days 0, 2, 4, 7, 9, and 11 by gavage (Supplementary Fig. S1A). The number of mice administered 0, 1, 5, 20, and 50 mg/kg ERGO was 14, 15, 14, 13, and 14, respectively. ERGO was orally administered to ERGO-free mice at the age of 6 weeks at 0, 5, 20, or 50 mg/kg on experimental days 0, 2, 4, 7, 9, and 11 by gavage

(Supplementary Fig. S1A). The number of mice administered 0, 5, 20, and 50 mg/kg ERGO was 12. On experimental day 14, NORT was first performed: each mouse was individually placed in an acrylic chamber (45 × 45 × 45 cm) without any objects and was allowed to explore for 10 min. On the next day, each mouse was placed in the same chamber with two identical objects located on a diagonal line. Animals were allowed to explore the chamber for five minutes (Supplementary Fig. S2). The time spent exploring each object was recorded. Twenty-four hours later, one of the objects was replaced by a novel object of a different shape at the same location in the chamber. Each mouse was allowed to explore the chamber under these conditions for five minutes. The exploration time for each object was recorded. The discrimination index was calculated as [(novel object exploration time/ total exploration time) – (familiar object exploration time/ total exploration time) × 100] (Table 1).

The SRT was conducted on the day after the final NORT day (Supplementary Fig. S1A): each mouse was individually placed in an acrylic chamber without any objects and allowed to explore for 10 min. On the next day, each mouse was placed in the same chamber with two identical objects located on a diagonal line. Animals were allowed to explore the chamber for five minutes (Supplementary Fig. S3). The time spent exploring each object was recorded. One hour later, one of the objects was moved, and each mouse was allowed to explore the chamber under these conditions for five minutes. The exploration time for each object was recorded. The discrimination index was calculated as [(moved object exploration time/ total exploration time) – (unmoved object exploration time/ total exploration time) × 100] (Table 1).

2.4. Measurement of ERGO Concentration

Repeated oral administration of ERGO at 0, 1, 5, 20, 50, or 100 mg/kg was performed in a separate set of normal mice at the age of 5 weeks, in the similar schedule to the behavioral tests. In these mice, the plasma was collected on experimental days 0, 7, 14, and 19 (Fig. S1A). Similarly, administration of ERGO was also performed in another set of mice at the age of 5 weeks in which the hippocampus was collected on experimental day 14. These experiments were performed to examine oral absorption and brain distribution of ERGO in mice. On the other hand, plasma and hippocampal samples were obtained in the same mice used for behavioral tests on the experimental day 19 (Supplementary Fig. S1A) to confirm reduction in basal level of ERGO and systemic absorption of ERGO in ERGO-free mice. All samples were preserved at –80 °C before the determination of ERGO concentration. Hippocampal samples were weighed, and portions were homogenized in 2 volumes of distilled water. Plasma and hippocampus homogenates were diluted 5- and 250-fold with water, respectively, deproteinized with methanol, and subjected to LC-MS/MS after centrifugation. The LC-MS/MS system was based on the LCMS-8040 model (Shimadzu, Kyoto, Japan). Chromatography was performed by means of step-gradient elution (flow rate, 0.4 mL/min) as follows: 0–0.5 min: 5% A/95% B; 0.5–3.5 min: 5% A/95% B to 70% A/30% B; 3.5–5.5 min: 70% A/30%

B; 5.5–5.6 min: 70% A/30% B to 5% A/95% B; 5.6–8 min: 5% A/95% B (A, water containing 0.1% formic acid; B, acetonitrile-containing 0.1% formic acid), using a Luna 3.0 μm HILIC column (200 Å, 150 × 2.0 mm; Phenomenex, Torrance, CA) at 40 °C. L-(+)-Ergothioneine-d9 was used as the internal standard.

2.5. Golgi Staining

Mice were purchased at the age of 5 weeks, 0 or 50 mg/kg ERGO was orally administered on experimental days 0, 2, 4, 7, 9, and 11 (Fig. S1B). Golgi staining was performed according to the recommended procedure of the FD Rapid GolgiStain Kit (PK401; FD Neuro Technologies, Columbia, MD, USA). On experimental day 14, mice were decapitated under anesthesia by pentobarbital, and brains were removed. Brains were put into the recommended solution and kept at room temperature in the dark for two weeks, followed by further incubation for 72 h in another solution. Brains were embedded in TFM (Triangle Biomedical Sciences, Durham, NC, USA), and coronal slices were cut at the thickness of 100 μm using a cryostat. The sections were placed on gelatin coated glass slides (Matsunami Glass, Osaka, Japan), dried overnight, washed with pure water, and immersed in the recommended solution for 10 min. The sections were washed with phosphate-buffered saline (PBS), sequentially immersed in 50, 75, and 90% ethanol, and then dehydrated in 100% ethanol, followed by 100% xylene. The sections were then coverslipped using Permount (Sigma-Aldrich, St. Louis, MO, USA) and observed with BZ9000 fluorescence microscope (Keyence, Osaka, Japan). Two to four neurons from the hippocampal dentate gyrus were randomly selected from each mouse for spine analysis. A total of nine to 10 neurons were analyzed in each group. Quantification of spines was performed using NIH ImageJ software. Spines were classified into 3 groups: mushroom, filopodia/thin, and stubby. Mushroom spines were characterized by a big head that was more than three times larger than its neck. Filopodia/thin spines were characterized by the absence of a head or the presence of a head that was not big. Stubby spines were characterized by their short and round appearance.

2.6. Neuronal Culture

Primary hippocampal neuronal cultures were performed according to the methods described by Nakamichi *et al.* [24], with minor modifications. In brief, hippocampi from 15-day-old embryonic ICR mice were dissected and incubated with 0.25% trypsin in PBS containing 28 mM glucose at 37°C for 20 min. Cells were mechanically dissociated using a 1,000-μL pipette tip in culture medium and plated at a density of 5×10^4 cells/cm² on plastic dishes that were coated with 7.5 μg/ml poly-L-lysine. Hippocampal neurons were cultured in Neurobasal™ media (Thermo Fisher Scientific, Waltham, MA, USA) that was supplemented with 100 U/mL penicillin, 100 μg/mL streptomycin, B-27 supplement, 0.5 mM glutamine, and 25 μM glutamate from 0 to 3 days *in vitro* (DIV) at 37°C in a humidified 5% CO₂ incubator (Fig. S1C). At three DIV, half of the culture medium was replaced with Neurobasal™ media supplemented with B-27

Table 1. Discrimination index in novel object recognition (NORT) and spatial recognition tests (SRT).

Discrimination index		ERGO (mg/kg) ^a				
		0	1	5	20	50
Normal mice	NORT ^b	1.83 ± 4.02	16.6 ± 5.6	16.3 ± 4.2	18.8 ± 3.6*	16.8 ± 4.6
	SRT ^c	1.63 ± 4.25	5.91 ± 6.18	10.5 ± 7.7	15.5 ± 6.5	24.9 ± 6.7*
ERGO-free mice	NORT ^b	-2.88 ± 7.55	- ^d	22.5 ± 4.0*	23.6 ± 3.4*	28.5 ± 4.3*
	SRT ^c	4.61 ± 4.38	- ^d	18.5 ± 5.0	18.9 ± 4.1	34.5 ± 3.4*

a) Orally administered in normal mice on days 0, 2, 4, 7, 9, and 11

b) Performed at three days after the last ERGO administration

c) Performed at six days after the last ERGO administration

d) Not performed

* Significant difference from the corresponding control values ($P < 0.05$)

supplement, 100 U/mL penicillin, 100 µg/mL streptomycin, and 0.5 mM glutamine, and cells were incubated for a further three days. At six DIV, the culture medium was replaced with NeurobasalTM media supplemented with 100 U/mL penicillin, 100 µg/mL streptomycin, and 0.5 mM glutamine. From 6 to 9 or 12 DIV, the cells were treated with 0, 5, 50, and 500 µM ERGO (Fig. S1C). For the inhibition study, 10 or 100 nM tropomyosin receptor kinase (Trk) inhibitor K252a dissolved in NeurobasalTM media that was supplemented with 100 U/mL penicillin, 100 µg/mL streptomycin, 0.5 mM glutamine, and 25 µM glutamate was added to the medium at six DIV and incubated for 20 min. The medium was then replaced with NeurobasalTM media that was supplemented with 100 U/mL penicillin, 100 µg/mL streptomycin, 0.5 mM glutamine, and 25 µM glutamate, and cells were incubated until 12 DIV (Fig. S1C).

2.7. Western Blot Analysis

Western blot analysis was performed according to the methods of Nakamichi *et al.* [25], with minor modifications. Hippocampal neurons were seeded at 5.0×10^4 cells/cm² on 12 well plastic dishes, cultured for 12 days, and washed twice with ice-cold PBS. Cells were centrifuged at 4°C for 5 min at 15,000 g after cell harvesting. Pellets thus obtained were suspended and sonicated in 20 mM Tris-HCl buffer (pH 7.5) containing 1 mM EDTA, 1 mM EGTA, 10 mM sodium fluoride, 10 mM sodium β-glycerophosphate, 10 mM sodium pyrophosphate, 1 mM sodium orthovanadate, and 1 µg/mL of various protease inhibitors [(p-amidinophenyl)methanesulfonyl fluoride, leupeptin, anti-pain, and benzamidin]. The suspensions were added at a volume ratio of 4:1 to 10 mM Tris-HCl buffer (pH 6.8) containing 10% glycerol, 2% sodium dodecylsulfate, 0.01% bromophenol blue, and 5% mercaptoethanol, and mixed at room temperature for one hour. The protein concentration was determined using a Bio-Rad Protein Assay Kit. The concentration of polyacrylamide gel was 7.5% for the detection of βIII-tubulin, microtubule-associated protein 2 (MAP2), and synapsin I, or 12.5% for the detection of mammalian target of rapamycin (mTOR), p-mTOR, S6K1, p-S6K1 (Ser371), p-S6K1 (Thr389), 4EBP1, and p-4EBP1. Each aliquot of 10 µg proteins was loaded on to a polyacrylamide

gel for electrophoresis at a constant current of 60 mA/2 plates for 100 min at room temperature, using a wide-mini-slab size PAGE system (Sima Biotech, Chiba, Japan), followed by blotting to a polyvinylidene fluoride membrane that was previously treated with 100% methanol. The membrane was blocked with a 2% bovine serum albumin (BSA) solution at 4°C overnight. The membrane was then reacted with antibodies against βIII-tubulin (1:10,000), MAP2 (1:10,000), Synapsin I (1:10,000), or β-actin (1:50,000) and diluted with buffer containing 0.2% BSA at room temperature for two hours while shaking [18], or reacted with antibodies against mTOR (1:1,000), p-mTOR (1:1,000), S6K1 (1:500), p-S6K1 (Ser371) (1:500), p-S6K1 (Thr389) (1:500), 4EBP1 (1:500), or p-4EBP1 (1:500) and diluted with Can Get Signal[®] at room temperature for two hours while shaking [26]. The membrane was then washed and reacted with an anti-mouse IgG (1:10,000–50,000) or anti-rabbit IgG (1: 2,000–10,000), diluted with 0.2% BSA or Can Get Signal[®]. Proteins reactive with these antibodies were detected with the aid of ECLTM detection reagents using a lumino image analyzer (LAS-4000; FUJIFILM, Tokyo, Japan). Densitometric determination was performed using ImageJ software.

2.8. Immunocytochemical Analysis

Hippocampal neurons were seeded at 1.25×10^4 cells/cm² on 12 well plastic dishes and cultured for 12 days. Neurons were washed with PBS, then fixed with 4% paraformaldehyde for 20 min at room temperature, and incubated for 30 min in blocking solution (3% BSA and 0.2% Triton X-100 in PBS) at room temperature. Cells were then incubated overnight in 10-times-diluted blocking solution containing antiserum against MAP2 (1:1,000) or an antibody against synapsin I (1:2,000) at 4°C, washed with PBS, and reacted with Alexa Fluor series-conjugated secondary antibodies (1:2,000) for one hour at room temperature. The cells were rinsed again with PBS, treated with mounting medium that contained DAPI, and observed under a confocal laser scanning microscope (LSM710) with a 63× objective. Five fields per well were chosen at random for analysis, and only non-clustered neurons were evaluated. The data were obtained from four wells in each preparation. To minimize

bias, neurons were evaluated blindly without the knowledge of the sample condition. Five neurons were analyzed from each well for the measurement of the number of synapsin I-positive puncta/10 μm neurite length, total neurite length, number of neurites, and Sholl analysis. Measurement of neurite length, total number of neurites, and Sholl analysis were conducted using the Simple neurite tracer plug-in [27] on Fiji, an open-source platform for biological-image analysis [28]. Sholl analysis was carried out at a 3.36 μm interval to a maximum radius of 137.2 μm . The area under the curve (AUC) was calculated using the trapezoidal rule for each Sholl profile.

2.9. Quantitative RT-PCR

Hippocampal neurons were seeded at 5.0×10^4 cells/cm² on 12 well plastic dishes and cultured for nine days. The total RNA was extracted from cultured cells according to the manufacturer's protocol of ISOGEN. cDNA was synthesized with oligo (dT)₁₂₋₁₈ primers, deoxynucleotide triphosphate mix, RT buffer, and MultiScribe Reverse Transcriptase, and amplified on Mx3005P (Agilent Technologies, Santa Clara, CA, USA) using a reaction mixture containing cDNA with the relevant forward and reverse primers and the THUNDERBIRD SYBR qPCR Mix. PCR reactions were initiated by template denaturation at 95°C for 15 min, followed by 40 cycles of amplification (denaturation at 95°C for 10 s, and primer annealing and extension at 60°C for 30 s). Relative quantification of expression levels of the target genes was determined by the delta-delta Ct method using transcripts of acidic ribosomal phosphoprotein P0 (36B4) as the internal standard. The sequences of the primers (5' to 3') were as follows: nerve growth factor (NGF) forward, TCTA-TACTGGCCGCAGTGAG and reverse, GGACATTGC-TATCTGTGTACGG; brain-derived neurotrophic factor (BDNF) forward, GCGGCAGATAAAAAGACTGC and reverse, TCAGTTGGCCTTTGGATACC; NT3 forward, GGAGGAAACGCTATGCAGAA and reverse, TTCTCT-GAGGCCGTGAAGTT; NT-5 forward, CCAAGTT-GAGGAAAACAA and reverse, TCCTCCGGGA-GAACTCCTAT; 36B4 forward, ACTGGTCTAGGACCC-GAGAAG and reverse, TCCCACCTTGTCTCCAGTCT.

2.10. Statistical Analysis

Data are expressed as the mean \pm S.E.M. The statistical significance of differences was determined by means of Student's t-test or one-way or repeated measures ANOVA, using Excel or IBM SPSS Statistics (Chicago, IL, USA), followed by the appropriate post-hoc tests. $P < 0.05$ was regarded as denoting a significant difference.

3. RESULTS

3.1. Enhancement of Object Recognition and Object Location Memory by Oral Administration of ERGO

To investigate whether oral intake of ERGO enhances the learning and memory ability under normal conditions, the experimental schedule in NORT was first constructed using mice that had not been exposed to ERGO treatment (Fig.

S2). The exploration time for the novel object was significantly longer than that for the familiar one under the condition that retention time was set to be three hours, whereas the exploration time was not different between the novel and familiar objects under the condition that retention time was set to 24 h (Fig. S2). This suggests that mice cannot recognize a difference between the novel and familiar object after a 24 h retention time. Thus, the enhancement effect of ERGO on object recognition memory was next observed under the condition that retention time was set to 24 h. ERGO was orally administered at 0–50 mg/kg three times per week for two weeks, and then NORT was performed (Fig. S1A). In retention trials, the exploration time for the novel object was significantly longer than that for the familiar object in normal mice administered 1–50 mg/kg ERGO, whereas the exploration time for the two objects was similar in normal mice that had not been treated with ERGO (Fig. 1A). The similar results were obtained in ERGO-free mice (Fig. 1B). The discrimination index at each dose was calculated to compare object recognition ability. The discrimination index was significantly higher in normal mice exposed to ERGO at a dose of 20 mg/kg than in the control group (Table 1). The discrimination index was significantly higher in ERGO-free mice exposed to ERGO at a dose of 5 mg/kg or higher dose than in the control group (Table 1). These results suggest that oral administration of ERGO enhances the object recognition memory under normal conditions in mice.

Next, the possible enhancement effect of oral administration of ERGO on object location memory was investigated using the SRT. In mice that were not exposed to ERGO treatment, the exploration time for the moved object was significantly longer than that for the unmoved object when measurement time was set to 10 min, whereas the exploration time was minimally different between the moved and unmoved objects when the measurement time was set to five minutes (Fig. S3). Thus, the enhancement effect of ERGO on object location memory was next examined under the condition that measurement time was five minutes. In retention trials, the exploration time for the moved object tended to be longer than that for the unmoved object in normal mice that were treated with 50 mg/kg ERGO (Fig. 1C). The exploration time for the moved object was significantly longer than that for the unmoved object in ERGO-free mice administered 5 or 50 mg/kg ERGO, whereas the exploration time for the two objects was similar in ERGO-free mice that had not been treated with ERGO (Fig. 1D). The discrimination index at each dose was calculated to compare spatial recognition ability. The discrimination index was significantly higher in normal and ERGO-free mice exposed to ERGO at a dose of 50 mg/kg than in the control group (Table 1). This suggests that oral administration of ERGO may also enhance object location memory under normal conditions in mice.

3.2. Plasma and Hippocampal Concentration of ERGO after Oral Administration

To support the findings that oral administration of ERGO has an enhancement effect on learning and memory ability

ty, we examined the gastrointestinal absorption and distribution to the hippocampus of ERGO following oral administration. During and after oral administration of ERGO (1–100 mg/kg) three times per week for two weeks, the plasma concentration profile of ERGO was measured. The plasma concentration of ERGO was remarkably higher in the mice that were treated with 100 mg/kg ERGO than in the control group from days 7 to 19 (Fig. 2A). In the group treated with 50 mg/kg ERGO, the plasma concentration of ERGO tended to be higher than that in the control on day 7 and this difference reached significance on day 14 (Fig. 2A). In the group treated with 20 mg/kg ERGO, the plasma concentration of ERGO also tended to be higher than that in the control group on day 14 (Fig. 2A). Meanwhile, the hippocampal concentration of ERGO on day 14 in the group treated with ERGO was also measured and showed a dose-dependent increase (Fig. 2B). The hippocampal concentration of ERGO in the group treated with ERGO at 20 mg/kg or more was significantly higher than that in the control group (Fig. 2B). The plasma and hippocampal concentrations of ERGO were also increased in a dose-dependent manner in ERGO-free mice (Table S1). These results indicate that orally administered ERGO is absorbed from the gastrointestinal tract and distributed to the hippocampus, after passing through the blood-brain barrier. These results support the finding that

learning and memory ability is enhanced after oral administration of ERGO and suggest that this may result from the action of ERGO being distributed to the hippocampus.

3.3. Promotive Effect of ERGO on Neuronal Maturation in the Hippocampal Dentate Gyrus

Neuronal maturation was next examined as a possible mechanism of action for the learning and memory enhancement observed after oral administration of ERGO. Golgi staining demonstrated that neurons with numerous neurites existed in the hippocampal dentate gyrus of the control group (Fig. 3A). Furthermore, morphological observation of the neurites revealed the existence of at least three types of spines (mushroom, filopodia/thin, and stubby; (Fig. 3B). In the dentate gyrus of mice that were orally administered 50 mg/kg ERGO three times per week for two weeks, there appeared to be more mushroom type spines than in the control group (Fig. 3C). Quantification of the number of each type of spines in each condition revealed that the population of mushroom type spines in the ERGO-treated group was significantly higher than that observed in the control group (Fig. 3D). These results suggest that oral administration of ERGO may promote neuronal maturation in the hippocampal dentate gyrus.

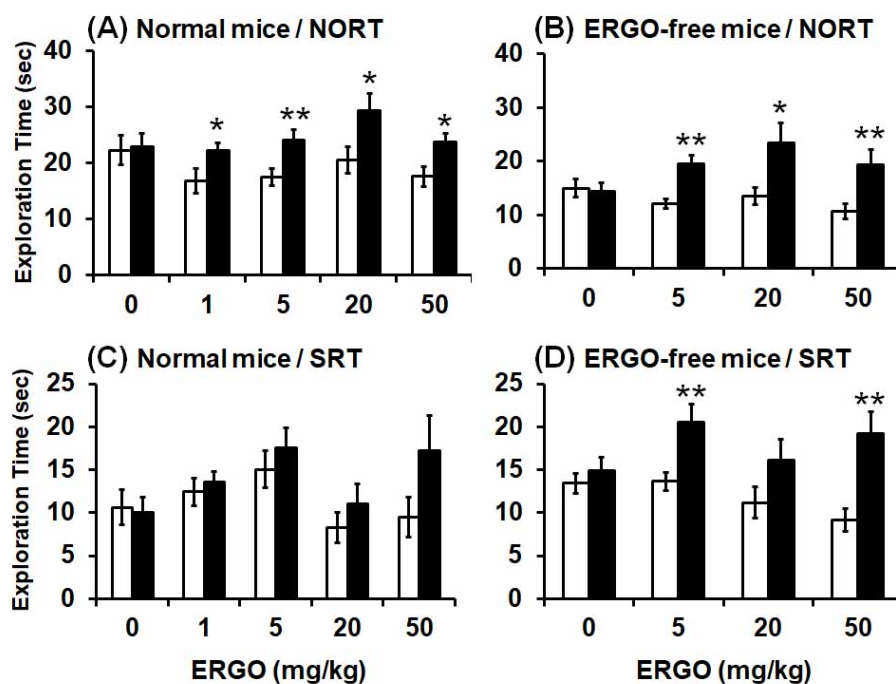


Fig. (1). Effect of oral administration of ERGO on object recognition and object location memory under normal conditions. Normal (A, C) and ERGO-free (B, D) mice were orally administered ERGO at 0, 1, 5, 20, or 50 mg/kg on days 0, 2, 4, 7, 9, and 11. Three and six days after the final ERGO administration, NORT (A, B) and SRT (C, D) were conducted, respectively, and the exploration time was measured. The white and black columns in panels (A) and (B) display the exploration time for the familiar and novel objects, respectively. The white and black columns in panels (C) and (D) show the exploration time for the unmoved and moved objects, respectively. Each value represents the mean \pm S.E.M. (n = 12–15). * Significant difference from the control ($P < 0.05$); ** Significant difference from the control ($P < 0.01$).

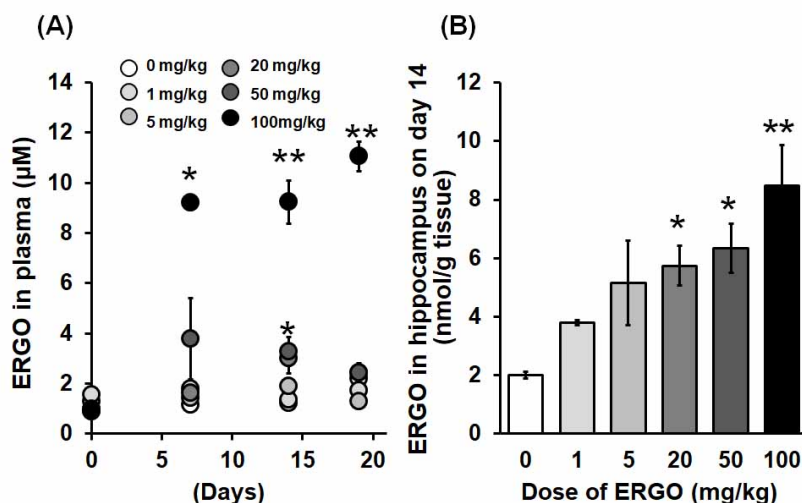


Fig. (2). ERGO concentration in the plasma (A) and hippocampus (B) after oral administration of ERGO. Mice were orally administered 0, 1, 5, 20, 50, or 100 mg/kg ERGO on days 0, 2, 4, 7, 9, and 11. Plasma samples were collected on days 0, 7, 14, and 19, and hippocampal samples were collected on day 14. The ERGO concentration was then measured by LC-MS/MS. Each value represents the mean ± S.E.M. (n = 3–6). * Significant difference from the values obtained in mice not treated with ERGO ($P < 0.05$); ** Significant difference the values obtained in mice not treated with ERGO ($P < 0.01$)

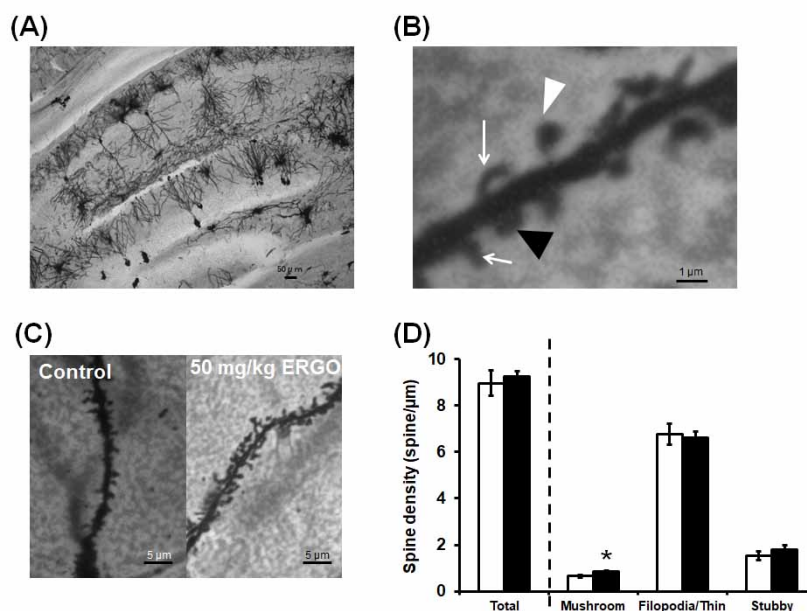


Fig. (3). Effect of oral administration of ERGO on spine morphology in the hippocampal dentate gyrus. Mice were orally administered 0 or 50 mg/kg ERGO on days 0, 2, 4, 7, 9, and 11. On day 14, the brain was collected for Golgi staining. Neurons in the hippocampal dentate gyrus were observed, and spines were classified. (A) A representative image of Golgi staining in the hippocampus of the control group. Scale bar: 50 µm. (B) Examples of the three classifications of spines in the control group. The white triangle indicates the mushroom-type spine, the white arrows indicate the filopodia/thin-type spines, and the black triangle indicates the stubby-type spine. Scale bar: 1 µm. (C) Representative images of dendritic branches in the hippocampal dentate gyrus of control mice and mice treated ERGO. Scale bar: 5 µm. (D) The quantitative results of spine morphological analysis in control mice (white) and mice treated with ERGO (black). Nine to 10 neurons from three mice were analyzed in each group. Each value represents the mean ± S.E.M. (n = 9–10). * Significant difference from the control group ($P < 0.05$).

3.4. Promotive Effect of ERGO on Cellular Maturation in Primary Cultured Hippocampal Neurons

To further investigate the promotive effect of ERGO on neuronal maturation, the expression of neuronal maturation-related markers was examined through quantitative PCR and Western blotting in primary cultured hippocampal neurons. The expression of mRNA for β III-tubulin and synapsin I was significantly higher in the hippocampal neurons that were exposed to 50 or 500 μ M ERGO than in the control group (Fig. 4A). Exposure of hippocampal neurons to 5–500 μ M ERGO also elevated the protein expression of β III-tubulin and synapsin I in a concentration-dependent manner (Fig. 4B, C). To confirm that exposure to ERGO increased the expression of these neuronal markers through a mechanism distinct from its neuroprotective effect, the protective effect of ERGO was also examined under the same culture condition. No significant difference was observed in

the number of Hoechst- and propidium iodide (PI)-positive cells between the control and ERGO-treated groups (Fig. S4). This result indicates a minimal protective effect of ERGO under this experimental condition. Meanwhile, exposure to ERGO minimally affected the expression of MAP2 at both the mRNA and protein level (Fig. 4). In cultured hippocampal neurons, more synapsin I-positive puncta per neurite were observed in the group exposed to 500 μ M ERGO than in the control group (Fig. 5A, B). However, ERGO exposure appeared to minimally affect neurite length (Fig. 5C) and the number of neurites per cell (Fig. 5D). However, the number of neurite intersections was significantly higher in the groups that were exposure to 50 and 500 μ M ERGO than in the control group (Fig. 5E, F). These results suggest that ERGO may promote synapse formation by increasing the number of neurite intersections in hippocampal neurons, supporting a promotive effect of ERGO on neuronal maturation.

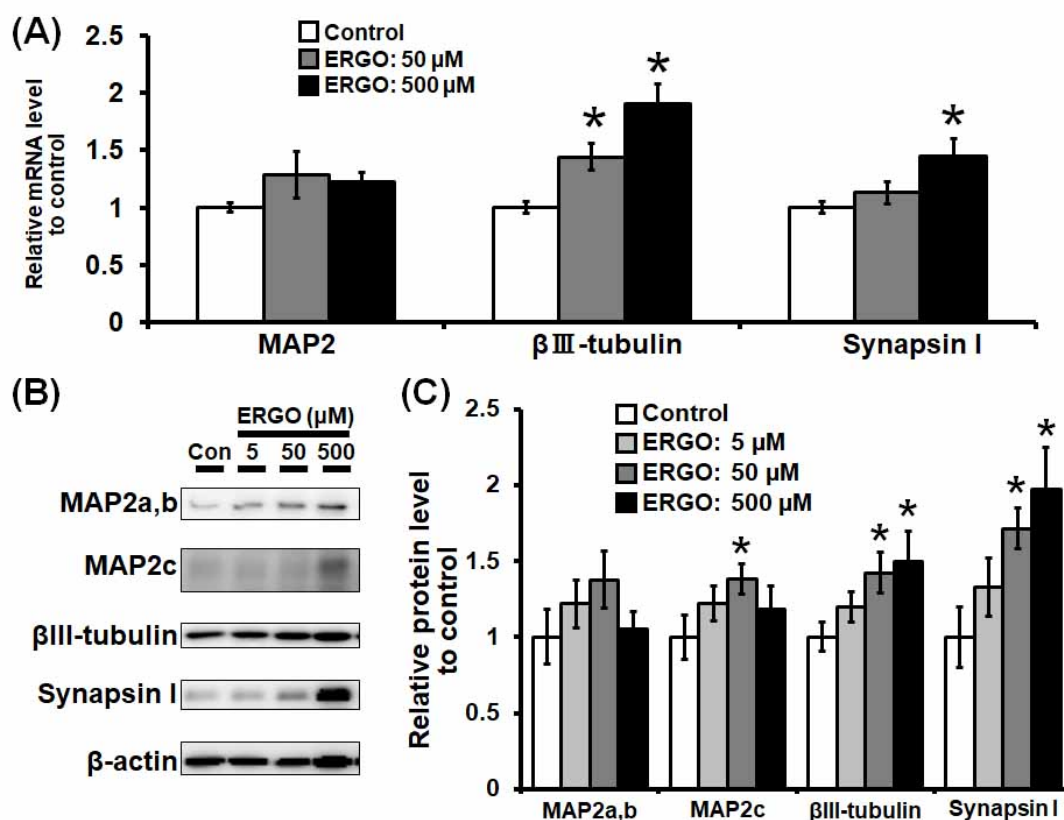


Fig. (4). Effect of ERGO on the expression of neuronal maturation markers in primary cultured hippocampal neurons. Hippocampal neurons were cultured in neurobasal medium supplemented with B-27 for six days, followed by further culture in neurobasal medium without B-27 in either the absence (white columns) or presence (gray or black columns) of ERGO until experimental day 12. (A) The total RNA was extracted from neurons cultured for 9 days for quantitative RT-PCR analysis. Data were normalized by the expression level of 36B4 mRNA and expressed as relative values to the corresponding control obtained in the absence of ERGO. The mRNA expression of MAP2, β III-tubulin, and synapsin I was evaluated in the control group and in mice treated with ERGO at 50 and 500 μ M. Each value represents the mean \pm S.E.M. ($n = 9$). (B, C) Neurons cultured for 12 days were homogenized, followed by SDS-PAGE for immunoblotting using antibodies against MAP2, β III-tubulin, and synapsin I. In panel (B), typical immunoblots were shown. In panel (C), data were normalized by the expression level of β -actin and expressed as relative values to the corresponding control obtained in the absence of ERGO. Each value represents the mean \pm S.E.M. ($n = 8-11$). * Significant difference from the control ($P < 0.05$).

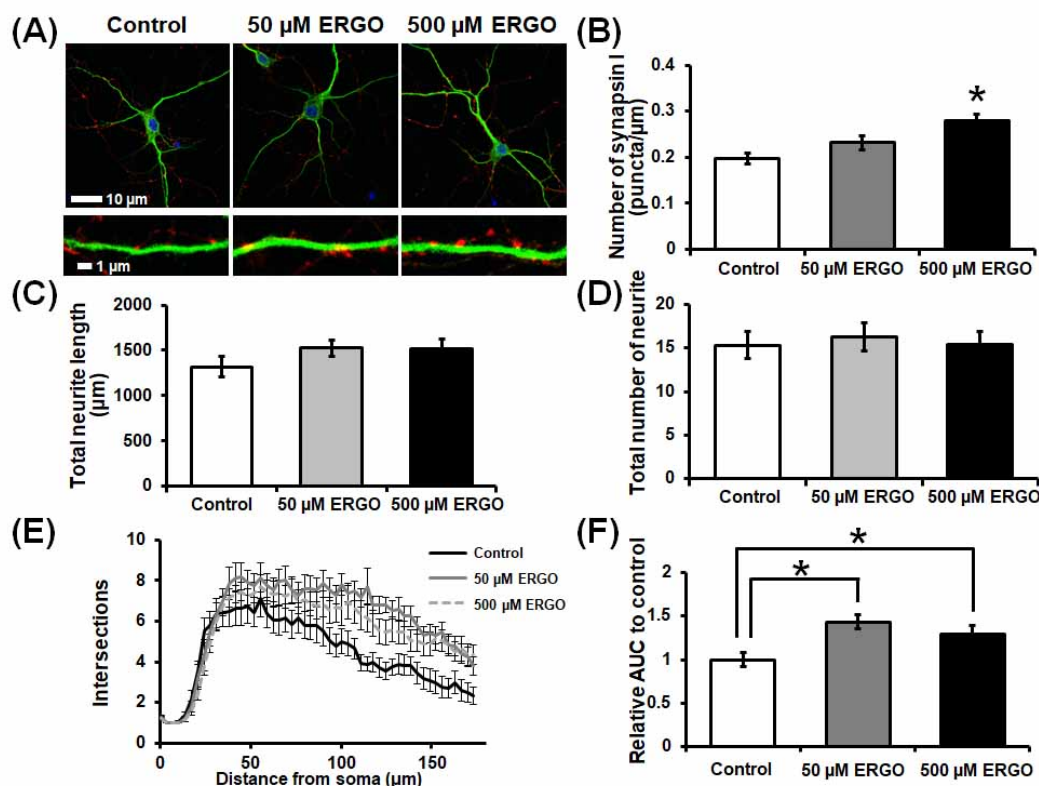


Fig. (5). Effect of ERGO on synapse formation and neurite outgrowth in primary cultured hippocampal neurons. Hippocampal neurons were cultured in neurobasal medium supplemented with B-27 for six days, followed by further culture in neurobasal medium without B-27 in either the absence (white columns) or presence (gray or black columns) of ERGO until experimental day 12. (A) Primary hippocampal neurons were fixed with 4% paraformaldehyde, followed by immunocytochemical detection of neuronal marker MAP2 (green), synapse marker synapsin I (red), and nuclear marker DAPI (blue). Scale bars: 1 (lower panel) or 10 μm (upper panel). The merged images are shown. (B) The number of puncta that were positive for synapsin I were counted by using ImageJ software and normalized by the length of neurites. Each value represents the mean ± S.E.M. (n = 15–20). (C–F) The length (C) and number (D) of neurites per cell were measured. Sholl analysis was also carried out using simple neurite tracer plug-in on Fiji (E), and the AUC was calculated using the trapezoidal rule for each Sholl profile (F). Twenty neurons in each group were analyzed. Each value represents the mean ± S.E.M. (n = 20). * Significant difference from the control ($P < 0.05$).

3.5. Induction of Neurotrophic Factors and Activation of mTORC1 Signaling by ERGO

To further investigate the mechanism underlying the promotion of neuronal maturation by ERGO, the possible induction of the expression of neurotrophic factors by ERGO was examined in cultured hippocampal neurons. The expression of mRNA for NT3 and NT5 was higher in the ERGO-treated group than in the control group (Fig. 6A). This ERGO-induced increase in the expression of NT3 and NT5 mRNA was concentration-dependent (Fig. 6A). However, the expression of NGF mRNA was slightly lower in the group exposed to 500 μM ERGO than in the control (Fig. 6A). Additionally, the mRNA expression of BDNF was minimally changed by ERGO (Fig. 6A). Next, the effect of inhibitor of Trk, which is the receptor for NT3 and NT5, on the expression of synapsin I was examined. The increase in the gene product of synapsin I that was provoked by ERGO was significantly suppressed in the presence of the Trk inhibitor

K252a at a concentration of 100 μM (Fig. 6B, C). This suggests the possible involvement of Trk signaling in the effects of ERGO.

Because ERGO is an amino acid and is incorporated into the intracellular space by the transporter OCTN1, the possible activation of the intracellular amino acid sensor mTORC1 signaling by ERGO was examined in cultured hippocampal neurons. In rodents, three isoforms of 4EBP1 are detected: α is the least phosphorylated form, β is an intermediate form, and γ is a hyperphosphorylated isoform [29]. The expression of phosphorylated mTOR and its downstream effector, 4EBP1, in hippocampal neurons was higher in the group exposed to ERGO than in the control group, whereas the phosphorylation of S6K1 was minimally changed by ERGO (Fig. 7). These results suggest that ERGO may promote cellular maturation at least in part through the induction of the neurotrophic factors NT3 and NT5, and activation of the Trk/mTORC1 signaling pathway in hippocampal neurons.

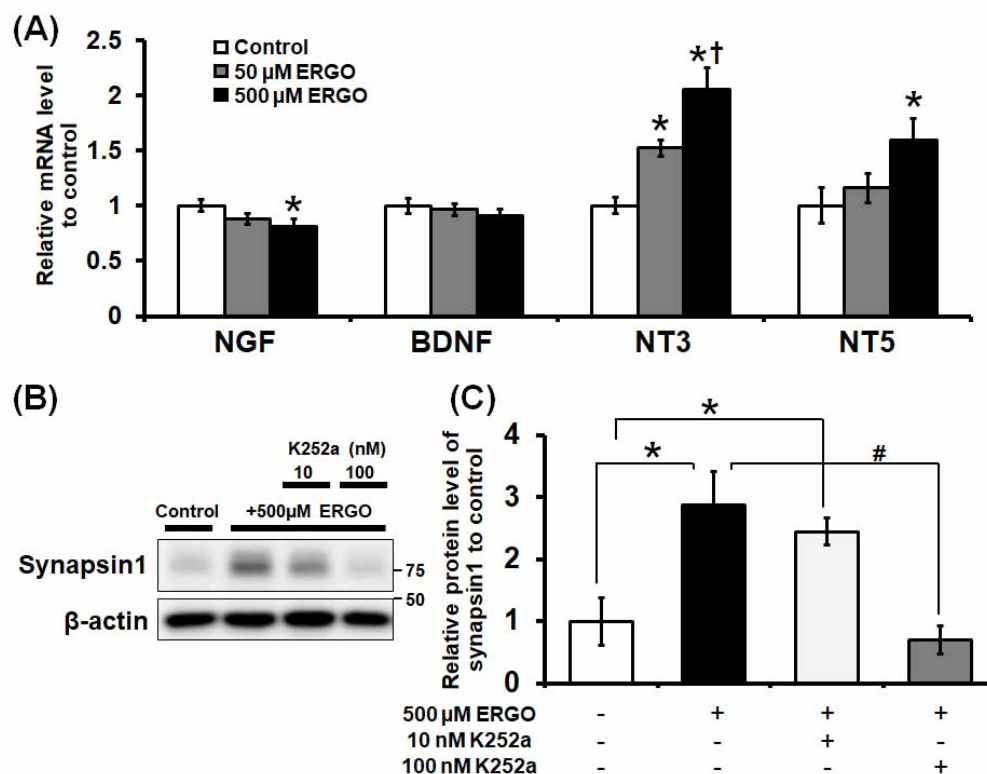


Fig. (6). Involvement of neurotrophic factor signaling in ERGO-induced neuronal maturation in cultured hippocampal neurons. Hippocampal neurons were cultured in neurobasal medium supplemented with B-27 for six days, followed by further culture in neurobasal medium without B-27 in either the absence (white columns) or presence (gray or black columns) of ERGO until experimental day 9 or 12. (A) The total RNA was extracted from neurons cultured for 9 days for quantitative RT-PCR analysis. Data were normalized by the expression level of 36B4 mRNA and expressed as relative values to the corresponding control obtained in the absence of ERGO. Each value represents the mean \pm S.E.M. ($n = 9$). (B, C) Neurons that were cultured for six days were exposed to the Trk inhibitor, K252a (10 or 100 nM), for 20 min and further cultured in either the absence (white columns) or presence (gray or black columns) of 500 μ M ERGO until experimental day 12. Cultured neurons were then homogenized, followed by SDS-PAGE for immunoblotting using an antibody against MAP2, β III-tubulin, and synapsin I. In panel (B), typical immunoblots are shown. In panel (C), data were normalized by the expression level of β -actin and expressed as relative values to the corresponding control obtained in the absence of ERGO. Each value represents the mean \pm S.E.M. ($n = 8-11$). * Significant difference from the control obtained in the absence of ERGO ($P < 0.05$); † Significant difference from the value obtained in neurons treated with 50 μ M of ERGO ($P < 0.05$); # Significant difference from the values obtained in the presence of ERGO alone ($P < 0.05$).

4. DISCUSSION

The present study demonstrated that the food-derived ingredient ERGO is distributed to the hippocampus through the blood-brain barrier after oral administration, and that ERGO may enhance learning and memory ability at least in part through the promotion of neuronal maturation in the hippocampus. It is noteworthy that the NORT results indicated a significant effect of ERGO at 5 mg/kg (Fig. 1A, Table 1), while both the NORT and SRT results indicated a promotive effect of ERGO at 20 or 50 mg/kg (Table 1). This dose of ERGO yielded a systemic concentration of 3–4 μ M (Fig. 2A). This ERGO concentration is clinically relevant since Cheah *et al.* recently reported a pharmacokinetic study of orally administered ERGO in healthy volunteers, which indicated that the plasma concentration of ERGO was 1 μ M at the basal level and 2–3 μ M after repeated daily oral adminis-

tration of ERGO at a dose of 25 mg/body [21]. Thus, the enhancement effect of ERGO on brain function may be advantageous in terms of its clinical application.

Because ERGO is ingested from the daily diet, ERGO exists in the plasma and hippocampus in normal mice that were not administered ERGO (Fig. 2). Nevertheless, exogenously administered ERGO displayed an enhancement effect on the learning and memory ability (Fig. 1, Table 1). The ERGO concentration in the hippocampus after oral administration for two weeks showed a significant increase at a dose of 20 mg/kg or than (Fig. 2B), whereas, the discrimination index for the NORT in the group that was exposed to ERGO at a dose of 20 mg/kg was significantly higher than in the control group. The discrimination index for the SRT tended to be higher in the group exposed to 20 mg/kg ERGO than in the control group (Table 1). These results support the

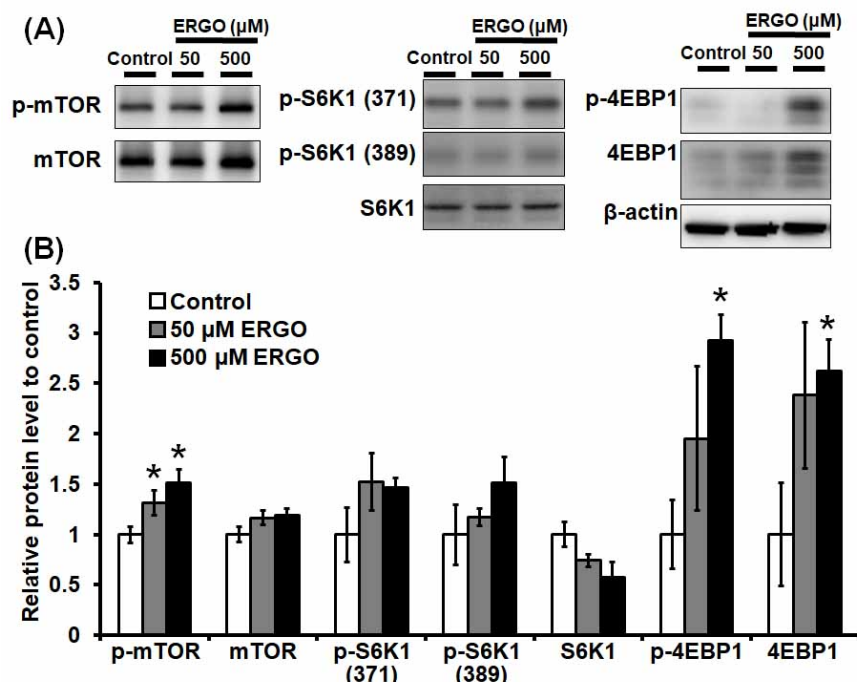


Fig. (7). Activation of the mTOR signaling pathway by ERGO in cultured hippocampal neurons.

Hippocampal neurons were cultured in neurobasal medium supplemented with B-27 for six days, followed by further culture in neurobasal medium without B-27 in either the absence (white columns) or presence (gray or black columns) of ERGO until experimental day 12. Cultured neurons were homogenized, followed by SDS-PAGE for immunoblotting using antibodies against p-mTOR, mTOR, p-S6K1 (Ser371), p-S6K1 (Thr389), S6K1, p-4EBP1, 4EBP1, and β -actin. In panel (A), typical immunoblots are shown. In panel (B), data were normalized by the protein level of β -actin and expressed as relative values to the corresponding control. Each value represents the mean \pm S.E.M. ($n = 4-12$). * Significant difference from the control ($P < 0.05$).

theory that ERGO may be incorporated in the hippocampus and may exert an enhancing effect on learning and memory. This hypothesis is also supported by the previous finding that OCTN1, which actively transports ERGO into the intracellular space, is expressed in both neurons [24] and neural stem cells [18]. Neural stem cells are abundantly present in the hippocampus. Additionally, exposure to ERGO leads to the uptake of ERGO in cultured neural stem cells and promotes cellular differentiation into neurons [18]. Learning and memory ability are improved by the promotion of neurogenesis in the hippocampus [30], whereas spatial memory declines when hippocampal neurogenesis is inhibited [31], suggesting that there is a potential association between hippocampal neurogenesis and brain function. The oral intake of a diet containing ERGO promotes neurogenesis in the murine hippocampus [14], further supporting a role of ERGO in the enhancement of learning and memory ability, at least in part through promotion of neurogenesis and neuronal maturation. Expression of the uptake transporter OCTN1 for ERGO in neurons and neural stem cells would be advantageous for ERGO to exert its biological activity in the brain since the concentration of ERGO in the hippocampus after 14 days of oral ERGO administration at 5–20 mg/kg was 5–6 μ M, which is 2–3 times higher than that in plasma (2–3 μ M) if we assume that the specific gravity of the hippocampal tissue is 1.

It is noteworthy that ERGO enhanced object recognition memory under normal conditions (Fig. 1, Table 1). Improvement of the learning and memory ability in dementia is an urgent social problem. Therefore, compounds that improve the impaired learning and memory ability in aged and/or brain-damaged animals have been extensively researched. In fact, it has been reported that curcumin and acetyl-L-carnitine both improve the impaired learning and memory ability in aged animals [32, 33]. However, limited reports are available on compounds that exert an enhancement effect on learning and memory under normal conditions. Advanced learning and memory abilities are advantageous for successful living in human society, which consists of diverse and advanced social tasks [34, 35]. The compounds that can be taken from daily diet and exert an enhancement effect on learning and memory could possess a prophylactic activity against dementia. Therefore, improvement of brain function through the daily diet is of great interest to healthy people as well as diseased people. Oral administration of ERGO exerted an improvement in learning and memory in the healthy condition (Fig. 1, Table 1). Because ERGO is a food-derived compound, improvement of brain function may be expected by its daily ingestion. Krill phosphatidylserine and certain types of nucleotide are also known as compounds that exert enhancement effects on the learning and memory ability in normal animals [36, 37]. However, limited informa-

tion is available regarding the clinical relevance of the dose required for such enhancement effect. Additionally, the mechanism controlling the systemic exposure of these compounds is mostly unknown, whereas the exposure of ERGO in the body is principally governed by OCTN1 [11, 13]. Mice were used at the age of 5 weeks in the present study. Further studies using aged mice are required to consider the prevention of dementia.

In the present study, the promotion of neuronal maturation, such as synapse formation, by ERGO was demonstrated in hippocampal neurons (Figs. 3, 4, 5). This may also be associated with the enhancement effect of ERGO on learning and memory, since neuronal activity in the hippocampus plays a crucial role in learning and memory, and synapse formation is essential for neuronal activity. This may also imply that the neuronal maturation that is provoked by ERGO may exert an enhancement effect not only on learning and memory, but also on other brain functions. The antidepressant effect of ERGO has already been demonstrated through oral administration in mice [14]. Antidepressants, such as fluoxetine and agomelatine, also exhibit a promotive effect on neuronal maturation and neurogenesis [38, 39]. Exposure to ERGO increased the expression of NT3 and NT5 in hippocampal neurons (Fig. 6). These neurotrophic factors caused neurite outgrowth [40, 41]. Administration of NT3 improves memory impairment in adult rats with damaged basal forebrain cholinergic neurons [42]. Furthermore, administration of NT5 also improves memory impairment in aged rats [43]. Thus, the induction of these neurotrophic factors may be at least partially associated with the enhancing effect of ERGO on learning and memory ability.

The transporter, OCTN1, is ubiquitously expressed in almost all of the bodily organs, at least in mice. This expression profile is compatible with the existence of ERGO in those organs, including brain, at the μM to sub mM range in wild-type mice, while ERGO is absent in the *octn1* gene knockout mice [11]. Exogenous administration of ERGO improved brain function in the present study (Fig. 1, Table 1). Similar beneficial effects of ERGO have also been observed in the peripheral organs. Administration of ERGO yields a protective effect against ischemia-reperfusion injury in the heart, small intestine, and liver [11, 44-46] and suppresses liver fibrosis [23], acute lesions in the lung [47], and skin aging [48]. These results support the existence of potential pharmacological activities of ERGO in various organs in the body, implying that it is a potential target of novel therapeutic agents for diseased conditions. However, the molecular mechanism(s) of ERGO, other than its antioxidant activity, that may underlie such pharmacological activities are largely unknown. In the present study, activation of the Trk/mTOR-C1 signaling pathway was proposed in hippocampal neurons (Figs. 6, 7). Yoshida *et al.* recently proposed that ERGO has immune-enhancing properties, through the potentiation of the toll-like receptor signaling pathway [49]. Further clarification of the mechanisms that underlie the action of ERGO will clarify its potential as a therapeutic target.

CONCLUSION

The food-derived hydrophilic amino acid, ERGO, is distributed to the hippocampus after oral administration and may enhance learning and memory abilities, at least in part, through the promotion of neuronal maturation in the hippocampus in normal mice. This pharmacological effect of ERGO in the brain is observed at a plasma ERGO concentration achievable in humans. Although further clarification of the mechanisms that underlie the action of ERGO, considering its safety, based on the ingestion of ERGO as a food ingredient for many years, and the transporter-mediated gastrointestinal absorption of ERGO followed by its uptake into brain parenchymal cells, this compound may be a unique target for improving brain function in normal subjects.

LIST OF ABBREVIATIONS

AUC	=	Area under the curve
BDNF	=	Brain-derived neurotrophic factor
BSA	=	Bovine serum albumin
DIV	=	Days <i>in vitro</i>
ERGO	=	Ergothioneine
MAP2	=	Microtubule-associated protein 2
NGF	=	Nerve growth factor
mTOR	=	Mammalian target of rapamycin
NORT	=	Novel object recognition test
NT	=	Neurotrophin
PBS	=	Phosphate-buffered saline
PI	=	Propidium iodide
SRT	=	Spatial recognition test
Trk	=	Tropomyosin receptor kinase
36B4	=	Acidic ribosomal phosphoprotein P0

ETHICS APPROVAL AND CONSENT TO PARTICIPATE

All animal procedures used in the present work were approved by the Kanazawa University Animal Care Committee (approval number: AP-183968).

HUMAN AND ANIMAL RIGHTS

All animal experiments were carried out in accordance with the NC3Rs ARRIVE guidelines. The animals were cared for in strict compliance with the guidelines outlined in the National Institutes of Health Guide for the Care and Use of Laboratory Animals.

CONSENT FOR PUBLICATION

Not applicable.

AVAILABILITY OF DATA AND MATERIALS

The datasets used and/or analysed during the current study are available from the corresponding author on reasonable request.

FUNDING

This work was partially supported by Grants-in-Aid for Scientific Research to NN (No. 19K07126) and YK (No. 15H04664) from the Ministry of Education, Culture, Sports, Science, and Technology of Japan, and by the Hoansha Foundation (Osaka, Japan) to YK

CONFLICT OF INTEREST

The author declares no conflict of interest, financial or otherwise.

ACKNOWLEDGEMENTS

The authors would like to thank Dr. Akihiro Tanaka in Yukiguni Maitake Co. Ltd. and Dr. Jean-Claude Yadan in TETRAHEDRON for their kind arrangement in providing ergothioneine. The authors would also like to thank Ms. Moe Mitamura at the Kanazawa University for technical assistance.

SUPPLEMENTARY MATERIAL

Supplementary material is available on the publisher's web site along with the published article.

REFERENCES

- [1] World Health Organization. *Dementia: Key facts.*, <http://www.who.int/news-room/fact-sheets/detail/dementia>
- [2] Briggs, R.; Kennelly, S.P.; O'Neill, D. Drug treatments in Alzheimer's disease. *Clin. Med. (Lond.)*, **2016**, *16*(3), 247-253. [<http://dx.doi.org/10.7861/clinmedicine.16-3-247>] [PMID: 27251914]
- [3] Weller, J.; Budson, A. Current understanding of Alzheimer's disease diagnosis and treatment. *F1000Res*, **2018**, *7* F1000 Faculty Rev-1161 [<http://dx.doi.org/10.12688/f1000research.14506.1>]
- [4] Venäläinen, O.; Bell, J.S.; Kirkpatrick, C.M.; Nishtala, P.S.; Liew, D.; Iiomäki, J. Adverse Drug Reactions Associated With Cholinesterase Inhibitors-Sequence Symmetry Analyses Using Prescription Claims Data. *J. Am. Med. Dir. Assoc.*, **2017**, *18*(2), 186-189. [<http://dx.doi.org/10.1016/j.jamda.2016.11.002>] [PMID: 28043802]
- [5] Li, Q.; Zhao, H.F.; Zhang, Z.F.; Liu, Z.G.; Pei, X.R.; Wang, J.B.; Cai, M.Y.; Li, Y. Long-term administration of green tea catechins prevents age-related spatial learning and memory decline in C57BL/6 J mice by regulating hippocampal cyclic amp-response element binding protein signaling cascade. *Neuroscience*, **2009**, *159*(4), 1208-1215. [<http://dx.doi.org/10.1016/j.neuroscience.2009.02.008>] [PMID: 19409206]
- [6] Kodali, M.; Parihar, V.K.; Hattiangady, B.; Mishra, V.; Shuai, B.; Shetty, A.K. Resveratrol prevents age-related memory and mood dysfunction with increased hippocampal neurogenesis and microvasculature, and reduced glial activation. *Sci. Rep.*, **2015**, *5*, 8075. [<http://dx.doi.org/10.1038/srep08075>] [PMID: 25627672]
- [7] Yook, J.S.; Okamoto, M.; Rakwal, R.; Shibato, J.; Lee, M.C.; Matsui, T.; Chang, H.; Cho, J.Y.; Soya, H. Astaxanthin supplementation enhances adult hippocampal neurogenesis and spatial memory in mice. *Mol. Nutr. Food Res.*, **2016**, *60*(3), 589-599. [<http://dx.doi.org/10.1002/mnfr.201500634>] [PMID: 26643409]
- [8] Park, H.R.; Kong, K.H.; Yu, B.P.; Mattson, M.P.; Lee, J. Resveratrol inhibits the proliferation of neural progenitor cells and hippocampal neurogenesis. *J. Biol. Chem.*, **2012**, *287*(51), 42588-42600. [<http://dx.doi.org/10.1074/jbc.M112.406413>] [PMID: 23105098]
- [9] Edwards, J.A.; Bellion, P.; Beilstein, P.; Rumbeli, R.; Schierle, J. Review of genotoxicity and rat carcinogenicity investigations with astaxanthin. *Regul. Toxicol. Pharmacol.*, **2016**, *75*, 5-19. [<http://dx.doi.org/10.1016/j.yrtph.2015.12.009>] [PMID: 26713891]
- [10] Kato, Y.; Kubo, Y.; Iwata, D.; Kato, S.; Sudo, T.; Sugiura, T.; Kagaya, T.; Wakayama, T.; Hirayama, A.; Sugimoto, M.; Sugihara, K.; Kaneko, S.; Soga, T.; Asano, M.; Tomita, M.; Matsui, T.; Wada, M.; Tsuji, A. Gene knockout and metabolome analysis of carnitine/organic cation transporter OCTN1. *Pharm. Res.*, **2010**, *27*(5), 832-840. [<http://dx.doi.org/10.1007/s11095-010-0076-z>] [PMID: 20224991]
- [11] Halliwell, B.; Cheah, I.K.; Tang, R.M.Y. Ergothioneine - a diet-derived antioxidant with therapeutic potential. *FEBS Lett.*, **2018**, *592*(20), 3357-3366. [<http://dx.doi.org/10.1002/1873-3468.13123>] [PMID: 29851075]
- [12] Gründemann, D.; Harlfinger, S.; Golz, S.; Geerts, A.; Lazar, A.; Berkels, R.; Jung, N.; Rubbert, A.; Schömig, E. Discovery of the ergothioneine transporter. *Proc. Natl. Acad. Sci. USA*, **2005**, *102*(14), 5256-5261. [<http://dx.doi.org/10.1073/pnas.0408624102>] [PMID: 15795384]
- [13] Sugiura, T.; Kato, S.; Shimizu, T.; Wakayama, T.; Nakamichi, N.; Kubo, Y.; Iwata, D.; Suzuki, K.; Soga, T.; Asano, M.; Iseki, S.; Tamai, I.; Tsuji, A.; Kato, Y. Functional expression of carnitine/organic cation transporter OCTN1/SLC22A4 in mouse small intestine and liver. *Drug Metab. Dispos.*, **2010**, *38*(10), 1665-1672. [<http://dx.doi.org/10.1124/dmd.110.032763>] [PMID: 20601551]
- [14] Nakamichi, N.; Nakayama, K.; Ishimoto, T.; Masuo, Y.; Wakayama, T.; Sekiguchi, H.; Sutoh, K.; Usumi, K.; Iseki, S.; Kato, Y. Food-derived hydrophilic antioxidant ergothioneine is distributed to the brain and exerts antidepressant effect in mice. *Brain Behav.*, **2016**, *6*(6)e00477 [<http://dx.doi.org/10.1002/brb3.477>] [PMID: 27134772]
- [15] Aruoma, O.I.; Spencer, J.P.; Mahmood, N. Protection against oxidative damage and cell death by the natural antioxidant ergothioneine. *Food Chem. Toxicol.*, **1999**, *37*(11), 1043-1053. [[http://dx.doi.org/10.1016/S0278-6915\(99\)00098-8](http://dx.doi.org/10.1016/S0278-6915(99)00098-8)] [PMID: 10566875]
- [16] Song, T.Y.; Chen, C.L.; Liao, J.W.; Ou, H.C.; Tsai, M.S. Ergothioneine protects against neuronal injury induced by cisplatin both in vitro and in vivo. *Food Chem. Toxicol.*, **2010**, *48*(12), 3492-3499. [<http://dx.doi.org/10.1016/j.fct.2010.09.030>] [PMID: 20932872]
- [17] Yang, N.C.; Lin, H.C.; Wu, J.H.; Ou, H.C.; Chai, Y.C.; Tseng, C.Y.; Liao, J.W.; Song, T.Y. Ergothioneine protects against neuronal injury induced by β -amyloid in mice. *Food Chem. Toxicol.*, **2012**, *50*(11), 3902-3911. [<http://dx.doi.org/10.1016/j.fct.2012.08.021>] [PMID: 22921351]
- [18] Ishimoto, T.; Nakamichi, N.; Hosotani, H.; Masuo, Y.; Sugiura, T.; Kato, Y. Organic cation transporter-mediated ergothioneine uptake in mouse neural progenitor cells suppresses proliferation and promotes differentiation into neurons. *PLoS One*, **2014**, *9*(2)e89434 [<http://dx.doi.org/10.1371/journal.pone.0089434>] [PMID: 24586778]
- [19] Sotgia, S.; Zinellu, A.; Mangoni, A.A.; Pintus, G.; Attia, J.; Carru, C.; McEvoy, M. Clinical and biochemical correlates of serum L-ergothioneine concentrations in community-dwelling middle-aged and older adults. *PLoS One*, **2014**, *9*(1)e84918 [<http://dx.doi.org/10.1371/journal.pone.0084918>] [PMID: 24392160]
- [20] Hatano, T.; Saiki, S.; Okuzumi, A.; Mohney, R.P.; Hattori, N. Identification of novel biomarkers for Parkinson's disease by metabolomic technologies. *J. Neurol. Neurosurg. Psychiatry*, **2016**, *87*(3), 295-301. [<http://dx.doi.org/10.1136/jnnp-2014-309676>] [PMID: 25795009]
- [21] Cheah, I.K.; Feng, L.; Tang, R.M.Y.; Lim, K.H.C.; Halliwell, B. Ergothioneine levels in an elderly population decrease with age and incidence of cognitive decline; a risk factor for neurodegeneration? *Biochem. Biophys. Res. Commun.*, **2016**, *478*(1), 162-167. [<http://dx.doi.org/10.1016/j.bbrc.2016.07.074>] [PMID: 27444382]
- [22] Song, T.Y.; Lin, H.C.; Chen, C.L.; Wu, J.H.; Liao, J.W.; Hu, M.L.

- Ergothioneine and melatonin attenuate oxidative stress and protect against learning and memory deficits in C57BL/6J mice treated with D-galactose. *Free Radic. Res.*, **2014**, *48*(9), 1049-1060. [http://dx.doi.org/10.3109/10715762.2014.920954] [PMID: 24797165]
- [23] Tang, Y.; Masuo, Y.; Sakai, Y.; Wakayama, T.; Sugiura, T.; Hara-da, R.; Futatsugi, A.; Komura, T.; Nakamichi, N.; Sekiguchi, H.; Sutoh, K.; Usumi, K.; Iseki, S.; Kaneko, S.; Kato, Y. Localization of xenobiotic transporter OCTN1/SLC22A4 in hepatic stellate cells and its protective role in liver fibrosis. *J. Pharm. Sci.*, **2016**, *105*(5), 1779-1789. [http://dx.doi.org/10.1016/j.xphs.2016.02.023] [PMID: 27020986]
- [24] Nakamichi, N.; Taguchi, T.; Hosotani, H.; Wakayama, T.; Shimizu, T.; Sugiura, T.; Iseki, S.; Kato, Y. Functional expression of carnitine/organic cation transporter OCTN1 in mouse brain neurons: possible involvement in neuronal differentiation. *Neurochem. Int.*, **2012**, *61*(7), 1121-1132. [http://dx.doi.org/10.1016/j.neuint.2012.08.004] [PMID: 22944603]
- [25] Nakamichi, N.; Kambe, Y.; Oikawa, H.; Ogura, M.; Takano, K.; Tamaki, K.; Inoue, M.; Hinoi, E.; Yoneda, Y. Protection by exogenous pyruvate through a mechanism related to monocarboxylate transporters against cell death induced by hydrogen peroxide in cultured rat cortical neurons. *J. Neurochem.*, **2005**, *93*(1), 84-93. [http://dx.doi.org/10.1111/j.1471-4159.2005.02999.x] [PMID: 15773908]
- [26] Ishimoto, T.; Masuo, Y.; Kato, Y.; Nakamichi, N. Ergothioneine-induced neuronal differentiation is mediated through activation of S6K1 and neurotrophin 4/5-TrkB signaling in murine neural stem cells. *Cell. Signal.*, **2019**, *53*, 269-280. [http://dx.doi.org/10.1016/j.cellsig.2018.10.012] [PMID: 30359715]
- [27] Longair, M.H.; Baker, D.A.; Armstrong, J.D. Simple Neurite Tracer: open source software for reconstruction, visualization and analysis of neuronal processes. *Bioinformatics*, **2011**, *27*(17), 2453-2454. [http://dx.doi.org/10.1093/bioinformatics/btr390] [PMID: 21727141]
- [28] Schindelin, J.; Arganda-Carreras, I.; Frise, E.; Kaynig, V.; Longair, M.; Pietzsch, T.; Preibisch, S.; Rueden, C.; Saalfeld, S.; Schmid, B.; Tinevez, J.Y.; White, D.J.; Hartenstein, V.; Eliceiri, K.; Tomancak, P.; Cardona, A. Fiji: an open-source platform for biological-image analysis. *Nat. Methods*, **2012**, *9*(7), 676-682. [http://dx.doi.org/10.1038/nmeth.2019] [PMID: 22743772]
- [29] Lin, T.A.; Kong, X.; Saltiel, A.R.; Blackshear, P.J.; Lawrence, J.C., Jr Control of PHAS-I by insulin in 3T3-L1 adipocytes. Synthesis, degradation, and phosphorylation by a rapamycin-sensitive and mitogen-activated protein kinase-independent pathway. *J. Biol. Chem.*, **1995**, *270*(31), 18531-18538. [http://dx.doi.org/10.1074/jbc.270.31.18531] [PMID: 7629182]
- [30] Bruel-Jungerman, E.; Laroche, S.; Rampon, C. New neurons in the dentate gyrus are involved in the expression of enhanced long-term memory following environmental enrichment. *Eur. J. Neurosci.*, **2005**, *21*(2), 513-521. [http://dx.doi.org/10.1111/j.1460-9568.2005.03875.x] [PMID: 15673450]
- [31] Winocur, G.; Wojtowicz, J.M.; Sekeres, M.; Snyder, J.S.; Wang, S. Inhibition of neurogenesis interferes with hippocampus-dependent memory function. *Hippocampus*, **2006**, *16*(3), 296-304. [http://dx.doi.org/10.1002/hipo.20163] [PMID: 16411241]
- [32] Goo, M.J.; Choi, S.M.; Kim, S.H.; Ahn, B.O. Protective effects of acetyl-L-carnitine on neurodegenerative changes in chronic cerebral ischemia models and learning-memory impairment in aged rats. *Arch. Pharm. Res.*, **2012**, *35*(1), 145-154. [http://dx.doi.org/10.1007/s12272-012-0116-9] [PMID: 22297753]
- [33] Yu, S.Y.; Zhang, M.; Luo, J.; Zhang, L.; Shao, Y.; Li, G. Curcumin ameliorates memory deficits via neuronal nitric oxide synthase in aged mice. *Prog. Neuropsychopharmacol. Biol. Psychiatry*, **2013**, *45*, 47-53. [http://dx.doi.org/10.1016/j.pnpbp.2013.05.001] [PMID: 23665290]
- [34] Batty, G.D.; Deary, I.J. Early life intelligence and adult health. *BMJ*, **2004**, *329*(7466), 585-586. [http://dx.doi.org/10.1136/bmj.329.7466.585] [PMID: 15361422]
- [35] Gottfredson, L.S. Life, Death, and Intelligence. *J. Cogn. Educ. Psychol.*, **2004**, *4*(1), 23-46. [http://dx.doi.org/10.1891/194589504787382839]
- [36] Sato, N.; Murakami, Y.; Nakano, T.; Sugawara, M.; Kawakami, H.; Idota, T.; Nakajima, I. Effects of dietary nucleotides on lipid metabolism and learning ability of rats. *Biosci. Biotechnol. Biochem.*, **1995**, *59*(7), 1267-1271. [http://dx.doi.org/10.1271/bbb.59.1267] [PMID: 7670187]
- [37] Lee, B.; Sur, B.J.; Han, J.J.; Shim, I.; Her, S.; Lee, H.J.; Hahn, D.H. Krill phosphatidylserine improves learning and memory in Morris water maze in aged rats. *Prog. Neuropsychopharmacol. Biol. Psychiatry*, **2010**, *34*(6), 1085-1093. [http://dx.doi.org/10.1016/j.pnpbp.2010.05.031] [PMID: 20677367]
- [38] Marcussen, A.B.; Flagstad, P.; Kristjansen, P.E.; Johansen, F.F.; Englund, U. Increase in neurogenesis and behavioural benefit after chronic fluoxetine treatment in Wistar rats. *Acta Neurol. Scand.*, **2008**, *117*(2), 94-100. [PMID: 18184344]
- [39] Rainer, Q.; Xia, L.; Guilloux, J.P.; Gabriel, C.; Mocaër, E.; Hen, R.; Enhamre, E.; Gardier, A.M.; David, D.J. Beneficial behavioural and neurogenic effects of agomelatine in a model of depression/anxiety. *Int. J. Neuropsychopharmacol.*, **2012**, *15*(3), 321-335. [http://dx.doi.org/10.1017/S1461145711000356] [PMID: 21473810]
- [40] Rabacchi, S.A.; Kruk, B.; Hamilton, J.; Carney, C.; Hoffman, J.R.; Meyer, S.L.; Springer, J.E.; Baird, D.H. BDNF and NT4/5 promote survival and neurite outgrowth of pontocerebellar mossy fiber neurons. *J. Neurobiol.*, **1999**, *40*(2), 254-269. [http://dx.doi.org/10.1002/(SICI)1097-4695(199908)40:2<254::AID-NEU11>3.0.CO;2-4] [PMID: 10413455]
- [41] Hechler, D.; Boato, F.; Nitsch, R.; Hendrix, S. Differential regulation of axon outgrowth and reinnervation by neurotrophin-3 and neurotrophin-4 in the hippocampal formation. *Exp. Brain Res.*, **2010**, *205*(2), 215-221. [http://dx.doi.org/10.1007/s00221-010-2355-7] [PMID: 20640412]
- [42] Lee, Y.S.; Danandeh, A.; Baratta, J.; Lin, C.Y.; Yu, J.; Robertson, R.T. Neurotrophic factors rescue basal forebrain cholinergic neurons and improve performance on a spatial learning test. *Exp. Neurol.*, **2013**, *249*, 178-186. [http://dx.doi.org/10.1016/j.expneurol.2013.08.012] [PMID: 24017996]
- [43] Fischer, W.; Sirevaag, A.; Wiegand, S.J.; Lindsay, R.M.; Björklund, A. Reversal of spatial memory impairments in aged rats by nerve growth factor and neurotrophins 3 and 4/5 but not by brain-derived neurotrophic factor. *Proc. Natl. Acad. Sci. USA*, **1994**, *91*(18), 8607-8611. [http://dx.doi.org/10.1073/pnas.91.18.8607] [PMID: 8078930]
- [44] Arduini, A.; Eddy, L.; Hochstein, P. The reduction of ferryl myoglobin by ergothioneine: a novel function for ergothioneine. *Arch. Biochem. Biophys.*, **1990**, *281*(1), 41-43. [http://dx.doi.org/10.1016/0003-9861(90)90410-Z] [PMID: 2383023]
- [45] Bedirli, A.; Sakrak, O.; Muhtaroglu, S.; Soyuer, I.; Guler, I.; Riza Erdogan, A.; Sozuer, E.M. Ergothioneine pretreatment protects the liver from ischemia-reperfusion injury caused by increasing hepatic heat shock protein 70. *J. Surg. Res.*, **2004**, *122*(1), 96-102. [http://dx.doi.org/10.1016/j.jss.2004.06.016] [PMID: 15522321]
- [46] Sakrak, O.; Kerem, M.; Bedirli, A.; Pasaoglu, H.; Akyurek, N.; Ofluoglu, E.; Gültekin, F.A. Ergothioneine modulates proinflammatory cytokines and heat shock protein 70 in mesenteric ischemia and reperfusion injury. *J. Surg. Res.*, **2008**, *144*(1), 36-42. [http://dx.doi.org/10.1016/j.jss.2007.04.020] [PMID: 17603080]
- [47] Repine, J.E.; Elkins, N.D. Effect of ergothioneine on acute lung injury and inflammation in cytokine insufflated rats. *Prev. Med.*, **2012**, *54*(Suppl.), S79-S82. [http://dx.doi.org/10.1016/j.ypmed.2011.12.006] [PMID: 22197759]
- [48] Obayashi, K.; Kurihara, K.; Okano, Y.; Masaki, H.; Yarosh, D.B.

L-Ergothioneine scavenges superoxide and singlet oxygen and suppresses TNF-alpha and MMP-1 expression in UV-irradiated human dermal fibroblasts. *J. Cosmet. Sci.*, **2005**, *56*(1), 17-27. [http://dx.doi.org/10.1111/j.0142-5463.2005.00265_2.x] [PMID: 15744438]

[49] Yoshida, S.; Shime, H.; Funami, K.; Takaki, H.; Matsumoto, M.;

Kasahara, M.; Seya, T. The anti-oxidant ergothioneine augments the immunomodulatory function of TLR agonists by direct action on macrophages. *PLoS One*, **2017**, *12*(1)e0169360 [<http://dx.doi.org/10.1371/journal.pone.0169360>] [PMID: 28114402]